Zootaxa 4901 (1): 001–092
https://www.mapress.com/j/zt/

Monograph

ISSN 1175-5326 (print edition)
ZOOTAXA
ISSN 1175-5334 (online edition)

https://doi.org/10.11646/zootaxa.4901.1.1
http://zoobank.org/urn:lsid:zoobank.org:pub:4458B8F9-505B-4598-8BF1-4AD48CCF155C

ZOOTAXA

4901

Revision of the Old World genus *Mesocomys* Cameron (Hymenoptera: Eupelmidae)

GARY A.P. GIBSON
Honorary Research Associate, Agriculture and Agri-Food Canada, Canadian National Collection of Insects, Arachnids and Nematodes, K. W. Neatby Bldg., 960 Carling Avenue, Ottawa, Ontario, Canada, K1A 0C6.
chalcidsrule@hotmail.com; Gary.Gibson@canada.ca; https://orcid.org/0000-0002-8161-7445

Magnolia Press
Auckland, New Zealand

Accepted by N. Dale-Skey: 2 Oct. 2020; published: 5 Jan. 2021

GARY A.P. GIBSON
REVISION OF THE OLD WORLD GENUS *MESOCOMYS* CAMERON (HYMENOPTERA: EUPELMIDAE)
(*Zootaxa* 4901)

92 pp.; 30 cm.

5 Jan. 2021

ISBN 978-1-77688-138-3 (paperback)

ISBN 978-1-77688-139-0 (Online edition)

FIRST PUBLISHED IN 2021 BY

Magnolia Press

P.O. Box 41-383

Auckland 1041

New Zealand

e-mail: magnolia@mapress.com

https://www.mapress.com/j/zt

ISSN 1175-5326 (Print edition)

ISSN 1175-5334 (Online edition)

Table of Contents

Abstract

The Old World genus *Mesocomys* Cameron (1905) (Hymenoptera: Eupelmidae: Eupelminae) is revised. Eleven species, including two newly described species, are recognized and keyed in two previously established species groups, the *albitarsis* and the *pulchriceps* species groups *sensu* Gibson (1995), but with additional features provided to distinguish members of the two groups. Five species are recognized in the *pulchriceps* group—*Mesocomys anelliformis* **n. sp.**, *M. longiscapus* **n. sp.**, *M. orientalis* Ferrière, 1935, *M. pauliani* Ferrière, 1951, and *M. pulchriceps* Cameron, 1905. Seven species are assigned to the *albitarsis* group, but one, *M. aegeriae* Sheng, 1996 is treated as a *nomen dubium*; the six recognized and keyed species in the *albitarsis* group are *M. albitarsis* (Ashmead, 1904), *M. breviscapis* Yao, Yang & Zhao, 2009, *M. menzeli* (Ferrière, 1930b), *M. obscurus* (Ferrière, 1930b) **revised stat.**, *M. superansi* Yao, Yang & Zhao, 2009, and *M. trabalae* Yao, Yang & Zhao, 2009. Within the *albitarsis* group, the species are further discussed relative to two newly established species subgroups, the *albitarsis* subgroup for *M. albitarsis*, *M. menzeli* and *M. obscurus*, and the *aegeriae* subgroup for *M. aegeriae*, *M. breviscapis*, *M. superansi* and *M. trabalae*. Females of the *albitarsis* subgroup possess a finely sculptured mesoscutal medial lobe in combination with partly infuscate fore wings and/or at least partly pale flagellum, whereas females of the *aegeriae* subgroup possess a much more coarsely sculptured mesoscutal medial lobe and hyaline fore wings in combination with a dark flagellum. Members of the *albitarsis* species group are restricted to the Oriental and eastern Palaearctic regions except for a single female of the *aegeriae* subgroup seen from Algeria that is provisionally identified as *M. breviscapis*; members of the *pulchriceps* group are restricted to the Afrotropical region except for *M. orientalis* from the Oriental region. Newly placed in synonymy are *M. aegeriae* Sheng, 1998 under *M. aegeriae* Sheng, 1996 **n. syn.**, *M. sinensis* Yao, Yang & Zhao, 2009 under *M. breviscapis* Yao, Yang & Zhao, 2009 **n. syn.**, *M. atulyus* Narendran, 1995 under *M. orientalis* Ferrière, 1935 **n. syn.**, *M. vuilleti* (Crawford, 1912) under *M. pulchriceps* Cameron, 1905 **n. syn.**, and *Semianastatus orientalis* Kalina, 1984 and *Mesocomys kalinai* Özdikmen, 2011 under *M. albitarsis* (Ashmead, 1904) **n. syns**. Lectotypes are newly designated for *M. menzeli*, *M. obscurus*, *M. orientalis*, *M. pauliani*, *M. pulchriceps* and *M. vuilleti*. Morphological features characteristic of the genus and of the highly dimorphic sexes are described and illustrated, and the species are keyed, described, and illustrated through macrophotography. Phylogenetics are discussed for the genus, the two species groups, and species within the *pulchriceps* group. Distribution and host records are also summarized for each species.

Key words: *Anastatus*, biology, egg parasitoid, morphology, pest management, sexual dimorphism, synonymy, taxonomy

Introduction

Cameron (1905) established *Mesocomys* (Hymenoptera: Eupelmidae: Eupelminae) for his newly described species *M. pulchriceps* from South Africa. However, the first species to now be classified in *Mesocomys* was described by Ashmead (1904) from Japan as *Anastatus albitarsis* (Eupelmidae). The latter species has sometimes also been identified in the biological literature as *Pseudanastatus albitarsis* (*e.g.*, Hirose 1964, 1969; Tong & Ni 1989, 1990; Ni *et al.* 1994), but was correctly recognized as a species of *Mesocomys* by Bouček (1988), who commented on the similarity of *Mesocomys* females to short-bodied females of *Anastatus* Motschulsky, especially to species he recognized as the *bifasciatus*-group in the latter genus. Kalina (1984) described the new genus and species *Semianastatus orientalis* for specimens reared from eggs of the Japanese giant silkworm, *Caligula japonica* Moore (Lepidoptera: Saturniidae), from Primorsky Krai in Russia, but Gibson (1995) synonymized *Semianastatus* under *Mesocomys*. Transfer of the type species of *Semianastatus* to *Mesocomys* resulted in junior homonomy of *M. orientalis* Kalina, 1984 under *M. orientalis* Ferrière, 1935, which was described originally from Myanmar (Burma). Gibson (1995) did not propose a replacement name for *M. orientalis* Kalina because he based his generic synonymy on the description and illustrations provided by Kalina (1984) and stated that examination of type material was required to determine whether the species was valid or the name was a synonym. However, Özdikmen (2011) subsequently provided the replacement name *Mesocomys kalinai* for *M. orientalis* (Kalina). Examination of type material of *Semianastatus orientalis* as part of the present study showed that this name is indeed a synonym for which a replacement name was unnecessary.

In addition to the above species, Ferrière (1930b) described *M. menzeli* and the variety *M. menzeli obscurus*, both originally in *Anastatus*, from eggs of the Atlas moth, *Attacus atlas* (L.) (Saturniidae) that were collected on the same date and locality on the island of Java, Indonesia. One other *Mesocomys* species has been described from the Oriental region, *M. atulyus* Narendran in Narendran & Sheela (1995) from India, from eggs of an unidentified species of *Antheraea* Hübner (Saturniidae). Two species other than *M. pulchriceps* have been described from the Afrotropical region, *M. vuilleti* (Crawford 1912), originally also in *Anastatus*, from eggs of *Cirina butyrospermi* (Vuillet) (Saturniidae) from Mali, and *M. pauliani* Ferrière (1951) from Madagascar. Finally, six names have been established for species from Palaearctic China, *M. aegeriae* Sheng in Sheng & Wang (1996), which was subsequently republished as a new species by Sheng (1998), plus *M. breviscapis* and *M. sinensis* Yao, Yang & Zhao (2009) from eggs of the Chinese pine caterpillar, *Dendrolimus tabulaeformis* Tsae & Liu (Lepidoptera: Lasiocampidae), *M. superansi* Yao, Yang & Zhao (2009) from eggs of the Sakhalin or white-lined silk moth, *Dendrolimus superans* (Butler), and *M. trabalae* Yao, Yang & Zhao (2009) from eggs of *Trabala vishnou* (Lefèbvre) (Lasiocampidae).

Species limits within the host genus *Dendrolimus* Gemar remain problematic, though recent molecular investigations suggest *D. tabulaeformis* should more correctly be treated as a subspecies of *D. punctatus* (Walker), which is closely related to *D. spectabilis* (Butler) but genetically is more distinct from such species as *D. houi* Lajonquière, *D. kikuchii* Matsumura, *D. pini* (L.), and *D. superans* (Qin *et al*. 2015; Kononov *et al*. 2016). Despite issues of host taxonomy, host biology of *Mesocomys* is comparatively well known relative to most genera of Eupelminae because all but three of the previously described species (*M. albitarsis*, *Semianastatus orientalis*, and *M. pulchriceps*) were reared originally from eggs of either Lasiocampidae or Saturniidae. Based on material examined for this study, other lepidopteran hosts include the eggs of species of Bombycidae, Erebidae, Eupterotidae, Hesperiidae, Lymantriidae, Notodontidae, Nymphalidae, and Papilionidae. Label data also indicates eggs of *Tessaratoma papillosa* (Drury) (Hemiptera: Tessaratomidae) and possibly eggs of Mantidae (Mantoidea) as hosts, and at least one label record indicates emergence from a pupa rather than an egg.

In Eupelminae, mesosomal structure differs conspicuously between the two sexes because females are characterized by several features that are correlated with the evolution of enhanced jumping ability, whereas males retain more plesiomorphic structures (Gibson 1986, 1995). As a result, males and females of Eupelminae are easily distinguished, with males more closely resembling males of some Cleonyminae (Chalcidoidea: Pteromalidae) than their conspecific females. However, the extreme sexual dimorphism that characterizes the subfamily makes association of the sexes of a single species usually difficult without rearing the two together or employing molecular techniques. Because most of the original *Mesocomys* descriptions were based on reared individuals of both sexes, males are reliably associated with females for most described species, though males have never previously been differentiated in keys to species other than for *M. sinensis* and *M. trabalae* (Yao *et al.* 2009). Of the 14 species-level taxa that were described in or subsequently assigned to *Mesocomys* prior to the present study, Ferrière (1951) provided a key (in French) to differentiate females of four species, Narendran & Sheela (1995) the females of five species (in English), Yao *et al*. (2009) the females of seven species (in Chinese), and Yang *et al*. (2015) the females of six species (in Chinese). The key of Yang *et al*. (2015) essentially repeats the key of Yao *et al*. (2009) except that *M. aegeriae* is not

included. Yang *et al.* (2015) did, however, provide some new host data for the treated Chinese species and included a colour habitus photograph of a male they identified as *M. albitarsis*, and of females they identified as *M. breviscapis*, *M. orientalis*, *M. sinensis*, *M. superansi* and *M. trabalae*.

As detailed by Chen *et al*. (2019), beginning in 2017 members of the Institute of Biological Control, Jilin Agricultural University, Changchun, China, reared individuals of two genera of Eupelminae, *Mesocomys* and *Anastatus*, from eggs of *C. japonica* as part of a survey for potential biocontrol agents of this pest of walnut trees in China. Laboratory colonies were subsequently established on eggs of the factitious host *Antherea pernyi* (Guérin-Méneville) (Saturniidae), the Chinese oak silk moth. Although it was evident that two species of *Mesocomys* had been reared it was not possible to confidently identify the species because of the lack of any comprehensive key to world species and because original species descriptions, although sometimes lengthy, not always included or illustrated the same features for comparison. The necessity to accurately identify the potentially beneficial species stimulated the present world revision of this economically important genus. Unfortunately, because of the lack of sufficient material, and the unavailability of some type material, the species limits and actual number of species comprising the *aegeriae* subgroup, newly defined herein, have not been resolved satisfactorily and additional research will be required to clarify concepts further.

Material and methods

Material. Specimens on which this study is based were obtained from the following 22 world collections; the associated codens are used to designate the museums in which specimens are deposited, and individuals facilitating specimen loans are given in parentheses:

AICF "Alexandru Ioan Cuza" University, Iaşi, Romania, Lucian Fusu personal collection (L. Fusu).
CFRB Chinese Academy of Forestry, Beijing, China (Z-Q. Yang).
CASC California Academy of Sciences, Department of Entomology, San Francisco, CA, USA (B. Fisher, R. Zuparko).
CNC Canadian National Collection of Insects, Arachnids and Nematodes, Agriculture and Agri-Food Canada, Ottawa, ON, Canada.
DZUC Department of Zoology, University of Calicut, Kerala, India (A.P. Ranjith).
ELKU Entomological Laboratory, Kyushu University, Fukuoka, Japan (T. Mita).
FAFU Fujian Agriculture and Forestry University, Jinshan, Fuzhou, Fujian, China (L-F. Peng).
JXAU Jiangxi Agricultural University, Nanchang, Jiangxi, China (L-F. Peng).
IAEE Institute of Applied Ecology and Ecotechnology, Kostelec nad Černými lesy, Czech Republic (V. Kalina). [Type material stated as deposited in IAEE, but currently in possession of V. Kalina, Prague, Czech Republic.]
IZCAS Chinese Academy of Sciences, Beijing, China (H. Cao, H. Xiao).
JLAU Institute of Biological Control, Jilin Agricultural University, Changchun, China (Y-M. Chen, L-S. Zang).
MHNG Museum d'Historie Naturelle, Geneva, Switzerland (B. Landry).
MNHN Museum National d'Histoire Naturelle, Paris, France (A. Touret-Alby).
NHMUK Department of Life Sciences, Natural History Museum, London, England (N. Dale-Skey Papilloud) [formerly, BMNH: British Museum of Natural History].
NMK National Museums of Kenya, Nairobi, Kenya (R. Copeland, M. Gikungu).
NMPC Narodni Muzeum v Praze, Prague, Czech Republic (J. Macek).
SAMC South African Museum, Iziko Museums of South Africa, Cape Town, South Africa (S. van Noort).
SANC South African National Collection of Insects, Plant Protection Research Institute, Pretoria, South Africa (W. Strumpher).
TARI Taiwan Agricultural Research Institute Insect Collection, Taichung City, Taiwan, Republic of China (C. Lee).
UCRC UCR Entomological Teaching and Research Collection, University of California, Riverside, CA, USA (S. Triapitzin, D. Yanega).
USNM National Insect Collection, National Museum of Natural History, Smithsonian Institution, Washington, DC, USA (M. Gates).
ZIN Zoological Institute of Russian Academy of Sciences, Zoological Museum, St. Petersburg, Russia (E. Tselikh).

Methods. *Microscopy/imaging*. Specimens were examined with a Nikon SMZ 1500 binocular microscope with an ocular grid having 100 divisions and were illuminated with a Leica 100-watt halogen light source. The halogen

light source was filtered through a piece of translucent Mylar® tracing acetate taped to the microscope objective in order to reduce glare. Images of the holotype of *M. atulyus* were provided by Avunjikkattu Ranjith (DZUC), of the remaining parts of the holotype of *M. aegeriae* by Ling-Fei Peng (FAFU), and of the lectotype of *M. pauliani* by Bernard Landry (MHNG). All other images in the plates of illustrations were taken at the CNC using a Leica DMC5400 20 megapixel camera attached to a Leica Z16 APO motorized macroscope and illuminated with three Leica KL2500 LCD fibre optic light sources fitted with 250-watt cold light reflector lamps. The fibre optic light sources were filtered through a polystyrene foam dome to reduce glare. The resulting image layers were combined electronically using Zerene Stacker™ and the final images enhanced as needed using Adobe® Photoshop. All CNC-imaged specimens, except for holotypes and allotypes, bear a unique "CNC Photo 2018-x" number, which is cited for the respective specimen in the list of material examined and in the figure captions. This is done so specimens can be readily matched with the published images if species concepts are changed in the future. For brevity, only the photo number is included in the figure captions.

Colour. In describing colour, the terms 'pale' and 'dark' are used as general terms relative to one another, with pale referring to yellow or orange to light brown, and dark referring to dark brown to black (then often also with variably conspicuous metallic lustre), as per Chen *et al*. (2019) and Gibson (2020). This is done for the reasons given in Gibson (2020). The appreciation of colour and of different metallic lustres can be affected by several factors, most particularly by differences in the type of light used to examine specimens, but also by the state of specimen preservation (*e.g.*, clean *versus* covered with some substance or faded because of exposure to light). Serial imaging of specimens can sometimes also produce colour artefacts. Imaging of three dimensional structures that are hyaline or pale on some levels but darker on other levels through the structure can result in the two dimensional montaged image appearing more extensively dark than is the actual structure. For example, the base of the gaster in Fig. 5G appears to lack a subbasal white band, but under some angles of viewing using the binocular microscope a paler subbasal region is evident, and a subbasal pale band is quite distinct in another paratype of the same species (Fig. 5H). Similarly, the mesotarsi of the female *M. albitarsis* appear infuscate in Fig. 1B. However, this results from the dark mesotarsal pegs and, except for the pegs, the basal four tarsomeres are actually mostly pale (Fig. 1G). The term 'infuscate' is used as a general term, simply meaning darkened to some extent relative to pale or hyaline (*e.g*., brownish-infuscate or yellowish-infuscate). Because of the factors that affect colour appreciation, the species descriptions are based on observations using the Nikon SMZ microscope and the halogen light source, and some images comprising the plates of illustrations may not match exactly the colours stated in the species descriptions.

Structure. Abbreviations used on the plates of photomicrographs to designate structures are listed alphabetically in Table 1 and explained below. Morphological terms largely follow Gibson (1986, 1995, 2004, 2017b) and Gibson and Fusu (2016), as amplified or modified below.

Head structures of the two sexes are quite similar; the term **face** is used for the entire frontal surface of the head (*e.g.*, Fig. 1C), whereas **frons** (Fig. 1D: **frs**) is used for the frontal region of the head between the dorsal limit of the scrobal depression and the posterior limit of the posterior ocelli, including the **ocellar triangle** (Fig. 1D: **oct**), the region encompassed by an imaginary line extending around the outer margins of the ocelli. The ocellar triangle sometimes has a somewhat different sculpture from the rest of the frons, as does the dorsal region of the head behind the posterior ocelli, which is treated as the **vertex** (Fig. 1D: **vtx**); the **temple** (Fig. 1D: **tmp**) is the dorsal region of the vertex behind the eye. The combined frons and vertex is the **frontovertex**. A ∩-shaped **scrobal depression** is formed from a concave **scrobe** (Fig. 1C: **sc**) above each torulus, with the scrobes dorsally convergent and continuous so as to differentiate a low-convex, triangular, **interantennal prominence** (Fig. 1C: **iap**) between them, and a slender **parascrobal region** (Fig. 1C: **psr**) between each lateral margin and inner eye margin; the dorsal part of the parascrobal region that is continuous with the frons is termed the **upper parascrobal region** (Figs 1C, D: **upr**). The **lower face** is that part of the face below the level of the toruli, which includes medially the **clypeus**, whose apical margin can be broadly incurved (Fig. 1F: **cly**) to deeply emarginate (*e.g.*, Figs 25E, F: arrow). The **gena** (Fig. 18B: **gen**) is the ventrolateral surface of the head lateral of the malar sulcus. The flagellum of the antenna is composed of 11 flagellomeres and is differentiated into two regions. The **funicle** (Fig. 2E: **fun**) is composed of the basal eight flagellomeres or **funiculars**; unlike in some literature on chalcidoids the first flagellomere (*e.g.,* Fig. 3G: fl_1) is not designated as the "anellus" and is included as part of the funicle. The **clava** (Fig. 2E: **clv**) is composed of the apical three flagellomeres, which although broadly fused are at least partly differentiated by fine sutures; the dorsal surface of the clava consists of a **micropilose sensory region** (*e.g*., Figs 2E: **msr**) that can appear to face laterally (*e.g*., Fig. 26G: **msr**) or even ventrally (*e.g*., Figs 6C, 11H) depending on how the flagellomeres are oriented, but which in air-

dried individuals often is collapsed (*e.g.*, Figs 9D, 20G) so that accurate width to length ratios of the clava cannot be calculated.

TABLE 1. List of abbreviations and illustrating figures for structural terms indicated on plates of figures.

Abbreviation	Term	Figures
ac	acropleuron	2B, 3E
acs	acropleural sulcus	2B, 3E
aml	anterior convex region of mesoscutal medial lobe	2C
aod	anterior ocellus diameter	1E, 6D, 22D
asl	apical setae of labrum	22C, 25F
ax	axilla	2A, 3D
bc	basal cell of fore wing	2F, 3F, 19D
cal	callus of propodeum	2D, G, H, 27H
cc	costal cell of fore wing	2F, 19D, 21I
clv	clava	2E
cly	clypeus	1F
cua	cubital area of fore wing	3F, 18H, 19D
cuf	cubital fold of fore wing	24B
dep	depression anterior to scutellar-axillar complex	2A, C
dso	distance between scrobal depression and anterior ocellus	1E, 6D, 22D
epm	mesepimeron	3E
eps	mesepisternum	3E
fl	flagellomere (funicular)	3G, 5C, D, F
fps	frontal surface of prepectus	2B
frs	frons	1D
fun	funicle (flagellomeres 1–8)	2E
gen	gena	18B
Gt	gastral tergite	5G–J, 17A, 21G
HH	head height	16C
HL	head length	18C
HW	head width	18C
iap	interantennal prominence	1C
IOD	interocular distance	18C
lab	labrum	1F
LOL	lateral ocellar line	16D
lps	lateral surface of prepectus	2B
mcf	mediocubital fold of fore wing	3F, 18H, 19D, 24B
mdf	medial fold of fore wing	24B
mll	mesoscutal lateral lobe	2C, 3D
mml	mesoscutal medial lobe	2C, 3D
mpb	parapsidal band on mesoscutal lateral lobe	4G
mpc	mesopectus	2B
MPOD	maximum diameter of posterior ocellus	16E
msr	micropilose sensory region of clava	2E, 26G
mv	marginal vein of fore wing	2F, 21I

...Continued on the next page

TABLE 1. (Continued)

Abbreviation	Term	Figures
no_1	pronotum	3D
not	notaulus	3D
oct	ocellar triangle	1D
OOL	ocellocular line	16E
pdl	pedicel	3G, 5C, F
pl_3	metapleuron	2B, G, H, 3E, 27F, H
pml	posterior depressed region of mesoscutal medial lobe	2C
pmv	postmarginal vein of fore wing	2F
pnc	pronotal collar	2D
pnp	pronotal panel	2D, 3E
POL	postocellar line	16D
ppd	propodeal plical depression	2D, G, H, 27H
pre	prepectus	3E
psr	parascrobal region	1C
pst	parastigma of submarginal vein	2F, 19D
sc	scrobe	1C
sct	scutellum	2A, 3D
sdc	scrobal depression convexity	1C, E
ser	setal row	7H, 15H, 19D, 24C, F
smv	submarginal vein of fore wing	2F, 21I
spc	speculum of fore wing disc	3F, 7F, H, 10F, 12F, 15G, H, 17G, H
spr	spur of stigmal vein	21D, 26H
stv	stigmal vein of fore wing	2F
syf	syntergal flange	5G, I
tg	tegula	2B, 19F, 23F, 24D
TL	temple length	18C
tmp	temple	1D
tsa	transscutal articulation	3D
unc	uncus of stigmal vein	2F, 14E, 21D, 26H
upr	upper parascrobal region	1C, D
vna	vanal area of fore wing	3F, 18H, 19D
vtx	vertex	1D

Although head structures are similar between the sexes, males and females differ conspicuously in mesosomal structure. In females, the dorsal surface of the pronotum is differentiated into a horizontal, quadrate to transverse-rectangular **pronotal collar** (Fig. 2C: **pnc**) that consists mostly of a bare, concave surface subdivided mediolongitudinally by a groove and/or pale line posterior to an inclined **pronotal neck**, the two regions also being differentiated by a variably distinctly developed but broadly arcuate (∩-like) margin bearing several long, spine-like setae (*e.g.*, Fig. 16F); the lateral, vertical surface of the pronotal collar is the **pronotal panel** (Fig. 2C: **pnp**). Males lack a distinctly differentiated pronotal collar and neck, the dorsal surface of the pronotum (Fig. 3D: **no_1**) being more-or-less uniformly inclined in front of the mesonotum and extensively though variably densely setose, but with a lateral, vertical pronotal panel (Fig. 3E: **pnp**) similar to females. Posterior to the pronotal panel in males is a large triangular sclerite, the **prepectus** (Fig. 3E: **pre**), whereas in females the prepectus is differentiated into a typically dark, more-or-less subrectangular **lateral prepectal surface** (Fig. 2B: **lps**) and a ventral, pale, **frontal prepectal surface** (Fig. 2B: **fps**). The contrastingly pale colour of the frontal prepectal surface is an important generic feature for *Mesoco-*

mys, but only features of the lateral prepectal surface are important for species recognition in the genus and, for this reason and for simplicity, the lateral surface of the prepectus is termed the prepectus in the species descriptions. In both sexes the combined lateral and ventral surfaces of the mesothorax is termed the **mesopleurosternum**. In males, the lateral surface of the mesothorax is differentiated into three principal regions. A small region below the fore wing base, the **acropleuron** (Fig. 3E: **ac**), is differentiated by the **acropleural sulcus** (Fig. 3E: **acs**) from a larger, convex **mesepimeron** (Fig. 3E: **epm**) behind the acropleuron, and a concave, oblique **mesepisternum** (Fig. 3E: **eps**) below both the acropleuron and mesepimeron. Sometimes males have a variably distinctly differentiated though paler, Y-like set of lines formed by a narrow pale band extending diagonally through the mesepisternum toward the prepectus, and from near the middle of this band another narrow pale band directed obliquely on the venter of the mesopleurosternum toward the base of the procoxa medially (Fig. 3E: arrows). In females, the lateral surface of the mesothorax is composed almost entirely of a large, convex, bare acropleuron (Fig. 2B: **ac**) that is differentiated by the acropleural sulcus (Fig. 2B: **acs**) (Gibson 1986, 1995). The rest of the mesopleurosternum in females (the surface ventrally between the acropleural sulci and in lateral view anterior to the dorsally recurved part of the acropleural sulcus below the prepectus) is called the **mesopectus** (Fig. 2B: **mpc**); unlike the acropleuron, the mesopectus is sparsely setose. The sexes also differ in mesonotal structure. In males, the **mesoscutal medial lobe** (Fig. 3D: **mml**) is separated by a linear **notaulus** (Fig. 3D: **not**) from a **mesoscutal lateral lobe** (Fig. 3D: **mll**) on either side, and the two notauli converge posteriorly so as to extend to but be widely separated at the **transscutal articulation** (Fig. 3D: **tsa**), the flexible line of articulation between the **mesoscutum** and the **scutellar-axillar complex**, which is composed of the two **axillae** (Fig. 3D: **ax**) and the **scutellum** (Fig. 3D: **sct**). In males, the mesoscutal medial lobe is uniformly convex and in a similar plane as the lateral lobes, and the scutellar-axillar complex is uniformly convex with the axillae separated from the scutellum by linear sutures (*e.g.*, Fig. 3D). However, in females the mesoscutal lateral lobes (Fig. 2C: **mll**) are differentiated from the medial lobe (Fig. 2C: **mml**) by notauli (Fig. 2A: **not**) that are more-or-less parallel anteriorly but which posteriorly curve toward each other to form a U-like furrow that further differentiates the medial lobe into an anterior, convex region (Fig. 2C: **aml**) and a posterior depressed region (Fig. 2C: **pml**). Females are also somewhat peculiar in that the depressed posterior part of the medial lobe between the lateral lobes articulates with the scutellar-axillar complex at a slightly lower level than the dorsal plane of the axillae. Because of this, the anterior margins of the axillae are vertical behind the mesoscutum so that in 'uncontorted' females (see further below) there appears to be a variably distinctly concave, transverse to broadly lenticular depression (*e.g.*, Figs 2A, C: **dep**) anterior to the axillae (Fig. 2A: **ax**). This is sometimes accentuated because the comparatively thin cuticle of the depressed posterior part of the mesoscutal medial lobe, even in critical-point dried females, often upfolds or is compressed anterior to the scutellar-axillar complex, possibly because of shrinkage of the underlying dorsolongitudinal flight muscles. Dorsolongitudinally on each mesoscutal lateral lobe is a differentiated, bare, more minutely coriaceous band, the **parapsidal band** (Fig. 4G: **mpb**), which is homologous with the parapsidal line, the site of origin of the dorsoventral flight muscle (Gibson 1986). Structure of the scutellar-axillar complex in females differs between the two species groups, with *albitarsis*-group females having a similar structure (*e.g.*, Fig. 2A) to that described for males, but *pulchriceps*-group females having a deep, subtriangular depression between each axilla and scutellum (*e.g.*, Figs 18F, 20E). Metapleural structure also differs between the sexes. In males, a triangular **metapleuron** (Fig. 3E: $\mathbf{pl_3}$) separates the posterodorsal angle of the mesepimeron (Fig. 3E: **epm**) from the base of the metacoxa. In females, a small and comparatively inconspicuous metapleuron (Figs 2B, G, H, 27F, H: $\mathbf{pl_3}$) is appressed to the posterodorsal surface of the acropleuron and separates this from the propodeum, though structure of the metapleuron differs between females of the two species groups (see respective species group diagnoses). Propodeal structure also differs both between the sexes and between females of the two species groups. In males, the propodeum has a complete median carina (*e.g.*, Figs 3H, 19G, 23G) whereas in females there is either a deep, V-shaped medial **propodeal plical depression** (Figs 2D, G: **ppd**) [*albitarsis* group] or a similarly shaped but flat or almost flat propodeal plical depression (*e.g.*, Figs 2H, 27H: **ppd**) [*pulchriceps* group]. In females, the part of the propodeum lateral to the propodeal spiracle, the **callus** (Figs 2D, G, H, 27H: **cal**), also differs in setal pattern between the two species groups, being either setose laterally along its length (*e.g.*, Figs 2D, 2G) [*albitarsis* group] or only apically (*e.g.*, Figs 2H, 27H) [*pulchriceps* group].

Fore wing venation is typical for Chalcidoidea in both sexes, that is, consisting of a **submarginal vein** (Fig. 2F: **smv**) that apically is broadened into a **parastigma** (Fig. 2F: **pst**) at the base of the **marginal vein** (Fig. 2F: **mv**), plus a **stigmal vein** (Fig. 2F: **stv**) and a **postmarginal vein** (Fig. 2F: **pmv**). The stigmal vein apically sometimes curves toward the postmarginal vein for a short distance as the **uncus** (Figs 2F, 14E: **unc**) or sometimes is apically

Y-like, with both a distinct uncus extending toward the postmarginal vein (Figs 21D, 26H: **unc**) and a variably long **spur** (Figs 21D, 26H: **spr**) extending beyond the uncus. The membranous part of the fore wing is arbitrarily subdivided into three main regions, the **costal cell**, the **basal region** and the **disc**. The **costal cell** (Fig. 2F: **cc**) is the membranous region in front of the submarginal vein, whereas the **basal region** is the membranous region behind the submarginal vein. The basal region is further subdivided into three areas by longitudinal folds: a **basal cell** (Figs 2F, 3F, 19D: **bc**) behind the submarginal vein that is delimited posteriorly by the **mediocubital fold** (Figs 3F, 18H, 19D, 24B: **mcf**) and apically by the base of the parastigma or, if developed, the **basal fold** *sensu* Gibson (2004, fig. 17: bf), a **cubital area** (Figs 3F, 18H, 19D: **cua**), the longitudinal region behind the mediocubital fold basally, and a **vanal area** (Figs 3F, 18H, 19D: **vna**), the longitudinal region behind the cubital area basally. The **disc** is the wing membrane beyond the basal region. The mediocubital fold (Fig. 24B: **mcf**) extends beyond the basal region for a short distance into the disc where it bifurcates into a more anterior **medial fold** (Fig. 24B: **mdf**) and more posterior **cubital fold** (Fig. 24B: **cuf**). The fore wing disc often differs in colour pattern among the species and sometimes in setal structure in females, but is entirely setose except males of some species have behind the parastigma a variably large and distinct bare region, the **speculum** (Figs 3F, 7H, 12F, 17G: **spc**); the speculum usually is separated from the parastigma by one or more rows of setae (*e.g.*, Figs 12F, 15H) and is always closed posteriorly by setae along the mediocubital fold (*e.g.*, Fig. 3F: **mcf**).

The gaster of males (*e.g.*, Fig. 3A) is similar to most other male Chalcidoidea, but the apical gastral tergite of females, the **syntergum**, is apically reflexed into a posteriorly rounded, often paler, flange-like extension, the **syntergal flange** (*e.g.*, Figs 5G, I: **syf**; 7A, B).

Additional abbreviations used in the text or on the images to indicate structures are: **aod** = anterior ocellar diameter (maximum longitudinal diameter of anterior ocellus, *e.g.*, Fig. 1E); **asl** = apical setae of labrum (Figs 22C, 25F); **dso** = distance between the dorsal margin of the scrobal depression and the anterior ocellus (*e.g.*, Fig. 1E); **EH** = eye height (maximum height of eye measured from an angle of view with all margins in focus); **EW** = eye width (maximum width of eye measured from an angle of view with all margins in focus); $\mathbf{fl}_{\mathbf{n}}$ = flagellomere (funicular) 1–8 (*e.g.*, Fig. 5F); $\mathbf{Gt}_{\mathbf{n}}$ = gastral tergite number (*e.g.*, Figs 5G–J); **HH** = head height (maximum height of head in frontal view, Fig. 16C); **HL** = head length (maximum length of head in dorsal or lateral views, Fig. 18C); **HW** = head width (maximum width of head in dorsal or frontal views, Fig. 18C); **IOD** = interocular distance (minimum distance between inner margins of eyes, Fig. 18C); **lab** = labrum (Fig. 1F); **LOL** = lateral ocellar line (minimum distance between anterior and a posterior ocellus, Fig. 16D); **MPOD** = maximum diameter of a posterior ocellus (Fig. 16E); **MS** = malar space (minimum distance between lower eye margin and oral margin in lateral view); **OOL** = ocellocular line (minimum distance between a posterior ocellus and eye margin, Fig. 16E); **pdl** = pedicel (Figs 3G, 5C, F); **POL** = postocellar line (minimum distance between posterior ocelli, Fig. 16D); **sdc** = scrobal depression convexity (Figs 1C, E); $\mathbf{St}_{\mathbf{n}}$ = gastral sternite number; **ser** = setal row (Figs 7H, 15H, 19D, 24C, F); **tg** = tegula (*e.g.*, Figs 2B, 23F); **TL** = temple length (in dorsal view, distance between upper eye margin and posterior margin of head, Fig. 18C).

Sculpture. There are two general types of body sculpture depending on whether it is formed by raised ridges or impressed lines or grooves. Sculpture consisting of concave cells formed by raised ridges is **reticulate**. Sculpture formed by impressed lines or grooves is **coriaceous** if the surface of the cell is flat, **pustulate** if the surface of the cell is noticeably convex, and **imbricate** if one margin of a sculptural cell is higher than the others so that the sculpture appears to overlap in a shingle-like manner. If any of the above sculptural types are more-or-less uniformly multisided it is **mesh-like**, whereas if noticeably elongated in one direction it is **alutaceous**. Irregular reticulate sculpture lacking distinctly delineated cells is **rugulose** to **rugose** depending on coarseness, and sculpture formed by almost parallel lines is **striate** or, if more irregular or wavy lines, **strigose**. However, these sculptural types often intergrade, and this is indicated by hyphenating any two sculptural terms. The difference between the types of sculpture is sometimes very slight and usually best appreciated from an oblique viewing angle with good lighting to better emphasize slightly raised edges, ridges or slightly depressed surfaces of the sculpture. In order to interpret sculpture correctly, regardless of the type of light used, some type of diffusing agent such as a translucent piece of artists film (*e.g.*, Mylar) placed between the light source and specimen, as close to the specimen as possible, is necessary to minimize glare. The necessity of using a diffusing agent with a light source (*e.g.*, see Talamas *et al*. 2017, figs 1, 2), regardless of the type of light, to correctly interpret sculpture relative to the species descriptions cannot be emphasized strongly enough.

Measurements. A range in body length, in millimeters, is provided for females and males of each species, but

both air-dried and critical-point dried specimens were measured for some species, which tends to increase the range in size. Because the gastral segments can telescope, the gaster is often shrivelled in air-dried specimens and therefore is typically shorter compared to critical-point dried specimens in which the gaster is usually more inflated. As a result of this artefact of preservation, critical-point dried specimens typically appear somewhat larger than air-dried specimens. Accurate body length measurement of females is also affected by whether or not they are 'contorted' in the sense of Gibson (1986). An uncontorted female is one in which the mesonotum forms a low-convex to almost flat surface (*e.g.*, Figs 4D, H; Gibson 1995, fig. 91) and whose body in lateral view forms a more-or-less straight line (*e.g.*, Figs 4B, F), whereas a contorted female is one in which the mesonotum is ∧-like arched along the transscutal articulation and, to varying extents, the head and gaster are reflexed dorsally above the mesosoma so that the body has a U-like (*e.g.*, Gibson 1995, fig. 92) or even O-like configuration if the gastral apex touches the top of the head. Consequently, accurate body length measurement of contorted females is not possible. Contorted females often also have the mesocoxae partly or completely rotated anteriorly out of their combined fossa so that the middle legs extend straight forward or are crossed over each other under the body (*e.g.*, Gibson 1995, fig. 92). All of these structural peculiarities, which are correlated with how female eupelmines jump (Gibson 1986), can also affect the visibility of different body parts, particularly of dorsal features.

All values other than body length are given as ratios between various body parts or as ocular grid units measured at the magnifications stated below. All measurements included in the female and male descriptions of the two newly described species are of the holotype and allotype, respectively, given as ocular grid units. Measurements are also given as ocular grid units for the descriptions of females and males of previously described species if the measurements were based on singletons. For previously described species with multiple specimens that result in ranges of values, HL, HH, HW, TL, EH, EW, and MS are given as ocular grid units, all taken at a magnification where one unit = 0.133 mm from individuals that include the smallest and largest specimens. As such, the actual range in length of each feature as well as the ratio range between any two of the features can be calculated. However, OOL, POL and LOL are compared to MPOD, and IOD is compared to HW as ratios, with the features measured at the maximum magnification possible with the Nikon microscope used, where 1 unit = 0.057 mm. Ratios are also given for cc/smv, mv and pmv length compared to stv length, but these features were measured at a magnification where 1 unit = 0.133 mm. Among type material of previously described species examined for this study were the holotypes of *M. albitarsis* and *M. superansi* and the newly designated lectotype of *M. pauliani*, and the respective measurements from these females are given between square brackets in addition to the respective ratios for the species; a question mark between square brackets indicates that a feature could not be measured accurately. Measurements and ratios are rounded to the nearest 10th except for IOD:HW. Lengths of the scape, pedicel, funiculars and clava, unless stated otherwise, were measured in lateral view; length of the scape does not include the radicle. Length of the costal cell, which is the same as the length of the submarginal vein, is measured from the basal constriction that differentiates the wing membrane from the humeral plate to the base of the marginal vein (Fig. 2F: vertical lines), whereas the marginal vein is measured from the point at which the costal cell/submarginal vein/parastigma attains the leading margin of the wing to the distal angle of the junction between the postmarginal and stigmal veins (Fig. 2F: vertical lines), and the postmarginal vein is measured from the point of junction between the postmarginal and stigmal veins to the apex of postmarginal vein (Fig. 2F: vertical lines). Although these measurements appear simple, they can be difficult to determine accurately because the costal cell gradually tapers to the base of the marginal vein and it can be difficult to determine the precise point of intersection, and the postmarginal vein typically tapers apically and it can be difficult to discern its exact apical limit. Measuring the length of the stigmal vein in a consistent manner is also made difficult by the described differences in structure of this vein. Typically, length of the stigmal vein is measured from the distal angle of the junction between the postmarginal vein and stigmal vein to the apex of the stigmal vein (Fig. 2F: oblique lines). However, in instances in which the stigmal vein apically curves into an uncus (Figs 2F, 14E: unc) or extends beyond the uncus as a variably long spur (Figs 21D, 26H: spr), length of the stigmal vein was measured to the posterior margin of the uncus. This was done so as to make measurements of the vein more comparable among the different species and specimens. For *pulchriceps*-group males, length of the basitarsomere is compared to the combined length of the apical four tarsomeres of the meso- and metatarsi. Length of each is the maximum dorsal length, but excluding the pretarsus and tarsal claws from the combined length of the apical four tarsomeres (Figs 23H, I: vertical lines).

Species treatments. My concept of *M. atulyus* is based on the original description plus the photomicrographs provided by Avunjikkattu Ranjith (DZUC), whereas my concepts of all other previously described species are based

on the original descriptions plus direct examination of at least one individual of the type series of the species, though this consisted of only the gaster and parts of some legs of the only remaining specimen of *M. aegeriae* (Fig. 5J). Dr Huanxi Cao (IZCAS) provided English translations of the label data for all IZCAS specimens cited under material examined, and identified most of the specimens using a provided draft key and macrophotographs; IZCAS specimens that I also examined are indicated with an asterisk (*). The FAFU specimens cited under material examined were identified by Dr Ling-Fei Peng using the final key and plates of illustrations of the present paper.

The species are treated in alphabetical order within the *albitarsis* and *pulchriceps* species groups, respectively. The differential features by which females and males are identified to species group are given in a diagnosis prior to the species group so that the features need not be repeated in each description. Consequently, the species descriptions are not rigorously comparable between the two species groups. Label data for holotypes and allotypes are cited as given on the labels, with a vertical line (|) indicating data on separate lines of the same label and an oblique line (/) indicating separate labels. Additional information given for female primary type material, if examined, is the method of mounting, condition of the specimen with missing parts listed, and whether or not the specimen is contorted. Collection data of non-type specimens are standardized similar to Gibson & Fusu (2016), with data on different labels or different lines of the same label not differentiated and the collection date month given in Roman numerals. Collection records for specimens examined are listed alphabetically within biogeographic realm and country, and when the locality is unequivocal within state for India and province or autonomous region for China. For this reason, depending on distribution, a species recorded from China can be listed under both the Oriental and Palaearctic regions for the sections 'specimens examined' and 'distribution'. The designations of Oriental or Palaearctic for Chinese and other localities follow Noyes (2019). For multiple collection events from the same locality an m-dash (—) separates the data common to all events from data that differs between the events. Newly reported country and provincial/state records within countries given under 'distribution', and host records given under 'biology', are indicated with an asterisk (*); previously published distribution and host and records are validated with Noyes (2019) or other references. Any information given between square brackets is by me, which for Lin *et al*. (2017) records is cited from Ling-Fei Peng (personal communication).

Mesocomys Cameron

Mesocomys Cameron, 1905: 210. Type species: *Mesocomys pulchriceps* Cameron, by monotypy.

Mesocomys; Schmiedeknecht, 1909: 171 (female keyed), 173 (male keyed), 175 (treatment); Ferrière, 1951: 265 (key to species); Bouček, 1988: 543 (keyed), 553–554 (treatment); Islam & Hayat, 1985: 191 (keyed); Gibson, 1995: 85 (female keyed), 90 (male keyed), 228–231 (treatment); Narendran & Sheela, 1995: 310–311 (key to species); Yao *et al*., 2009: 155–156 (key to species); Yang *et al*., 2015: 167–168 (key to species).

Semianastatus Kalina, 1984: 18–19. Type species: *Semianastatus orientalis* Kalina, by monotypy and original designation. Synonymy by Gibson, 1995: 228, 229.

Diagnosis. FEMALE. Head with antennae inserted much closer to oral margin than middle of face (*e.g.*, Figs 1C, 16C) such that ventral margins of toruli obviously below level of lower orbit, and toruli widely separated such that distance between toruli about 3× minimum diameter of a torulus, and distance between a torulus and inner orbit subequal to minimum diameter of a torulus; scrobal depression (*e.g.*, Figs 1C, 16C) with lateral margins convergent toward anterior ocellus for at least two-thirds distance and often extending to within about one ocellar diameter of ocellus, carinately margined at least laterally so face with comparatively slender, abruptly delineated, subequally wide parascrobal region (Fig. 1C: psr) along most of height of eye, and with comparatively deep scrobes (Fig. 1C: sc) separated by a large, triangular, low-convex interantennal prominence (Fig. 1C: iap). Eye superficially bare, only exceedingly sparsely microsetose. Mandibles bidentate, with truncate dorsoapical margin and small, acute, ventroapical tooth (*e.g.*, Fig. 22C). Pronotum with pronotal collar (Fig. 2C: pnc) divided by paler line of weakness (*e.g.*, Figs 11E, 16F) and mostly variably conspicuously concave and bare except for more-or-less broadly ∩-like row of long, spine-like setae along lateral and anterior margins (*e.g.*, Fig. 16F). Prepectus with frontal surface (Fig. 2B: fps) yellowish, contrasting with darker, bare, subrectangular lateral surface (Fig. 2B: lps), and lateral surface much larger than tegula (Fig. 2B: tg). Mesoscutum with notauli (Fig. 2A: not) extending about two-thirds length, broadly U-like so as to separate mesoscutal lateral lobes (Fig. 2C: mll) from mesoscutal medial lobe (Fig. 2C: mml) and differentiate medial lobe into anterior convex region (Fig. 2C: aml) and posterior depressed region (Fig. 2C:

pml). Mesosoma with *either* scutellar-axillar complex having deep, subtriangular, paramedial depression between each axilla and scutellum (*e.g.*, Figs 18F, 20E) *or* propodeum with deeply concave, V-shaped medial plical depression (*e.g.*, Figs 2D, G: ppd). Acropleuron (Fig. 2B: ac) broadly rounded posteriorly with acropleural sulcus (Fig. 2B: acs) curved around anterolateral margin of mesocoxa slightly onto ventral surface of mesopleurosternum. Mesotibia without apical groove or apical pegs (Figs 1G, I); mesotarsus with single row of dark pegs along either side of basal two or three tarsomeres (Figs 1G, I). Fore wing disc without oblique bare band (linea calva); hyaline or variably infuscate, sometimes with hyaline cross-band (*e.g.*, Figs 2F, 11G) or anterior and posterior hyaline regions (*e.g.*, Fig. 18H) with white setae behind marginal vein. Metapleuron bare, but different in structure depending on species group (*cf.* Figs 2G & H: pl_3) (see respective species group diagnoses). Propodeum with large V- to U-shaped medial plical depression, but plical depression different in structure (*cf.* Figs 2G & H: ppd) and associated with different setal pattern of callus in the two species groups (*cf.* Figs 2G & 27H: cal) (see respective species group diagnoses). Gaster sometimes with variably distinct subbasal pale band in dorsal (*e.g.*, Fig. 1A) and/or lateral (*e.g.*, Figs 1B, 18B) views because Gt_1 dorsoapically or Gt_2 in part transversely, variably paler to white, though often Gt_1 apically and Gt_2 almost or completely hyaline so colour of cuticle below shows through and they appear dark (hyaline nature of Gt_1 and Gt_2 often obvious only if sclerites raised slightly above the others); syntergum with syntergal flange (Figs 5G, I: syf; 7A, B).

MALE. Head with insertion of antennae and structures of scrobal depression, interantennal prominence and mandibles similar to female (*cf.* Figs 1C & 3C). Antenna with pedicel variably conspicuously elongate-triangular, ventrally with row of several setae along length (*e.g.*, Figs 3G, 7G); flagellum robust-filiform (funiculars and clava subequal in width, *e.g.*, Figs 3G, 17F) to clavate (funiculars obviously widened to clava, *e.g.*, Fig. 23E), and clava with micropilose sensory region along length (*e.g.*, Fig. 26G: msr). Mesosoma and legs not atypically modified for subfamily except basitarsomere of hind and middle legs sometimes distinctively long relative to remaining tarsomeres, sometimes noticeably longer than combined length of apical four tarsomeres (Figs 23H, I). Fore wing colour pattern often similar to conspecific female (*cf.* Figs 5A & 7F, 9I & 10F, 21D & 24B); disc without (*e.g.*, Figs 24B–G) or with variably large and distinct speculum (*e.g.*, Figs 3F, 7H, 12F, 15H: spc), but if evident then speculum closed posteriorly by setae along mediocubital fold (*e.g.*, Fig. 3F: mcf). Mesepimeron (Fig. 3E: epm) not subdivided into upper and lower mesepimeron by pit or line. Metapleuron (Fig. 3E: pl_3) bare.

Recognition. Gibson (1995) provided a comprehensive description of both sexes as well as keys to differentiate individuals from other eupelmine genera, but the features given above are sufficient to recognize both sexes of *Mesocomys* from other eupelmine genera. Structure of the scutellar-axillar complex in combination with the propodeum alone is sufficient to recognize *Mesocomys* females, as is the combination of head structure and pedicel structure and setal pattern for males. However, since the generic key of Gibson (1995), the males of some species of genera other than *Eupelmus* Dalman and *Xenanastatus* Bouček have been shown to possess a broad fore wing speculum extending between the parastigma and mediocubital fold, including the males of *M. albitarsis* (Fig. 3F: spc) and *M. obscurus* (Fig. 12F: spc).

Relationships. Putative relationships of *Mesocomys* with other eupelmine genera remain unresolved because of a unique combination of features possessed by females. Gibson (1995) hypothesized that *Mesocomys* belonged to a basal group of Eupelminae whose females share three symplesiomorphic features: absence of a mesotibial apical groove (Figs 1G, I; Gibson 1995, character 34, state 1), absence of mesotibial apical pegs (Figs 1G, I; Gibson 1995, character 35, state 1) and a mesotrochantinal plate with two separate articulatory lobes (Gibson 1995, fig. 93; character 22, state 1). Females also have a light coloured, digitiform frontal prepectal surface (Fig. 2B: fps; Gibson 1995, character 19, state 2) and a sinuate acropleural sulcus (Fig. 2B: acs; Gibson 1995, character 21, state 2). These shared features support *Mesocomys* as most closely related to, or some part of, *Australoodera* Girault + *Tineobius* Ashmead + *Ecnomocephala* Gibson + *Eupelmus*. Gibson (1995) noted four similarities shared between *Mesocomys* females and those of the subgenus *E.* (*Eupelmus*), but all were hypothesized as likely convergences because of the presumption of monophyly for *Eupelmus*. Males of *M. albitarsis* (Fig. 3F: spc) and *M. obscurus* (Fig. 12F: spc) are now known to possess a similarly large fore wing speculum as most *Eupelmus* males, which represents another feature that is either convergent in the two genera or possibly a groundplan feature of both that was subsequently reduced (*e.g.*, Fig. 15H) or lost in other species of *Mesocomys*. The currently ambiguous relationships of *Mesocomys* also result in part because females possess bidentate mandibles consisting of a broad dorsoapical margin and a small ventroapical angulation (*e.g.*, Fig. 22C; Gibson 1995, character 1, state 2a), have a flanged syntergum (*e.g.*, Figs 5G, I: syf; Gibson 1995, character 39, state 3), often a subbasally white-banded gaster (*e.g.*, Figs 1A, B; Gibson

1995, character 42, state 2a), and fore wings that sometimes have a hyaline cross-band or anterior and posterior regions with white setae behind the marginal vein (*e.g.*, Figs 11G, 18H; Gibson 1995, character 31, states 5b, 5c). In these latter four features females more closely resemble typical females of *Anastatus*, and thus Kalina's (1984) generic name *Semianastatus* was quite appropriate. As discussed below, *Anastatus* is another genus whose members are mainly endoparasitoids of eggs of various insects and Gibson (2016) suggested that bidentate mandibles may be prone to evolve in eupelmines that are egg parasitoids; if so, mandibular structure is not a reliable indicator of phylogenetic relationships. Further, fore wing colour patterns similar to those of typical *Anastatus* females, and a subbasally white gaster, also seem to be prone to evolve in conjunction, possibly as an adaptation to avoid predation (Fusu & Polaszek 2017; Gibson 2017a). No functional advantage for the evolution of a flanged syntergum has yet been proposed and the evolutionary significance of this feature remains unknown. Though the resemblance of *Mesocomys* and *Anastatus* females likely is entirely the result of convergence, the similarities do explain why *M. albitarsis*, *M. menzeli*, *M. obscurus* and *M. vuilleti* were all described originally in *Anastatus*.

Gibson (1995) differentiated two species groups within *Mesocomys*, the *albitarsis* and *pulchriceps* groups. As discussed under the two species groups below, monophyly of the *pulchriceps* group is supported minimally by the autapomorphic scutellar-axillar structure of females (*e.g.*, Figs 18F, 25G) and possibly also by common possession by both sexes of similar fore wing colour patterns with anterior and posterior hyaline regions (*cf.* Figs 21D & 24B). The monophyly of the *albitarsis* group is less well-supported, possibly by the distinctively deeply concave, V-shaped medial plical depression of the propodeum of females (Figs 2D, G: ppd), though females of the *pulchriceps* group have a similarly shaped though almost flat plical region (Figs 2H, 27H: ppd). The latter plical structure of *pulchriceps*-group females is also associated with a propodeal callus that is setose only posterolaterally (Figs 2H, 27H: cal) rather than along its length (Figs 2D, G: cal), and a metapleuron that is right-angled bent into a vertical band along the callus and a horizontal band over the posterodorsal surface of the acropleuron (Figs 2H, 27H: pl_3) rather than in a single plane flat over the acropleuron (Fig. 2G: pl_3) as in *albitarsis*-group females. The conspicuous difference in structure of the metapleuron within two lineages of a single genus is interesting because the metapleuron was postulated by Gibson (1995) to form an integral part of the skeletomusculature of females related to jumping—its association with the posterior margin of the acropleuron acting as the lock mechanism to enable stretching the resilin pad by the acropleural muscles when the mesoscutum is arched prior to release of the stored energy to produce a jump. However, based on similar structures in such putatively closely related genera as *Australoodera*, *Eupelmus* and *Tineobius*, a more extensively setose callus and a flat metapleuron likely are symplesiomorphic groundplan features of *Mesocomys*. If so, the associated deeply concave plical depression (Figs 2D, G) of *albitarsis*-group females may also be a groundplan feature and the almost flat plical depression of *pulchriceps*-group females (Figs 2H, 27H: ppd) secondarily derived within *Mesocomys* and yet another synapomorphy supporting monophyly of the group. Because only the *pulchriceps* group is reliably supported as a monophyletic lineage, which could render the *albitarsis* group paraphyletic, I retain both as species groups within *Mesocomys* rather than treating the two as subgenera. However, this means that two morphologically different groups of species within the *albitarsis* group have to be treated as subgroups within the species group, as discussed under the *albitarsis* group.

Distribution. *Mesocomys* is restricted to the Afrotropical, Oriental and Palaearctic regions. Species of the *pulchriceps* group are restricted to the Afrotropical region other than for *M. orientalis*, which is known only from the Oriental region, whereas species of the *albitarsis* group are restricted to the Oriental and eastern Palaearctic regions except for a single known female from the western Palaearctic region in northern Africa (Algeria).

Biology. The biologies of two species of *Mesocomys* have been studied in detail, *M. albitarsis* (*e.g.*, Clausen 1927; Hirose 1969; Peng *et. al*. 1984; Tong & Ni 1989; Fang & Hu 1993; Chen *et al*. in press) and *M. pulchriceps* (*e.g.*, Berg 1970, 1971a, 1971b, 1972; Webb 1961). The immature stages of *M. albitarsis* were described and illustrated by Clausen (1927), and those of *M. pulchriceps* by Berg (1970). All but two publications citing host records and/or biology of *Mesocomys* support species as being exclusively endoparasitoids of Lepidoptera eggs. Label data of specimens examined for this study indicate species can minimally parasitize eggs of the families Bombycidae, Erebidae, Eupterotidae, Hesperiidae, Lasiocampidae, Lymantriidae, Notodontidae, Nymphalidae, Papilionidae, and Saturniidae. Hosts are recorded for all 11 herein recognized species of *Mesocomys* except for *M. longiscapus*, and Lasiocampidae is a recorded host family for all but *M. pauliani*, whereas Saturniidae is a host family for all but *M. breviscapis*, *M. superansi* and *M. orientalis*. The families Bombycidae, Eupterotidae, Hesperiidae, Nymphalidae and Papilionidae are recorded only for *M. pulchriceps*, Notodontidae only for *M. albitarsis*, and Erebidae only for *M. orientalis*.

One highly anomalous non-Lepidopteran host record for the genus is *Chrysomya chloropyga* (Wiedemann) (Diptera: Calliphoridae) for *M. pulchriceps*, which Ferrière (1930a) attributed to Cameron (1905). Ferrière stated "Cameron gives as host [of *M. pulchriceps*] the larva of a Calliphorid fly, *Chrysomyia* [*sic*] *chloropyga*, but his information was probably erroneous, as all specimens found later have been bred from Lepidopterous eggs" (Ferrière 1930a, p. 35). However, the original description of *M. pulchriceps* by Cameron (1905) mentions nothing of a host, nor does the label data of the remaining type specimens (see species treatment). Berg (1970, p. 127) also stated that Cameron (1905) "gave" *C. chloropyga* as a host, and like Ferrière (1930a) he questioned the validity of that host, but based on his statements he was just quoting Ferrière (1930a), as was Gibson (1995). As such, why Ferrière (1930a) stated *C. chloropyga* was a host of *M. pulchriceps* and why he attributed this host record to Cameron (1905) are mysteries. The only other published non-lepidopteran host is by van Noort *et al*. (2007), who recorded two unidentified morphospecies of *Mesocomys* as parasitoids in the galls of *Scyrotis* Meyrick (Lepidoptera: Cecidosidae) on *Searsia* [= *Rhus*] *lucida* (L.) (Anacardiaceae) attacked by the lethal inquiline *Rhoophilus loewi* Mayr (Hymenoptera: Cynipidae), which modifies the primary *Scyrotis* gall. *Mesocomys* species B was recorded as a parasitoid in *Scyrotis* galls and *Mesocomys* species A as a larval parasitoid in *Rhoophilus* galls (van Noort *et al*. 2007, table 5). However, images (available on www.waspweb.org) provided by Simon van Noort (SAMC) of a contorted, brachypterous female voucher specimen (SAM-HYM-P088419 deposited in SAMC, collecting event number KB02-R16) from van Noort *et al.* (2007), which was reared from a *Scyrotis* gall, proved to be of a female *Anastatus*. There should be an additional two reared specimens from the study in SAMC, which although not located are undoubtedly also *Anastatus* females and reared either as a primary parasitoid or hyperparasitoid of *Scyrotis* larvae/pupae in galls formed on *S. lucida* or of the larvae/pupae of *R. loewi* (S. van Noort, personal communication).

Anastatus is another, though much more speciose genus whose members are mostly endoparasitoids of eggs of various insects (Bouček 1988; Gibson 1995; Noyes 2019). However, a few have been described from immature stages other than the egg, including *A. longipalpus* Risbec (1951b) from a larva of *Peizotrachelus varium* (Wagner) (Coleoptera: Curculionidae), *A. bostrychidi* Risbec (1951b) as possibly from the larva of *Simoxylum ceratoniae* (L.) (Coleoptera: Bostrichidae), *A. osmyli* (Girault 1927) from a cocoon of *Porismus* [= *Osmylus*] *strigatus* (Burmeister) (Neuroptera: Osmylidae), *A. leithi* (Walker 1872) from "blister galls" on leaves of *Duranta* L. (Verbenaceae) (Bouček 1979) and, according to Burks (1967), *A. drassi* (Riley *in* Howard 1892) from a cocoon of an unidentified species of Dryinidae (Hymenoptera) rather than from a spider nest as originally stated by Riley. Boldt & White (1992) also reported an unidentified species of *Anastatus* as reared from the larvae of *Exema elliptica* Karren (Coleoptera: Chrysomelidae). Other *Anastatus* have been reared and described from Diptera puparia, including *A. urichi* (Waterston *in* Urich *et al*. 1922) from a puparium of *Cyclopodia greeffi* Karsch (Nycterbiidae), *A. viridiceps* Waterston (1915) as a pupal parasitoid of the tsetse flies *Glossina morsitans* Westwood and *G. austeni* Newstead (Diptera: Glossinidae) (Noyes 2019), *A. dipterae* Risbec (1955) from an unidentified though presumably dipteran puparium, *A. pipunculi* Perkins (1906) from a puparium of *Eudorylus* [= *Pipunculus*] *cinerascens* (Perkins) (Pipunculidae), and both *A. catamarencensis* (Brèthes 1922) and *A. sirphidi* Risbec (1951a) from the puparia of unidentified species of Syrphidae. Some species have also been shown to develop both as primary endoparasitoids of eggs and as hyperparasitoids because they have been reared from the cocoons of Braconidae (Hymenoptera: Ichneumonoidea). Risbec (1951a) originally described *A. apantelesi* from an *Apanteles* Förster cocoon, but stated that he had also obtained a specimen of the species from an egg of *Charaxes epijasius* Reiche (Lepidoptera: Nymphalidae), which led Prinsloo (1980) to suggest *A. apantelesi* could develop both as a primary egg endoparasitoid and as a hyperparasitoid through Braconidae. *Anastatus amarus* Subba Rao (1957) was also described originally as a hyperparasitoid, as a parasitoid of *Apanteles delhiensis* Muesebeck & Subba Rao parasitic on *Spoladea* [= *Hymenia*] *recurvalis* (Fabricius) (Lepidoptera: Pyralidae). Further, *A. bifasciatus* (Geoffroy *in* Fourcroy 1875) has been reported as reared from a cocoon of *Cinara schimitscheki* Börner (Hemiptera: Aphididae) through *Pauesia pini* (Haliday) (Viggiani & Tremblay 1978), and from the Gypsy moth, *Lymantria dispar* (L.), through *Cotesia* [= *Apanteles*] *melanoscela* (Ratzeburg) and *Meteorus versicolor* (Wesmael) (Vasic & Minic 1979). Three other species also recorded as hyperparasitoids of the Gypsy moth are *A. japonicus* Ashmead (1904) through *Rhogas dendrolimi* (Matsumura) (Tong 1987) and *C. melanoscela* (Schedl 1936; Weseloh *et al*. 1979), *A. kashmirensis* Mathur (1956) through *C. melanoscela* and *Aleiodes* [= *Rhogas*] *indiscretus* (Reardon) (Weseloh *et al*. 1979), and *A. pearsalli* through *C. melanoscela* (Muesebeck & Dohanian 1927). Gibson (1995), among others (*e.g.*, Wheeler & Miller 1990), also reported *Anastatus* as a hyperparasitoid through Scelionidae (Hymenoptera: Platygastroidea), which are also egg parasitoids, but such examples likely reflect multiparasitism of egg masses and egg competition (*e.g.*, Ni *et al*. 1994) rather than hyper-

parasitism. Regardless, some species of *Anastatus* are known to be facultative hyperparasitoids as well as primary egg endoparasitoids and it is possible that species of *Mesocomys* might also sometimes develop as facultative hyperparasitoids. For example, *R. dendrolimi* is a primary pupal parasitoid of *Dendrolimus* species, including *D. superans* (He & Chen 1990), the eggs of which are the recorded host stage for *M. superansi*. Consequently, the anomalous host-stage record of a pupa of *D. superans* reported herein for *M. superansi* might be correct if the specimen actually developed as a hyperparasitoid through *R. dendrolimi*. Additionally, two mounts of *M. pulchriceps* from Angola have handwritten labels with what appears to be "pu. *Papilio demodocus*" Esper (Papilionidae), and the "pu." might be an abbreviation for pupa. Further, specimens examined for this study include some of *M. orientalis* reared from eggs of the litchi stink bug, *Tessaratoma papillosa* (Drury) (Hemiptera: Tessaratomidae), and four females of *M. pulchriceps* from Nigeria labelled as reared from a mantid (Mantodea) egg mass.

Regardless of whether *Mesocomys* can rarely parasitize hosts other than Lepidoptera and/or host stages other than the egg, species are mostly economically beneficial because they are mainly parasitoids of defoliating pest Lepidoptera, though sometimes they can be considered as pests when they parasitize eggs of wild silk moths, thereby reducing potential population levels and thus the economic value of what might have been derived from silk production (Kioko 1998; Koidzumi & Shibata 1940; Veldtman *et al.* 2004).

Key to species of *Mesocomys* Cameron

1 Female. . . . 2
- Male. . . . 12

2(1) Scutellar-axillar complex with scutellum (Fig. 2A: sct) and axillae (Fig. 2A: ax) similarly convex and separated by linear sutures; fore wing hyaline (Figs 5A, 13A, 14E, 16H) to variably brownish-infuscate (Figs 2F, 9I, 11G) but without separated anterior and posterior hyaline regions with white setae behind marginal vein; propodeum with deeply concave, V-shaped medial plical depression (Figs 2D, G: ppd), and callus (Figs 2D, G: cal) setose laterally along most or entire length . . . . 3 (*albitarsis* group)
- Scutellar-axillar complex anteriorly with paramedial triangular depressions between scutellum and axillae (*e.g.*, Figs 18F, 26E); fore wing disc brownish-infuscate from level of base of parastigma to near apex of postmarginal vein except for separated anterior and posterior hyaline region with white setae behind marginal vein (*e.g.*, Figs 18H, 26H); propodeum with relatively flat U- to V-shaped medial plical depression (Figs 2H, 27H: ppd), and callus (Figs 2H, 27H: cal) setose only posterolaterally . . . . 8 (*pulchriceps* group)

3(2) Mesoscutal medial lobe with anterior convex region isodiametric mesh-like coriaceous posteriorly, and posterior depressed region very finely mesh-like coriaceous to variably extensively smooth and shiny (Figs 2C, 9H, 11E); fore wing disc at least distinctly brownish-infuscate behind stigmal and postmarginal veins (Figs 2F, 9I) and sometimes also behind parastigma and base of marginal vein (Fig. 11G) or appearing bifasciate because setae in hyaline region behind marginal vein white compared to darker setae basally and apically (Fig. 2F); antenna sometimes with at least apical third of scape, and pedicel and flagellum more-or-less extensively and conspicuously paler than scape basally and clava (Figs 9C–E) . . . . 4 (*albitarsis* subgroup)
- Mesoscutal medial lobe with anterior convex region mostly transversely reticulate-strigose to reticulate-rugose posteriorly, and posterior depressed region reticulate to finely reticulate-rugose (Figs 4C, G, 6F, 13E, 16F); fore wing hyaline (Figs 5A, 6G, 13A, 16H) or if very faintly infuscate behind stigmal vein then flagellum entirely dark . . . . 6 (*aegeriae* subgroup)

4(3) Antenna at least with about apical third or more of scape, and usually pedicel and funicle variably extensively, obviously paler than scape basally and clava (Figs 9C–E); fore wing disc hyaline or brownish-infuscate only behind stigmal and postmarginal veins, and setae basal to infuscate region uniformly brownish to pale (Fig. 9I) . . . . ***Mesocomys menzeli* Ferrière**
- Antenna entirely dark or at most extreme apical margin of scape pale (Figs 2E, 11H); fore wing disc sometimes variably distinctly bifasciate, with brownish region behind parastigma and base of marginal vein and behind stigmal and postmarginal veins (Fig. 11G) or, if with evident brownish-infuscate region only behind stigmal and postmarginal veins, then hyaline region basal to infuscate region with white setae compared to darker setae behind parastigma and base of marginal vein (Fig. 2F) 5

5(4) Mesotarsus (Fig. 1G) and metatarsus (Fig. 1H) pale or at most slightly brownish in part; fore wing variably distinctly unifasciate to bifasciate, but at least infuscation behind parastigma and base of marginal vein obviously paler than infuscation behind stigmal and postmarginal veins, and setae behind marginal vein white and inconspicuous compared to darker setae more basally and apically (Fig. 2F) . . . . ***Mesocomys albitarsis* (Ashmead)**
- Mesotarsus (Fig. 1I) and metatarsus (Fig. 1J) variably dark brownish-infuscate; fore wing more-or-less similarly brownish-infuscate behind parastigma and base of marginal vein and behind stigmal and postmarginal veins, and setae within hyaline region behind marginal vein brownish or at least conspicuous and not distinctly white (Fig. 11G) . . . . ***Mesocomys obscurus* Ferrière**

6(3) Gaster in dorsal view with Gt_1 similarly dark as remaining tergites (Figs 13F, H), though in lateral view pale subbasally (Figs 13B, D); scape entirely dark or at most with only extreme dorsoapical margin distinctly paler beyond level of apical-most setae (Figs 14D, F); legs with both pro- and metafemur extensively brownish-infuscate to dark (Fig. 13D); basal cell entirely, uniformly, setose (Figs 8G, H) . . . . . ***Mesocomys superansi* Yao, Yang & Zhao**

- Gaster in dorsal view usually with about apical half of Gt_1 distinctly paler than remaining tergites and in lateral view pale subbasally (*e.g.*, Figs 16A, B), though appearance variable depending on condition of specimen (*e.g.*, Figs 5G–I); scape with outer and inner surfaces more extensively pale apically, including part of setose region (Figs 5B, C, 16G); legs sometimes with all femora similarly pale as tibiae and tarsi; basal cell sometimes setose only basally and apically and variably extensively bare mesally (Figs 8D–F) 7

7(6) Legs sometimes entirely pale beyond coxae or if metafemur (Fig. 16B) and profemur variably extensively dark then at least anterior surface of profemur extensively pale longitudinally and/or body longer than 3 mm . . . . . ***Mesocomys trabalae* Yao, Yang & Zhao**

- Legs with both pro- and metafemora similarly infuscate over all surfaces except apically and basally, and body at most 3 mm in length (Figs 4A, B, E, F) . . . . . ***Mesocomys breviscapis* Yao, Yang & Zhao**

8(2) Fore wing brownish-infuscate behind most of submarginal vein, including medially along mediocubital fold (Fig. 18H: mcf) into disc, except for hyaline region anteroapically near base of parastigma (Figs 18H, 20H), and with marginal vein at least 2.5× length of stigmal vein (Figs 18H, 20H); clypeus broadly, shallowly emarginate (Fig. 18D) 9

- Fore wing usually brownish-infuscate basally for distance at most about equal to apical hyaline region or if infuscation extending more extensively posteriorly along mediocubital fold then separated from infuscation of disc (Figs 21D, I, 25H, 26H) and/or marginal vein obviously less than 2.5× length of stigmal vein (*e.g.*, Figs 21D, 26H); clypeus deeply and narrowly emarginate, more-or-less bidentate (*e.g.*, Figs 22C, 25E, F, 26F: arrow) 10

9(8) Scape only about 4× as long as greatest width (Fig. 18G); flagellum with fl_1–fl_8 transverse or at most basal funiculars subquadrate such that clava about as long as apical 5 funiculars (Fig. 18G) . . . . . ***Mesocomys anelliformis* Gibson n. sp.**

- Scape about 6× as long as greatest width, elongate-tubular (Fig. 20G); flagellum with at least fl_2–fl_5 obviously longer than wide and most other funiculars subquadrate such that clava only about as long as apical 3 funiculars (Fig. 20G) . . . . . ***Mesocomys longiscapus* Gibson n. sp.**

10(8) Fore wing (Figs 25B, H) with marginal vein comparatively long, at least about 3× length of stigmal vein, and disc with distinct hyaline region along parastigma and marginal vein basally; upper parascrobal region and frons smooth, mesh-like coriaceous to alutaceous, but surface of all sculptural cells flat (Fig. 25D); currently known only from Madagascar . . . . . ***Mesocomys pauliani* Ferrière**

- Fore wing (Figs 21D, I, 26H) with marginal vein comparatively short, at most 2.5× length of stigmal vein, and disc usually without distinct hyaline region along parastigma and marginal vein; specimen either Oriental in distribution or with upper parascrobal region and frons variably extensively and conspicuously roughened, at least partly mesh-like reticulate (Fig. 26D) 11

11(10) Frons and upper parascrobal region smooth, uniformly coriaceous to coriaceous-imbricate, the mostly isodiametric mesh-like sculpture defined by engraved lines with surface of sculptural cells flat (Figs 22D, E) [Oriental] . . . . . ***Mesocomys orientalis* Ferrière**

- Frons and upper parascrobal region usually distinctly roughened, at least in part, most commonly mesh-like reticulate to reticulate-strigose, the sculpture irregular and formed by raised ridges such that sculptural cells concave (Fig. 26D), though sometimes similar to condition described above (frons coriaceous-reticulate to transversely coriaceous-imbricate and upper parascrobal region imbricate or if almost mesh-like coriaceous then with some cells slightly depressed medially) [Afrotropical] . . . . . ***Mesocomys pulchriceps* Cameron**

12(1) Fore wing hyaline (Figs 3F, 7F) or brownish-infuscate only behind stigmal vein (Figs 10F, 12F, 17G) and metatarsus entirely pale or at least uniformly coloured (Figs 3B, 7D, 10B, 17B) . . . . . 13 (*albitarsis* group)

- Fore wing distinctly brownish-infuscate behind parastigma and behind stigmal vein so as to differentiate hyaline region or separated anterior and posterior hyaline regions behind marginal vein (Figs 19A, 24B, F) and/or metatarsus bicoloured with basitarsomere and apical one or two tarsomeres obviously darker than usually much paler medial tarsomeres (Figs 19A, 23H, I: upper) . . . . . 19 (*pulchriceps* group)

13(12) Antenna with scape and pedicel yellow in contrast to brown flagellum (Figs 10C, D) . . . . . ***Mesocomys menzeli* Ferrière**

- Antenna entirely dark (Figs 3G, 7G, 12E) or at most scape yellow apically (Fig. 17F) 14

14(13) Fore wing disc with large, quadrangular speculum extending between parastigma and mediocubital fold (Figs 3F, 12F); pedicel only about as long as combined length of basal two funiculars (Figs 3G, 12E); legs often with all femora extensively and similarly dark (Figs 3B, 12B) 15

- Fore wing disc usually with small, subcircular to transverse speculum (Figs 15H, 17G), but even if higher than wide then separated from parastigma by at least one row of setae (Fig. 7F); pedicel distinctly longer than combined length of basal two

funiculars, usually almost as long as combined length of basal three funiculars (Figs 7G, 15F, 17F); legs often with at least mesofemur pale (Figs 7D, 17B) 16

15(14) Fore wing disc uniformly hyaline or almost so, at most with only very faint and inconspicuous infuscation behind stigmal vein (Fig. 3F) . . . . . ***Mesocomys albitarsis* (Ashmead)**
- Fore wing disc with distinct brownish infuscation behind stigmal vein (Fig. 12F) . . . . . ***Mesocomys obscurus* Ferrière**

16(14) Legs beyond coxae more-or-less uniformly yellowish (Figs 17A, B) . . . . . ***Mesocomys trabalae* Yao, Yang & Zhao** [part]
- Legs with at least metafemur extensively brownish-infuscate to dark (Fig. 7D). 17

17(16) Front leg with posterior surface of profemur partly brownish-infuscate (Fig. 15B) and mesofemur extensively, distinctly brownish-infuscate to dark, noticeably darker than respective tibia (Figs 15A, B) . . . . . ***Mesocomys superansi* Yao, Yang & Zhao**
- Front and middle legs uniformly pale beyond coxae (Figs 7D, 17B) 18

18(17) Fore wing without dorsal setae in costal cell basal to row of setae in front of parastigma or with at most 3 quite inconspicuous setae, but not on both wings (Figs 7F, H); speculum conspicuous, distinctly higher than wide (Figs 7F, H) . . . . . ***Mesocomys breviscapis* Yao, Yang & Zhao**
- Fore wing with at least 4 distinct dorsal setae forming row within cell basal to setae in front of parastigma (Fig. 17H); speculum comparatively small and subcircular to transversely oval (Figs 17G, H) . . . . . ***Mesocomys trabalae* Yao, Yang & Zhao** [part]

19(12) Fore wing basal cell at least setose along entire length of mediocubital fold, though variably extensively setose within cell (Fig. 19D); cubital cell dorsally with row of setae closely paralleling leading margin over about apical half (Fig. 19D: ser); clypeus shallowly emarginate medially (*cf.* Fig. 18D) . . . . . ***Mesocomys anelliformis* Gibson n. sp.**
- Fore wing mostly bare behind submarginal vein to or near level of parastigma (Figs 24B, F), at most with a few setae basally along mediocubital fold; cubital cell dorsally with row of setae apically, but setae directed obliquely to within cell basally rather than closely paralleling leading margin (Figs 24C, F: ser) (less obvious for smaller individuals); clypeus deeply emarginate medially so as to almost appear bilobed (*cf.* Figs 25E & 26F: arrow) 19

20(19) Fore wing hyaline region behind marginal vein with mostly inconspicuous white setae, the setae not distinct from hyaline membrane (Figs 24B, C); head with upper parascrobal region and frons lateral to anterior ocellus uniformly mesh-like coriaceous to coriaceous-imbricate, but surface of all sculptural cells flat (Fig. 24A) [Oriental] . . . . . ***Mesocomys orientalis* Ferrière**
- Fore wing hyaline region behind marginal vein with dark setae or mostly dark setae distinct from hyaline membrane (Figs 24F, G); head with at least frons lateral to anterior ocellus and often upper parascrobal region mesh-like reticulate to punctate-reticulate, with the surface of some sculptural cells depressed (Fig. 24E) [Afrotropical] . . . . . ***Mesocomys pulchriceps* Cameron**

Taxonomy

albitarsis species group

Diagnosis. FEMALE. Head with scrobal depression separated from anterior ocellus by distance (Figs 1E, 6D: dso) at most equal to longitudinal diameter of ocellus (Figs 1E, 6D: aod); scrobal depression dorsally with lateral margin slightly, sinuately incurved (*e.g.*, Fig. 11F: arrows) rather than uniformly ∩-like, and with differentiated convexity dorsally (Figs 1C, E: sdc); clypeus broadly, shallowly emarginate (Fig. 1F: cly). Head, other than for bare scrobes (Fig. 1C: sc), more-or-less uniformly setose with hair-like setae, including along oral margin (*e.g.*, Figs 1C, F). Scutellar-axillar complex with linear sutures separating similarly low-convex axillae (Fig. 2A: ax) and scutellum (Fig. 2A: sct). Middle leg with tibial spur and tarsomeres (excluding pegs) similarly coloured, pale (*e.g.*, Fig. 1G) to dark brown (*e.g.*, Fig. 1I). Fore wing hyaline (Figs 5A, 6G, 14E, 16H) to variably distinctly brownish-infuscate, sometimes bifasciate with hyaline band with white setae behind marginal vein (Figs 2F, 9I, 11G), but without separated anterior and posterior hyaline regions, and with all setae hair-like; costal cell hyaline except usually light yellowish-infuscate dorsoapically, with hair-like setae in front of parastigma, and ventrally with setae along entire length, one to two rows medially but more numerous apically in front of parastigma; marginal vein about 3× length of stigmal vein. Metapleuron (Fig. 2G: pl_3) more-or-less semicircular or tapered ventrally, but flat and on same plane as lateral propodeal surface over incised posterodorsal surface of acropleuron. Propodeum medially with deeply concave, V-shaped plical depression (Figs 2D, G: ppd), and with callus (Figs 2D, G: cal) setose laterally along most or all of length. Gaster in dorsal view with or without subbasal pale to white band, but at least Gt_2 dark brown and similarly sclerotized and sculptured as subsequent tergites.

MALE. Head with scrobal depression separated from anterior ocellus by distance similar to longitudinal diameter of anterior ocellus (*e.g.*, Figs 7C, 15C); clypeus broadly, shallowly emarginate similar to female. Middle

leg with tibial spur and tarsomeres similarly pale; middle and hind legs with basitarsomeres not distinctively long, at least slightly shorter than combined length of respective apical four tarsomeres; mesotarsus and metatarsus uniformly pale or at most apical tarsomeres somewhat darker (Figs 3B, 7D, 10B). Fore wing hyaline (Figs 3F, 7F) or at most with brownish-infuscate region behind stigmal vein (Figs 10F, 12F, 17G); costal cell setation similar to female except also with row of setae (Figs 7H, 15H: ser) closely paralleling leading margin apically and often with additional off-set setae paralleling leading margin basal to setae in front of parastigma; basal cell partly to sometimes completely setose (Figs 7H, 12F, 15H, 17G, H), at least with setae along mediocubital fold both basally and apically and with some setae within cell apically; disc virtually without (Fig. 10F) or with variably large and distinct speculum (Figs 3F, 7H, 12F, 15H, 17G, H: spc).

Remarks. Although head structure is similar between the sexes for *albitarsis*-group species, males have a somewhat more broadly and uniformly ∩-like scrobal depression (*cf.* Figs 1C & 3C) that lacks the developed dorsal convexity of females (Figs 1C, E: sdc). Both sexes have the scrobal depression separated from the anterior ocellus by a distance similar to the longitudinal diameter of the anterior ocellus, but so do *pulchriceps*-group males (*e.g.*, Figs 23C, 24A, E), suggesting that the greater separation between the scrobal depression and anterior ocellus of *pulchriceps*-group females (*e.g.*, Figs 18E, 20F) is secondarily derived for that species group. As discussed for the genus, monophyly of the *albitarsis* group remains questionable. The dorsally, slightly sinuate scrobal depression (Fig. 11F: arrows) and dorsal scrobal depression convexity (Figs 1C, E: sdc) of females could support monophyly of the *albitarsis* group. The distinctively deep, V-shaped propodeal plical depression of *albitarsis*-group females (Figs 2D, G: ppd) is a much more conspicuous difference between the two species groups and unique within Eupelminae and Eupelmidae. This structure could therefore also support monophyly of the *albitarsis* group but, as discussed under the genus, it is associated with two other putative symplesiomorphies of the propodeum and thus may also be a symplesiomorphic groundplan feature of the genus. Basal cell and costal cell setal features characteristic of *albitarsis*-group males are shared with at least *M. anelliformis* males, and possibly also with the unknown males of *M. longiscapus* within the *pulchriceps* group, and thus likely also represent symplesiomorphies for the *albitarsis*-group (see further under *M. anelliformis*).

Two morphologically different groups of species are evident within the *albitarsis* group based on females, which I newly designate as the ***aegeriae* subgroup** and the ***albitarsis* subgroup** based on the first described species in each of the two subgroups. Females of the *albitarsis* subgroup have a comparatively finely sculptured mesoscutal medial lobe (Figs 2C, 9H, 11E) in combination with partly infuscate fore wings (Figs 2F, 9I, 11G) and/or at least partly pale flagellum (Figs 9C, E), whereas females of the *aegeriae* subgroup have a much more coarsely sculptured mesoscutal medial lobe (Figs 4C, G, 13E, 16F) and hyaline fore wings (Figs 5A, 6G, 14E, 16H) in combination with a dark flagellum (Figs 6C, 14D, 16G). Although *M. aegeriae* can be recognized to subgroup based on its original description, type material is lost except for the gaster and parts of some legs of the holotype (Fig. 5J) that, along with the original description, are insufficient to confidently recognize the species within the subgroup (see further below). I therefore use the available name for the subgroup but treat it as a *nomen dubium*, as discussed under 'Remarks' for *M. aegeriae*. The actual number of species in the *aegeriae* subgroup is not confidently resolved, in part because of the lack of sufficient available material to confidently differentiate intra- from interspecific variation. Further study is necessary to determine whether *M. aegeriae* differs from or is a senior synonym of one or more of the other *aegeriae*-subgroup species, which were all described by Yao *et al*. (2009). Species of the *aegeriae* subgroup occur in the eastern Palaearctic and Oriental regions except for a single female from Algeria that I provisionally identify as *M. breviscapis*. The *albitarsis* subgroup consists of *M. albitarsis*, *M. menzeli* and *M. obscurus*, which are restricted to the Oriental and eastern Palearctic regions.

Mesocomys aegeriae Sheng, *nomen dubium*

Fig. 5J

Mesocomys aegeriae Sheng in Sheng & Wang, 1996: 416–417 (Chinese description), 418 (English description), figs 1–5 (female). Described from holotype ♀, allotype ♂, and another 5♀ and 3♂ paratypes (all JXAU).

Mesocomys aegeriae Sheng, 1998: 26–28, figs 1–5 (female). Described from holotype ♀, allotype ♂, and another 6♀ and 4♂ paratypes (all JXAU). Junior homonym of *M. aegeriae* Sheng, 1996. **New synonymy**.

Mesocomys aegeriae; Yao *et al*., 2009: 155 (keyed).

Type material examined. *Mesocomys aegeriae*. Holotype ♀ (JXAU; Fig. 5J): collection data in Chinese on two labels, plus two labels with both Chinese and English, one with "*Neomesocomys aegeriae* Sheng" in English and the other with "Holotype *Mesocomys aegeriae* Sheng" in English; publication-cited data: [China], Hancheng, Shaanxi, 15.VIII.1965, Dang Xinde, parasitic in eggs of *Dendrolimus tabulaeformis* Tsae & Liu.

The holotype (Fig. 5J) is almost completely destroyed except for the following: gaster (dark brown with Gt_1 whitish-hyaline except dorsobasally, and broadly rounded syntergal flange paler, light brownish-yellow) glued to point; right mesofemur (?) glued to point near base of gaster, plus left mesotibia and mesotarsus in glue on one side of gaster and apex of right mesotibia (projecting out of glue) and mesotarsus in glue under gaster (all yellow except mesotarsal pegs dark).

No other specimens of the type series were located and are presumed destroyed (Ling-Fei Peng, personal communication).

Distribution. PALAEARCTIC: China (Shaanxi) (Sheng & Wang 1996; Sheng 1998).

Biology. Host: LEPIDOPTERA. **Lasiocampidae**. *Dendrolimus tabulaeformis* Tsae & Liu (Sheng & Wang 1996; Sheng 1998).

Remarks. The name *Mesocomys aegeriae* Sheng was validated twice, originally in Sheng & Wang (1996) and then subsequently by Sheng (1998). In both instances the name was stated as a "*sp. nov*." with the same holotype female and type depository information, but with some differences in the descriptions of the sexes and with one extra female and male paratype designated by Sheng (1998). As such, *M. aegeriae* Sheng (1998) is both a homonym and an objective synonym of *M. aegeriae* Sheng in Sheng & Wang (1996).

As discussed above, the type material of *M. aegeriae* is missing except for parts of the female holotype that along with the original description are insufficient to unambiguously distinguish the species. This is unfortunate because *M. aegeriae* is the oldest available name among the species of *Mesocomys* originally described from China. Its correct interpretation is therefore critical for stable nomenclature. Description and illustration of the scutellar-axillar complex and propodeum of the female in Sheng & Wang (1996, fig. 2) and by Sheng (1998, fig. 1) are sufficient to place the species within the *albitarsis* group of *Mesocomys.* Further, the description of the female by Sheng (1998, p. 27), which is somewhat more detailed and informative than in Sheng & Wang (1996), states "fore wing hyaline … without spots or band", and "thoracic dorsum almost regularly sculptured, without distinct duller parts, always beset with rather sparse light bristles", which is sufficient to also place it as the first described species of what I designate as the *aegeriae* subgroup. Sheng (1998, p. 26) also described the female gaster as "with yellow band at the middle of first tergite" and the antenna as having "end of scape and pedicel yellow or yellowish brown". These latter features at least preclude *M. aegeriae* from being conspecific with *M. superansi*, females of which have the gaster uniformly dark basally in dorsal view (Figs 13F, H) and the antenna either entirely dark (Fig. 14D) or at most with only the extreme dorsoapical margin of the scape obviously paler (Fig. 14F) beyond the level of the apical-most setae on the scape (Fig. 14F, insert). In addition to the holotype of *M. superansi*, I also examined two female paratypes of *M. breviscapis* and one female paratype each of *M. sinensis* and *M. trabalae*, plus six additional *M. trabalae* females from the original rearing as the type material. Females described under these three names have the scape variably extensively yellowish apically, but at least partly yellow over the setose area (Figs 5C, 16G; Yao *et al*. 2009, figs 2, 4, 7), and usually have a variably distinct pale band on the gaster subbasally (Figs 5H, 16A), though this sometimes is not conspicuous (Figs 5G, I) because of specimen condition (see further below). Therefore, *M. breviscapis*, *M. sinensis* and *M. trabalae* are all potentially conspecific with *M. aegeriae*.

Females of *M. aegeriae* were described by Sheng (1998) as having the legs beyond the coxae yellowish-brown except for the hind femur being darker. Other than the mesotarsal pegs, the remaining parts of the legs of the holotype are all pale, more-or-less yellowish (Fig. 5J). The examined paratype of *M. trabalae* also has entirely yellowish front and middle legs (except for the mesotarsal pegs), but the hind leg has the outer surface of the metafemur dark basally and more extensively ventrolongitudinally (Fig. 16B, insert). Of the other six females of *M. trabalae* examined from the same rearing as the type specimens, all have similar leg colour patterns as the examined paratype except one has entirely yellow legs beyond the coxae. The holotype of *M. superansi* (Figs 13A, B) and the examined paratypic females of *M. breviscapis* (Figs 4A, B) and *M. sinensis* (Fig. 4F) have both the pro- and metafemora extensively dark except apically and basally. Therefore, if *M. aegeriae* is conspecific with one of the species later described by Yao *et al*. (2009), female leg colour pattern suggests it more likely is conspecific with *M. trabalae* than with *M. breviscapis*, *M. sinensis* or *M. superansi*. However, the description of leg colour pattern and the non-description of fore wing colour pattern for *M. aegeriae* males may not support this. The much shorter male description

for *M. aegeriae* does not specifically describe leg colour pattern, but does state "hind femur dark brown", which suggests that, as for females, the legs were pale except for the metafemur. I did not examine male type material of *M. breviscapis* or *M. superansi*, for which leg colour pattern was not described. However, males I identify as *M. superansi* have all femora at least in part brownish-infuscate to dark (Figs 15A, B), another feature supporting non-synonymy of *M. superansi* with *M. aegeriae*. The examined male paratype of *M. trabalae* has entirely pale legs, including the metafemur (Fig. 17B), as do all the males I identify as *M. trabalae* reared in the laboratory on *A. pernyi* (Fig. 17A), whereas the examined *M. sinensis* male paratype has the metafemur dark (Fig. 7D) as described for *M. aegeriae*. If male leg colour pattern is a stable diagnostic feature of the species then this would indicate *M. aegeriae* more likely is synonymous with what was described as *M. sinensis* (and possibly *M. breviscapis*) than with *M. trabalae*. Further, there is no mention of fore wing colour pattern in the original male description of *M. aegeriae*, which would suggest the fore wings were hyaline rather than having an infuscate region behind the stigmal vein, as was described by Yao *et al*. (2009) for *M. superansi* (Fig. 15G) and *M. trabalae* (Fig. 17G). However, the examined male paratype of *M. trabalae* appears to have uniformly hyaline fore wings and it is difficult to be certain whether the wings are completely hyaline or there is slight infuscation behind the stigmal vein in some other males I identify as *M. trabalae* or *M. superansi*. Further, of four males with the same collection data from Yunnan Forestry College (IZCAS), two have entirely pale legs beyond the coxae and two have the metafemur variably darkly infuscate. This leg colour pattern could indicate that two of the males are *M. trabalae* and the other two are *M. sinensis* or *M. breviscapis*; however, all four have fore wing setal features similar to those exhibited by male *M. trabalae*, which brings into question the validity of metafemoral colour pattern as a differential feature for this species (see further below and under *M. trabalae*). Described body length also tends to support *M. aegeriae* as more likely synonymous with *M. trabalae* than with what was described as *M. breviscapis* or *M. sinensis*. The described body lengths for females was 2.1–2.5 mm for *M. breviscapis*, 2.3 mm for *M. superansi* (but newly measured as 3.3 mm), 2.4–2.8 mm for *M. sinensis*, 2.7–3.5 mm for *M. aegeriae*, and 3.4–3.9 mm for *M. trabalae*. Thus, although the ranges overlap, the type specimens of *M. aegeriae* were somewhat larger and more similar in size to females of *M. trabalae* and *M. superansi* than those of *M. breviscapis* and *M. sinensis*.

Although some of the features described for *M. aegeriae* could support synonymy with *M. trabalae*, basal cell setal pattern does not. Sheng (1998, p. 27) described the fore wing of female *M. aegeriae* as having the basal cell "entirely setose which behind the submarginal vein are whitish and extend to the base of the wing along the posterior margin". As discussed under *M. breviscapis*, basal cell setal pattern differs among *aegeriae*-group females, and the limits of intraspecific variation remain uncertain because of the lack of sufficient material to confidently assess species limits. However, the few females I identify as *M. superansi* all have a completely setose basal cell (Figs 8G, H), except sometimes for a small, comparatively inconspicuous bare region anteroapically behind the submarginal vein (Fig. 8H: arrow). Most females that I identify as *M. breviscapis* (Figs 8A–C) also have the basal cell essentially entirely setose, though setation sometimes is limited to a single longitudinal row within the basal cell in addition to it being entirely setose posteriorly along the mediocubital fold (Fig. 8B); the only exception is the examined *M. sinensis* paratype, which has the basal cell extensively bare except basally and apically (Fig. 8D) (see further under *M. breviscapis*). Females of *M. trabalae* usually also have the basal cell extensively bare behind the submarginal vein (Fig. 8E) other than sometimes being setose along the entire length of the mediocubital fold, but if more-or-less extensively setose within the basal cell then it is at least broadly bare along the mediocubital fold (Fig. 8F). Consequently, no yet observed *M. trabalae* female has a basal cell setal pattern that matches the setal pattern described for *M. aegeriae*.

Another feature that may not support synonymy of *M. aegeriae* and *M. trabalae* is host data. *Mesocomys trabalae* was originally reared from eggs of *Trabala vishnou*, whereas the type material of *M. superansi* was reared from eggs of *Dendrolimus superans* and that of *M. aegeriae*, *M. breviscapis* and *M. sinensis* were all reared from eggs of *Dendrolimus tabulaeformis*. However, based on known host range of other *Mesocomys* species for which several rearings are known, it is unlikely that any of the species are strictly host specific, including *M. trabalae*. Following its original description, specimens of this latter species were reared from *Dendrolimus houi* as well as from field-collected eggs of *Caligula japonica* and on the factitious host *Antherea pernyi* in the laboratory, showing that it is not even host-family specific. Distributions of the described species also do not provide any substantive evidence of potential synonymy because all were described from the eastern part of Palaearctic China (*M. aegeriae*, *M. sinensis* and *M. trabalae* from Shaanxi Province and *M. breviscapis* and *M. superansi* from Hebei Province).

Yao *et al*. (2009) recognized *M. aegeriae* as a valid species different from the four species they newly described,

but based on their key their concept of *M. aegeriae* appears to have been based only on the original description rather than examination of type specimens. Yao *et al*. (2009) keyed *M. breviscapis* from *M. aegeriae*, *M. sinensis* and *M. trabalae* by differences in two antennal and one fore wing setal feature of females. Females of *M. breviscapis* were stated as having the first funicular nearly equal in length to the second funicular, whereas the first funicular was stated as obviously shorter than the second funicular in females of the other three species. Even though Sheng (1998, fig. 2) illustrated the first funicular as being much smaller than the second and subsequent funiculars for female *M. aegeriae*, the description of Sheng (1998, p. 26) states "all 8 funicular segments mostly subequal in length…" ("all seven funiculars" in Sheng & Wang 1996, p. 418). As discussed under *M. breviscapis*, although only three female paratypes were examined, there does not appear to be a conspicuous difference between the lengths of the first and second funiculars for the examined *M. breviscapis* (Fig. 5F) and *M. sinensis* (Fig. 5C) paratypes. Further, because of its attachment to the pedicel, apparent length of the first funicular often differs slightly if measured dorsally *versus* ventrally (*e.g.*, Fig. 6E: lower antenna), and because the other funiculars articulate with each other the length of each can vary slightly depending on their position relative to each other and the angle from which they are viewed. Relative length of the funiculars also appears to vary to some extent correlated with body size.

Yao *et al*. (2009) also stated in their key that females of *M. breviscapis* have the basal two-thirds of the costal cell bare, but they did not provide an alternative state for the other three species in the second half of the couplet. The validity of setal pattern of both the costal cell and basal cell as specific features is discussed under *M. breviscapis*, but their mention of costal cell in the first part of the couplet may have been a *lapsus* for the basal cell (see under *M. breviscapis*). Finally, Yao *et al*. (2009) keyed *M. breviscapis* as having a short scape not reaching the anterior ocellus as opposed to a long scape reaching or exceeding the vertex in females of *M. aegeriae*, *M. sinensis* and *M. trabalae*. They then keyed *M. aegeriae* from the other two species by the scape reaching the anterior ocellus as opposed to exceeding the vertex in *M. sinensis* and *M. trabalae*. Neither Sheng & Wang (1996) nor Sheng (1998) described length of the scape relative to the anterior ocellus or vertex, but they did provide line illustrations of the head in frontal view with the scape within the scrobal depression extending to the upper margin of the head (Sheng & Wang 1996, fig. 1; Sheng 1998, fig. 2). The validity as a specific feature of scape length relative to the level of the anterior ocellus or vertex is discussed under *M. breviscapis*, but the level to which the scape appears to extend to in specimens depends in part on whether it is appressed to the head within the scrobal depression or is angled away from the head, and the view from which the head is observed. For example, the scape does not appear to extend to the level of the anterior ocellus in either Fig. 6C or Fig. 6D, seen in frontal view, whereas in lateral view the apex of the scape appears to extend to the level of the anterior ocellus and vertex (Fig. 6B).

Yao *et al*. (2009) also differentiated *M. aegeriae* females from those of *M. sinensis* and *M. trabalae* based on the pronotum being almost square with an arcuate, often ridge-like margin differentiating the neck from the collar, and the gaster being apically yellow, as opposed to females of the latter two species having the pronotum wider than long and without a ridge-like margin between the collar and neck, and the gaster dark brown apically. The key states given for *M. aegeriae* by Yao *et al*. (2009) apparently were taken from the original description by Sheng (1988), which states "end point of abdomen yellow (p. 26)" and "pronotum subquadrate, with arcuate, often ridge-like margin differentiating neck from transverse, depressed collar (p. 27)". However, pronotal structure is very similar for all species of *Mesocomys* and the absence of a distinct, arcuate margin separating the collar from the neck in at least *M. breviscapis* (Fig. 4C) and *M. sinensis* (Fig. 4G) is correlated with their comparatively small body size. The larger holotype of *M. trabalae* has a more evident, though not distinctly ridge-like arcuate angulation (Fig. 16F). Also, even though Yao *et al*. (2009) stated that the female gaster of *M. trabalae* and *M. sinensis* are dark brown apically, the examined paratype of *M. trabalae* does have the syntergal flange distinctly paler, brownish-yellow to apically yellow, than the remainder of the syntergum, and in some females from the same rearing as the type material the flange is hyaline apically so that the underlying ovipositor sheaths are visible through it (Fig. 14H). The syntergal flange is also at least somewhat paler, lighter brown to brownish-yellow and very narrowly hyaline apically than the rest of the syntergum for examined type material of *M. breviscapis* (Fig. 7A) and *M. sinensis* (Fig. 7B). Differences between how conspicuously pale is the syntergal flange likely is at least partly correlated with body size and specimen condition.

The original descriptions of *M. aegeriae* in Sheng & Wang (1996) and by Sheng (1998) do include one anomalous feature, the described lengths of the submarginal, marginal, postmarginal and stigmal veins. These were described as 30: 40: 30: 17, respectively, for females. If accurate, length of the submarginal vein is atypically short relative to females of other species because, based on my measurements, the costal cell/submarginal vein is always

longer than the marginal vein for female *Mesocomys*. However, neither Sheng & Wang (1996) nor Sheng (1998) noted how length of the submarginal vein was measured. Rather than being a diagnostic feature that differentiates *M. aegeriae* females from other *aegeriae*-subgroup species, more likely the unusually short submarginal vein length given was because either the parastigma was not included in its length or, more likely, the measurement did not include the true point at which the leading margin of the costal cell merged with the base of the marginal vein. This latter possibility is suggested by the figures of the fore wing in both publications, in which the leading margin of the costal cell does not merge smoothly with the marginal vein but abuts the apex of the parastigma somewhat to the base of the marginal vein (Sheng & Wang 1996, fig. 2; Sheng 1998, fig. 1).

Based on the above discussion, *M. aegeriae* is certainly the correct name for one *aegeriae* subgroup species in China, but the original description and the remaining parts of the holotype are insufficient to confidently establish whether it is the senior synonym of one or more of the species described by Yao *et al.* (2009) other than *M. superansi*. As discussed further under the relevant names, what constitutes intra- and interspecific variation, and thus the species limits and the actual number of valid species included in the *aegeriae* subgroup, remains questionable. In order to more confidently establish correct nomenclature, new rearings from type-host eggs (*D. superans*, *D. tabulaeformis*, and *T. vishnou*), ideally from the type localities, are required to obtain fresh specimens of both sexes for comparison and for molecular analyses. Also, to more confidently establish species limits and differentiate intraspecific from interspecific variation, more geographically extensive collections from China and elsewhere in the eastern Palearctic and Oriental regions are required, as are rearings from other potential Lepidoptera hosts. Until these can be accomplished I prefer to treat *M. aegeriae* as a *nomen dubium*.

Mesocomys albitarsis (Ashmead)

Figs 1A–H, 2A–G, 3

Anastatus albitarsis Ashmead, 1904: 154. Described from holotype ♀ (USNM, type no. 7171).

Anastatus albitarsis; Clausen, 1927: 461–472 (life history, description of immature stages), plate XXIII (immature stages and female figured); Chu, 1937: 59–60 (redescription), fig. 2 (female); Kalina, 1981: 9 (generic classification).

Pseudanastatus albitarsis (Ashmead); Yasumatsu & Watanabe, 1964: 85 (new combination).

Semianastatus orientalis Kalina, 1984: 19–22, 28, figs 64–82 (female), plate II figs 1–6 (female). Described from holotype ♀ (ZIN) plus 7♀ paratypes, 2♀ deposited in IAEE and 5♀ in ZIN. **New synonymy**.

Mesocomys albitarsis (Ashmead); Bouček, 1988: 573, fig. 987 (new combination, name given in figure caption without author name or indication of generic transfer); Gibson, 1995: 230 (incorrectly attributed as new combination), figs 73, 74, 143, 144, 199, 264, 300 (female), figs 350, 411, 412 (male); Narendran & Sheela, 1995: 311 (keyed); Yao *et al*., 2009: 155 (keyed); Yang *et al*., 2015: 167 (keyed), 167–169 (Chinese description and data), 256–257 (English data summary), fig. 87 (male).

Mesocomys orientalis (Kalina); Gibson, 1995: 229 (new combination, homonym).

Mesocomys kalinai Özdikmen, 2011: 834–835. Unnecessary replacement name for *Mesocomys orientalis* (Kalina 1984), preoccupied by *Mesocomys orientalis* Ferrière (1935). **New synonymy**.

Description. FEMALE (habitus: Figs 1A, B). Length = 2.0–4.6 mm [?]. Head sometimes entirely green though usually with variably extensive coppery to reddish-violaceous lustre or more rarely blue to purple lustre on one or more of parascrobal region and frons below or around anterior ocellus (Figs 1C, E), interantennal prominence (Fig. 1C), scrobes, and vertex (Fig. 1D). Face with upper parascrobal region and frons mesh-like coriaceous in smaller individuals to variably distinctly mesh-like reticulate in larger individuals (Figs 1D, E), the sculptural cells formed by at least slightly raised ridges, vertex (Fig. 1D) more transversely alutaceous to alutaceous-strigose, parascrobal region mostly much more distinctly roughened than frons, rugulose to transversely reticulate-strigose, and scrobes and interantennal prominence above about level of dorsal limit of toruli imbricate to reticulate-imbricate, the face between toruli much more minutely mesh-like coriaceous (Fig. 1C). Head measurements: HL = 2.6–4.3 [3.3], HH = 4.6–6.0 [4.9], HW = 4.9–7.7 [6.5], TL = 0.9–1.7 [?], EH = 2.5–4.3 [3.4], EW = 2.2–3.5 [3.0], MS = 1.3–2.1 [1.8], IOD 0.30–0.34 [0.32]× HW, MPOD: OOL: POL: LOL = 1.0: 0.5–0.8: 1.8–2.4: 1.4–2.0 [1.0: 0.5: ?: 1.8], and dso 0.5–1.0× aod [1.0:1.1]. Labiomaxillary complex with maxillary and labial palps dark brown or labial palps only slightly paler. Antenna (Fig. 2E) uniformly dark or at most scape pale only along extreme apical or anteroapical margin; scape elongate-rectangular, only slightly tapered apically, about 3.7–4.0× [?] as long as greatest width; pedicel about twice as long as apical width and as long as or only slightly longer than combined length of basal

two funiculars; flagellum with fl_1 slightly transverse to slightly longer than wide and increasing in width apically so basal funiculars beyond fl_1 quadrate to slightly longer than wide but increasingly more quadrate to transverse apically; clava about as long as apical three funiculars.

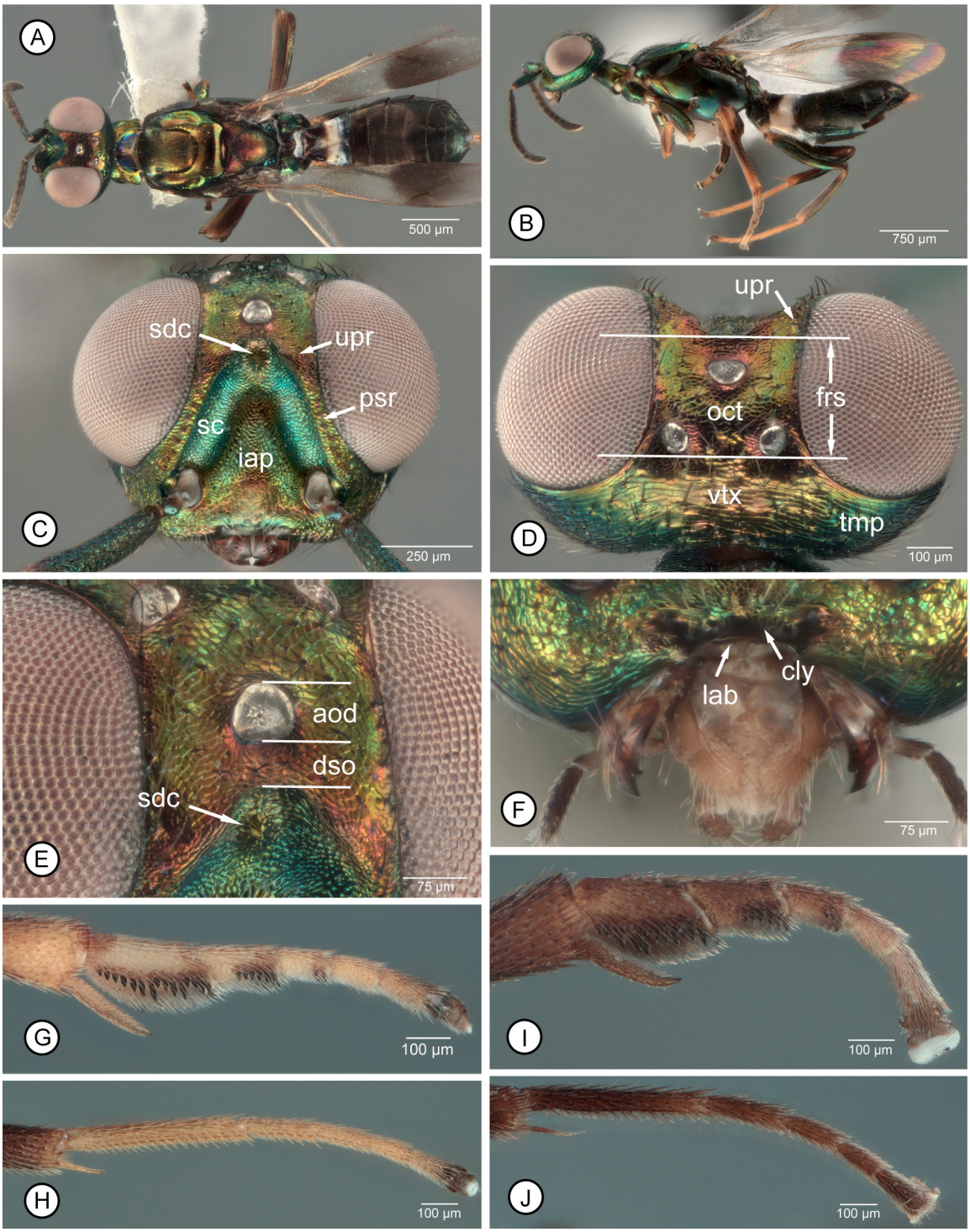

FIGURE 1A–J. *Mesocomys* spp. ***A–H***, *M. albitarsis* ♀: **A**, dorsal habitus (#27); **B**, lateral habitus (#26); **C**, head, frontal (#26); **D**, head, dorsal (#26); **E**, frontodorsal part of head (#26); **F**, clypeus and mouthparts (#27) [apical setae missing from labrum]; **G**, mesotarsus and apex of mesotibia (#26); **H**, metatarsus and apex of metatibia (#26). ***I & J***, *M. obscurus* ♀ (#62): **I**, mesotarsus and apex of mesotibia; **J**, metatarsus and apex of metatibia. [See 'Methods' and Table 1 for explanation of abbreviations.]

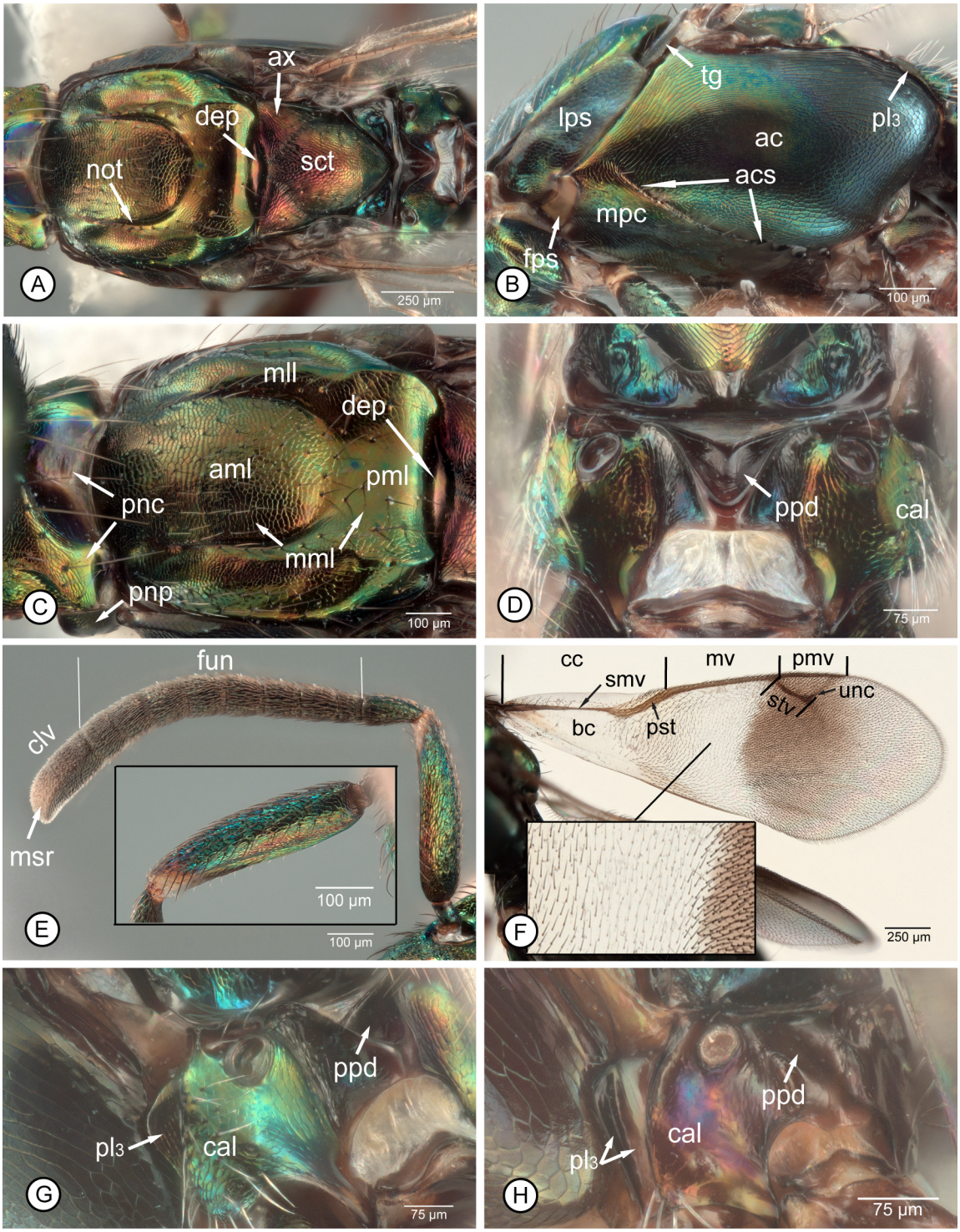

FIGURE 2A–H. *Mesocomys* spp. ***A–G***, *Mesocomys albitarsis* ♀. **A**, mesosoma, dorsal (#27); **B**, mesosoma, lateral (#56); **C**, pro- and mesonotum (#27); **D**, metanotum and propodeum (#27); **E**, antenna, inner view [insert: scape, outer view] (#26); **F**, fore wing (#26) [insert: enlargement of central part of disc]; **G**, metapleuron and propodeum (#56). **H**, *Mesocomys pulchriceps* ♀: metapleuron and propodeum (#47). [See 'Methods' and Table 1 for explanation of abbreviations.]

Pronotum dorsally usually brown or with concave part with blue to purple lustre under some angles of light, but green on convex lateral and anterior parts (Figs 2A, C); mesonotum with mesoscutum mostly green, to bluish-green posteriorly, but with variably distinct and extensive coppery to reddish-violaceous lustre (Figs 2A, 2C), and scutellar-axillar complex variably extensively reddish-violaceous anteriorly to green or bluish-green posteriorly (Fig. 2A); in lateral view (Fig. 2B) similarly metallic green with some coppery to reddish-violaceous lustre as

dorsally, but prepectus usually more bluish to purple compared to lateral panel of pronotum and acropleuron under most angles of light. Mesoscutum (Fig. 2C) with convex anterior part of medial lobe mesh-like coriaceous or at most inconspicuously coriaceous-imbricate in larger individuals, depressed posterior part similarly but much more finely mesh-like coriaceous to smooth and shiny medially, and lateral lobe also mesh-like coriaceous; mesoscutum, excluding parapsidal band, similarly setose with brown hair-like setae except depressed posterior part of medial lobe more sparsely setose and setae often somewhat longer and more bristle-like. Scutellar-axillar complex (Fig. 2A) with axillae obliquely alutaceous to alutaceous-strigose and scutellum mesh-like coriaceous mediolongitudinally but with more elongate sculpture on sides; setose laterally, with brown hair-like setae. Acropleuron finely mesh-like sculptured, though with more minute sculpture mesally below level of fore and hind wing bases and larger, more isodiametric, coriaceous-reticulate sculpture posteriorly. Front leg at least with femur dark, except apically, and tarsus pale, but with tibia variably extensively dark, pale apically and basally, and often with anterior and posterior surfaces variably extensively to entirely pale. Middle leg beyond coxa sometimes more-or-less similarly pale, including tibial spur, except for dark mesotarsal pegs (Fig. 1G), but usually femur and tibia variably extensively brownish-yellow to dark brown, most commonly with knee and tibia apically, and sometimes femur basally, paler (Fig. 1B). Hind leg with trochantellus and tarsus pale, the tarsus at most light brownish in part (Fig. 1H), and femur and tibia mostly dark with tibia usually narrowly paler basally and apically and femur sometimes with green lustre (Fig. 1B). Fore wing (Fig. 2F), at least in larger individuals, with basal cell light brownish-infuscate basally and disc often distinctly bifasciate, with darker brown region with dark setae behind stigmal and postmarginal veins and with lighter brown region with dark setae behind parastigma and base of marginal vein, the two regions separated medially behind marginal vein by more hyaline region with white setae, though sometimes infuscate region behind parastigma indistinct or lacking so wing appears unifasciate, but then also with much paler, white setae behind marginal vein in contrast to dark setae basally and apically (Fig. 2F, insert); costal cell bare dorsally excluding setae in front of parastigma; basal cell bare or with up to 2 setae basally on mediocubital fold; measurements of cc: mv: pmv: stv = 4.0–4.8: 3.1–3.6: 1.8–2.0: 1.0 [4.1: 3.3: 1.8: 1.0].

Gaster mostly dark brown but in dorsal view with variably distinct and large subbasal white band (Fig. 1A) formed by apically whitish-hyaline Gt_1, and in lateral view (Fig. 1B) St_1 entirely white and Gt_1 apically with vertical sides white; Gt_2–syntergum dark brown except syntergal flange yellowish-hyaline and apical tergites sometimes with slight greenish lustre; Gt_1 smooth, shiny and bare, and, at least when raised above Gt_2, noticeably hyaline apically, and usually comparatively narrow with subparallel sides relative to more uniformly ovate Gt_2–syntergum; Gt_2–syntergum similarly mesh-like coriaceous to alutaceous and Gt_3 or Gt_4–syntergum with at least one row of hair-like setae across surface. Ovipositor sheaths pale, yellowish.

MALE (habitus: Figs 3A, B). Length = 1.7–3.1 mm. Head (Fig. 3C) sometimes entirely green to bluish-green, but usually with variably extensive and distinct coppery to reddish violaceous lustre on one or more of frons medially to entirely, scrobal depression, interantennal prominence, lower face, and/or gena. Face with upper parascrobal region and frons at least slightly roughened, mesh-like coriaceous-imbricate to partly, shallowly reticulate; vertex transversely alutaceous-imbricate to strigose, but rounded into occiput; scrobal depression and most of interantennal prominence similarly mesh-like reticulate to imbricate, but more finely mesh-like coriaceous ventrally between toruli. Head measurements: HL = 2.4–3.6, HH = 3.2–5.0, HW = 4.0–6.2, EH = 2.0–3.0, EW = 1.8–2.7, MS = 1.2–1.8, IOD 0.42–0.45× HW, MPOD: OOL: POL: LOL = 1.0: 0.5–0.8: 2.1–2.8: 1.3–1.4, and dso subequal to aod. Labiomaxillary complex with palpi variably yellow to brownish. Antenna (Fig. 3G) entirely dark, but scape and pedicel with green lustre similar to head; scape about 2.5–2.8× as long as wide; pedicel about 1.7–2.0× as long as apical width and about 0.8–0.9× combined length of basal two funiculars; flagellum robust-filiform to slightly clavate; fl_1 transverse and much smaller than fl_2, fl_2–fl_8 subquadrate to slightly longer than wide, and clava about 2.1–2.3× as long as wide and equal in length or only slightly longer than combined length of basal two funiculars (up to about 0.6× combined length of apical three funiculars).

Mesosoma dorsally (Fig. 3D) similarly green to bluish-green as head except usually with slight coppery lustre on scutellum medially and sometime more extensively on mesonotum; in lateral view similar in colour to dorsal surface, and mesopleurosternum with (Fig. 3E) or without evident Y-like set of pale lines. Mesoscutum with medial lobe very shallowly mesh-like reticulate to reticulate-imbricate, usually somewhat more coarsely sculptured anteriorly than posteriorly. Scutellar-axillar complex with axillae mesh-like coriaceous to very shallowly reticulate, and scutellum mesh-like coriaceous medially and posteriorly but more longitudinally alutaceous to coriaceous-imbricate laterally. Legs (Fig. 3B) with at least metafemur and sometimes all femora dark and then usually with green to bluish-green lustre, though profemur and/or mesofemur sometimes only partly brown to dark, with base and apex variably extensively pale or anterior and/or dorsal surfaces more extensively to entirely pale, yellowish-brown to

yellow; trochanters sometimes, at least in part, trochantelli, tibiae (including mesotibial spur) and tarsi much paler, yellowish to brownish-yellow, than metafemur, but with metatibia sometimes slightly darker apically. Fore wing entirely or essentially entirely hyaline, at most very faintly and inconspicuously brownish behind stigmal vein (Fig. 3F); costal cell dorsally without or with up to 3 setae off-set from row of setae paralleling leading margin basal to setae in front of parastigma; basal cell closed posteriorly by setae along length of mediocubital fold and closed apically by at least 1 row of setae along basal fold, and usually more extensively setose apically, but with at least basal half of cell bare; speculum (Fig. 3F: spc) large and broad, extending to parastigma without intervening setae; measurements of cc: mv: pmv: stv = 3.0–3.3: 1.6–1.8: 1.6–1.8: 1.0.

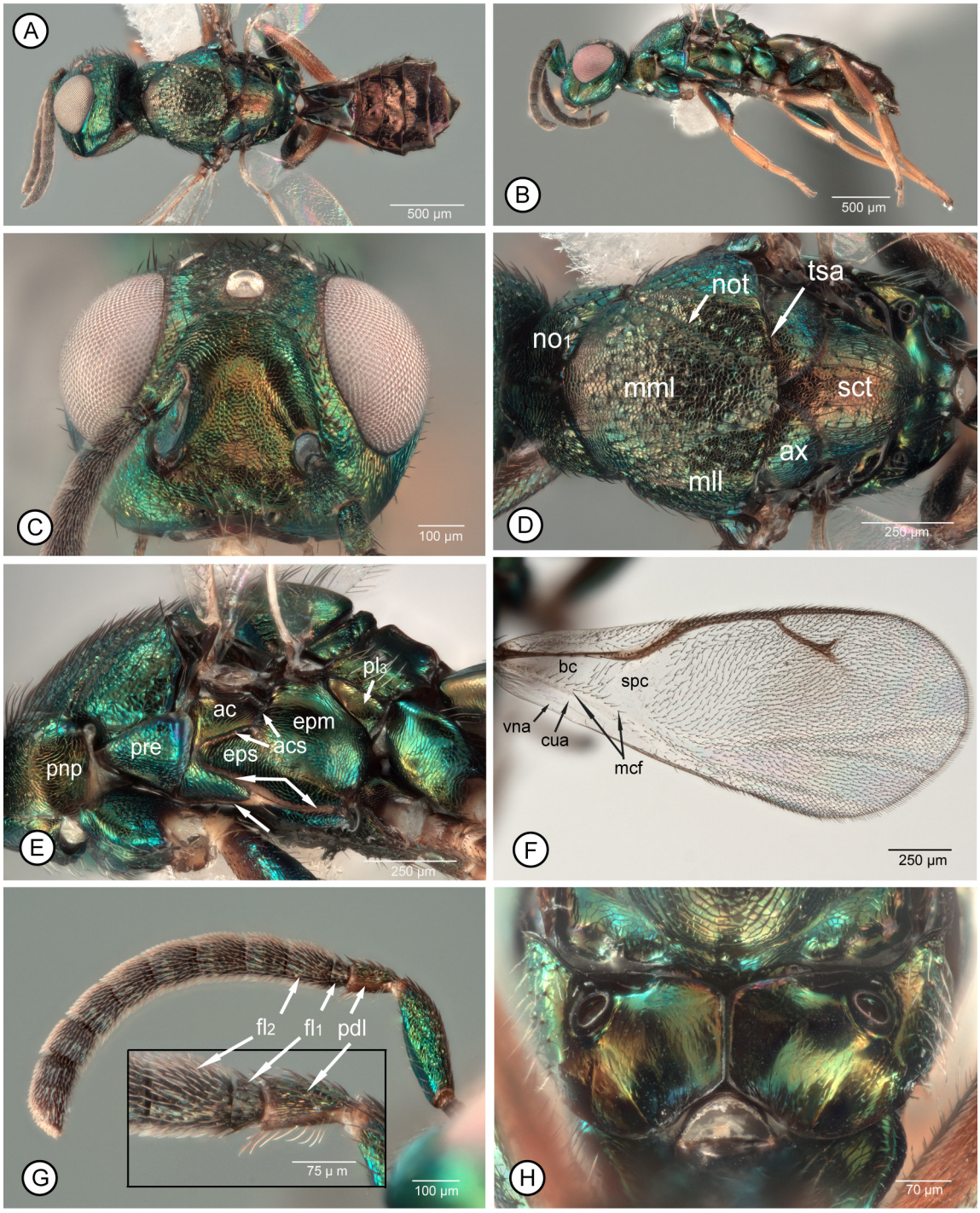

FIGURE 3A–H. *Mesocomys albitarsis* ♂. **A**, dorsal habitus (#29); **B**, lateral habitus (#28); **C**, head, frontal (#30); **D**, mesosoma, dorsal (#29); **E**, mesosoma, lateral (#28) [bottom three arrows point to Y-like set of pale lines on mesopleurosternum]; **F**, fore wing (#29); **G**, antenna, inner view [insert: pedicel–fl_2] (#30); **H**, propodeum (#29). [See 'Methods' and Table 1 for explanation of abbreviations.]

Gaster dark brown or with variably extensive green lustre basally and/or apically (Fig. 3A).

Type material examined. *Anastatus albitarsis*. Holotype ♀ (USNM): "Hakone / JAPAN | KOEBELE / Type | No. 7171 | U.S.N.M. / *Anastatus* | *albitarsis* | Ash ♀ / USNM ENT | 00802456". Holotype glued by left acropleuron on top of card point such that right side faced dorsally, with head pointed toward pin; contorted, with mesonotum strongly arched such that head over and obscuring most of dorsal surface of mesoscutum, and gaster detached from body and glued by left side on top of point, but entire except extreme apex of right clava missing. Images available at: http://www.usnmhymtypes.com/default.asp?Action=Show_Types&Single_Type=True&TypeID=3479.

Semianastatus orientalis. Paratypes examined (1♀ IAEE, 5♀ ZIN): "Primorsk. Territory | Suchanskii forest | establ. from eggs | *Dictyoploca japonica* | V.– Kazakova / *Semianastatus* | *orientalis* | gen. & sp. n. | det. Kalina 19."

Other material examined. CHINA. No data other than: egg of *Dendrolimus* sp. (4♀ IZCAS); Lin Wei, egg of *Dendrolimus* sp. (4♀ IZCAS). East China Academy of Agriculture Sciences, 1954 (3♀ IZCAS). Yuantou, 14.IX.1956, egg of *Odonestis pruni* L. (2♀ IZCAS).

ORIENTAL. **CHINA**. ***Fujian***. Chong-An, 9.V.1982, Naiquan Lin (1♀ IZCAS). Shaowu County, Longhu, 11.IV.2015 (1♀ FAFU). ***Guangxi***. Institute of Forestry Sciences, V.1974, Lin Wei (3♀ IZCAS). ***Hubei***. Wuchang, Shengwen Li—9.VI.1984, egg of *Dendrolimus punctatus* Walker (13♀, 1♂ IZCAS); Mailongshan, 9.VI.1984, egg of *Dendrolimus punctatus* Walker (5♀ IZCAS). ***Hunan***. Dao-An, 20.VIII.1955, *Dendrolimus* sp. (4♀, 1♂ IZCAS). Dong-AN, 20.VIII.1955, egg of *Dendrolimus* sp. (3♂ IZCAS). Jing County, IV.1980, Lijun Zhou, *Antherea pernyi* (Guérin-Méneville, 1855) (1♀, 1♂ IZCAS). Qing County, IV.1979, Xinwang Tong, *Dictyoploca japonica* Moore (2♀ IZCAS). Xupu, VIII.1978 (2♀ IZCAS), IV.1979 (10♀ IZCAS), Xinwang Tong, egg of *Dendrolimus punctatus* Walker. You County, 15.VI.1960, egg of *Dendrolimus* sp. (5♀ IZCAS). ***Jiangsu***. Nanjing—1957 (1♀ IZCAS); ex. *Dendrolimus* VIII.1956, laboratory stock, A. Huba (1♀, 1♂ NHMUK). ***Jiangxi***. Kuling, 1200m, 7.I.1934, H. Höne, ex. egg *Rhodinia fugax-diana* (1♀ NHMUK, 1♀ NMPC). ***Yunnan***. Gejiu, Shiyan, VIII.1980, Guoxiang Li, *Dendrolimus kikuchii* Matsumura (1♀ IZCAS). Pu-Er, 8.XII.1981, Dingxi Liao, egg of *Dendrolimus* sp. (1♀ IZCAS). ***Zhejiang***. Changshan, East China Academy of Agriculture Sciences, 1955 (2♀, 2♂ IZCAS). Mt. Siming, Malaise trap, 5.VI.2017 (1♀ FAFU). **TAIWAN**. Taoyuan Hsien road S of Shan Paling to Paling, 700-900m, 25.V.1990, J. Heraty (1♂ CNC).

PALAEARCTIC. **CHINA**. ***Anhui***. Xiuning, Lingnan Forest, VI.1984, Xueshang Zhou, egg of *Dendrolimus kikuchii* Matsumura (3♀ IZCAS). ***Gansu***. Kang Co., Longnan City, 23.I.2018, Y. Chen, ex. *Caligula japonica* Moore egg, lab. reared on eggs of *Antherea pernyi* (Guérin-Méneville) (Lep: Saturniidae) (45♀, 15♂ CNC, 1♀ CNC Photo 2018-27, 1♂ CNC Photo 2018-29). ***Hebei***. Fengning, Yunwushan, 27.VIII.1985, Shihua Song, pine tree (6♀ IZCAS). Qianxi, 26.VIII.1954, egg of *Dendrolimus* sp. (2♀ IZCAS). ***Henan***. Tongbai, 6.VI.1988, *Dendrolimus punctatus* Walker (14♀ IZCAS). ***Liaoning***. Benxi, Manchu Autonomous Co., Benxi City, Tai Shan Forest Farm, 23.IV.2017, Y. Chen, ex. *Caligula japonica* Moore egg, lab. reared on eggs of *Antherea pernyi* (Guérin-Méneville) (Lep: Saturniidae) (30♀, 15♂ CNC, 2♀ CNC Photo 2018-26, -56, 2♂ CNC Photo 2018-28, -30). Xingcheng Forestry Bureau, 19.V.1981, Yanli Zhao (1♀ IZCAS). ***Shaanxi***. Hanzhong, VIII.1978, egg of *Dendrolimus tabulaeformis* (Tsai et Liu, 1962) (2♀ IZCAS). Huanglongshan, 27.III.1981, Jian Zhu (1♀, 2♂ IZCAS). ***Shandong***. Huang County, Daixiang Zhang—22, 24.IV.1955, egg of Saturniidae sp. (2♀ IZCAS); 11 (4♀ IZCAS), 22 (1♀ IZCAS).V.1955, *Dendrolimus* sp. **JAPAN**. 97.137 (1♀ NHMUK). VII.1963, M. Brown, ex. ova *Antherea yamami* [*sic*], dead in ovum (1♀ NHMUK). bred from imported egg of *Antheraea yamamai*, 29.V.1893 (1♀ NHMUK). II.1961, ex. *Dictyoploca japonica* egg, CIE 18628 (3♀ NHMUK). III.1961, ex. *Antheraea yamamai*, CIE18628 (3♀, 1♂ NHMUK). Aichi, Mt. Sanage-Yama, 18-24.VI.1993, T. Kanbe (1♀ CNC, CNC Photo 2018-22). Ehime, 30.VIII.1957 (2♀ USNM). Fuduoka, Mt. Hiko, 25.VIII-4.IX.1989 (1♀ CNC), 18-25.IX.1989 (1♀ CNC), Takeno & Sharkey. Kunitachi, VI.1936 (1♀ NHMUK). Ishikawa-ken, Oshimizu, 17.IV.1974, I. Togashi, ex. *Dictyoploca japonica* (1♀ NHMUK). Matsuyama, VI.1961, Tachikawa, ex. eggs *Dictyoploca japonica* (1♀ USNM). Tokyo, 26.I.1921, C.P. Clausen, ex. moth eggs, c. #1503 (25♀, 6♂ UCRC) [another 10♂ in UCRC that are similarly mounted and with similar handwritten labels as Tokyo specimens apparently erroneously labelled as "France, Bergerac, Dordogne, 22-26.VII.1955, Parker & Moniaenkov, R.1503", because of similar record numbers]. Tokyo, C. Lasaki [?] (22), ex. eggs *Caligula japonica* (4♀, 4♂ USNM). Yokohama, 20.IX.1921, C.P. Clausen (4♀, 4♂ USNM).

Distribution. ORIENTAL: China [*Fujian, *Guangxi, *Hubei, Hunan & Jiangsu (Noyes 2019), *Jiangxi, *Yunnan, Zhejiang (Noyes 2019)], Taiwan (Herting 1976). PALAEARCTIC: China [*Anhui, Beijing (Yang *et al*. 2015), *Gansu, *Hebei, *Henan, *Liaoning, *Shaanxi, Shandong (Noyes 2019)], Japan (Ashmead 1904), South Korea (Anonymous 1965).

Biology. Hosts: LEPIDOPTERA. **Lasiocampidae**. *Dendrolimus kikuchii* Matsumura and *D. punctatus* (Walker) (Chu 1937; Yang *et al*. 2015) on *Pinus massoniana* Lamb (Pinaceae) (Tong & Ni 1990), *D. spectabilis* (Butler) (Ishii 1938) on pines (Hirose 1964), *D. tabulaeformis* Tsai & Liu (Yang *et al*. 2015); **Odonestis pruni* (L); *Lebeda nobilis* Walker (Yang *et al*. 2015). **Lymantriidae**. *Lymantria dispar* (L.) (Fukaya 1936), *L. dissoluta* Swinhoe (Ge *et al.*, 1996). **Notodontidae**. *Fentonia ocypete* (Bremer), *Phalera assimilis* (Bremer & Grey) and *Trabala* [= *Lampronadata*] *cristata* Butler (Fry 1989). **Saturniidae**. **Antherea pernyi* (Guérin-Méneville), **A. yamamai* Guérin-Méneville; *Caligula japonica* (Moore) [as *Dictyoploca* (*Caligula*) *japonica*] (Clausen 1927; Yang *et al*. 2015); *Eriogyna pyretorum* (Westwood) (Koidzumi & Shibata 1940); **Rhodinia fugax diana* Oberthür.

Aspects of the biology of *M. albitarsis* have been studied extensively (*e.g.*, Chen *et al*. in press), though mostly either under its original *Anastatus* combination (*e.g.*, Clausen 1927; Fang & Hu 1993; Koidzumi & Shibata 1940; Xu *et al*. 2006) or, more commonly, under *Pseudanastatus* (*e.g.*, Hirose 1969; Ni *et al*. 1994; Schaefer *et al*.1988; Tong & Ni 1989, 1990; Wang 1990).

Remarks. Examination of paratypic material of *Semianastatus orientalis* Kalina (1984) showed the material to be conspecific with *M. albitarsis*, thus confirming the generic synonymy of *Semianastatus* under *Anastatus* by Gibson (1995) and that the replacement name of *M. kalinai* Özdikmen (2011) for *M. orientalis* (Kalina) was unnecessary. Type females of both names are of the form with distinct infuscation only behind the stigmal and postmarginal veins (*cf.* Fig. 2F), though the *S. orientalis* type material has the head and mesosoma brighter green than the *M. albitarsis* holotype, and the upper parascrobal region and frons are very slightly coriaceous-imbricate compared to coriaceous in the holotype of *M. albitarsis*.

As discussed under the *albitarsis* species group, *M. albitarsis* comprises a species trio along with *M. menzeli* and *M. obscurus*. Females of the three species are very similar to each other in structure, sculpture and setal patterns, but share different colour pattern combinations. Females of *M. albitarsis* and *M. obscurus* are similar to each other in having virtually entirely dark antennae (Figs 2E, 11H) compared to the more extensively pale antennae of *M. menzeli* females (Figs 9C–E). However, females of *M. obscurus* have tarsi that are mostly to entirely brownish-infuscate, even if variably dark brown (Figs 1I, J), whereas those of *M. albitarsis* and *M. menzeli* have pale tarsi or these at most only in limited part light brownish (Figs 1G, H). Fore wing colour pattern of *M. albitarsis* intergrades with that of females of the other two species. Females of *M. menzeli* have only a single infuscate region behind the stigmal and postmarginal veins (Fig. 9I), whereas females of *M. obscurus* have a distinctly bifasciate fore wing with infuscation behind the stigmal and postmarginal veins and behind the parastigma and base of the marginal vein (Fig. 11G). However, in both *M. menzeli* and *M. obscurus* the discal setae are uniformly brownish or, if somewhat paler in the more hyaline region behind the marginal vein in *M. obscurus*, then not contrastingly white (Fig. 11G, insert). Females of *M. albitarsis* most commonly have the fore wing distinctly infuscate only behind the stigmal and postmarginal veins (Fig. 2F) similar to *M. menzeli* (Fig. 9I), though the wing can also be variably distinctly, though paler brownish-infuscate behind the parastigma and base of the marginal vein so as to be similar to *M. obscurus* (Fig. 11G). However, regardless of the visibility of the basal infuscation, females of *M. albitarsis* have white setae in the hyaline region behind the marginal vein (Fig. 2F, insert). Because of this the medial setae are less obvious than are the darker setae basally and apically, and the wing appears bifasciate even if without obvious basal infuscation. Female *M. albitarsis*, as for the other two species of the species trio, usually have quite a distinct subbasal white band on the gaster in dorsal view (Fig. 1A). However, this may not be apparent or only obscurely developed in smaller females or even larger air-dried females with the gaster collapsed or shrivelled, though in lateral view the gaster usually is quite obviously paler to whitish basally (Fig. 1B).

Within the *albitarsis* subgroup, males of *M. albitarsis* are more similar to those of *M. obscurus* than to those of *M. menzeli* in three conspicuous features: 1) scape and flagellum similarly dark (Figs 3G, 12E) *versus* scape and pedicel pale compared to brown flagellum (Fig. 10D); 2) fore wing disc with a large, quadrangular speculum extending between the parastigma and mediocubital fold (Figs 3F, 12F) *versus* disc often more-or-less uniformly setose beyond basal cell, but if with evident bare region (*e.g.*, Fig. 10F) then comparatively slender and separated from parastigma by setae; and 3) pedicel only about as long as combined length of basal two funiculars (Figs 3G, 12E) *versus* pedicel almost as long as combined length of basal three funiculars (Fig. 10D). Males of *M. albitarsis* (Fig. 3B) and *M. obscurus* (Fig. 12B) also have all femora at least partly brown to dark, whereas males of *M. menzeli* have the legs entirely pale beyond the coxae (Figs 10A, B) or only the metafemur partly dark. Males of *M. albitarsis* are differentiated from those of *M. obscurus* by fore wing colour pattern, the former having hyaline or essentially hyaline fore wings (Fig. 3F) and the latter a distinct brownish-infuscate region behind the stigmal vein (Fig. 12F).

Because of a similar leg colour pattern, males of *M. albitarsis* might also be confused with males of *M. superansi* within the *aegeriae* subgroup, but the two are differentiated by differences in size of the fore wing speculum (*cf*. Figs 3F & 15H) and relative length of the pedicel (*cf*. Figs 3G & 15F), as is discussed under the latter species.

Mesocomys breviscapis Yao, Yang & Zhao

Figs 4, 5A–I, 6, 7, 8A–D

Mesocomys breviscapis Yao, Yang & Zhao 2009: 155 (keyed), 156–157 (Chinese description), 160 (English summary), figs 4–6 (female). Described from holotype ♀ plus 11♀ and 2♂ paratypes from a single rearing (all CFRB).

Mesocomys sinensis Yao, Yang & Zhao, 2009: 156 (keyed), 157 (Chinese description), 160 (English summary), figs 7–9 (female). Described from holotype ♀ and 2♀ and 6♂ paratypes from one rearing, plus 12♀ paratypes from a separate rearing from a different locality and date but same host as the holotype (all CFRB). **New synonymy**.

Mesocomys breviscapis; Yang *et al*., 2015: 167 (keyed), 169–170 (Chinese description and data), 257 (English data summary), fig. 88 (female); Lin *et al*., 2017: 842–848 (misidentification of *M. menzeli*), fig. 1a (female, misidentification of *M. trabalae*).

Mesocomys sinensis; Yang *et al*., 2015: 167 (keyed), 172–173 (Chinese description and data), 257 (English data summary), fig. 92 (female).

Description. FEMALE (habitus: Figs 4A, B, E, F, 6A, B). Length = 2.1–3.0 mm. Head (Fig. 6C) dark with variably distinct green lustre except frontovertex with variably extensive and distinct reddish-violaceous lustre under some angles of light (Fig. 6D). Face with upper parascrobal region and frons mesh-like coriaceous imbricate to very shallowly reticulate in part (Fig. 6D), vertex more transversely alutaceous to mesh-like reticulate, parascrobal region finely but more distinctly roughened than frons, and scrobes and interantennal prominence above about level of dorsal limit of toruli similarly mesh-like imbricate to very shallowly, obscurely reticulate, the face between toruli more finely mesh-like coriaceous. Head measurements (all as ocular grid units measured from Algeria female, see Remarks): HL = 3.1, HH = 4.1, HW = 5.5, IOD = 1.7, TL = 1.1, EH = 2.8, EW = 2.0, MS = 1.2, MPOD: OOL: POL: LOL = 0.9: 0.5: 1.9: 1.5, and dso about 0.5× aod (Fig. 6D). Labiomaxillary complex dark brown or maxillary palps brown. Antenna (Figs 5B–F, 6C) with scape at least pale dorsally for distance extending beyond level of apical-most setae (Figs 5C, 6E) and sometimes up to about apical quarter pale, but pedicel and flagellum dark (Figs 5D–F, 6C); scape elongate-rectangular, at most only slightly tapered apically about 4.0–4.4× as long as wide; pedicel slightly longer than twice apical width and about as long as combined length of basal two funiculars plus basal half of third funicular to as long as combined length of basal three funiculars; flagellum with fl_1 quadrate to slightly transverse, with funiculars increasing in width apically so basal funiculars beyond fl_1 slightly longer than wide but apical funiculars quadrate to slightly transverse; clava about as long as apical three funiculars.

Mesosoma dorsally (Figs 4C, G, 6F) variably distinctly green similar to head or with slight bluish-green or coppery lustre under some angles of light; in lateral view with similar metallic lustre as dorsally or more brown with only slight metallic lustre (Figs 4D, H), with prepectus uniformly coloured (Fig. 4D) or somewhat thinner cuticle of margins brownish-hyaline (Fig. 4H), but without distinctly paler margins. Mesoscutum (Figs 4C, G, 6F) with convex anterior part of medial lobe entirely reticulate-rugulose or somewhat more finely though distinctly mesh-like coriaceous-reticulate posteriorly, depressed posterior part at least distinctly sculptured, mesh-like reticulate or reticulate-rugulose anteriorly to more finely mesh-like coriaceous posteriorly, and lateral lobe mostly mesh-like coriaceous; mesoscutum, excluding parapsidal band, more-or-less uniformly setose, though with somewhat longer setae posteriorly and bare along transscutal articulation. Scutellar-axillar complex (Figs 4C, G, 6F) with axillae obliquely alutaceous and scutellum mesh-like coriaceous to coriaceous-imbricate mediolongitudinally but with more elongate sculpture on sides; setose laterally with dark hair-like setae becoming longer posteriorly. Acropleuron finely mesh-like sculptured, though with more minute sculpture mesally below level of fore and hind wing bases and much larger coriaceous-reticulate sculpture posteriorly (Figs 4D, H). Legs with pro- and metafemora brownish to dark (Figs 4B, F), but mesofemur similarly pale, yellowish (Figs 4B, E, F) to brownish-orange (Fig. 6A), as remainder of middle leg, including tibial spur, except for dark mesotarsal pegs (Fig. 4E); pro- and metatibiae pale or variably distinctly and extensively infuscate similar to femora, but tarsi pale. Fore wing (Figs 5A, 6G) uniformly hyaline other than for yellowish venation; costal cell without (Figs 8B–D) or with up to 2 dorsal setae (Fig. 8A: upward directed arrows) basal to setae in front of parastigma; basal cell sometimes (examined *M. sinensis* paratype) with about basal half bare except for broadly separated row of setae along mediocubital fold basally and apically (Fig. 8D), though

more commonly (see Remarks) entirely setose between submarginal vein and mediocubital fold (Figs 8A–C) except sometimes for small, inconspicuous bare region basally (Fig. 8A: downward directed arrow) and with setae along mediocubital fold at most only narrowly separated medially (Fig. 8C: arrows); fore wing measurements: cc: mv: pmv: stv = 3.9–4.0: 3.0–3.3: 1.7–1.9: 1.0.

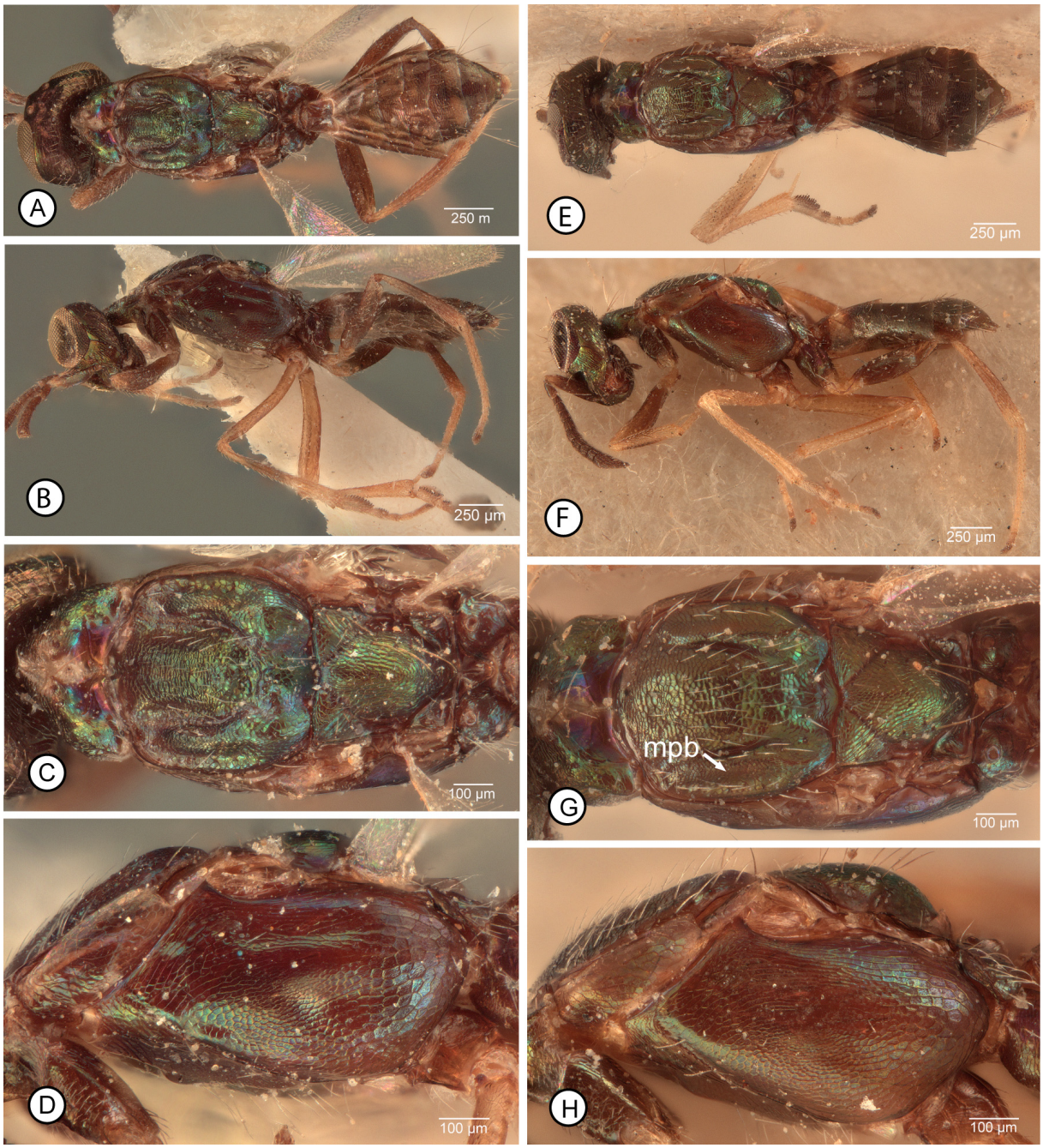

FIGURE 4A–H. *Mesocomys breviscapis* ♀. ***A–D***, *M. breviscapis* (PT, #98): **A**, dorsal habitus; **B**, lateral habitus; **C**, mesosoma, dorsal; **D**, mesosoma, lateral. **E–H**, *M. sinensis* (PT, #95): **E**, dorsal habitus; **F**, lateral habitus; **G**, mesosoma, dorsal [mpb = parapsidal band]; **H**, mesosoma, lateral. Figure caption abbreviation: PT = paratype.

Gaster in dorsal view dark brown except one or more apical tergites sometimes with slight greenish lustre and syntergal flange variably distinctly paler, yellowish-brown to yellow, and usually with evident, transverse, subbasal white band (Fig. 5H), though sometimes only slightly paler subbasally (Fig. 5I) or superficially entirely brown (Fig. 5G) in air-dried individuals; in lateral view with dorsally tapered subbasal white band because side of Gt_1 white apically and St_1 extensively white; Gt1 dorsally shiny and bare, though at least obscurely mesh-like coriaceous, and sometimes with subparallel or only slightly divergent sides relative to more

uniformly ovate, more distinctly mesh-like coriaceous to transversely coriaceous-reticulate Gt_2–syntergum; Gt_2–syntergum with at least one row of hair-like setae across surface. Ovipositor sheaths pale, yellowish.

MALE (based on *M. sinensis* paratype, habitus: Fig. 7D). Length about 2 mm. Head (Fig. 7C) mostly green but with slight reddish-violaceous lustre under some angles of light, most extensively on frons. Face with upper parascrobal region and frons distinctly roughened, mesh-like imbricate to inconspicuously reticulate; vertex more transversely reticulate to imbricate-strigose, rounded into occiput; scrobal depression and most of interantennal prominence similarly mesh-like reticulate to imbricate, but more finely mesh-like coriaceous ventrally between toruli. Head measurements: HL = 2.7, HH = 3.5, HW = 4.8, IOD = 1.9, EH = 2.3, EW = 1.9, MS = 1.4, MPOD: OOL: POL: LOL = 1.1: 0.5: 2.0: 1.4, and dso subequal to aod (Fig. 7C). Labiomaxillary complex dark brown. Antenna (Fig. 7G) dark brown except extreme apex and base of scape pale; scape about 3× as long as wide; pedicel slightly more than twice as long as apical width and about 0.9× combined length of basal three funiculars; flagellum clavate-filiform, only slightly widened toward clava; fl_1 transverse, fl_2 and fl_3 slightly transverse to subquadrate depending on view, but subsequent funiculars quadrate to slightly longer than wide apically, and clava (collapsed) about 2.1× as long as wide and about 0.6× (right antenna) to 0.8× (left antenna) combined length of apical three funiculars.

Mesosoma dorsally (Fig. 7E) similarly green as head except scutellum medially with variably extensive and distinct coppery lustre depending on angle of view; in lateral view similar in colour to dorsal surface, and mesopleurosternum with Y-like set of pale lines (Fig. 7D). Mesonotum (Fig. 7E) with mesoscutal medial lobe distinctly reticulate to reticulate-rugulose. Scutellar-axillar complex (Fig. 7E) with axillae anteriorly similarly reticulate as mesoscutal medial lobe, but posteriorly more reticulate-imbricate and scutellum mesh-like coriaceous medially and posteriorly but more imbricate laterally. Legs beyond coxae similarly pale except metafemur mostly dark, paler apically and basally (Fig. 7D). Fore wing (Fig. 7F) hyaline; costal cell dorsally with 1 (right wing, Fig. 7H) to 3 (left wing, Fig. 7F) setae off-set from setae paralleling leading margin (Fig. 7H: ser) basal to setae in front of parastigma; basal cell appearing almost entirely setose (left wing, Fig. 7F) or more extensively bare over about basal half (right wing, Fig. 7H) (see Remarks); speculum comparatively small and inconspicuous, separated from base of parastigma by more than one row of setae (Figs 7F, H); measurements of cc: mv: pmv: stv (left wing) = 3.6: 2.3: 2.1: 1.0.

Gaster dark brown.

Type material examined. *Mesocomys breviscapis*. Paratypes examined (2♀ CFRB; CNC-Photo 2018-98, -99): label data in Chinese, except determination label with name written as *Mesocomys breviscapus* [*sic*], publication-cited data: [China], Hebei Province, Xinglong County, 40.42°N, 117.48°E, 28.IX.1980, BA Hong-Ze, collected and reared from eggs of *Dendrolimus tabulaeformis* Tsae & Liu.

Mesocomys sinensis. Paratypes examined (1♀, 1♂ CFRB; ♀: CNC-Photo 2098-85, ♂: CNC-Photo 2018-97) from the same rearing as the holotype: label data in Chinese, publication-cited data: [China], Shaanxi Province, Liuba County, Miaotaizi, 33.65°N, 106.95°E, 20.IV.1985, Qi-Ji Hu and Zhong-Qi Yang, collected and reared from eggs of *Dendrolimus tabulaeformis* Tsae & Liu.

Other material examined. ORIENTAL. **CHINA**. ***Sichuan***. Qingchengshan, 19.X.1983, Changfang Li (1♀ IZCAS, CNC Photo 2018-96). ***Zhejiang***. Mt. Fengyang, Malaise trap, 7-10.VIII.2003 (1♀ FAFU).

PALAEARCTIC. **ALGERIA**. Biskra, 1917 (1♀ NHMUK, NHMUK 011515672, CNC Photo 2018-100).

Distribution. ORIENTAL. China [*Sichuan, *Zhejiang]. PALAEARCTIC: *Algeria, China [Hebei, Shaanxi (Yao *et al*. 2009; Yang *et al.* 2015)].

Biology. Host: LEPIDOPTERA. **Lasiocampidae**. *D. tabulaeformis* Tsae & Liu (Yao *et al*. 2009).

Remarks. My concept of *M. breviscapis* is based on five females and one male consisting of two *M. breviscapis* female paratypes, one female and one male *M. sinensis* paratype, plus one other female from China and Algeria. I identify the latter two females as *M. breviscapis* based on their similar size, leg colour patterns, and fore wing setal patterns to the *M. breviscapis* paratypes, as is discussed more fully below. Additionally, the colour photographs of females in Yang *et al*. (2015) identified as *M. breviscapis* (fig. 88), *M. sinensis* (fig. 92) and possibly *M. trabalae* (fig. 90) (see further under *M. superansi* and *M. trabalae*) fit my concept of *M. breviscapis*. However, most of the specimens identified in Lin *et al*. (2017, table 2, species 5) as *M. breviscapis* are a misidentification of *M. menzeli* (see further under the latter species), except the photographed female (Lin *et al*. 2017, fig. 1a) appears to be *M. trabalae*, a species that was also reared by Lin *et al*. (2017) (see further under the latter species). For this reason I list the distribution and host data reported for *M. breviscapis* by Lin *et al.* (2017) under *M. menzeli*. The above publications demonstrate an uncertain concept of *M. breviscapis*, and my concept of the species is similarly uncertain. My uncertainty results not only because I have seen so few specimens but also because of apparent discrepancies in

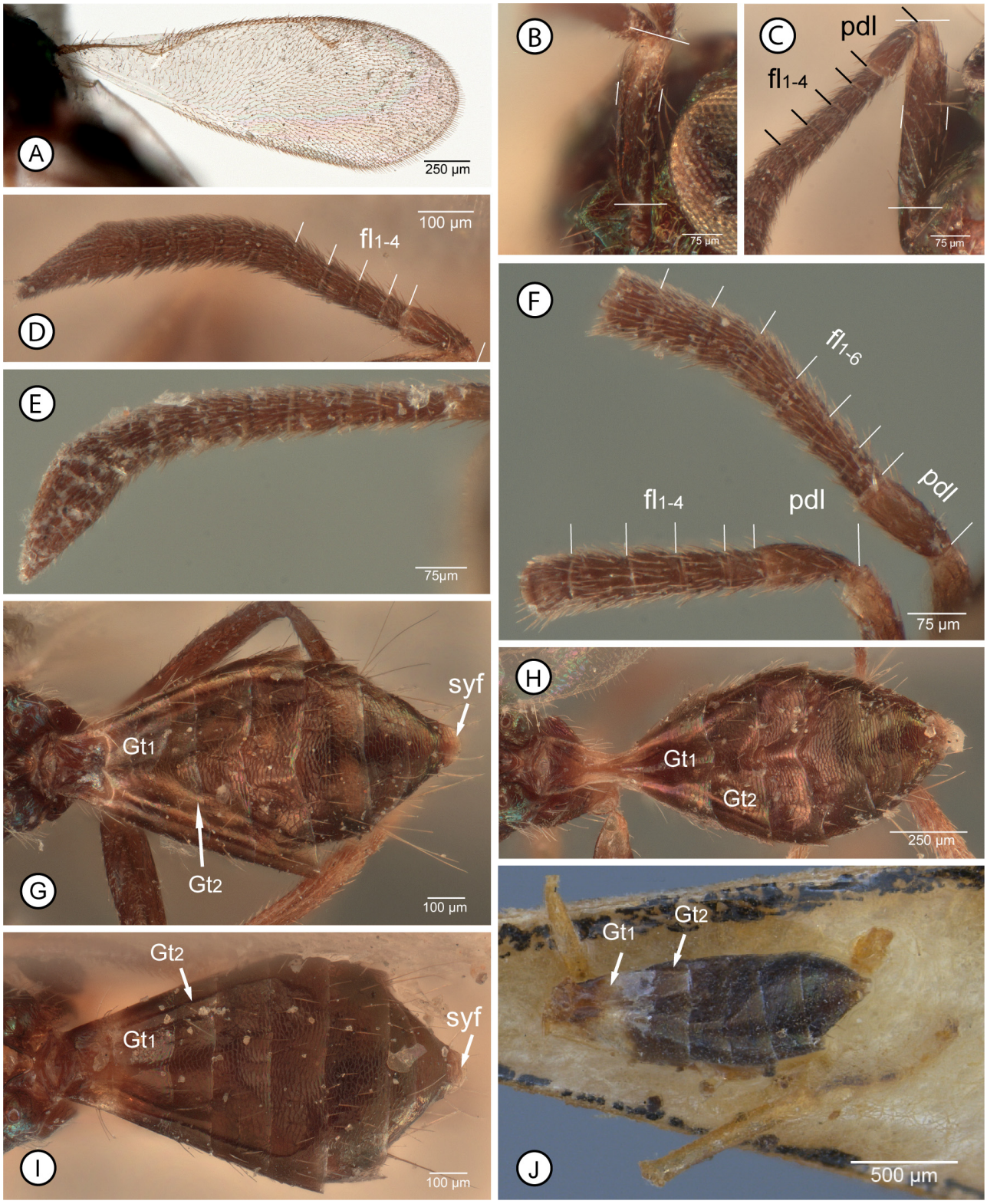

FIGURE 5A–J. *Mesocomys* spp. ♀. ***A–I***, *M. breviscapis*: **A**, fore wing (PT, #99); **B**, scape, outer view (PT, #98); **C**, scape and basal funiculars, outer view (*M. sinensis* PT, #95); **D**, pedicel and flagellum (*M. sinensis* PT, #95); **E**, flagellum (PT, #99); **F**, partial antennae (PT, #98); **G**, gaster, dorsal (PT, #98); **H**, gaster, dorsal (PT, #99); **I**, gaster, dorsal (*M. sinensis* PT, #95). **J**, *M. aegeriae*, gaster and parts of legs remaining of holotype. [See 'Methods' and Table 1 for explanation of abbreviations; white lines on Figs 5B & C indicate length and width limits of scape, whereas other lines on Figs 5C, D & F indicate basal and apical limits of pedicel and basal funiculars; figure caption abbreviation: PT = paratype.]

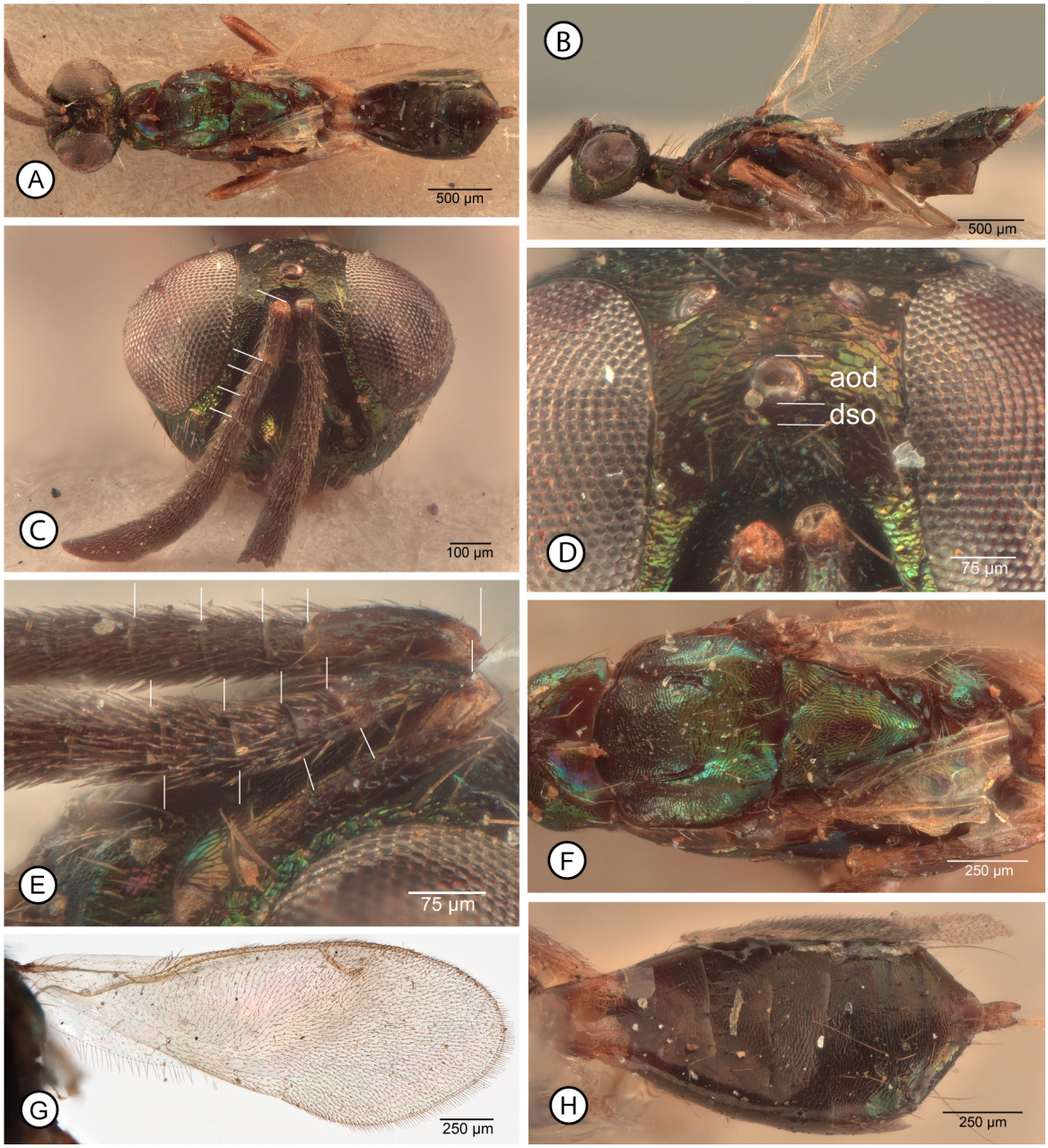

FIGURE 6A–H. *Mesocomys breviscapis* ♀ (#100) [Algeria]. **A**, dorsal habitus; **B**, lateral habitus; **C**, head, frontal; **D**, frontodorsal part of head; **E**, basal half of antennae [white lines indicate basal and apical limits of basal three funiculars of both antennae, including dorsal and ventral lengths for left antenna]; **F**, mesosoma, dorsal; **G**, fore wing; **H**, gaster, dorsal. [See 'Methods' and Table 1 for explanation of abbreviations.]

the original descriptions and key to species by Yao *et al*. (2009) that make inferences of intra- *versus* interspecific variation among what they described as *M. breviscapis*, *M. sinensis* and *M. trabalae* unreliable. Further, the head is strongly collapsed medially in all three examined *M. breviscapis* and *M. sinensis* paratype females and the non-type female from China is so strongly contorted that the end of the gaster touches the head so that dorsal features are not visible. Consequently, accurate head measurements are possible only for the Algeria female and these measurements are used for the female description. The head measurements given for the male description are also based on just a single individual, the *M. sinensis* paratype.

As noted under *M. aegeriae*, Yao *et al*. (2009) differentiated *M. breviscapis* from *M. aegeriae*, *M. sinensis* and *M. trabalae* by relative length of the scape, relative length of the first and second funiculars, and by costal cell setal pattern. However, because the examined *M. breviscapis* and *M. sinensis* paratype females have their heads strongly collapsed it is not possible to accurately evaluate the relative position of the apex of the scape to that of the anterior

ocellus and vertex. Regardless, this feature is at least partly affected by how the scape is held relative to the frontal surface of the head and the direction and angle from which the head is viewed (see Remarks for *M. aegeriae*). There does, however, appear to be a difference in the scape length to width ratios illustrated by Yao *et al*. (2009, figs 4, 7) for *M. breviscapis* and *M. sinensis*, which I measure from the photographs as 4.1× longer than wide in fig. 4 for *M. breviscapis* and 4.4× longer than wide in fig. 7 for *M. sinensis*. Microscope measurements from a direct lateral view of the outer surface of the left scape of the one female *M. breviscapis* paratype examined for which accurate scape measurements can be made (Fig. 5B) indicates a scape that is 4.0× as long as wide, which is very similar to that of the photograph. However, the same measurements for the examined *M. sinensis* paratype indicates a scape that is only 4.25× as long as wide (Fig. 5C). The non-type female from China also has a scape that is 4.1× as long as wide, whereas it is 4.2× as long as wide for the female from Algeria, and thus intermediate between the ratios of the measured *M. breviscapis* and *M. sinensis* paratypes. Further, the difference in relative length of the scape among the measured females is comparatively small, and within the range of what might be expected from intraspecific variation based on measurements made for females of *M. superansi* (4.1–4.4×) and *M. trabalae* (4.0–4.5×). As also discussed under *M. aegeriae*, the difference in relative lengths of the first and second funiculars for the examined *M. breviscapis* and *M. sinensis* paratypes are at least not conspicuous (*cf*. Figs 5C & F), and observation of more numerous females identified as *M. superansi* and *M. trabalae* indicates relative length of the funiculars varies to some extent for various reasons. Variation in funicular length is at least partly correlated with body size, but can even appear to differ between the two antennae of the same individual. Because the funiculars articulate with each other they can be held at slightly different angles relative to each other in either antenna, resulting in slightly different dorsal *versus* ventral lengths and a different appearance depending on the angle of view (*e.g.*, Fig. 6E). Finally, Yao *et al*. (2009) keyed *M. breviscapis* females as having the basal two-thirds of the costal cell bare; however, the English description states "costal cell having a row of hairs on lower side at most, *basal cell never hairy proximally half* (my italics), speculum present", as does the Chinese description. The discrepancy between the key and description suggests that "costal cell" given in the key either was a *lapsus* for the basal cell or, perhaps less likely, that the statement in the description that the basal half of the basal cell is bare was a *lapsus* for the dorsal setal pattern of the costal cell. Regardless, the described basal cell setal pattern does not match the observed setal patterns of the two examined *M. breviscapis* paratypes, which have the basal cell almost completely setose anterior of the mediocubital fold except for quite a small and inconspicuous bare region basally behind the submarginal vein (Fig. 8A: larger arrow). This setal pattern is similar to the setal patterns exhibited by the non-type female from China (Fig. 8B) and from Algeria (Fig. 8C). The difference between the described basal cell setal pattern for *M. breviscapis* by Yao *et al*. (2009) and that exhibited by the two examined paratypes (Fig. 8A) suggests that the original description may have been based on the holotype and that at least some of the paratypes have a much more extensively setose basal cell, including the two examined paratypes.

In addition to a possible discrepancy between the key and description relative to costal cell *versus* basal cell setation, and a definite discrepancy between the described and observed setal patterns of the basal cell for *M. breviscapis*, neither setal pattern was mentioned in the second half of the couplet leading to *M. sinensis* and *M. trabalae*. No English description of this feature was given for *M. sinensis*, but the Chinese description states the costal cell has at least one complete row of setae along its length ventrally, and dorsally has setae over the apical third but is bare over the basal two-thirds. The description also states that the basal cell has several setae within its basal two-thirds and the apical third densely setose. These described features do match the single examined *M. sinensis* paratype (Fig. 8D), which has the costal cell dorsally setose in front of the parastigma but bare basal to the base of the parastigma (Fig. 8D), and the basal cell setose over about its apical half (Fig. 8D: right-directed arrows point to basal-most setae within the basal cell and upward directed setae point to apical-most setae along the mediocubital fold), but bare over at least its basal half except for five setae near the mediocubital fold basally (Fig. 8D: upward directed arrows), and a single, somewhat more anteriorly placed seta within the cell submedially (Fig. 8D: downward directed arrow). The Chinese description of *M. trabalae* describes the costal cell as having several rows of setae ventrally but dorsally densely setose only apically, and the basal cell as having several scattered setae, open ventrally, and without a speculum. I am uncertain as to what Yao *et al.* (2009) refer to relative to presence or absence of a speculum in females because the fore wing of females is always uniformly setose below the parastigma into the disc (Figs 8A–H), unlike that of males (see below). However, description of the basal cell setal pattern does match the examined *M. trabalae* paratype and other non-type females from the original rearing, which have the basal cell broadly bare medially (Fig. 8E) or at least broadly bare medially along the mediocubital fold (open posteriorly) if with scattered setae within the cell (Fig. 8F).

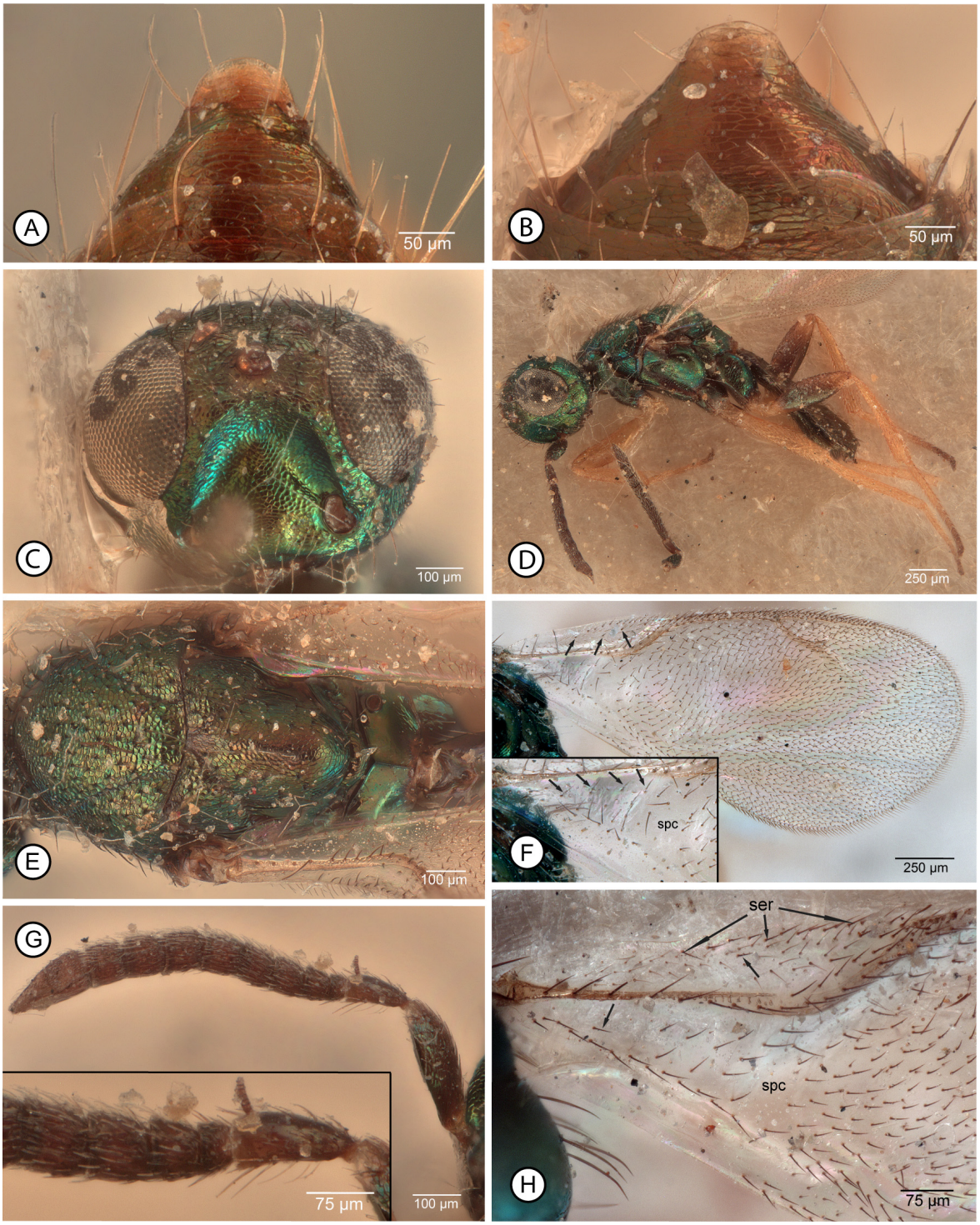

FIGURE 7A–H. *Mesocomys breviscapis*. ***A & B***, ♀ gastral apex: **A**, *M. breviscapis* PT (#98); **B**, *M. sinensis* PT (#95). ***C–H***, male (*M. sinensis* PT, #97): **C**, head, frontal; **D**, lateral habitus; **E**, mesosoma, dorsal; **F**, left fore wing from ventral view [insert: enlargement of basal cell and speculum]; **G**, antenna [insert: pedicel and basal four funiculars]; **H**, right fore wing from dorsal view. [See 'Methods' and Table 1 for explanation of abbreviations; arrows in Figs 7F & H point to dorsal setae in costal and basal cells; figure caption abbreviation: PT = paratype.]

As noted above, the examined *M. sinensis* female paratype has the costal cell dorsally bare basal to the setae in front of the parastigma (Fig. 8D), as does one of the examined *M. breviscapis* paratypes and the non-type females from China (Fig. 8B) and Algeria (Fig. 8C). However, the other examined *M. breviscapis* paratype has two dorsal setae (Fig. 8A: upward directed arrows) basal to the setae in front of the parastigma. The examined *M. trabalae*

paratype female has the costal cell bare dorsally except for setae in front of the parastigma (*cf*. Fig. 8E). However, some of the non-type females from the same rearing as the type specimens have up to four setae dorsally within the costal cell basal to the setae in front of the parastigma, and one female I identify as *M. trabalae* from Japan has about ten setae dorsally in the costal cell apically other than in front of the parastigma (Fig. 8F, insert). Even if this latter female is incorrectly identified to species, the females from the original *M. trabalae* rearing show that setal patterns of the costal cell is more variable than described, as is basal cell setal pattern.

Yao *et al*. (2009) differentiated *M. trabalae* from *M. sinensis* in their key by body size (see under *M. aegeriae*), body colour (bright green *versus* dark blue-green, respectively), and by setal patterns of the costal cell and basal cell in males. Males of *M. trabalae* were keyed as having the basal and costal cells covered with setae and lacking a speculum, whereas males of *M. sinensis* were keyed as having the basal half of the costal cell bare and having a speculum. Based on observed females, head and mesosomal colour is variable and some *M. trabalae* females can have quite distinct bluish to purple lustre (Figs 16A, C, D). As for male fore wing setal pattern, all *aegeriae*-subgroup males have at least a small, circular to oval speculum on the disc adjacent to an at least apically setose basal cell. The examined *M. sinensis* male paratype does have quite a conspicuous, higher than wide speculum (Figs 7F, H: spc) that is at least as large as that of examined males of the other species (Figs 15H, 17G, H: spec), and thus does not contradict the key. However, because the two male paratypes from the original rearing of *M. breviscapis* were not examined it is unknown whether these have a speculum similar to the examined *M. sinensis* male. Further, size of the speculum can differ even between the two wings of a single male. The right wing of the male from Thailand I identify as *M. superansi* has a transverse-oval speculum that is separated from the parastigma by two rows of setae (Fig. 15H: spc), whereas the left wing has a larger, higher than wide speculum because there is only a single row of setae adjacent to the parastigma (Fig. 15H, insert: spc).

Similarly to females, males of all *aegeriae*-subgroup species have one to two rows of setae ventrally along the length of the costal cell, with the setae becoming more numerous apically in front of the parastigma, and dorsally there is a row of setae immediately in front of the parastigma. However, unlike females, there is also a row of setae dorsally that closely parallel the leading margin over about the apical half of the costal cell (Figs 7H, 15H: ser). Like females, males differ in whether there are additional setae dorsally within the costal cell basal to the setae in front of the parastigma that are more-or-less distinctly off-set from the more marginal setae. In the examined *M. sinensis* paratype male, the right wing costal cell has a single off-set seta (Fig. 7H: upward directed arrow) in front of the parastigma, whereas the left wing (seen only from ventral view) appears to have three dorsal setae (Fig. 7F: upward directed arrows). The two wings differ even more conspicuously in setation of the basal cell. The setation of the right wing is similar to the original description because almost the basal half of the basal cell is bare anterior to a completely setose mediocubital fold, except for a single seta within the cell (Fig. 7H: downward directed arrow) that is off-set slightly from the other setae along the mediocubital fold. However, the basal cell of the left wing appears almost completely setose because of a complete row of setae along the length of the cell behind the submarginal vein (Fig. 7F, insert: downward directed arrows). The examined paratype male of *M. trabalae* closely matches the original description because the basal cell is entirely, uniformly setose and, more conspicuously, the costal cell dorsally is much more extensively setose than for the *M. sinensis* paratype, being almost completely setose dorsoapically (right wing with at least 15 setae dorsally within cell excluding setae along margin), with the setal region tapered basally over about its apical half (Fig. 17H). Although this difference is certainly conspicuous between the two male paratypes, other males I identify as *M. trabalae* usually have the costal cell less extensively setose dorsally. However, most often there is an obvious row of several setae behind the setal row paralleling the margin, though some males have as few as three dorsal setae within the cell more toward the base of the parastigma (Fig. 17H, insert: upward directed arrows). The latter setal pattern is thus more similar to that of the left wing of the *M. sinensis* male paratype (Fig. 7F). Males of *M. trabalae* therefore also demonstrate variation in costal setal pattern but, as discussed under *M. aegeriae* and *M. trabalae*, the limits of intraspecific *versus* interspecific variation remain uncertain for both costal and basal cell setal patterns. Two of the three males I identify as *M. superansi* have one to three dorsal setae off-set from the more marginal setae within the costal cell (Fig. 15H: upward directed arrows), the number sometimes differing between the two wings of the same individual, whereas one has several slightly off-set setae (see under *M. superansi*).

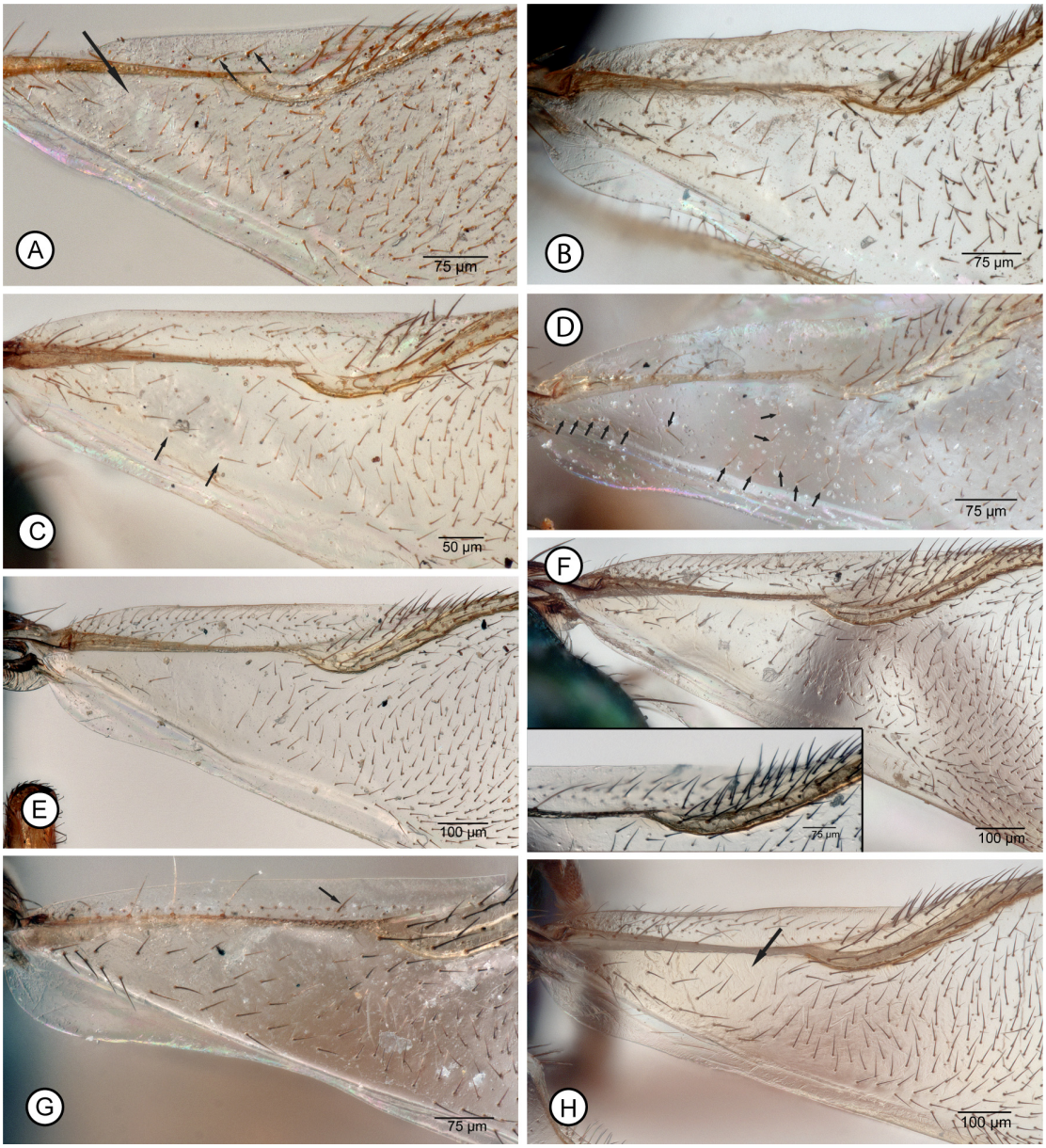

FIGURE 8A–H. *Mesocomys aegeriae*-subgroup species, basal part of fore wing, ♀. **A**, *M. breviscapis* (PT, #98); **B**, *M. breviscapis* (#96) [China]; **C**, *M. breviscapis* (#100) [Algeria]; **D**. *M. breviscapis* (*M. sinensis* PT, #95); **E**, *M. trabalae* (#23) [China]; **F**, *M. trabalae* (#102) [Japan; insert: enlargement of apex of costal cell]; **G**, *M. superansi* (#103) [China]; **H**, *M. superansi* (#104) [Thailand]. [Downward directed arrow in Figs A & H points to bare region, whereas other arrows in figures point to dorsal setae within costal and basal cells; figure caption abbreviation: PT = paratype.]

Although not included as a key character, Yao *et al*. (2009) described the male fore wing of *M. trabalae* as having a brown region under the stigmal vein. Many examined males have quite a distinct brownish-infuscate region (Fig. 17G), but sometimes (including in the examined paratype male of *M. trabalae*) it is so faint that it is difficult to be certain whether slight infuscation is present or absent. Infuscation behind the stigmal vein was also described for males of *M. superansi* (Fig. 15G), but one male with the same collection and rearing data as the type material has essentially uniformly hyaline fore wings (see under *M. superansi*). Whether or not there is noticeable infuscation behind the stigmal vein is thus indicated as yet another variable feature for males of at least some species. Fore wing infuscation was described as lacking from *M. breviscapis* males; it was not described for *M. sinensis* males, but the examined male has uniformly hyaline fore wings (Fig. 7F). There does appear to be slight infuscation behind the stigmal vein in Fig. 7F, but the right fore wing in ventral view appears uniformly hyaline and the infuscation in Fig. 7F likely is an artefact resulting from the leading margin of the wing being glued to the card rectangle and the

rest of the wing being angled away from the card beyond the stigmal vein. Presence or absence of male fore wing infuscation may also be at least partly correlated with body size.

As discussed above, condition of the examined female paratypes of *M. breviscapis* and *M. sinensis* does not permit appraisal of the length of the scape relative to the anterior ocellus and vertex in any of the specimens. There is a conspicuous difference in observed basal cell setal patterns between the examined paratype females of *M. breviscapis* (Fig. 8A) and *M. sinensis* (Fig. 8D), but the observed condition for *M. breviscapis* does not match the original description, suggesting the setal pattern is more variable than described. Further, both costal and basal cell setal patterns differ between the two wings of the examined male paratype of *M. sinensis* (Figs 7F, H), and the *M. superansi* male from Thailand shows that size of the speculum can even vary between the two wings of a single individual (Fig. 15H). There is also noticeable variation in both costal cell and basal cell setal patterns for *M. trabalae* females (Figs 8E, F). Both *M. breviscapis* and *M. sinensis* were reared originally from the same host, *D. tabulaeformis*, and the three examined paratype females are very similar in size and leg colour pattern (*cf*. Figs 4A–D with Figs 4E–H). Although additional, freshly collected and well-preserved and mounted specimens females reared from *D. tabulaeformis* are necessary to more accurately assess relative length of the scape, relative length of the funiculars, and basal and costal cell setal patterns for both sexes, I do not currently interpret any of these features as reliable specific features. I therefore newly synonymize the name *M. sinensis* under *M. breviscapis*, though I retain *M. trabalae* for the reasons discussed under that species.

The female from Algeria (Figs 6A–H) I identify as *M. breviscapis* certainly results in a highly anomalous collection record for the species, but it closely resembles the examined *M. breviscapis* paratypes in most features, including having a very similar basal cell setal pattern (Fig. 8C). The relative length of the pedicel is slightly longer than for the examined females from China, fully equalling the combined length of the basal three funiculars under most angles of view (Figs 6C, E) compared to about the combined length of the basal two funiculars and basal half of the third funicular (Figs 5C, D, F), but this difference is not great. The middle femora and tibiae are also slightly infuscate, light brownish except for a paler yellow knee (Figs 6A, B), whereas the Chinese females have uniformly yellowish femora and tibiae.

Mesocomys menzeli (Ferrière)

Figs 9, 10

Anastatus menzeli Ferrière, 1930b: 354–355. Described from 7♀ and 4♂ syntypes; lectotype ♀, here designated (NHMUK).
Mesocomys menzeli (Ferrière); Bouček, 1988: 554 (new combination); Narendran & Sheela, 1995: 311 (keyed).
Mesocomys breviscapis; Lin *et al*., 2017: 842–848 (misidentification, except fig. 1a misidentification of *M. trabalae*).

Description. FEMALE (habitus: Figs 9A, B). Length = 2.1–4.1 mm. Head (Figs 9E–G) dark with variably extensive and distinct metallic lustres, variably extensively green to bluish-green on face below frontovertex though usually with blue to violet or purple lustre dorsally over interantennal prominence and/or scrobes, and sometimes also with green and/or reddish-violaceous lustre on frontovertex (Figs 9F, G) under some angles of light. Face with upper parascrobal region and frons mesh-like coriaceous to very shallowly coriaceous-reticulate or imbricate (Figs 9F, G) with some sculpture formed by slightly raised ridges, but at most only very slightly roughened, vertex (Fig. 9F) more transversely alutaceous to alutaceous-strigose, parascrobal region mostly much more distinctly roughened than frons, rugulose to transversely reticulate-strigose, and scrobes and interantennal prominence above about level of dorsal limit of toruli imbricate to reticulate-imbricate, the face between toruli much more minutely mesh-like coriaceous. Head measurements: HL = 2.4–4.1, HH = 3.1–5.7, HW = 4.3–8.0, TL = 0.9–1.5, EH = 2.2–4.2, EW = 1.9–3.6, MS = 1.2–2.0, IOD 0.33–0.40× HW, MPOD: OOL: POL: LOL = 1.0: 0.5–0.9: 1.8–2.0: 1.4–1.6, and dso 0.6–1.0× aod (Fig. 9G). Labiomaxillary complex with maxillary palps variably dark brown and labial palps paler or both palps pale, yellowish. Antenna (Figs 9C–E) with scape variably extensively pale apically and usually pedicel and most of flagellum except clava pale, yellowish (Fig. 9C), with clava at least dorsally and scape basally darker brown (darker part of scape often also with some green lustre), but rarely most of pedicel and flagellum variably dark brown (Fig. 9D); scape elongate-rectangular, only slightly tapered apically, about 3.5–4.0× as long as greatest width; pedicel about twice as long as apical width and about as long as basal two funiculars; flagellum with fl_1 at least as long as wide and funiculars increasing in width apically so basal funiculars beyond fl_1 quadrate to slightly longer than wide but increasingly more quadrate to transverse apically; clava about as long as apical three funiculars.

Pronotum dorsally variably extensively brown though often with some bright green, blue and/or reddish-violaceous to violet lustre at least laterally; mesonotum (Fig. 9H) at least with depressed part of mesoscutal medial lobe distinctly bright green or blue to reddish-violaceous or violet, with anterior convex part of medial lobe and lateral lobes dark brown to variably distinctly green to reddish-violaceous under different angles of light, and scutellar-axillar complex usually with more coppery to reddish-violaceous lustre anteriorly and green to bluish-green lustre posteriorly; in lateral view mesosoma mostly dark brown though usually at least lateral panel of pronotum and acropleuron with similar metallic lustres as mesothorax dorsally. Mesoscutum (Fig. 9H) with convex anterior part of medial lobe mesh-like coriaceous to mesh-like coriaceous-imbricate, depressed posterior part similarly but much more finely mesh-like coriaceous to smooth and shiny medially, and lateral lobe also mesh-like coriaceous; mesoscutum, excluding parapsidal band, similarly setose with brown hair-like setae except depressed posterior part of medial lobe usually more sparsely setose with longer, more bristle-like setae. Scutellar-axillar complex (Fig. 9H) with axillae obliquely alutaceous to alutaceous-strigose and scutellum coriaceous to coriaceous-imbricate, the sculpture usually more-or-less elongate though sometimes more isodiametric mesh-like anteromedially or medially; setose laterally with brown hair-like setae. Acropleuron finely mesh-like sculptured, though with more minute sculpture mesally below level of fore and hind wing bases and larger, more isodiametric, coriaceous-reticulate sculpture posteriorly. Front leg entirely pale beyond coxa or only femur variably extensively dark (Fig. 9B). Middle leg sometimes entirely pale beyond coxa except for dark mesotarsal pegs, though often tibia medially and/or femur variably extensively brownish to dark, but tibial spur pale. Hind leg (Fig. 9B) beyond coxa at least with outer surface of femur extensively dark and sometimes tibia variably darkly and extensively brown mesally, but tarsus pale. Fore wing of smallest individuals sometimes almost completely hyaline with only inconspicuous brownish-infuscate region behind stigmal vein, but at least larger individuals with basal cell light brownish-infuscate basally and disc more distinctly brownish-infuscate behind stigmal and postmarginal veins (Fig. 9I), the setae within infuscate region usually darker, but otherwise all setae uniformly brown to variably pale without region of distinctly contrasting white setae behind marginal vein; costal cell bare dorsally excluding setae in front of parastigma; basal cell of smallest individuals variably extensively setose, sometimes more-or-less completely setose along mediocubital fold and with scattered setae within basal cell, but larger individuals with basal cell bare or almost so, with only a few setae apically below parastigma and 1 to a few setae basally on mediocubital fold (Fig. 9I); stigmal vein curved apically into uncus; measurements of cc: mv: pmv: stv = 3.4–4.8: 2.8–3.8: 1.8–2.1: 1.0.

Gaster mostly dark brown but in dorsal view with variably large and conspicuous subbasal white band (Fig. 9A) formed by apically whitish-hyaline Gt_1, and in lateral view (Fig. 9B) St_1 entirely white and Gt_1 apically with vertical sides white; Gt_2–syntergum dark brown except syntergal flange yellowish-hyaline and apical tergites sometimes with slight greenish lustre; Gt_1 smooth, shiny and bare, and, at least when raised above Gt_2, noticeably hyaline apically, and usually comparatively narrow with subparallel sides relative to more uniformly ovate Gt_2–syntergum; Gt_2–syntergum similarly mesh-like coriaceous to alutaceous and Gt_3 or Gt_4–syntergum with at least one row of hair-like setae across surface. Ovipositor sheaths pale, yellowish.

MALE (habitus: Figs 10A, B). Length = 1.8–3.4 mm. Head (Fig. 10C) mostly green to blue with limited purple lustre except frons or frontovertex sometimes variably extensively dark or with slight coppery to reddish-violaceous lustre (Figs 10A, C). Face with upper parascrobal region and frons mesh-like coriaceous in smaller individuals to slightly roughened, coriaceous-imbricate, in larger individuals; vertex transversely alutaceous-imbricate in smaller individuals to strigose in larger individuals, but rounded into occiput; scrobal depression and most of interantennal prominence similarly mesh-like reticulate to imbricate, but more finely mesh-like coriaceous ventrally between toruli. Head measurements: HL = 2.5–4.0, HH = 3.3–5.4, HW = 4.3–7.0, EH = 2.1–3.5, EW = 1.9–2.9, MS = 1.1–1.8, IOD 0.37–0.40× HW, MPOD: OOL: POL: LOL = 1.0: 0.5–0.7: 1.7–1.9, 1.2–1.3, and dso subequal to aod. Labiomaxillary complex yellow. Antenna (Fig. 10D) with scape and pedicel yellow and flagellum variably dark brown; scape about 2.5–2.7× as long as wide; pedicel about 2.4–2.5× as long as apical width and about 0.8–0.9× as long as combined length of first three funiculars; flagellum clavate-filiform, slightly widened to clava; fl_1 strongly transverse and much smaller than fl_2, fl_2–fl_8 subquadrate, slightly wider to slightly longer than wide, and clava about 2.2–2.6× as long as wide and about 0.8–1.0× combined length of apical three funiculars.

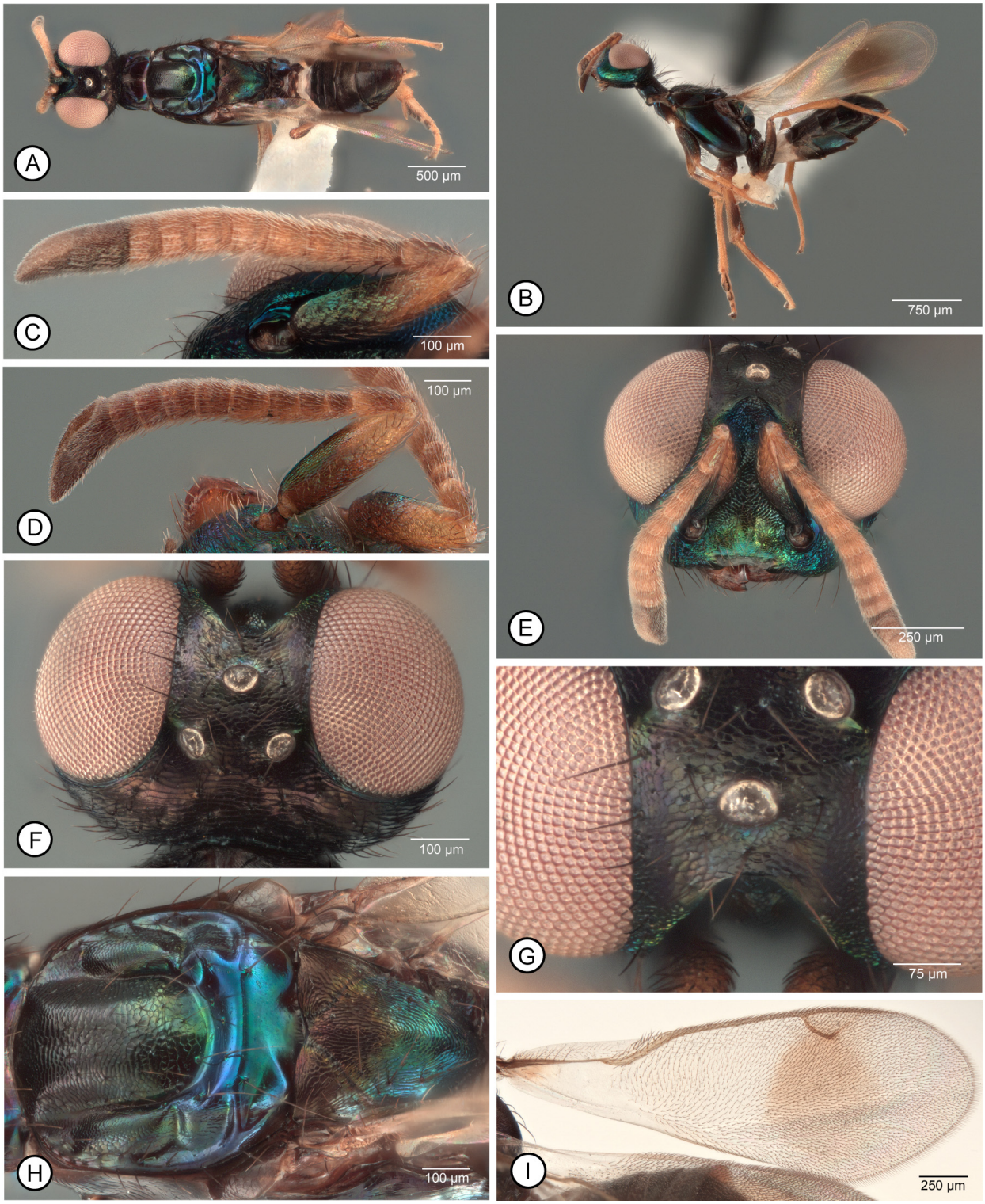

FIGURE 9A–I. *Mesocomys menzeli* ♀. **A**, dorsal habitus (#32); **B**, lateral habitus (#32); **C**, antenna, inner view (#32); **D**, antenna, outer view (#59); **E**, head and antennae, frontal (#32); **F**, head, dorsal (#32); **G**, frontodorsal part of head (#32); **H**, mesonotum (#32); **I**, fore wing (#32) [most setae missing from basal cell].

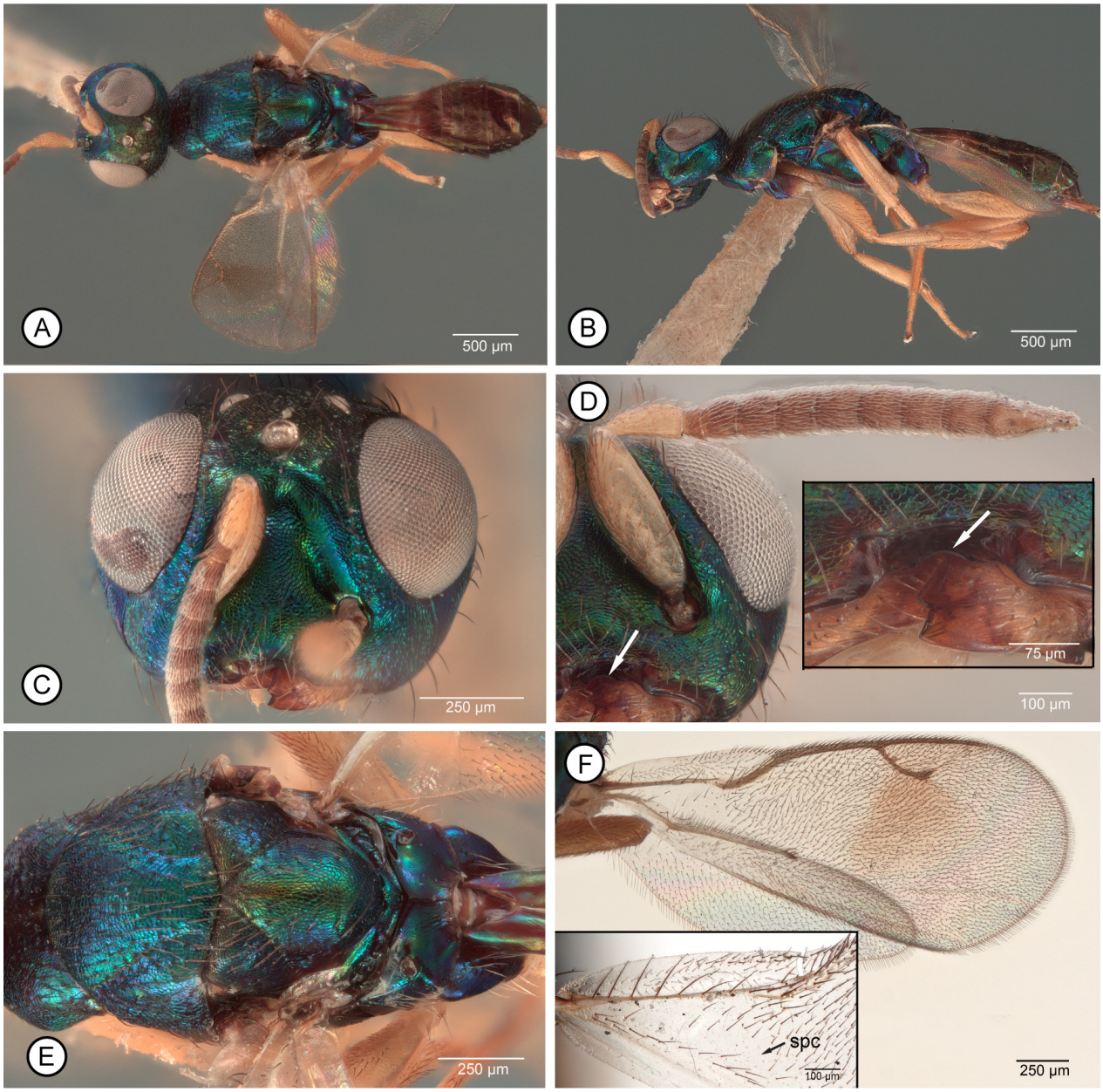

FIGURE 10A–F. *Mesocomys menzeli* ♂. **A**, dorsal habitus (#34); **B**, lateral habitus (#34); **C**, head, frontal (#34); **D**, antenna, inner view [insert: clypeus and mandibles, arrows point to clypeal margin] (#58); **E**, mesosoma, dorsal (#34); **F**, wings (#34) [insert: fore wing base (#58)].

Mesonotum dorsally (Fig. 10E) mostly green to blue with some purple lustre similar to head, except scutellar-axillar complex often with variably distinct and extensive coppery lustre medially; in lateral view (Fig. 10B) similar in colour to dorsal surface, and mesopleurosternum with Y-like set of pale lines. Mesonotum (Fig. 10E) with mesoscutal medial lobe very shallowly mesh-like reticulate to reticulate-imbricate, usually somewhat more coarsely sculptured anteriorly than posteriorly; scutellar-axillar complex with axillae mesh-like coriaceous to very shallowly reticulate, and scutellum mesh-like coriaceous medially and posteriorly but more longitudinally alutaceous to coriaceous-imbricate laterally. Legs similarly pale, yellowish, beyond coxae (Figs 10A, B) or smaller individuals often with metafemur variably extensively brown medially, but mesotibial spur pale. Fore wing hyaline or at most with light brownish infuscation between stigmal and postmarginal veins and behind stigmal vein (Fig. 10F); costal cell dorsally without or sometimes with up to several setae off-set from setae paralleling leading margin (Fig. 10F, insert) basal to setae in front of parastigma; basal cell closed posteriorly by setae along mediocubital fold and at least setose anteriorly over at least apical half (Fig. 10F, insert); speculum absent from larger individuals or evident only

as posterior transverse bare region contiguous with basal cell (Fig. 10F, insert: spc) but often more conspicuous and higher than wide in smaller individuals, though separated from parastigma by at least two rows of setae; measurements of cc: mv: pmv: stv = 3.0–3.3: 1.7–1.8: 1.7–1.8: 1.0.

Type material examined. Lectotype ♀ (hereby designated, NHMUK). Specimen not re-examined for study, but examined in 2015 at NHMUK, with following data based on notes taken at that time and on image of designated lectotype and type labels provided by N. Dale-Skey Papilloud (NHMUK) in 2018: "Type [red-bordered circular label] / Ex oeufs de | *Attacus atlas* / JAVA | Buitenzorg | R. Menzel / Eiparasit von | *Attacus atlas* | IV.1923 / Pres. by | Imp. Inst. Ent. | Brit. Mus. | 1931-140. / *Anastatus* | *menzeli* sp. n. | Ch. Ferriere det. ♀ type / B.M. TYPE | HYM. | 5.1,024 / NHMUK 010198548"; also newly labelled with "LECTOTYPE ♀ | *Anastatus* | *menzeli* Ferrière". Lectotype glued by venter on card triangle with head extending beyond apex of triangle; uncontorted and entire except following missing: left hind wing (left fore wing detached and glued to one side of point); right antenna beyond fl_4.

Paralectotypes examined, here designated: 4♀ (2♀ NHMUK, 2♀ MHNG) and 3♂ (2♂ NHMUK, CNC Photo 2018-57, -58; 1♂ MHNG), all with yellow-bordered "Co-type" label and similar collection data as lectotype; also newly labelled with "PARALECTOTYPE | *Anastatus* | *menzeli* Ferrière".

Other material examined. Eggs of Lep. (1♀ NHMUK). ORIENTAL. **CHINA**. ***Fujian***. Jiangle County, Longqishan, 10.IX.1991, Changming Liu (1♀ IZCAS). Jiangle County, Moyuan, [Pukeng], 6.XI.2016, [Lin Haoyu], ex. egg of *D. houi* (2♀, 8♂ FAFU). Yongtai County, 11-18.IV.2018, [Lin Haoyu], ex. egg of *D. houi* (1♀, 1♂ FAFU). **INDIA**. ***Karnataka***. Anoor, VIII.1982, ex. eggs of hairy caterpillar, CIE 54-61 (6♀, 10♂ NHMUK). 25 km W Mudigere, 3.X.1979, J.S. Noyes (1♀ NHMUK). ***Uttar Pradesh***. Dehra Dun, 17.V.1985, J. LaSalle, on citrus trees underneath mango trees (2♀ CNC). **INDONESIA**. Java**,** Buitenzorg, ex. *Attacus atlas*, R. Menzel (1♀ NHMUK; 7♀, 1♂ USNM, 1♀ CNC Photo 2018-33, ♂ CNC Photo 2018-34); Proefst, W Java, Tjinjiroean, 20.VIII.1941, Fr. A. Th. H. Verbeek, No. 202 (2♀ NHMUK). **MALAYSIA**. Malay Penins., Pahang, Fraser's Hill, 4200 ft., 12.VII.1936, F.M.S. (1♀ NHMUK). **TAIWAN**. Chutzuhu, N. Taipei City, 26.V.1983, K.C. Chou (1♀ TARI). Paling, Taoyuan, Hsien, 800 m, 3-5.V.1983, K.C. Chou & C.C. Pan (1♀ TARI, CNC Photo 2018-59). Tsaoshan, 20 km N. Taipei City, 21.VII.1977, K.S. Lin (1♀ TARI). **THAILAND**. Chiang Mai, Doi Phahompok NP, Mae Fang Hotspring, 19°57.961′N 99°9.355′E, 560m, 21-28.X.2007, P. Wongchai, MT T6193 (1♀ CNC, CNC Photo 2018-32).

Distribution. ORIENTAL: *China [Fujian], *India [Karnataka, Uttar Pradesh], Indonesia [Java (Ferrière 1930b)], *Malaysia, *Taiwan, *Thailand.

Biology. Host: LEPIDOPTERA. ***Lasiocampidae**. *Dendrolimus houi* Lajonquière. **Saturniidae**. *Attacus atlas* (L.) (Ferrière 1930b).

Remarks. Ferrière (1930b) did not designate a holotype from among the seven females and four males that constitute the type series and, as such, all are syntypes, and the reason for designating one as lectotype herein. *Mesocomys menzeli* is hypothesized to form a species trio along with *M. albitarsis* and *M. obscurus* based on the shared features by which the *albitarsis* subgroup is defined. Features by which both sexes of *M. menzeli* are differentiated from the other two species are discussed under those species.

The females imaged do not adequately encompass colour variation because some females have the head and mesosoma much more extensively green (*cf.* Figs 1C & 2A) and/or with other metallic lustres under some angles of light. There is also a series of males and females (NHMUK) from India labelled as reared from eggs of a "hairy caterpillar" that comprise the small end of the range in size given for both sexes and which otherwise increase apparent intraspecific variation. In particular, most of these reared females from India have a more extensively setose basal cell than larger females, often being more-or-less completely setose along the mediocubital fold and more extensive setae apically or with scattered setae along most of the length of the cell. Associated males have the metafemur variably extensively brown to dark medially as well as a hyaline fore wing with a variably conspicuous speculum, though if the bare region is higher than wide it is quite slender and is separated by setae from the base of the parastigma. One of the three male paralectotypes also has entirely hyaline wings, though it has the disc entirely setose as for other larger males (Fig. 10F). I consider the differences between the smaller individuals reared from "hairy caterpillar" eggs as variation correlated possibly with size and/or host difference.

Ling-Fei Peng (FAFU) originally identified the two *Mesocomys* species reported in Lin *et al*. (2017) as *M. breviscapis* and *M. trabalae* using the key of Yao *et al*. (2009) (L-F. Peng, personal communication). The latter key did not include *M. menzeli*. Voucher material of the species reported as *M. breviscapis* in Lin *et al*. (2017, table 2, species 5) (32 individuals from Pukeng, Jiangle County, Fujian) is preserved in FAFU. Using the key and plates

of illustrations from the present species revision, Dr Peng identified remaining voucher specimens as consisting of two species, *M. menzeli* (two females and eight males) and *M. trabalae* (one female). These identifications confirm the identification of *M. trabalae* in Lin *et al*. (2017), but show that the identification of *M. breviscapis* was mostly a misidentification of *M. menzeli*, other than the photograph of the female identified as *M. breviscapis* (Lin *et al.* 2017, fig. 1a), which appears to be *M. trabalae* (see further under the latter species). Images sent to me by Dr Peng of one of the females he identified as *M. menzeli* is this species under my concept.

Mesocomys obscurus (Ferrière) revised stat.

Figs 1I & J, 11, 12

Anastatus menzeli var. *obscurus* Ferrière, 1930b: 355. Described from 5♀ and 1♂ syntypes; lectotype ♀, here designated (NHMUK).

Mesocomys menzeli obscurus (Ferrière); Narendran & Sheela, 1995: 307 (new combination, stated as probably the same as *M. albitarsis*).

Description. FEMALE (habitus: Figs 11A, B). Length = 3.8–4.3 mm. Head (Figs 11C, D) dark with variably extensive and distinct though dull metallic lustres, variably extensively green on face below frontovertex, though usually with blue to violet or purple lustre dorsally over interantennal prominence and/or scrobes, coppery to reddish-violaceous lustre on interantennal prominence between toruli, and sometimes also with slight green to reddish-violaceous lustre on frontovertex (Figs 11D, F) under some angles of light. Face with upper parascrobal region and frons mesh-like coriaceous to very shallowly coriaceous-reticulate or imbricate with some sculpture formed by slightly raised ridges, but at most only very slightly roughened (Figs 11D, F), vertex (Fig. 11D) more transversely alutaceous to alutaceous-strigose, parascrobal region mostly much more distinctly roughened than frons, rugulose to transversely reticulate-strigose, and scrobes and interantennal prominence above about level of dorsal limit of toruli imbricate to reticulate-imbricate, the face between toruli much more minutely mesh-like coriaceous (Fig. 11C). Head measurements: HL = 4.0–4.1, HH = 5.5–5.8, HW = 7.7–7.9, TL = 1.4–1.6, EH = 4.0–4.3, EW = 3.5–3.6, MS = 1.9–2.0, IOD 0.30–0.35× HW, MPOD: OOL: POL: LOL = 1.0: 0.5: 2.3–2.5: 1.9, and dso about 0.8–0.9× aod (Fig. 11F). Labiomaxillary complex with palps similarly dark brown or labial palps slightly paler. Antenna (Fig. 11H) dark, the scape and pedicel with slight green lustre under some angles of light; scape elongate-rectangular, only slightly tapered apically, about 3.6–4.0× as long as greatest width; pedicel about twice as long as apical width and only about as long as basal two funiculars; flagellum with fl_1 slightly transverse to slightly longer than wide, but at least fl_2–fl_4 longer than wide and with flagellum increasing in width and decreasing in length apically so funiculars increasingly more quadrate to slightly transverse apically; clava about as long as apical three funiculars.

Pronotum dorsally partly dark brown but usually with bright green, blue and/or reddish-violaceous to violet lustres at least laterally; mesonotum (Figs 11A, E) at least with depressed part of mesoscutal medial lobe distinctly bright green or blue to violet, with anterior convex part of medial lobe and lateral lobes mostly dark brown with only slight green or reddish-violaceous lustre under some angles of light, and scutellar-axillar complex paler brown or with coppery to reddish-violaceous anteriorly and green to bluish-green posteriorly; in lateral view mesosoma mostly dark brown though usually at least lateral panel of pronotum and acropleuron with similar metallic lustres as mesothorax dorsally. Mesoscutum (Fig. 11E) with convex anterior part of medial lobe mesh-like coriaceous to coriaceous-imbricate, depressed posterior part similarly but much more finely mesh-like coriaceous to smooth and shiny medially, and lateral lobe also mesh-like coriaceous; mesoscutum excluding parapsidal band similarly setose with brown hair-like setae except depressed posterior part of medial lobe bare with longer, more bristle-like setae anteriorly and bare over about posterior half. Scutellar-axillar complex with axillae obliquely alutaceous to alutaceous-strigose and scutellum variably coriaceous to coriaceous-imbricate, the sculpture often more elongate laterally than medially and sometimes with somewhat larger sculpture anteromedially than laterally and posteriorly; setose laterally with brown hair-like setae. Acropleuron finely mesh-like sculptured, though with more minute sculpture mesally below level of fore and hind wing bases and larger, more isodiametric, coriaceous-reticulate sculpture posteriorly. Legs mostly brownish beyond coxae, including tarsi (Figs 1I, J, 11B), even if mesotarsomeres only brownish-yellow and obviously not as dark as mesotarsal pegs, with mesotibial spur similar in colour to mesotarsomeres, but front leg with knee and tibia apically usually distinctly paler, middle leg with anterior margin of femur apically pale to hyaline, tibia basally somewhat paler, yellowish-brown, and hind leg with trochantellus pale. Fore wing (Fig.

11G) with basal cell light brownish-infuscate basally and disc distinctly bifasciate, even if somewhat lighter brownish behind parastigma and base of marginal vein than behind stigmal and postmarginal veins, with all setae dark or with some setae in hyaline region behind marginal vein paler, more yellowish, but not distinctly white (Fig. 11G, insert); costal cell bare dorsally excluding setae in front of parastigma; basal cell with 1–4 setae on mediocubital fold basally; stigmal vein curved apically into uncus; measurements of cc: mv: pmv: stv = 4.0–4.1: 3.2–3.3: 1.7–2.0: 1.0.

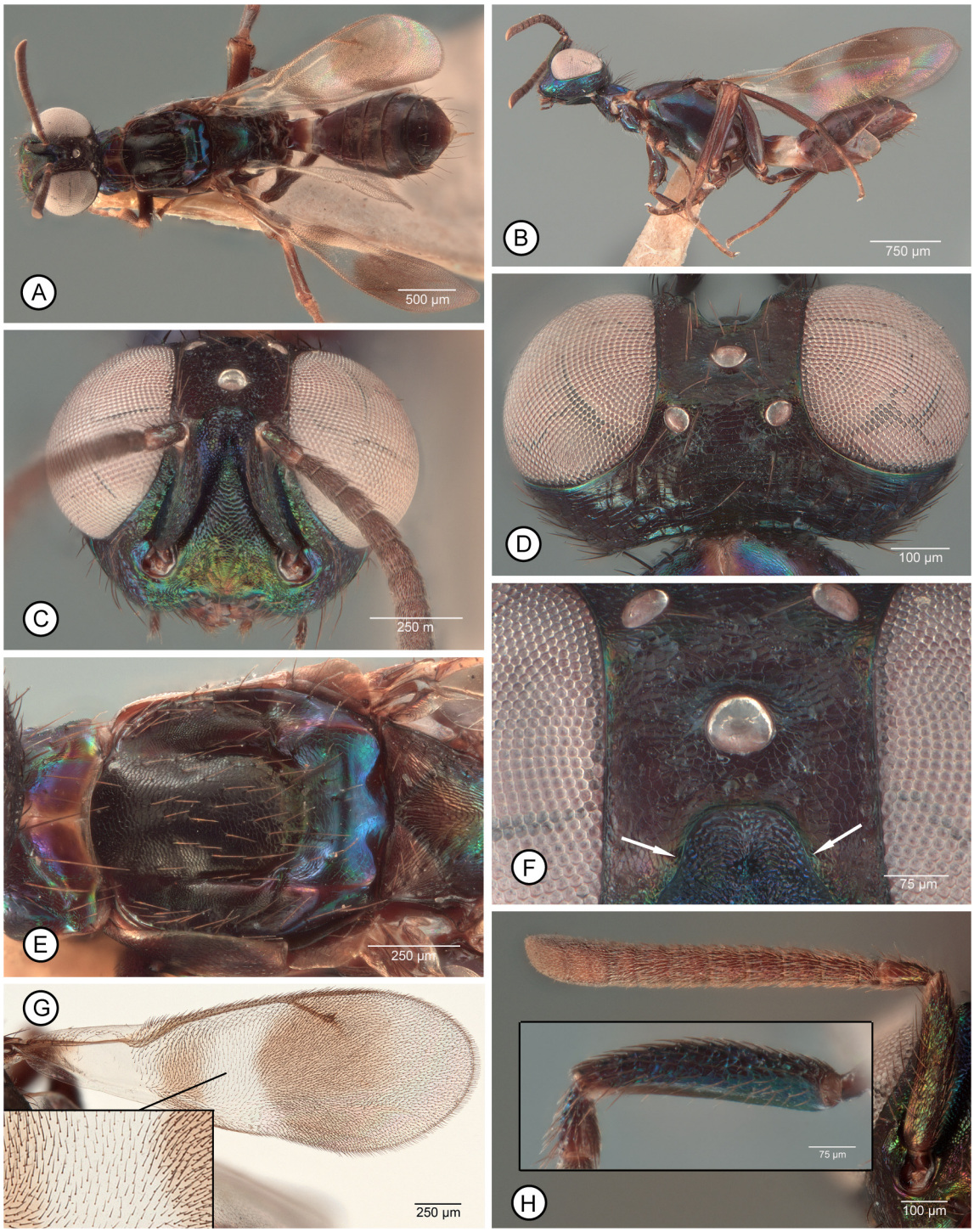

FIGURE 11A–H. *Mesocomys obscurus* ♀. **A**, dorsal habitus (#31); **B**, lateral habitus (#62); **C**, head, frontal (#62); **D**, head, dorsal (#62); **E**, mesosoma, dorsal (PLT, #67); **F**, frontodorsal part of head (#62) [arrows point to incurved margin of scrobal depression]; **G**, fore wing (PLT, #67); **H**, antenna, inner view (PLT, #67) [insert: scape and pedicel, outer view (#82)]. Figure caption abbreviation: PLT = paralectotype.

Gaster mostly dark brown but at least in lateral view with variably conspicuous pale to white region basally to subbasally (Fig. 11B) formed by St_1 and apically paler sides of Gt_1, with Gt_1 dorsally usually also whitish-hyaline apically so in dorsal view gaster also with distinct subbasal white band (Fig. 11A), but rarely Gt_1 dorsally almost uniformly dark brown similar to subsequent tergites so in dorsal view gaster without subbasal white band, with Gt_2–syntergum dark brown except syntergal flange brownish-yellow to yellowish-hyaline (Fig. 11A) and apical tergites sometimes with very slight greenish lustre; Gt_1 smooth, shiny and bare, and usually comparatively narrow with subparallel sides relative to more uniformly ovate Gt_2–syntergum; Gt_2–syntergum similarly mesh-like coriaceous to alutaceous and Gt_3 or Gt_4–syntergum with at least one row of hair-like setae across surface. Ovipositor sheaths pale, yellowish.

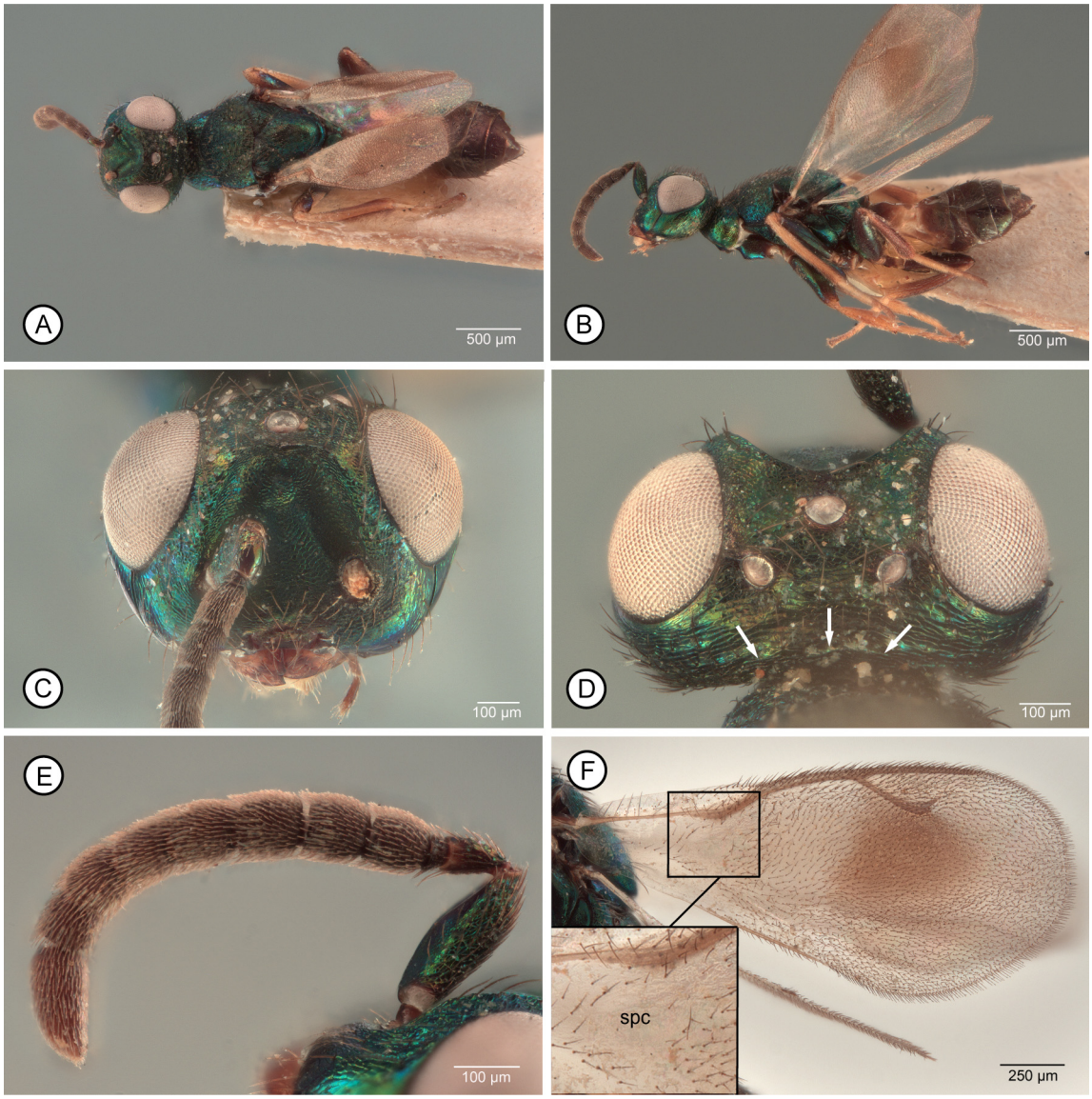

FIGURE 12A–F. *Mesocomys obscurus* ♂ (paralectotype). **A**, dorsal habitus; **B**, lateral habitus; **C**, head, frontal; **D**, head, dorsal [arrows point to transverse ridge delimiting posterior margin of vertex]; **E**, antenna, outer view; **F**, fore wing [spc = speculum].

MALE (based on single paralectotype, habitus: Figs 12A, B). Length about 3.1 mm. Head mostly green, but under some angles of light with slight coppery to dark reddish-violaceous lustre on frontovertex (Fig. 12D) and limited blue to purple lustre within scrobal depression dorsally and lower face lateral of clypeus. Face with upper parascrobal region and frons slightly roughened, mesh-like coriaceous-imbricate; vertex transversely alutaceous except posterior margin delimited by irregular transverse ridge between about level of inner margin of eyes (Fig. 12D: arrows); scrobal depression and most of interantennal prominence similarly mesh-like reticulate to imbricate, but more finely mesh-like coriaceous ventrally between toruli. Head measurements (all as ocular grid units): HL =

4.0, HH = 4.7, HW = 6.6, IOD = 3.0, EH = 3.0, EW = 2.7, MS = 1.8, MPOD: OOL: POL: LOL = 1.3: 0.8: 3.6: 2.2, and dso slightly less than aod (Fig. 12D). Labiomaxillary complex with maxillary palps dark brown (Fig. 12C) but labial palps paler, light brownish-yellow. Antenna (Fig. 12E) dark, but scape and pedicel with green lustre similar to head; scape about 2.7× as long as wide; pedicel about 1.8× as long as apical width and only about 0.8× as long as combined length of first two funiculars; flagellum robust-filiform, subequal in width; fl_1 strongly transverse and much smaller than fl_2, fl_2–fl_8 subquadrate to slightly longer than wide, and clava about twice as long as wide and about 0.7× combined length of apical three funiculars (length approximate because flagellum curved apically).

Mesosoma dorsally (Fig. 12A) similarly green as head except with slight coppery lustre on mesoscutum posteriorly and scutellum medially under some angles of light; in lateral view (Fig. 12B) similar in colour to dorsal surface or somewhat more bluish, and mesopleurosternum without evident, paler, Y-like set of lines. Mesonotum with mesoscutal medial lobe distinctly mesh-like reticulate; scutellar-axillar complex with axillae shallowly mesh-like reticulate, and scutellum mesh-like coriaceous-reticulate medially and posteriorly but somewhat more distinctly, though shallowly, reticulate-imbricate to imbricate laterally. Front leg with trochantellus pale but femur otherwise dark with green lustre except apically light brownish-yellow, and tibia and tarsus similarly pale as femur apically. Middle leg similar in colour to front leg except tibia apically and apical three tarsomeres somewhat darker brownish compared to more whitish-yellow basal two tarsomeres, tibial spur, and tibia basally. Hind leg with femur, except trochantellus, dark with slight greenish lustre under some angles of light, tibia dark brown except slightly paler basally and apically, and tarsus whitish-yellow basally but becoming slightly darker brown apically. Fore wing (Fig. 12F) with distinct brownish infuscation behind stigmal vein and, much less conspicuously, between postmarginal and stigmal veins; costal cell dorsally with 1 (left wing) or 2 (right wing) setae slightly off-set from row of setae paralleling leading margin basal to setae in front of parastigma; basal cell closed posteriorly by row of setae along mediocubital fold but otherwise extensively bare except for about 3 rows of setae apically; speculum (Fig. 12F: spc) large and broad, extending to parastigma without intervening setae over about apical half of parastigma; measurements of cc: mv: pmv: stv = 2.8: 1.4: 1.6: 1.0.

Gaster dark brown except with pale band subbasally (Fig. 12B).

Type material examined. Lectotype ♀ (hereby designated, NHMUK). Specimen not re-examined for study, but examined in 2015 at NHMUK, with following data based on notes taken at that time and on image of designated lectotype and type labels provided by N. Dale-Skey Papilloud (NHMUK) in 2018: "Type [red-bordered circular label] / Ex oeufs de | *Attacus atlas* / JAVA | Buitenzorg | R. Menzel / Pres. by | Imp. Inst. Ent. | Brit. Mus. | 1931-140. / *Anastatus* | *menzeli* Ferr. | var. *obscurus* nov. | Ch. Ferriere det. | ♀ type / B.M. TYPE | HYM. | 5.1,025 / NHMUK 010198545"; also newly labelled with "LECTOTYPE ♀ | *Anastatus menzeli obscurus* | Ferrière". Lectotype glued by venter on card triangle with head extending beyond apex of triangle, uncontorted and entire.

Paralectotypes examined, here designated: 4♀ (2♀ NHMUK, 1♀ CNC Photo 2018-67; 2♀ MHNG, 1♀ CNC Photo 2018-31) and 1♂ (NHMUK), all with yellow-bordered "Co-type" label and similar collection data as lectotype; also newly labelled with "PARALECTOTYPE | *Anastatus* | *menzeli obscurus* | Ferrière".

Other material examined. ORIENTAL. **INDONESIA**. Java, Buitenzorg, R. Menzel, ex. *Atticus atlas* (4♀ USNM, 1♀ CNC Photo 2018-62).

Distribution. ORIENTAL: Indonesia [Java (Ferrière 1930b)].

Biology. Host: LEPIDOPTERA. **Saturniidae**. *Attacus atlas* (L.) (Ferrière 1930b).

Remarks. Ferrière (1930b) did not designate a holotype from among the five females and one male originally stated as constituting the type series and, as such, all are syntypes, and the reason for designating one as lectotype herein. The USNM females have similar label data as the type material and thus might be from the same rearing, but are mounted on a different type of card point and are excess in number to the number of individuals cited in the original description.

Because of the very few specimens available, the species description undoubtedly does not adequately encompass intraspecific variation. The range in length described for females likely is mostly the result of differences resulting from air-drying and body-part position because head measurements among specimens are the same or very similar. At least seven of the nine known females have the first gastral segment white apically and comparatively narrow with subparallel sides relative to an abruptly ovate, dark brown gaster beginning with Gt_2. Dorsal gastral shape and colour pattern is not visible for one female because it is strongly contorted, but in one female Gt_1 is only slightly narrowed and similarly brown as the other tergites so in dorsal view a distinct subbasal pale band is lacking, though in lateral view Gt_1 is seen to be pale apically on its vertical sides. Females also vary in how darkly infuscate

the tarsi are, with the mesotarsomeres sometimes dark brown similar to the tarsal pegs (Fig. 1I), but sometimes only brownish-yellow and noticeably paler than the tarsal pegs, but always darker than in Fig. 1G.

Individuals of *M. obscurus* may have been reared only once, and from the same host, place and time as *M. menzeli*. Females of the two species are structurally very similar, but differ in at least three colour features. Compared to *M. menzeli*, females of *M. obscurus* have the antennae uniformly dark (Fig. 11H) *versus* at least the scape pale apically, and usually the funicle also extensively, through variably conspicuously paler relative to a darker clava and scape basally (Figs 9C–E), the legs are mostly dark, including the tarsi (Figs 1I, J, 11B) *versus* legs usually extensively pale or at least all tarsi (except for mesotarsal pegs) pale, yellowish (Figs 9A, B, *cf*. Figs 1G & H), and the fore wing disc is bifasciate (Fig. 11G) *versus* unifasciate (Fig. 9I). The single known male of *M. obscurus* (Figs 12A–F) is insufficient to evaluate possible intraspecific variation in such features as the absence of a visible Y-like set of pale lines on the mesopleurosternum, the presence of an irregular, transverse vertexal ridge (Fig. 12D: arrows), and a subbasally pale gaster (Fig. 12B), though males very likely are variable for all three features. Some critical-point dried males of *M. trabalae* also have a subbasal pale region (Fig. 17A, insert), and the presence or absence of this feature in both sexes appears to be at least partly correlated with specimen preservation. Although I describe one or two off-set setae dorsally in the costal cell for the examined male paralectotype of *M. obscurus*, these are only slightly off-set from the other setae forming a row closely paralleling the leading margin. Unlike females, males of *M. obscurus* are more similar to those of *M. albitarsis* than males of *M. menzeli*, including the presence of a large fore wing speculum (Fig. 12F: spc) and comparatively short pedicel (Fig. 11H), as is discussed under *M. albitarsis*.

Mesocomys superansi Yao, Yang & Zhao

Figs 8G & H, 13, 14A–G, 15

Mesocomys superansi Yao, Yang & Zhao, 2009: 155 (keyed), 157, 159 (Chinese description), 160 (English summary), figs 10, 11 (female). Described from holotype ♀ and 1♂ paratype (both CFRB).

Mesocomys superansi; Yang *et al*., 2015: 167 (keyed), 172 (Chinese description and data), 257–258 (English data summary), fig. 91 (female, misidentification of *M. trabalae* or *M. breviscapis*).

Description. FEMALE (habitus: Figs 13A–D). Length = 2.6–3.5 mm [3.3]. Head (Figs 14A–C) dark brown to almost completely green or with scrobal depression sometimes blue to purple (Fig. 14A), and frontovertex often with variably extensive reddish-coppery to reddish-violaceous lustre. Face with upper parascrobal region and frons mesh-like coriaceous in smaller individuals (Fig. 14C) to slightly roughened, coriaceous-imbricate to very shallowly reticulate in larger individuals, vertex similar in sculpture to frons or somewhat more transversely alutaceous (Fig. 14B), parascrobal region finely but more distinctly roughened than frons, and scrobes and interantennal prominence above about level of dorsal limit of toruli similarly mesh-like coriaceous to very shallowly, obscurely reticulate, the face between toruli more finely, minutely mesh-like coriaceous (Fig. 14A). Head measurements: HL = 2.8–3.6 [3.3], HH = 3.5–4.8 [4.7], HW = 4.8–6.4 [5.9], TL = 1.1–[1.3] EH = 2.5–3.6 [3.2], EW = 2.3–3.1 [2.5], MS = 1.3–[1.6], IOD 0.27–[0.34]× HW, MPOD: OOL: POL: LOL = 1.0: 0.5–0.6: 1.8–2.0: 1.3–1.4 [1.0: 0.6: 2.0: 1.4], and dso about 0.5–0.8× aod [0.5:1.0] (Fig. 14C). Labiomaxillary complex dark brown. Antenna (Figs 14D, F) entirely dark or at most only extreme dorsoapical margin of scape distinctly paler beyond level of apical-most row of setae (Fig. 14F, insert); scape elongate-rectangular, at most only slightly tapered apically, about [4.1]–4.4× as long as greatest width; pedicel slightly longer than twice apical width and about as long as combined length of basal two funiculars plus basal half of third funicular (Fig. 14D); flagellum with fl_1 and fl_2 slightly longer than wide and funiculars increasing in width apically so funiculars beyond fl_2 somewhat longer than wide basally to quadrate or slightly transverse apically; clava about as long as apical three funiculars.

Mesosoma dorsally sometimes mostly similarly dark brown as head (Fig. 13A), though usually distinctly green to bluish-green (Fig. 13C), except concave dorsal part of pronotum and sometimes scutellum apically with coppery to reddish-violaceous lustre; in lateral view similarly dark brown (Figs 13B, G) to distinctly green or bluish-green as for dorsal surface, though acropleuron sometimes with variably distinct darker blue or reddish-violaceous lustre, and prepectus sometimes (see Remarks) with margins variably extensively, though narrowly, distinctly paler (Fig. 13G). Mesoscutum (Fig. 13E) with convex anterior part of medial lobe distinctly sculptured, mostly variably coarsely reticulate-rugulose though usually somewhat more finely though distinctly mesh-like coriaceous-reticulate

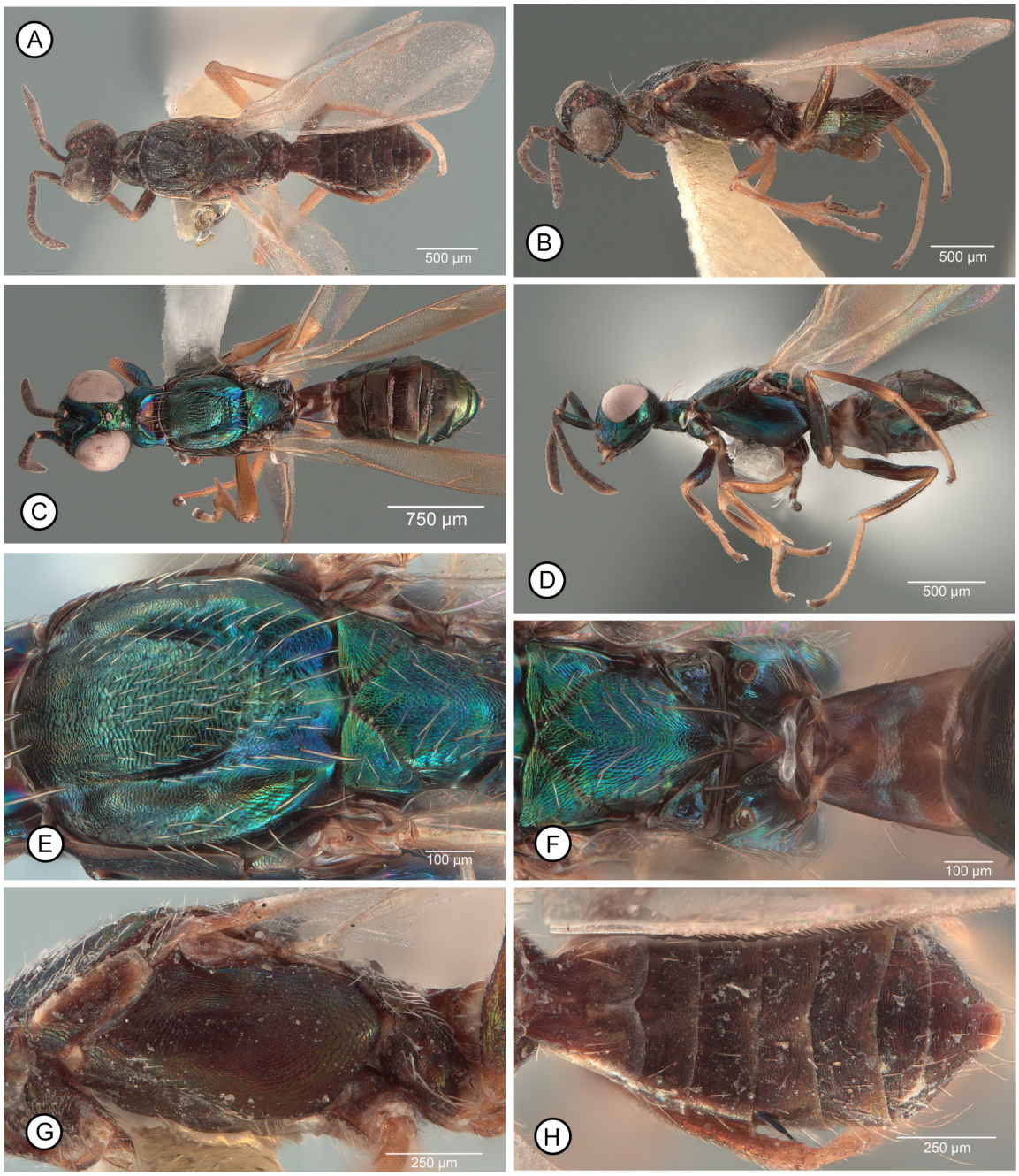

FIGURE 13A–H. *Mesocomys superansi* ♀. **A**, dorsal habitus (HT); **B**, lateral habitus (HT); **C**, dorsal habitus (#60); **D**, lateral habitus (#61); **E**, mesonotum (#60); **F**, scutellum–Gt_1 (#60); **G**, mesosoma, lateral (HT); **H**, gaster, dorsal (HT). Figure caption abbreviation: HT = holotype.

posteriorly, and depressed posterior part with about anterior half to two-thirds distinctly sculptured similar to anterior convex region and more finely mesh-like coriaceous anterior of transscutal articulation, and lateral lobe mostly mesh-like coriaceous; mesoscutum, excluding parapsidal band, more-or-less uniformly setose, though with somewhat longer setae posteriorly and bare along transscutal articulation. Scutellar-axillar complex (Figs 13E, F) with axillae obliquely alutaceous and scutellum mesh-like coriaceous to coriaceous-imbricate mediolongitudinally but with more elongate sculpture on sides; setose laterally with dark hair-like setae becoming longer posteriorly. Acropleuron (Fig. 13G) finely mesh-like sculptured, though with more minute sculpture mesally below level of fore and hind wing bases and much larger coriaceous-reticulate sculpture posteriorly. Front leg (Fig. 13D) with trochantellus pale, but femur mostly dark except apically, and tibia mostly pale but variably extensively and distinctly dark dorso- and ventrolongitudinally. Middle leg (Figs 13B, D) pale beyond coxa except for dark mesotarsal pegs. Hind

leg (Figs 13B, D) with trochanter and trochantellus at least slightly paler than femur basally, femur dark basally but variably extensively pale apically, tibia entirely pale or at most slightly, inconspicuously brownish-infuscate apically, and tarsus pale. Fore wing (Fig. 14E) uniformly hyaline other than for yellowish venation; costal cell dorsally sometimes with 1–4 setae apically basal of setae in front of parastigma (Fig. 8G: arrow); basal cell uniformly setose posteriorly along mediocubital fold and otherwise entirely or mostly setose except sometimes for comparatively small and inconspicuous bare region basally or anteroapically behind submarginal vein (Figs 8G, H); measurements of cc: mv: pmv: stv = 3.2–4.0: 2.8–3.2: 1.8–2.0: 1.0 [4.0: 3.2: 1.9: 1.0].

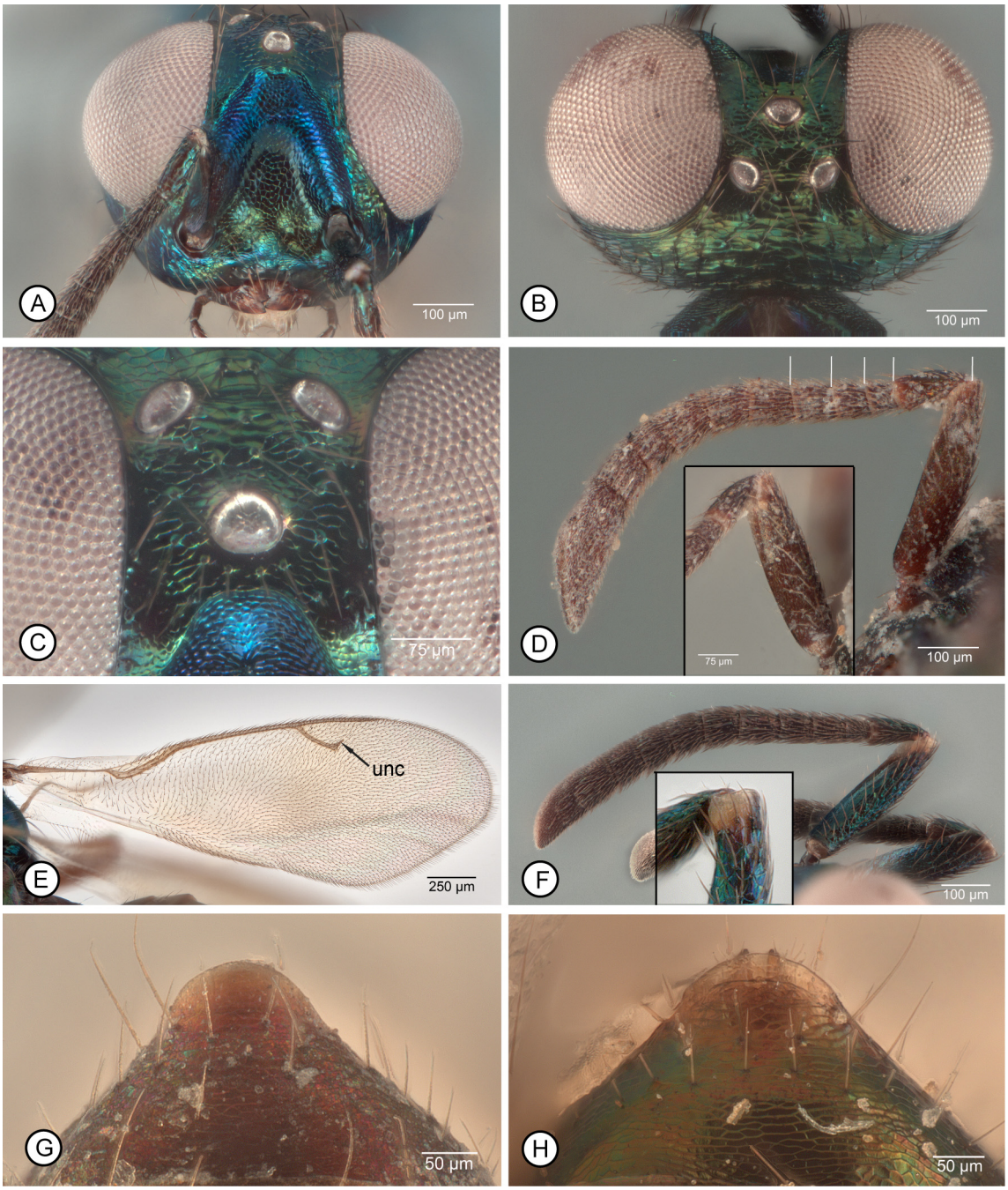

FIGURE 14A–H. *Mesocomys* spp. ***A–G****, M. superansi* ♀: **A**, head, frontal (#61); **B**, head, dorsal (#60); **C**, frontodorsal part of head (#60); **D**, antenna, inner view [insert: scape–fl_1, outer view] (holotype); **E**, fore wing (#60) [unc = uncus]; **F**, antennae (#60) [white lines indicate basal and apical limits of scape and basal funiculars; insert: enlargement of apex of scape in dorsal view]; **G**, gastral apex (holotype). **H**, *M. trabalae* (#35): gastral apex.

Gaster in dorsal view without a subbasal white band (Figs 13A, C, F, H) though Gt_1 sometimes noticeably hyaline apically, dark brown or one or more tergites sometimes with slight greenish lustre depending on angle of light (Figs 13C, D), and syntergal flange at least slightly paler brown (Fig. 14G) to distinctly paler, yellowish; in lateral view with dorsally tapered subbasal white band (Figs 13B, D) because side of Gt_1 white apically and St_1 extensively white; Gt1 dorsally shiny and bare, though at least obscurely mesh-like coriaceous, and usually with subparallel or only slightly divergent sides relative to more uniformly ovate, more distinctly mesh-like coriaceous to transversely coriaceous-reticulate Gt2–syntergum; Gt2–syntergum with at least one row of hair-like setae across surface. Ovipositor sheaths pale, yellowish.

MALE (habitus: Figs 15A, B). Length = 2.2–2.6 mm. Head uniformly green to bluish-green (Fig. 15C) except usually frons partly dark or with very slight coppery lustre under some angles of light. Face with upper parascrobal region and frons roughened, mesh-like imbricate-reticulate; vertex more transversely strigose, rounded into occiput; scrobal depression and most of interantennal prominence similarly mesh-like reticulate to imbricate, but more finely mesh-like coriaceous ventrally between toruli. Head measurements: HL = 2.5–3.2, HH = 3.5–3.8, HW = 4.4–5.4, EH = 2.3–2.7, EW = 2.0–2.2, MS = 1.2–1.5, IOD 0.37–0.40×HW, MPOD: OOL: POL: LOL = 1.0–1.1: 0.5–0.8: 1.8–2.4: 1.2–1.4, and dso subequal to aod (Fig. 15C). Labiomaxillary complex with palpi brownish-yellow to brown. Antenna (Fig. 15F) dark except extreme apex and base of scape yellowish, remainder of scape and pedicel with bluish to bluish-green lustre similar to head; scape about 3× as long as wide, pedicel about 2.0–2.4× as long as apical width and about 0.8–0.9× combined length of basal three funiculars; flagellum clavate-filiform, only slightly widened toward clava; fl_1 transverse, subsequent funiculars all similar in length, more-or-less quadrate, but length to width ratios variable depending on antenna and view (see Remarks), and clava about twice as long as wide and about 0.8× combined length of apical three funiculars.

Mesosoma dorsally (Fig. 15D) similarly green to bluish-green as head except scutellum medially usually with variably extensive and distinct coppery lustre depending on angle of view; in lateral view similar in colour to dorsal surface except lateral surface of mesoscutal medial lobe and acropleuron sometimes more bluish to purple, and mesopleurosternum with at least obscurely paler Y-like set of lines (Fig. 15E). Mesonotum (Fig. 15D) with mesoscutal medial lobe distinctly reticulate to reticulate-rugulose; scutellar-axillar complex with axillae anteriorly similarly coarsely reticulate as mesoscutal medial lobe, but posteriorly more finely imbricate and scutellum mesh-like coriaceous to coriaceous-imbricate medially and posteriorly but more imbricate to imbricate-reticulate laterally. Front leg with trochantellus, tibia, tarsus, and usually trochanter pale, but femur variably extensively brownish-infuscate to dark, sometimes entirely dark with slight green to violaceous lustre except narrowly pale apically, though often more extensively pale except ventral and posterior surfaces medially variably dark brown (Fig. 15B). Middle leg with trochantellus, tarsus, and sometimes trochanter pale, but femur at least extensively brownish medially (Fig. 15A) and sometimes almost entirely dark except basally and apically (Fig. 15B), and tibia pale to variably extensively and distinctly darker, brownish-yellow apically, though tibial spur pale. Hind leg with trochanter, trochantellus and tarsus pale, but femur entirely dark except narrowly apically (Fig. 15B), and tibia variably distinctly and extensively darker, brownish apically (Figs 15A, B). Fore wing sometimes essentially uniformly hyaline, but usually with variably distinct brownish-infuscate region behind stigmal vein (Fig. 15G); costal cell dorsally with variable number of setae (Fig. 15H: upward directed arrows) off-set from row of setae paralleling leading margin (Fig. 15H: ser) basal to setae in front of parastigma; basal cell sometimes entirely setose, but at least setose along length of mediocubital fold and over about apical half of cell; speculum usually small, wider than high, and separated from parastigma by 2 or 3 rows of setae (Fig. 15H), but sometimes variable even between two wings of one individual, and if higher than wide then separated from parastigma by at least 1 row of setae (Fig. 15H, insert); measurements of cc: mv: pmv: stv = 2.9–3.2: 1.8–2.0: 1.6–1.9: 1.0.

Gaster dark brown (Figs15A, B) or sometimes one or more tergites with slight greenish lustre under some angles of light.

Type material examined. Holotype ♀ (CFRB; Figs 13A, B, G, H, 14D, G): label data in Chinese, publication cited data: [China], Hebei Province, Fengning, 41.2°N, 116.63°E, IX.1978, Hong-Ze BA, collected and reared from eggs of *Dendrolimus superans* (Butler). Holotype point-mounted, uncontorted, and entire except fl_7–clava of left antenna, and left front leg beyond trochanter missing.

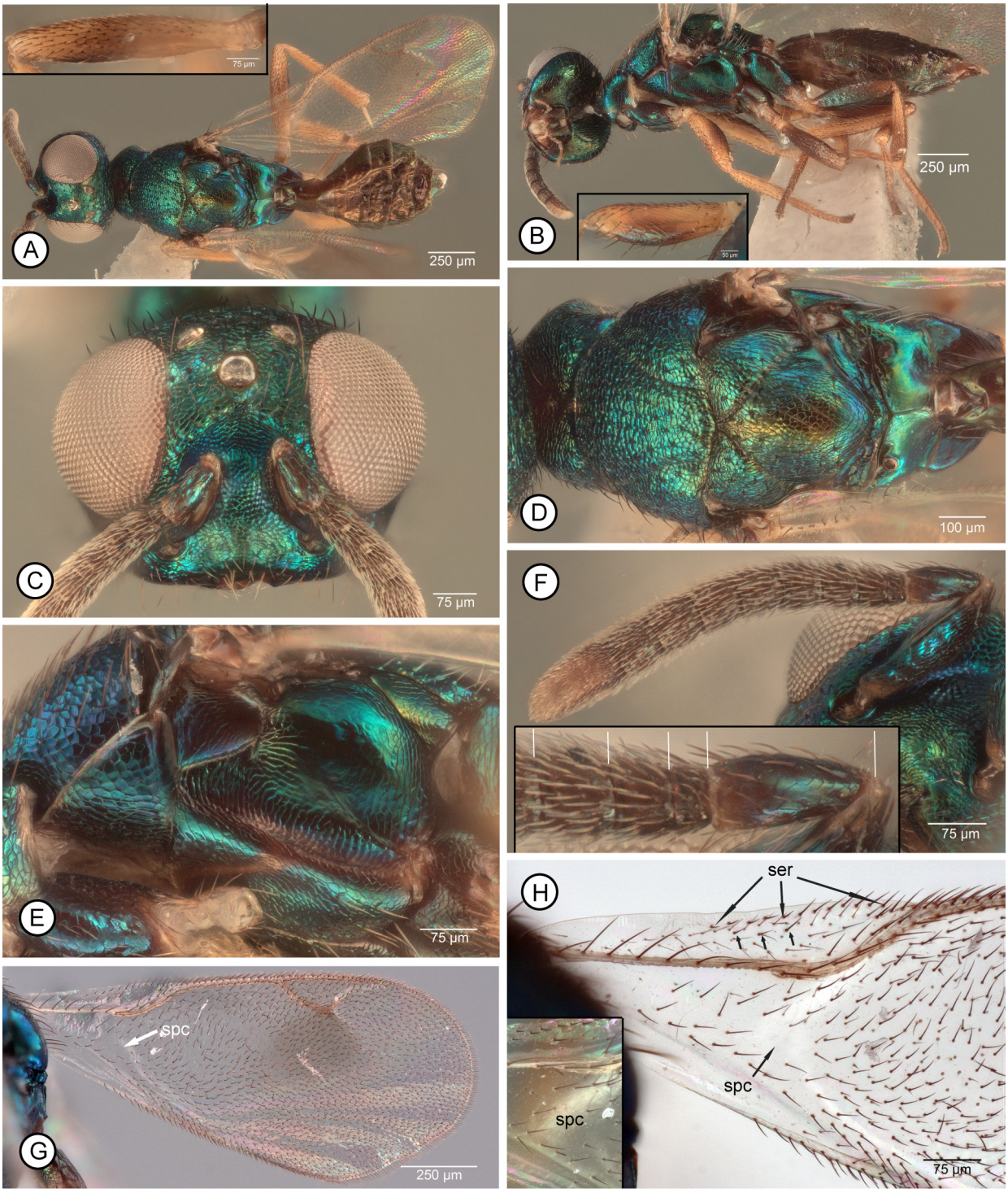

FIGURE 15A–H. *Mesocomys superansi* ♂. **A**, dorsal habitus [insert: mesofemur, posterior] (#65); **B**, lateral habitus (#106) [insert: profemur, posterior]; **C**, head, frontal (#65); **D**, mesosoma, dorsal (#65); **E**, mesosoma, lateral (#65); **F**, antenna [insert: pedicel and basal three funiculars, white line indicate length of articles] (#65); **G**, right fore wing (#65); **H**, base of right fore wing [insert: speculum of left fore wing] (#65). [Abbreviations: ser = setal row, spc = speculum.]

Other material examined. ORIENTAL. **THAILAND**. Chiang Mai, Doi Pha Hom Pok NP—20º3.455'N 99º8.551'E, 2174 m, 7-14.XI.2007, Kiewlom 1: Montaine forest, MT T2819, Komwuan Srisom & Prasit Wongchai (1♀ CNC, CNC Photo 2018-61); 20º3.331'N 99º8.552'E, 2112 m, 11-18.VII.2007, Kiewlom 2: Montaine forest, MT T2823, Komwuan Srisom (2♀ CNC, 1♀ CNC Photo 2018-60). Chiang Mai, Huai Nam Dang NP, 19º17.56'N 98º36.029'E, 31.III-7.IV.2008, MT T5657, Anuchart & Thawatchai (1♂ CNC, CNC Photo 2018-65).

PALAEARTCIC. **CHINA**. ***Hebei***. Fengning County, IX.1978, egg of *Dendrolimus superans* (Butler), number 660, original number 7, no. 20 (1♂ IZCAS); Hebei Academy of Forestry Sciences, VIII.1978, egg of *Dendrolimus* sp. (1♀ IZCAS); Xinglong, V.1979, Weiliang Qin, pupa of *Dendrolimus* sp. (1♀ IZCAS). ***Xizang***. Tibet, Nielamu, Youyi Bridge, 1700-2400m, 2.IX.2001, Chaodong Zhu, camphor tree (1♂ IZCAS, CNC Photo 2018-106).

Distribution. ORIENTAL: *Thailand. PALAEARCTIC: China [Hebei (Yao *et al.* 2009), *Xizang].

Biology. Host: LEPIDOPTERA. **Lasiocampidae**. *Dendrolimus superans* (Butler) (Yao *et al.* 2009) attacking *Larix principis-rupprechtii* Mayr (Pinaceae) (Yang *et al*. 2015).

The single IZCAS record indicating emergence from of a pupa of *Dendrolimus* sp. is anomalous (see further under 'Biology' for the genus).

Remarks. *Mesocomys superansi* was described from a single holotype female and paratype male, of which I examined the holotype (Figs 13A, B, G, H, 14D, G). The dorsal habitus photograph in Yang *et al.* (2015, fig. 91) apparently is also of the holotype. Length given in the original description for the holotype is 2.3 mm, but my measurement results in a length of 3.3 mm. The holotype body is also almost completely brown with only quite obscure metallic lustre (Figs 13A, B, G, H; Yang *et al*. 2015, fig. 91) except the frontovertex is more distinctly reddish-coppery under most angles of light. The head and mesosoma of the other two examined females from China have somewhat more distinct, mostly greenish lustre, but with the frons also reddish-coppery to violaceous, whereas the Thailand females have a much brighter, mostly bluish-green head and mesosoma (Figs 13C–F, 14A–C), including the frontovertex other than for a very small reddish-coppery region between the posterior ocellus and inner orbit (Fig. 14C). Based on the original description of *M. superansi*, the lack of distinct metallic lustres from the Chinese females may result from exposure to light and some fading over the years. However, additional specimens are required to more fully assess the significance of a reddish-coppery frontovertex for the holotype and the other two Chinese females compared to a more uniformly greenish head (Figs 14A–C) for the Thailand females. Further, all three examined females from China have the margins of the prepectus, particularly apically, quite obviously pale (Fig. 13G), whereas those from Thailand have the prepectus uniformly dark (Fig. 13D). Again, the significance of this difference between the females from China and Thailand needs to be investigated with additional specimens to determine whether the pale colouration is an artefact of preservation for the specimens or is diagnostic for *M. superansi* and thus indicates the presence of a similar but separate species in Thailand.

The holotype female varies in dorsal setal pattern of the costal cell between the two wings, with the costal cell of the left wing having a row of four setae, and that of the right fore wing having only a single seta (*cf.* Fig. 8G: arrow), more basal to the apical setae in front of the parastigma. The other females I identify as *M. superansi* have the costal cell dorsally bare basal to the setae in front of the parastigma (Fig. 8H) except for one female from China, which has three setae on one wing and two on the other, and one female from Thailand and one from China with just a single seta on one wing (Fig. 8G: arrow). Yao *et al.* (2009, fig. 11) also illustrated the basal cell as being entirely setose, which is true for the holotype (evident from right fore wing), though some females either have the extreme base of the cell bare or have a small, inconspicuous bare region apically behind the submarginal vein (Fig. 8H: arrow). The fore wing venation illustrated for *M. superansi* in the original description by Yao *et al.* (2009, fig. 11) shows the postmarginal vein as extending only to a level equal with the apex of the stigmal vein, but this is incorrect, the postmarginal vein being distinctly longer than the stigmal vein (*cf.* Fig. 14E) as for other species. The line drawing of the female antenna by Yao *et al.* (2009, fig. 10) is also incorrect because only seven funiculars are illustrated and the apparent first funicular is as long as the pedicel. Apparently, the division between the first and second funiculars (Fig. 14D) was omitted from the line drawing so the unusually long first funicular actually was of the basal two funiculars.

As discussed above under *M. aegeriae* and *M. breviscapis*, *M. superansi* appears to be a distinct species whose females are readily distinguished from those described as *M. aegeriae*, *M. breviscapis*, *M. sinensis* and *M. trabalae*. Females of *M. superansi* uniquely have the scape entirely dark (Fig. 14D) or with only the extreme apex pale beyond the level of the apical-most setae (Fig. 14F, insert). Further, the gaster in dorsal view lacks a subbasal pale band so as to be uniformly dark except for an at least slightly paler syntergal flange (Figs 13H, 14G), though in lateral view there is a subbasal white band (Figs 13B, D). Though a subbasal pale band dorsally on the gaster is not always obvious in mounted females of other species (Figs 5G, I), the exceptions appear to be because of artefacts of preservation, mostly likely as result of being air-dried and some shrivelling. Based on the pro- and metafemora being mostly dark and the antennal scapes appearing to be entirely dark, the female identified as *M. trabalae* in Yang *et al*. (2015, fig. 90) more likely is a female of *M. superansi* or possibly *M. breviscapis* (see further under *M. trabalae*).

I did not examine the single male paratype of *M. superansi*, and the original description is the briefest of the four species described by Yao *et al*. (2009). The description states only that the length of the male is 2.8 mm, the body is bluish-green, the first to third funiculars of the flagellum are transverse and the remaining funiculars are about quadrate, the fore wing has a slight brownish region around the stigmal vein, the basal third of the basal cell is bare and closed, the apical half of the costal cell has some setae, and the speculum is very small. I do identify one male from Thailand as *M. superansi* based on its association with three females I identify as this species. This male matches the original description by having quite a distinct brownish-infuscate region behind the stigmal vein (Fig. 15G), having some setae apically in the costal cell (Fig. 15H), and having the basal cell closed posteriorly by setae along the length of the mediocubital fold but having about the basal half of the cell bare (Fig. 15H). Although the original description does not include leg colour pattern, the Thailand male, in addition to having the metafemur dark, also has the posterior surface of the mesofemur distinctly infuscate (Fig. 15A) and the posterior and ventral surfaces of the profemur slightly infuscate medially. A similar leg colour pattern is also exhibited by another male from Xizang Province (Tibet), though with the pro- and mesofemora somewhat more extensively and distinctly infuscate (Fig. 15B). Finally, a male from Fengning county with almost the same data as the original type material, including being reared from a *D. superans* egg, also appears to be *M. superansi*, but with the most extensively dark pro- and mesofemora of the three males, with all the femora almost completely dark except narrowly apically. The three different numbers given on the specimen labels of this male suggests it likely was part of some rearing or experiment, possibly the same as the original type material, but it is card-mounted rather than point-mounted and the labels are different from those for the material examined from Yao *et al*. (2009). Further, it differs from the original description in having essentially entirely hyaline fore wings, with at most only very faint and inconspicuous infuscation behind the stigmal vein under some angles of light, and the basal cell is entirely setose rather than being bare in its basal half. Both the Fengning county and Xizang males have a small fore wing speculum (*cf*. Fig. 15H), as stated in the original description, with the bare region being separated from the parastigma by at least two rows of setae. However, size of the speculum differs between the two wings in the Thailand male. The right wing has a small bare region separated from the parastigma by two to three rows of setae (Figs 15G, H), but the left wing has a larger, higher than wide bare region that is separated from the parastigma by only a single row of setae (Fig. 15H, insert). There is also variation in the number of setae dorsally within the costal cell that are off-set from the setae paralleling the leading margin, particularly for the Fengning county male in which there are several setae that are only slightly off-set and thus less certainly designated as marginal or as off-set setae. The original description also states that the first three funiculars are transverse and the remaining funiculars are "about quadrate" (English description). The males I identify as *M. superansi* have only the first funicular distinctly transverse, and in the Thailand male the length to width ratios of the subsequent funiculars differ somewhat depending on the antenna and the view. The differences between the two antennae are most apparent for the apical two funiculars, with fl_7 appearing slightly longer than wide and fl_8 quadrate for the right antenna (Fig. 15F), but fl_7 slightly transverse and fl_8 more distinctly transverse for the left antenna. However, the pedicel of the three males is at least 0.8× the combined length of the subsequent three funiculars, which is an important supplemental feature to distinguish *M. superansi* males from those of *M. albitarsis*, which they might be confused with because of their extensively brownish-infuscate to dark femora. Males of *M. superansi* have a somewhat longer pedicel, almost as long as the combined length of the basal three funiculars (Fig. 15F) compared to only about as long as the combined length of the basal two funiculars (Fig. 3G) for *M. albitarsis* males. Males of the two species also differ in size of the fore wing speculum. Males of *M. albitarsis* always have a large, quadrangular speculum that extends to the base of the parastigma (Fig. 3F). Although size of the speculum varies for *M. superansi* males, known males at least have a narrower speculum that is separated from the parastigma by at least one row of setae (Fig. 15H, insert).

Mesocomys trabalae Yao, Yang & Zhao

Figs 8E & F, 14H, 16, 17

Mesocomys trabalae Yao, Yang & Zhao, 2009: 155 (keyed), 156 (Chinese description), 159–160 (English summary), figs 1–3 (female). Described from holotype ♀ plus 35♀ and 3♂ paratypes (all CFRB).

Mesocomys trabalae; Yang *et al*., 2015: 167 (keyed), 171–172 (Chinese description and data), 257 (English data summary), fig. 90 (female, misidentification of *M. superansi* or *M. breviscapis*); Lin *et al*., 2017: 842–848 (host and distribution records), fig. 1a (female, misidentified as *M. breviscapis*).

Description. FEMALE (habitus: 16A, B). Length = 3.3–4.9 mm. Head (Figs 16C–E) dark with variably distinct green lustre to mostly bright green, except sometimes blue to purple within scrobes and frontovertex sometimes with variably extensive coppery to reddish-violaceous lustre under some angles of light. Face with upper parascrobal region and frons mesh-like coriaceous-imbricate to very shallowly reticulate, vertex increasingly more transversely alutaceous-strigose posteriorly (Fig. 16D), parascrobal region finely but more distinctly roughened than frons, and scrobes and interantennal prominence above about level of dorsal limit of toruli similarly mesh-like imbricate to very shallowly, obscurely reticulate, the face between toruli more finely mesh-like coriaceous (Fig. 16C). Head measurements: HL = 3.5–4.4, HH = 4.8–6.0, HW = 6.4–7.8, TL = 1.1–1.6, EH = 3.4–4.2, EW = 3.0–3.6, MS = 1.8–2.1, IOD 0.30–0.33×HW, MPOD: OOL: POL: LOL =1.0: 0.4–0.5: 1.9–2.0: 1.3–1.4, and dso about 0.3–0.6× aod (Fig. 16E). Labiomaxillary complex dark brown or maxillary palps brown and labial palps variably paler (Fig. 16C). Antenna (Fig. 16G) with at least about apical quarter of scape pale and sometimes much more extensively pale along ventral and dorsal margins (Fig. 16G, insert), but pedicel and flagellum dark; scape elongate rectangular, at most only slightly tapered apically, about 4.0–4.5× as long as greatest width; pedicel slightly longer than twice apical width and about as long as combined length of basal two funiculars plus basal half of third funicular; flagellum often with up to six basal funiculars longer than wide, though fl_2 and/or fl_1 sometimes subquadrate, and funiculars increasing in width apically so apical two to four funiculars quadrate to slightly transverse; clava about as long as apical three funiculars.

Mesosoma dorsally (Fig. 16A) variably dark with blue or purple (Fig. 16F) and/or green lustres to mostly bright green, though concave dorsal part of pronotum (Fig. 16F) dark to reddish-violaceous and mesonotum sometimes with some coppery or reddish-violaceous lustre under some angles of light; in lateral view similarly coloured as mesonotum, with prepectus uniformly dark or at most margins very slightly paler, brownish-hyaline. Mesoscutum (Fig. 16F) with convex anterior part of medial lobe entirely reticulate-rugulose or somewhat more finely though distinctly mesh-like coriaceous-reticulate posteriorly, depressed posterior part at least distinctly sculptured, mesh-like reticulate or reticulate-rugulose anterior to more finely mesh-like coriaceous posteriorly, and lateral lobe mostly mesh-like coriaceous; mesoscutum, excluding parapsidal band, more-or-less uniformly setose, though with somewhat longer setae posteriorly and bare along transscutal articulation. Scutellar-axillar complex with axillae obliquely alutaceous and scutellum mesh-like coriaceous to coriaceous-imbricate mediolongitudinally but with more elongate sculpture on sides; setose laterally with dark hair-like setae becoming longer posteriorly. Acropleuron finely mesh-like sculptured, though with more minute sculpture mesally below level of fore and hind wing bases and much larger coriaceous-reticulate sculpture posteriorly. Legs often entirely pale, orangish, beyond coxae or only metafemur partly dark (Fig. 16B), though sometimes profemur variably distinctly and extensively, to entirely dark except apically and basally, and then metatibia and/or protibia also partly brownish-infuscate to dark, but mesotibial spur pale (see Remarks). Fore wing (Fig. 16H) uniformly hyaline other than for yellowish venation; costal cell bare dorsally or with up to 5 (China) to 10 (Japan: Fig. 8F, insert) setae forming one or more rows apically in costal cell basal of setae in front of parastigma; basal cell setation highly variable, often setose basally and apically but broadly bare medially (Fig. 8E) or sometimes extensively bare behind submarginal vein but setose along length of mediocubital fold, or more-or-less extensively, though only partly setose within basal cell behind submarginal vein and then broadly bare along mediocubital fold medially (Fig. 8F); fore wing measurements: cc: mv: pmv: stv = 3.7–4.3: 3.2–3.6: 1.8–2.2: 1.0.

Gaster in dorsal view dark brown except usually with distinct, transverse, subbasal white band (Fig. 16A) [sometimes apparently absent because of specimen preservation], one or more apical tergites sometimes with slight greenish lustre, and syntergal flange variably distinctly paler, yellowish-brown to yellowish-hyaline (Fig. 14H); in lateral view (Fig. 16B) with dorsally tapered subbasal white band because side of Gt_1 white apically and St_1 extensively white; Gt1 dorsally shiny and bare, though at least obscurely mesh-like coriaceous, and usually with subparallel or only slightly divergent sides relative to more uniformly ovate, more distinctly mesh-like coriaceous to transversely coriaceous-reticulate Gt2–syntergum; Gt2–syntergum with at least one row of hair-like setae across surface. Ovipositor sheaths pale, yellowish.

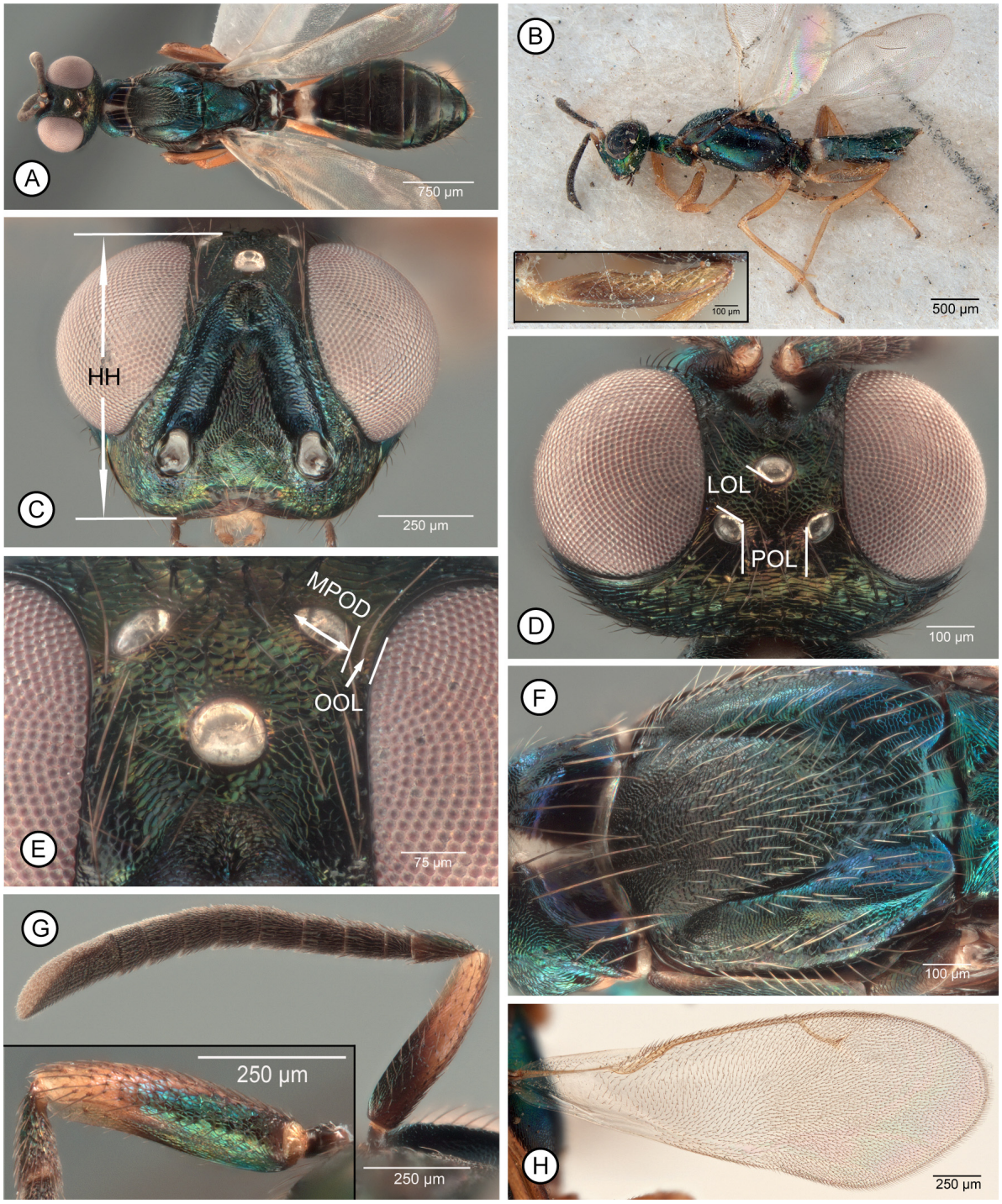

FIGURE 16A–H. *Mesocomys trabalae* ♀. **A**, dorsal habitus (#40); **B**, lateral habitus (paratype, #24) [insert: enlargement of metafemur]; **C**, head, frontal (#66); **D**, head, dorsal (#40); **E**, frontodorsal part of head (#40); **F**, pro- and mesoscutum (#40); **G**, antenna, inner view [insert: scape and pedicel, outer view] (#36); **H**, fore wing (#23). [See 'Methods' and Table 1 for explanation of abbreviations.]

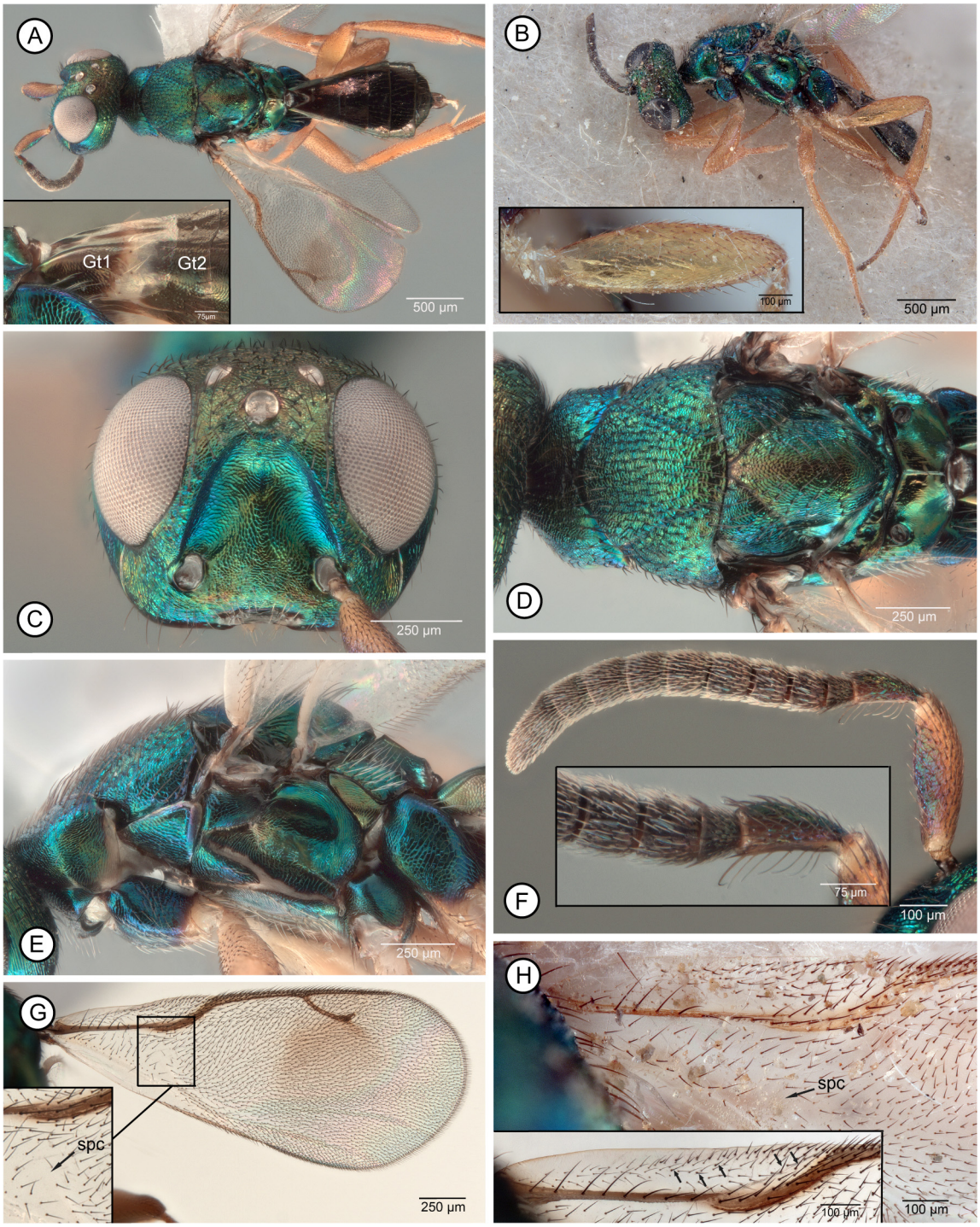

FIGURE 17A–H. *Mesocomys trabalae* ♂. **A**, dorsal habitus (#38) [insert: basal two gastral tergites, lateral (#105)]; **B**, lateral habitus (paratype, #25) [insert: enlargement of metafemur]; **C**, head, frontal (#38); **D**, mesosoma, dorsal (#38); **E**, mesosoma, lateral (#37); **F**, antenna, inner view [insert: pedicel–fl_3] (#39); **G**, fore wing (#38); **H**, fore wing (paratype, #25) [insert: costal cell (#101) arrows point to non-marginal setae on dorsal surface within costal cell]. [See 'Methods' and Table 1 for explanation of abbreviations.]

MALE (habitus: Figs 17A, B). Length = 2.4–3.5 mm. Head usually entirely or mostly green to bluish-green (Fig. 17C), with males from China having variably extensive and distinct reddish-violaceous lustre on frontovertex (Fig. 17A) and sometimes elsewhere on face under some angles of light. Sculpture of face variable, larger males with upper parascrobal region and frons distinctly roughened, mesh-like reticulate to reticulate-rugulose and vertex transversely imbricate-strigose, but sometimes in smaller males upper parascrobal region and frons smoother, more

mesh-like coriaceous-reticulate, and vertex transversely alutaceous, but vertex rounded into occiput; scrobal depression and most of interantennal prominence similarly mesh-like reticulate to imbricate, but more finely mesh-like coriaceous ventrally between toruli. Head measurements: HL = 3.0–4.0, HH = 4.1–5.6, HW = 5.1–7.2, EH = 2.6–3.4, EW = 2.2–2.9, MS = 1.4–2.0, IOD 0.39–0.43× HW, MPOD: OOL: POL: LOL = 1.0: 0.5–0.6: 1.8–2.0: 1.2–1.3, and dso about 0.7–1.0× aod (Fig. 17C). Labiomaxillary complex dark brown to pale brownish-yellow. Antenna (Fig. 17F) sometimes with scape entirely dark with green to bluish-green lustre, but often variably extensively pale, brownish-yellow to yellowish-brown (Figs 17A, C, F) except for at least outer surface ventrally (Fig. 17F), pedicel dark and usually with green to bluish-green lustre, but flagellum dark brown; scape about 2.6–3.2× as long as wide; pedicel about 2.5× as long as apical width and about 0.7–0.8× combined length of basal three funiculars; flagellum clavate-filiform, only slightly widened toward clava; fl_1 slightly transverse to quadrate but tapered basally, and subsequent funiculars subquadrate or only slightly longer than wide, and clava about 1.9–2.5× as long as wide and about 0.7–0.8× combined length of apical three funiculars.

Mesosoma dorsally (Fig. 17 D) similarly green to bluish-green as head or somewhat more blue to purple under some angles of light, except usually scutellum dark or with variably extensive and distinct coppery lustre medially, and mesoscutum sometimes with limited coppery lustre; in lateral view similar in colour to dorsal surface, mostly green to blue, except mesopleurosternum usually with Y-like set of pale lines (Fig. 17E). Mesonotum (Fig. 17D) with mesoscutal medial lobe distinctly reticulate to reticulate-rugulose; scutellar-axillar complex with axillae anteriorly similarly reticulate as mesoscutum, but posteriorly more reticulate-imbricate and scutellum mesh-like coriaceous medially and posteriorly but more imbricate laterally. Legs usually completely pale beyond coxae (Figs 17A, B), though sometimes metafemur variably dark brown (see Remarks). Fore wing often with variably distinct brownish region behind stigmal vein (Fig. 17G), but sometimes uniformly hyaline; costal cell dorsally sometimes uniformly setose apically in front of parastigma, with setal region tapered basally to about mid length of cell (Fig. 17H), but usually with differentiated row of setae closely paralleling leading margin, row of setae in front of parastigma, and variable number of setae (at least 3 on both wings, Fig. 17H, insert: upward directed arrows) forming one to two rows between row of setae along leading margin and setae in front of parastigma; basal cell entirely setose (Figs 17G, H) or at most only extreme base bare; speculum comparatively small and inconspicuous, separated from base of parastigma by at least 2 rows of setae (Figs 17G, H); measurements of cc: mv: pmv: stv = 3.2–3.7: 1.7–2.1: 1.6–1.8:1.0.

Gaster dark brown (Fig. 17A) or in dorsal view sometimes with up to about apical one third of Gt_1 whitish-hyaline and in lateral view with slender but more distinct subbasal white band (Fig. 17A, insert).

Type material examined. Paratypes examined (1♀ CFRB, CNC Photo 2018-24; 1♂ CFRB, CNC Photo 2018-25): label data in Chinese, publication cited data: [China], Shaanxi Province, Huanglongshan, Guanzhuang Forest Farm, collected 3.IV.1985, emerged 12.IV.1985, Zhong-Qi Yang and Fei Huang, collected and reared from eggs of *Trabala vishnou* Lefèbvre.

Other material examined. ORIENTAL. **CHINA**. ***Fujian***. Jiangle County, Moyuan, [Pukeng], 6.XI.2016, [Lin Haoyu], ex. egg of *D. houi* (1♀ FAFU); Minqing County, Dongqiao [= Baiyunshan Forestry Farm], 3.V.2017, [Lin Haoyu], ex. egg of *D. houi* (2♀ FAFU); Yongtai County, Heipingshan, IV.2018 (1♀ FAFU). ***Sichuan***, E-Mei Mountain, Jiulaodong, 2.VIII.1967, Youcai Yu (1♀ IZCAS). ***Yunnan***. Yunnan Forestry College, Kunming, An-Ning Hot Spring, 1.III.1981, Yingxia Li (4♂ IZCAS). ***Zhejiang***. Yunhe, V.1984, *Dendrolimus houi* Lajonquière (4♀, 2♂ IZCAS). **TAIWAN**. Nantou Hsien—Meifeng, 2150 m, 8-11.V.1984, K.C. Chou & C.C. Pan (1♀ TARI); Tungpu, 1200 m, 25-29.IX.1980 (2♀ TARI), 18-21.X.1982 (1♀ TARI), K.C. Chou & T. Lin. Nantou, Tungpu, 1.VI.1990, 1200 m, J. Heraty (1♂ UCRC #119641). **THAILAND**. Chiang Mai, Doi Phahompok NP, Doi Phaluang, 20°1.06′N 99°9.5815′E, 1449 m, 7-14.V.2008, P. Wongchai, MT T6106 (1♀ CNC).

PALAEARCTIC. **CHINA**. ***Gansu***. Kang Co., Longnan City, 23.I.2018, Y. Chen, ex. *Caligula japonica* Moore egg, lab. reared on eggs of *Antherea pernyi* (Guérin-Méneville) (Lep: Saturniidae) (63♀, 23♂ CNC, 3♀ CNC Photo 2018-36, -40, -66, 3♂ CNC Photo 2018-37, -38, -39). ***Shaanxi***. Huanglong County, Guanzhuang, 3.IV.1985, ex. eggs *Trabala vishnou*, Z.-Q. Yang (6♀ plus 4 host eggs, CNC, 2♀ CNC Photo 2018-23, -35) [non-type specimens from same rearing as type series]. **JAPAN**. Hokkaido, Shimamaki-mura, 17.VIII.1976, K. Kamijo (1♀ SEHU, CNC Photo 2008-102).

Distribution. ORIENTAL. China [Fujian (Lin *et al*. 2017), *Sichuan, *Yunnan, *Zhejiang], *Taiwan, *Thailand. PALAEARCTIC: China [*Gansu, Shaanxi (Yao *et al.* 2009)], *Japan [Hokkaido].

Biology. Hosts: LEPIDOPTERA. **Lasiocampidae**. *Dendrolimus houi* Lajonquière (Lin *et al.* 2017); *Trabala*

vishnou (Lefèbvre) (Yao *et al.* 2009) defoliating *Hippophae rhamnoides* L. (Elaeagnaceae) (Yang *et al*. 2015). **Saturniidae**. **Antherea pernyi* (Guérin-Méneville) [factitious host]; **Caligula japonica* Moore.

Remarks. As discussed under *M. aegeriae* and *M. breviscapis*, the morphological limits of both sexes and potential synonymy of *M. trabalae* remain questionable. My concept of the species is based primarily on one male and female paratype plus six females from the original type rearing, as well as numerous males and females reared in the laboratory on the factitious host *A. pernyi* from individuals originally reared from *C. japonica* eggs in the field, and a few other females collected in China. The females all differ from what I treat as *M. breviscapis* (including *M. sinensis*) by having entirely yellow legs beyond the coxae or at most the metafemur partly dark (Fig. 16B, insert) as well as being somewhat larger. Under this concept, the colour photograph of the female in lateral view in Yang *et al*. (2015, fig. 90) identified as *M. trabalae* is either *M. breviscapis* or *M. superansi* because both the pro- and metafemora are mostly dark and the flagellum is entirely dark. The antennal scapes in the image appear to be entirely dark, which would indicate *M. superansi* as the more likely species, but the quality of the image is insufficient to be certain. On the other hand, the colour photograph of the female in Lin *et al*. (2017, fig. 1a) identified as *M. breviscapis* appears to definitely be that of a *M. trabalae* female, as discussed under *M. breviscapis* and *M. menzeli*. Lin *et al*. (2017, table 2, species 6) reported 18 specimens of *M. trabalae* from Baiyunshan, Minqing County, Fujian, reared from *D. houi*, of which two female voucher specimens are preserved in FAFU. One of the females from the locality from which *M. breviscapis* [= *M. menzeli*] was reported by Lin *et al*. (2017) is also a *M. trabalae*, indicating the two species at least occur together and possibly sometimes parasitize the same egg mass.

The extralimital females from Taiwan and Japan I identify as *M. trabalae* expand the morphological limits of the species by having the profemur also partly brownish-infuscate to dark and, except for their comparatively large size, they are thus more similar to what I distinguish as *M. breviscapis*. Three of four females from Taiwan have the costal and basal cell setal patterns visible, of which one has three dorsal setae within the costal cell on one wing and none on the other, and the other two have one dorsal seta on one wing but not the other. The female from Japan has about ten setae dorsally within the costal cell on both wings, whereas the female from Thailand lacks dorsal setae within the costal cell. Females from China display a range from no dorsal setae within the costal cell to up to five dorsal setae. Basal cell setal pattern is also quite variable, though unlike *M. superansi* females (Figs 8G, H) and females I treat as *M. breviscapis* (Figs 8A–C) other than the examined *M. sinensis* paratype (Fig. 8D), the basal cell is broadly bare medially (Fig. 8E) or bare behind the submarginal vein if setose along the mediocubital fold or, if more-or-less extensively setose longitudinally within the cell, then broadly bare long the mediocubital fold medially (Fig. 9F).

The examined male paratype of *M. trabalae* has the gaster uniformly dark, as originally described, as do other air-dried males. However, some critical-point dried males reared on *A. pernyi* eggs are similar to females in having up to about the apical third of the basal gastral tergite whitish-hyaline and with a somewhat more distinct subbasal whitish band in lateral view (Fig. 17A, insert). Critical-point dried males of *M. breviscapis* and *M. superansi* are necessary to determine whether males of at least *M. breviscapis* might also sometimes have a subbasal pale band, depending on state of preservation. The original Chinese description of *M. trabalae* also states that there is a brownish region behind the stigmal vein in males, but the examined male paratype has uniformly hyaline fore wings or at most very faint and inconspicuous infuscation behind the stigmal vein. Some other males from China I identify as *M. trabalae* also have the wings hyaline or essentially hyaline (see below), but the male from Taiwan and males reared on *A. pernyi* eggs have a noticeable infuscate region behind the stigmal vein (Figs 17A, G). The male from Taiwan differs from other males by having the head and body somewhat more bluish-green and having the frontovertex similarly coloured as the face (Fig. 17C), without a differentiated region of reddish-coppery to violaceous lustre, though males from China are variable in how distinct and extensive is this lustre. The examined male paratype of *M. trabalae* has the costal cell densely setose apically (Fig. 17H), as originally described for the species but, as discussed under *M. breviscapis*, other males typically have a less extensively dorsally setose costal cell. Usually there is at least one row of several setae that are off-set from the setae paralleling the leading margin, but sometimes there are as few as three setae (Fig. 17H: upward directed arrows). This latter setal pattern is therefore more similar to the examined *M. sinensis* paratype, which has three dorsal setae on one wing (Fig. 7F: upward directed arrows), though only a single seta on the other wing (Fig. 7H: upward directed arrow). The examined *M. trabalae* paratype male also has a comparatively small, subcircular speculum that is distinctly separated from the parastigma by setae (Fig. 17H: spc), and the basal cell is entirely setose, as also originally described. Similar fore wing setal features are possessed by four males from China that are not associated with females but share the same label data (Yunnan

Forestry College, 1.III.1981). As discussed under *M. aegeriae*, two of these males have entirely yellow legs like other *M. trabalae* males, whereas two have the metafemora variably dark brown, more similar to what I interpret as *M. breviscapis* males (Fig. 7D). All four males have hyaline fore wings or with only faint, inconspicuous infuscation behind the stigmal vein. The two different metafemoral colour patterns either indicate that metafemoral colour pattern is variable for *M. trabalae* males or that males of two different species, *M. trabalae* and *M. breviscapis*, were collected together at the same time and place. The rearing of the type material of *M. menzeli* and *M. obscurus* together from eggs collected at the same time and place shows the former alternative to certainly be possible. However, based on the similar fore wing setal patterns among the four males, particularly the presence of several setae dorsally within the costal cell apically, I consider it more likely that metafemoral colour pattern can vary in males similar to females. Because of this, in the key to males I include a couplet to differentiate males of *M. trabalae* with dark metafemora from *M. breviscapis* males. However, the hypothesis that metafemoral colour pattern is variable for males of *M. trabalae* needs to be tested by further collecting and rearings and, ideally, by molecular studies, as do the hypotheses that *M. breviscapis* and *M. sinensis* are synonymous and a separate species from *M. trabalae*.

pulchriceps species group

Diagnosis. FEMALE. Head with scrobal depression separated from anterior ocellus by distance (Fig. 22D: dso) at least about twice longitudinal diameter of ocellus (Fig. 22D: aod); scrobal depression dorsally uniformly flat to low-convex without differentiated convexity, and uniformly ∩-like tapered dorsally (*e.g.*, Fig. 22E) or only very slightly, inconspicuously sinuate (*e.g.*, Fig. 24A); clypeus either broadly, shallowly emarginate (Fig. 18D) or deeply, ∩-like emarginate medially so to appear almost bidentate (Figs 22C, 25E, F, 26F: arrow) [feature sometimes not clearly visible if apical setae of labrum project beneath emargination (Fig. 22C: asl) or if apex of labrum itself underlies emargination (Fig. 25F: arrow)]. Head with hair-like setae on frontovertex and upper parascrobal region (*e.g.*, Figs 18C, E), denser and more conspicuous fringe of mostly brown, elongate-lanceolate setae along oral margin lateral of clypeus to malar sulcus (*e.g.*, Fig. 18D), row of similarly elongate-lanceolate setae on parascrobal region at least ventrally, and whitish-translucent elongate-lanceolate setae on interantennal prominence medially (*e.g.*, Fig. 18D). Head with sculpture of upper parascrobal region and frons variable, but interantennal prominence and scrobes more-or-less uniformly mesh-like imbricate to reticulate-imbricate (*e.g.*, Figs 22A, E). Scutellar-axillar complex with deep, paramedial triangular depression between each axilla and scutellum (*e.g.*, Figs 18F, 26E). Middle leg with tibial spur usually dark and distinctly contrasting in colour with tarsomeres (excluding pegs), though sometimes only orangish. Fore wing disc infuscate from base of parastigma to near apex of postmarginal vein except for separated anterior and posterior hyaline regions with white setae behind marginal vein, and with some setae of basal infuscate region variably distinctly lanceolate (*e.g.*, Fig. 18H); costal cell hyaline to distinctly brownish-infuscate apically, dorsally bare except densely setose with hair-like to lanceolate dark setae in front of parastigma, and ventrally with hair-like setae over at least much of length, the setae more numerous apically but usually interrupted by variably broad bare region basal of parastigma; marginal vein often only about 2.5× as long as stigmal vein, or less (*e.g.*, Figs 21D, 26H). Metapleuron (Figs 2H, 27H: pl_3) consisting of smooth and shiny, vertical region along lateral margin of propodeum and abruptly reflexed, smooth and shiny, elongate-slender band at right angle to vertical band over incised posterodorsal surface of acropleuron. Propodeum with flat to only shallowly depressed U- to V-shaped medial plical depression (Figs 2H, 27H: ppd), and callus setose only posterolaterally (Figs 2H, 27H: cal). Gaster in dorsal view with or without subbasal pale to white band formed in part by Gt_2 and/or Gt_1, but at least Gt_2 variably distinctly hyaline [often not obvious unless tergite raised slightly above Gt_3 because colour or underlying sclerite shows through].

MALE. Head with scrobal depression separated from anterior ocellus by distance similar to or greater than, but by less than twice longitudinal diameter of anterior ocellus (*e.g.*, Figs 19B, 23C); clypeus similarly incurved, to deeply emarginate, as for conspecific female (*e.g.*, Fig. 23C). Head with sculpture of upper parascrobal region and frons variable, but interantennal prominence and scrobes more-or-less uniformly mesh-like imbricate to reticulate-imbricate similar to female. Middle leg often with tibial spur dark and then often distinctly contrasting in colour with paler tarsomeres; middle and hind legs sometimes with basotarsomeres distinctively long, as long as or longer than combined length of respective four apical tarsomeres (Figs 23H, I); mesotarsus sometimes (Fig. 23I: lower tarsus) and metatarsus always bicoloured with at least basitarsus and one or two apical tarsomeres obviously darker than paler medial tarsomeres (Figs 19A, 23H, I). Fore wing variably distinctly infuscate behind stigmal vein and

behind parastigma such that hyaline region or anterior and posterior hyaline regions with diffuse margins differentiated behind marginal vein (Figs 19A, 24B, F), the hyaline region sometimes with white setae (Fig. 24C) similar to conspecific female (Fig. 21D); costal cell ventrally usually with setae separated by variably broad bare region basal to parastigma, and dorsally with variable pattern of setae; basal cell often bare except for partial row of setae along mediocubital fold basally; disc uniformly setose, without evident speculum (Figs 19D, 24C, G).

Remarks. Head structure of the two sexes differ in two distinctive features by which females of the two species groups differ. Males have the scrobal depression separated from the anterior ocellus by a distance obviously less than twice the longitudinal diameter of the ocellus (*e.g.*, Figs 19B, 23C) and they have hair-like setae on the lower face (*e.g.,* Fig. 23C) rather than the lanceolate setae of females (*e.g.,* Fig. 18D). Both features are thus indicated as secondarily derived for females of the *pulchriceps* group and support monophyly of the group. Females of some other genera of Eupelminae, such as *Anastatus*, sometimes also have similarly long and dense, lanceolate setae along the oral margin as for *pulchriceps*-group females. This suggests independent origin for some unknown functional reason. As discussed under the genus, monophyly of the *pulchriceps* group is likely also supported by metapleural structure (Figs 2H, 27H: pl_3), an only posterolaterally setose propodeal callus (Figs 2H, 27H: cal), and possibly by the associated, only shallowly depressed to flat propodeal plical depression (Figs 2H, 27H: ppd) of females. Monophyly may also be supported by fore wing colour pattern, with both females and males having partly infuscate fore wings with anterior and posterior hyaline regions behind the marginal vein apically (*cf*. Figs 21D & 24B). Some *albitarsis*-group species also have partly infuscate fore wings, but the patterns likely are convergent to those of the *pulchriceps* group because females have at most a hyaline cross-band behind the marginal vein rather than separated anterior and posterior regions, and conspecific males have entirely hyaline fore wings or ones that are infuscate only behind the stigmal vein. As discussed below under *M. anelliformis*, the species pair *M. anelliformis* + *M. longiscapus* is indicated as the sister group of *M. pauliani* + (*M. orientalis* + *M. pulchriceps*).

Mesocomys anelliformis Gibson n. sp.

Figs 18, 19, 27A

Description. FEMALE (habitus: Figs 18A, B). Length about 3.5 mm. Head with at least frontovertex mostly dark (Fig. 18C), but scrobal depression, interantennal prominence, lower face, lower part of parascrobal region, and gena dorsally to temple (Fig. 18B) with variably bright metallic green lustre and one or more also with variably distinct and extensive reddish-violaceous lustre (*e.g.*, Fig. 18D). Face with upper parascrobal region and frons (Fig. 18E) at least very shallowly mesh-like reticulate except ocellar triangle and vertex, including temple, transversely reticulate to reticulate-alutaceous or reticulate-strigose posteriorly, and lower parascrobal region more transversely reticulate-imbricate roughened to reticulate-rugose. Clypeus with apical margin broadly, shallowly incurved (Fig. 18D). Head measurements: HL = 3.7, HH = 6.2, HW = 8.1, IOD = 3.2, TL = 1.1, EH = 4.3, EW = 3.3, MS = 2.1, MPOD: OOL: POL: LOL = 1.3: 1.4: 3.6: 2.4, and dso 2.8× [2.8: 1.0] aod. Scrobal depression dorsally evenly ∩-like arched (Fig. 18E). Labiomaxillary complex with maxillary palps dark brown, but labial palps paler, lighter brown (Fig. 18D) (visible only for holotype). Antenna (Fig. 18G) with scape mostly yellow but radicle, scape very narrowly basally and somewhat more extensively ventrobasally, pedicel, and flagellum dark brown; scape broadest subbasally and narrowed apically, with ventral margin sinuate, and about 4× as long as greatest width; pedicel about twice as long as apical width and subequal in length to combined length of basal three funiculars; flagellum with all funiculars transverse and increasing in width apically such that apical funiculars strongly transverse; clava subequal in length to combined length of apical five funiculars.

Mesosoma dorsally (Figs 18A, F) mostly dark with slight green to bluish lustre under different angles of light, but in lateral view at least prepectus paler brown (Figs 18B, 27A) and acropleuron sometimes with more distinct green to bluish or purple lustre (Fig. 27A). Mesoscutum (Fig. 18F) with convex anterior part of medial lobe shallowly mesh-like reticulate to mesh-like coriaceous posteriorly, depressed posterior part of medial lobe obviously smoother, much more finely mesh-like coriaceous, to obliquely alutaceous on inclined inner surface of lateral lobe, and with dorsal and outer inclined surfaces of lateral lobe also mesh-like coriaceous; mesoscutum, excluding parapsidal band, almost uniformly setose with brownish hair-like setae except depressed posterior part of medial lobe somewhat more sparsely setose than convex anterior part. Scutellar-axillar complex (Fig. 18F) mesh-like coriaceous; with 2 or 3 hair-like setae within each axillar depression and scutellum with 2 or 3 similar hair-like setae laterally along length, the posterior-most setae the longest (exact number of setae uncertain because of condition

of specimens). Prepectus coriaceous-reticulate to shallowly reticulate with sculpture somewhat more isodiametric (mesh-like) apically than basally (Fig. 27A). Acropleuron (Fig. 27A) finely sculptured, mesh-like coriaceous-reticulate anterodorsally near lateral margin of mesoscutum and similarly but somewhat more distinctly mesh-like reticulate ventrally above acropleural sulcus to more longitudinally reticulate-coriaceous posteroventrally, shiny and virtually smooth mesolongitudinally below level of both fore and hind wing bases except longitudinally striate dorsally posterior of level of fore wing base, and mesh-like reticulate over about posterior third with somewhat larger-sized cells than elsewhere. Front leg dark brown except dorsal and inner surfaces of tibia variably distinctly paler, more yellowish (Fig. 18B). Middle leg, including tibial spur, dark brown except extreme apex of femur dorsally and narrow region subbasally on tibia pale, and tarsomeres yellowish-white or if yellowish-infuscate then at least obviously paler than mesotarsal pegs. Hind leg dark brown except following paler: trochantellus, femur apically, tibia basally, and tarsus variably extensively and distinctly mesally. Fore wing (Fig. 18H) with costal cell hyaline except brownish-infuscate apically in front of parastigma; basal region also mostly brownish-infuscate, including vanal area variably extensively basally (Fig. 18H: vna), except following hyaline: basal cell apically adjacent to base of parastigma, cubital area (Fig. 18H: cu) longitudinally, and vanal area apically behind mediocubital fold (Fig. 18H: mcf), the apical anterior and posterior hyaline regions behind base of parastigma separated medially by infuscation extending along mediocubital fold into disc, and sometimes basal cell with slightly paler band of infuscation medially across cell; disc extensively brownish-infuscate except with slender but distinct hyaline region along parastigma and base of marginal vein, and with separated anterior and posterior hyaline regions behind marginal vein apically, the anterior hyaline region not quite extending to junction of marginal and stigmal veins, and wing subhyaline apically beyond about level of postmarginal vein. Fore wing (Fig. 18H) with costal cell dorsally bare except densely setose with mostly slightly lanceolate dark setae in infuscate region in front of parastigma; basal cell bare except for several dark hair-like setae (6 on left wing and 10 on right wing of holotype) along mediocubital fold over about basal half, and with short, white, hair-like setae apically in hyaline region adjacent to base of parastigma; disc with setae white in anterior and posterior hyaline regions but otherwise dark, mostly broadly lanceolate basally to and between anterior and posterior hyaline regions to stigmal vein anteriorly, but hair-like posterobasally behind cubital fold, apically beyond posterior hyaline region, and anteroapically beyond stigmal vein, and with at least some hair-like setae within hyaline region along parastigma; stigmal vein curved apically into uncus, but without spur projecting beyond uncus (Fig. 18H); measurements of cc: mv: pmv: stv = 7.0: 4.2: 2.6: 1.5.

Gaster with dorsal surface of Gt_1 brown, to hyaline apically, but Gt_2 hyaline so colour of Gt_3 shows through and therefore in dorsal view usually appearing more-or-less uniformly brown (Fig. 18A), and in lateral view also more-or-less uniformly brown (most air-dried paratypes) to distinctly white (critical-point dried holotype, Fig. 18B) (see Remarks); Gt_1 and Gt_2 dorsally shiny, at most very obscurely mesh-like coriaceous, and bare but with hair-like setae laterally; Gt_3 and Gt_4 also brown, quite shiny but somewhat more distinctly mesh-like coriaceous, and bare dorsally but setose laterally; G_5–syntergum dark with distinct greenish lustre, less shiny than preceding tergites, with much more distinct mesh-like coriaceous to imbricate or shallowly reticulate sculpture, and more extensively setose with at least one row of hair-like setae across surface dorsally; syntergum with syntergal flange similarly sculptured as rest of syntergum, but much paler, brown to brownish-yellow. Ovipositor sheaths pale, yellowish.

MALE (habitus: Fig. 19A). Length about 2.8 mm. Head (Figs 19B, C) with face green except frontovertex mostly more bluish-green (Fig. 19C) and interantennal prominence mediolongitudinally (Fig. 19B), and under some angles of light scrobal depression dorsally and frons anteriorly (Fig. 19C) with coppery to reddish-violaceous lustre. Face with upper parascrobal region and frons distinctly roughened, mesh-like reticulate, except more finely sculptured medially between anterior ocellus and scrobal depression; vertex transversely reticulate to transversely reticulate-strigose (Fig. 19C). Clypeus with apical margin broadly, shallowly incurved (*cf*. Fig. 18D). Head measurements: HL = 3.5, HH = 5.2, HW = 6.4, IOD = 2.4, EH = 2.5, EL = 3.2, MS = 1.6, MPOD: OOL: POL: LOL = 1.3: 1.0: 2.5: 1.6, and dso slightly greater [13:12] than aod. Scrobal depression dorsally evenly ∩-like arched (Figs 19B, C). Labiomaxillary complex not visible. Antenna (Fig. 19E) with scape yellow and clava brown, but pedicel and funicle intermediate in colour between scape and clava, variably dark brownish-yellow under different angles of light; scape about 3.2× as long as wide; pedicel about 2.3× as long as apical width, and about equal to combined length of basal four funiculars; flagellum clavate; fl_1 similar in size to fl_2, with all funiculars subquadrate to slightly transverse, and clava slightly longer than combined length of apical three, transverse, funiculars (clava collapsed so that length to width ratio not measurable with accuracy).

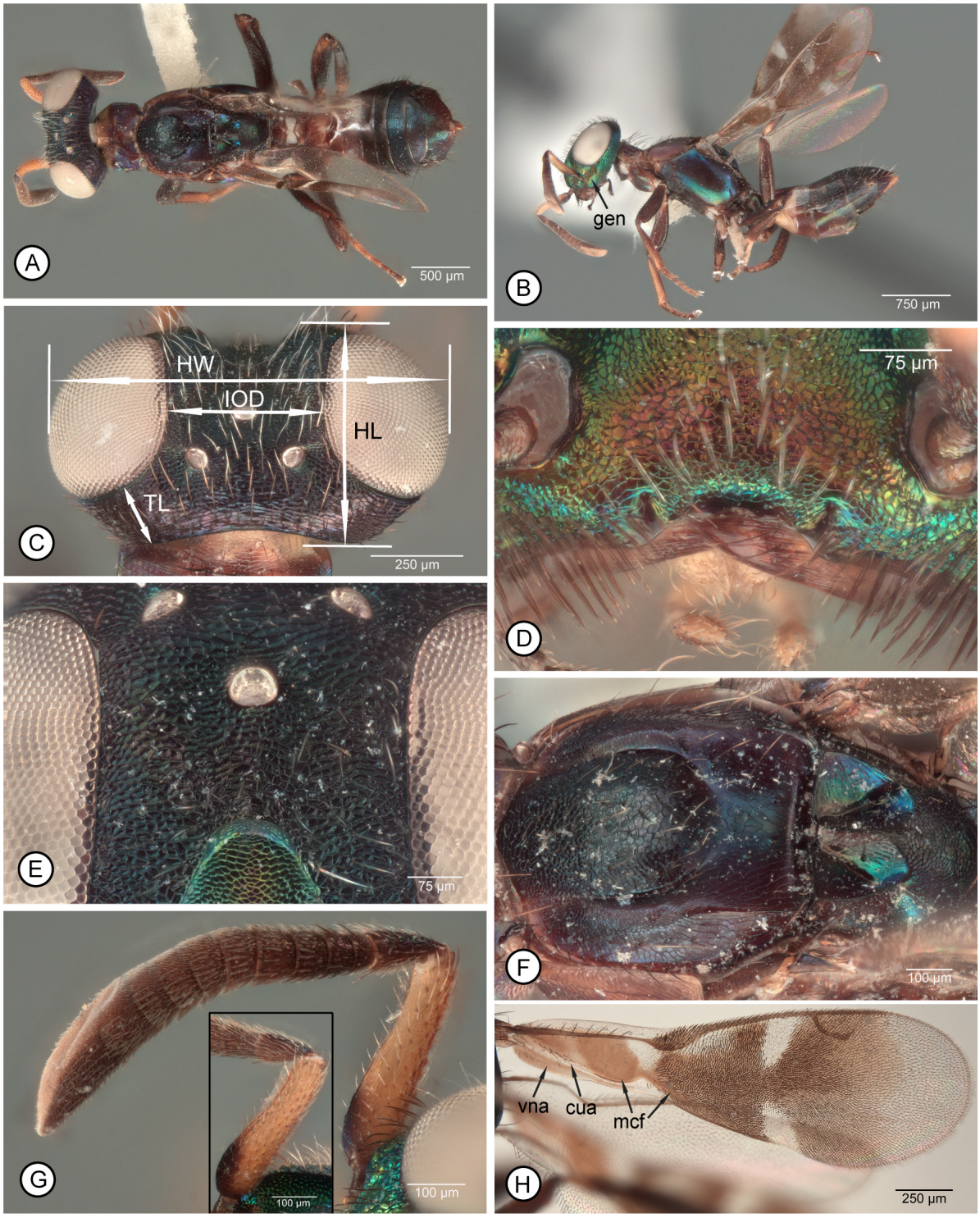

FIGURE 18A–H. *Mesocomys anelliformis* ♀ holotype. **A**, dorsal habitus; **B**, lateral habitus; **C**, head, dorsal; **D**, lower face; **E**, frontodorsal part of head; **F**, mesonotum; **G**, antenna, outer view [insert: scape–fl_1, inner view]; **H**, fore wing. [See 'Methods' and Table 1 for explanation of abbreviations.]

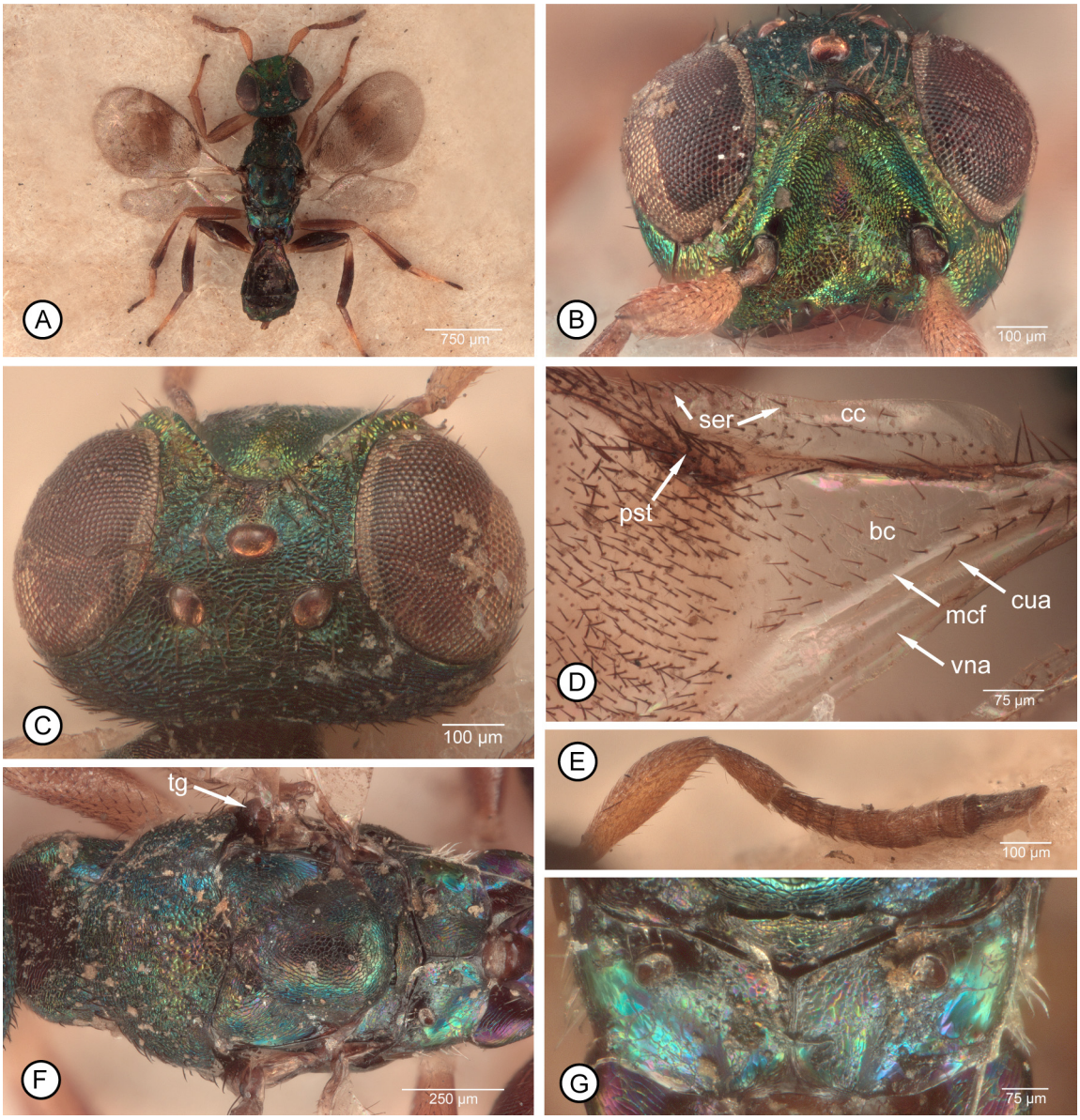

FIGURE 19A–G. *Mesocomys anelliformis* ♂ paratype (#52). **A**, dorsal habitus; **B**, head, frontal; **C**, head, dorsal; **D**, base of left fore wing, **E**, right antenna; **F**, mesosoma, dorsal; **G**, metanotum and propodeum. [See 'Methods' and Table 1 for explanation of abbreviations.]

Mesosoma dorsally (Fig. 19F) similarly green to bluish-green as head but with variably extensive coppery to reddish-violaceous lustre on pronotum, mesoscutum, and scutellar-axillar complex medially under different angles of light; lateral view mostly concealed by wings. Tegula dark brown (Fig. 19F: tg). Mesoscutum (Fig. 19F) with medial lobe distinctly reticulate to reticulate-rugulose; scutellar-axillar complex with axillae anteriorly similarly reticulate as mesoscutal medial lobe, but posteriorly more reticulate-imbricate and scutellum mesh-like coriaceous medially and posteriorly but more imbricate laterally. Legs with all coxae dark; front leg beyond coxa pale, yellowish to somewhat brownish-yellow (ventral margin of left femur brown to dark over about apical half, but right femur uniformly pale in the only known male); middle leg beyond coxa with trochanter and femur similarly pale as front leg except trochantellus paler, yellowish-white, tibia variably extensively pale basally depending on view, with at least about apical quarter dark brown but with brownish colour extending much more extensively basally on posterior surface, and tibial spur dark brown, and tarsus with basal three tarsomeres pale and apical two tarsomeres dark brown; hind leg beyond coxa with femur and tibia mostly dark brown, but trochanter and about basal quarter of tibia pale, and tarsus with second and third tarsomeres pale, but basitarsomere and apical two tarsomeres yellowish-brown to dark brown; mesotarsus with basitarsus about 0.7× and metatarsus

with basitarsus about 0.8× combined length of respective apical four tarsomeres. Fore wing (Fig. 19A) with basal cell brownish-infuscate basally, and disc comparatively dark brownish-infuscate from base of parastigma to level about equal with apex of stigmal vein except for hyaline region behind most of length of marginal vein, the hyaline region tapered posteriorly and separated by infuscation from similarly hyaline, though smaller region along posterior margin of wing, but all setae, including within hyaline region, dark brown; costal cell (Fig. 19D: cc) ventrally with single, uninterrupted row of setae extending to more numerous setae in front of parastigma (Fig. 19D: pst), and dorsally bare except for setae in front of parastigma and row of setae paralleling leading margin over about apical half (Fig. 19D: ser); basal cell setose along entire length of mediocubital fold but variably setose within cell, the basal cell of left wing (Fig. 19D) extensively setose except bare anteriorly behind most of length of submarginal vein other than for single setae near midlength, and basal cell of right wing bare with only two setae within cell other than setae along mediocubital fold; stigmal vein recurved apically into slender uncus, without developed spur beyond uncus; accurate measurements of venation not possible because of specimen condition, but marginal vein about 1.6× and postmarginal vein about 1.9× length of stigmal vein.

Gaster dark brown.

Type material. Holotype ♀ (CNC). "GUINEA: (Conakry), Mount Nimba | Gouan camp, Gallery forest of Zié | nr. "Station de Pompage Zié: [*sic*], tree canopy | understory shrub layer, Fogging 01 | N07°40'23''W08°22'24'', 1250m, 3.x.2011 | Arnaud Henrand & Didier Van den Spiegel / HOLOTYPE ♀ | *Mesocomys* | *anelliformis* Gibson". Holotype point-mounted, uncontorted, and entire (Figs 18A, B).

Paratypes (3♀, 1♂ NHMUK). **Uganda**. Bulago Isle, L. Victoria, VII.1914, Dr. G.D.H. Carpenter, bred from Lasiocampid ova, sp. not known, *Mesocomys* det. J. Waterston (3♀ NHMUK, NHMUK 011515723, 011515725 & 011515726; 1♂: NHMUK 011515730, CNC Photo 2018-52). All labelled also with paratype labels.

Etymology. A combination of the Latin words *anellus*, little ring, and *forma*, shape, in reference to the comparatively very short, ring like funiculars of the female flagellum.

Distribution. AFTROTROPICAL: Guinea, Uganda.

Biology. Host unknown, but paratypes reared from eggs of an unknown species of Lasiocampidae.

Remarks. All three female paratypes from Uganda are card-mounted by their venter and have the wings glued to the card on either side so that the lateral and ventral surfaces of the body are partly to completely concealed and accurate measurements of wing venation is not possible. The specimens are also dirtier than the holotype and with some setae abraded, and the species description thus relies to a great extent on observation of just the holotype. The critical-point dried holotype has Gt_2 hyaline so in dorsal view the gaster is more-or-less uniformly brown, but in lateral view there is a distinct white region subbasally (Fig. 18B). Of the three air-dried paratypes, two have the gaster more-or-less uniformly brown, except for a hyaline Gt_2, in both dorsal and lateral views, but one not only has a distinct whitish region subbasally in lateral view but also a transverse whitish band in dorsal view across the base of Gt_2.

Within the *pulchriceps* group, females of *M. anelliformis* are differentiated most readily by the features given in the key and, based on the few available specimens, from those of *M. longiscapus* by additional features discussed under the latter species. Males of *M. longiscapus* are unknown, but the known male of *M. anelliformis* has a similar clypeal structure as for females, the apical margin being shallowly incurved (Fig. 18D) so as to be similar to that of *albitarsis*-group species rather than deeply emarginate (*e.g.*, Figs 25E, F) unlike at least *M. orientalis* and *M. pulchriceps* males. Because both sexes of *M. anelliformis* share the same clypeal structure it is possible that both sexes of *M. anelliformis* and *M. longiscapus* also share similar antennal structures. If so, *M. longiscapus* males may have a longer scape and less strongly transverse funiculars than do *M. anelliformis* males (Fig. 19E).

Because a shallowly incurved clypeus is shared with *albitarsis*-group species, this structure is hypothesized as symplesiomorphic within the *pulchriceps* group. The deeply emarginate, almost bidentate clypeal structure of females and possibly males (males of *M. pauliani* are unknown), therefore supports *M. pauliani* + *M. orientalis* + *M. pulchriceps* as a monophyletic group. A basal relationship of at least *M. anelliformis* to that of at least *M. orientalis* + *M. pulchriceps* may also be supported by male fore wing setal patterns. The only known male of *M. anelliformis* has the basal cell at least setose along the entire length of the mediocubital fold (Fig. 19D), though the extent of setation within the basal cell differs between the two wings. Males of the *albitarsis*-group also have an extensively setose basal cell, at least along the mediocubital fold (Figs 3F, 7H, 10F, 12F, 15H), and thus this setal pattern is hypothesized as symplesiomorphic within the *pulchriceps*-group. Further, the costal cell of the

only known *M. anelliformis* male has an uninterrupted row of setae along its length ventrally, and dorsally has a row of setae that closely parallel the leading margin of the costal cell over about its apical half (Fig. 19D: ser), also similar to *albitarsis*-group males (*e.g.*, Figs 7H, 15H), and thus likely also symplesiomorphic features. Males of at least *M. orientalis* and *M. pulchriceps* have a bare basal cell or, some *M. pulchriceps*, with the basal cell closed posteriorly by only a few setae basally on the mediocubital fold. Males of these two species also have the ventral row of setae of the costal cell more-or-less broadly interrupted basal to the parastigma, and dorsally although there is one or two rows of setae in the costal cell apically, these setae extend somewhat obliquely into the cell rather than closely paralleling the leading margin (Figs 24C, F: ser), though this difference is not so obvious for smaller individuals. Further, the tegula of the known *M. anelliformis* male is dark brown and all the coxae are similarly dark, similar to conspecific females and both sexes of the *albitarsis*-group. Males of *M. orientalis* and *M. pulchriceps* are variable in both these colour features, with the variation at least partly correlated with body size. Typical males of both *M. orientalis* and *M. pulchriceps* have a pale tegula that contrasts distinctly in colour with the rest of the mesosoma (Figs 23F, 24D: tg); they also typically have at least the procoxa extensively to entirely pale (Figs 23B, F), and often the mesocoxa pale at least ventrally. However, smaller males sometimes have a variably dark brown to brownish-hyaline tegula and more extensively dark legs, including the pro- and mesocoxae. Another feature that appears to be at least partly correlated with body size, but more similar for *M. orientalis* and *M. pulchriceps* males, is relative length of the basitarsi of the middle and hind legs. The known male of *M. anelliformis* has the basitarsus of the middle leg only about 0.7 times and the basitarsus of the hind leg only about 0.8 times the combined length of the respective apical four tarsomeres (Fig. 19A), whereas at least males at the upper end of the range in body length for *M. orientalis* and *M. pulchriceps* have conspicuously longer basitarsi (Figs 23H, I), as described for the two species. Females of *M. anelliformis* and *M. longiscapus* also share a more extensively infuscate basal cell, with the infuscation extending uniformly into the disc along the mediocubital fold (Figs 18H, 20H) than for other *pulchriceps*-group females (Figs 21D, I, 25H, 26H). The more extensive fore wing infuscation could support *M. anelliformis* + *M. longiscapus* as a monophyletic lineage, though a single *M. pulchriceps* female was seen with similarly extensive infuscation (see further under *M. pulchriceps*). Although the features discussed above support *M. anelliformis* and *M. longiscapus* as basal to the other three *pulchriceps*-group species, such a relationship is not supported by marginal vein length. Females of *M. pauliani* have a comparatively long marginal vein (Fig. 25H) similar to *albitarsis*-group females (*e.g.*, Figs 2F, 5A), and thus another putative symplesiomorphy, whereas females of *M. orientalis* (Fig. 21D) and *M. pulchriceps* (Fig. 26H) have comparatively short marginal veins. The length of the marginal vein of *M. anelliformis* (Fig. 18H) and *M. longiscapus* (Fig. 20H) females is intermediate between the two extremes. Therefore, if *M. anelliformis* and *M. longiscapus* are basal to *M. pauliani* + *M. orientalis* + *M. pulchriceps*, the marginal vein must have been secondarily reduced independently to that of *M. orientalis* + *M. pulchriceps*.

***Mesocomys longiscapus* Gibson n. sp.**
Figs 20, 27B

Description. FEMALE (habitus: Figs 20A, B). Length about 3.9 mm. Head (Figs 20C, D) mostly dark with extensive reddish-violaceous lustre over parascrobal region ventrally, interantennal prominence and lower face, but with slight greenish lustre under some angles of light elsewhere, particularly within scrobal depression, on vertex, and gena. Face with upper parascrobal region and frons (Fig. 20F) mesh-like coriaceous-pustulate to imbricate except ocellar triangle and vertex, including temple, increasing more imbricate-alutaceous to reticulate-alutaceous posteriorly (Fig. 20C), and lower parascrobal region more transversely reticulate-imbricate roughened. Clypeus with apical margin broadly, shallowly incurved (*cf.* Fig. 18D). Head measurements: HL = 3.7, HH = 7.2, HW = 9.2, IOD = 3.4, TL = 1.5, EH = 4.3, EW = 3.4, MS = 2.5, MPOD: OOL: POL: LOL = 1.3: 1.3: 4.2: 2.3, and with dso 2.0× [2.4: 1.2] aod. Scrobal depression dorsally slightly M-like emarginate (Fig. 20F). Labiomaxillary complex with maxillary palps dark brown but labial palps paler, yellowish. Antenna (Fig. 20G) with scape mostly yellow but extreme apex dorsally, extreme base ventrally and radicle brownish; pedicel and flagellum dark brown; scape subequal in width along length; about 6× as long as greatest width; pedicel about 2.5× as long as apical width and subequal to combined length of basal two funiculars plus basal half of third funicular; flagellum with fl_1 quadrate to slightly longer than apical width, and at least fl_2–fl_5 all slightly longer than

wide, and increasingly slightly in width apically such that apical 1–3 funiculars quadrate to slightly transverse; clava subequal in length to combined length of apical three funiculars.

Mesosoma dorsally (Figs 20A, E) mostly dark brown with at most obscure metallic lustre except pronotum dorsally with neck much paler, yellowish, and collar with bluish to reddish-violaceous lustre laterally; in lateral view pronotal panel paler ventrally than dorsally, prepectus orangish-brown to brown with at least slight bluish to purple lustre under some angles of light and acropleuron darker brown with green to partly coppery to blue or purple lustre under different angles of light (Fig. 27B). Mesoscutum (Fig. 20E) with convex anterior part of mesoscutal lobe shallowly mesh-like reticulate, depressed posterior part similarly shallowly and distinctly mesh-like reticulate, and lateral lobe mesh-like coriaceous-reticulate; mesoscutum, excluding parapsidal band, almost uniformly setose with brownish hair-like setae except depressed posterior part of medial lobe somewhat more sparsely setose than convex anterior part. Scutellar-axillar complex (Fig. 20E) mesh-like coriaceous-imbricate to slightly reticulate-imbricate; with 2 hair-like setae within each axillar depression and scutellum with 3 hair-like setae laterally along length, the posterior-most setae the longest. Prepectus distinctly mesh-like reticulate (Fig. 27B). Acropleuron (Fig. 27B) entirely sculptured, mesh-like reticulate-imbricate to shallowly reticulate anterodorsally near lateral margin of mesoscutum, only minutely and obscurely mesh-like dorsally near fore wing base but distinctly, almost longitudinally, finely striate below fore wing base, with sculpture becoming more coarsely longitudinally strigose-striate posteromedially, but more mesh-like coriaceous-reticulate over about posterodorsal and posteroventral half and isodiametric coriaceous-reticulate posteriorly. Front leg (Figs 20A, B) dark brown except tibia and tarsus paler, yellowish. Middle leg (Fig. 20B) with trochanter, trochantellus, most of femur, tibia basally except for subbasal pale band, mesotibial spur and mesotarsal pegs dark, but femur apically, narrow subbasal band on tibia and at least apical half of tibia, and tarsomeres other than pegs paler, more yellowish. Hind leg (Fig. 20B) mostly dark except femur distinctly paler apically and variably extensively ventrobasally, tibia at least with distinct, narrow pale band basally and variably extensively paler apically, and tarsomeres pale, yellowish. Fore wing (Fig. 20H) with costal cell hyaline except brownish-infuscate apically in front of parastigma; basal region mostly brownish-infuscate except basal cell apically hyaline adjacent to base of parastigma and slightly paler medially across cell (paler region not visible in Fig. 20H because of leg below wing), and cubital and vanal areas hyaline to subhyaline, lighter brown than basal cell, but infuscation of basal cell extending into disc along mediocubital fold; disc extensively brownish-infuscate except with slender but distinct hyaline region along parastigma and base of marginal vein, and with separated anterior and posterior hyaline regions behind marginal vein apically, the anterior region not quite extending to junction of marginal and stigmal veins, and wing subhyaline apically beyond about level of postmarginal vein. Fore wing (Fig. 20H) with costal cell dorsally bare except densely setose with mostly slightly lanceolate dark setae in infuscate region in front of parastigma, and apically along leading margin with row of dark hair-like setae (Fig. 20H: arrows) for distance equal to about two-thirds length of parastigma; basal cell bare except dorsally with about 20 dark hair-like setae over about basal half along mediocubital fold, and with short, white, hair-like setae in anteroapical hyaline region adjacent to parastigma; disc with setae white in anterior and posterior hyaline regions but otherwise dark and mostly broadly lanceolate except hair-like posterobasally behind cubital fold and apically beyond about level of stigmal vein; stigmal vein curved apically into uncus, but without spur projecting beyond uncus; measurements of cc: mv: pmv: stv = 7.6: 3.7: 2.0: 1.5.

Gaster with Gt_1 and St_1 somewhat paler brown than subsequent tergites and Gt_2 hyaline so colour of Gt_3 shows through and therefore in dorsal view more-or-less uniformly brown (Fig. 20A), though slightly paler basally, and in lateral view with or without evident vertical white band at junction of Gt_1 and Gt_2; Gt_1 and Gt_2 dorsally shiny, at most very obscurely mesh-like coriaceous, and bare but with hair-like setae laterally; Gt_3–syntergum similarly or somewhat increasingly more coarsely though shallowly mesh-like reticulate, with Gt_3 and Gt_4 setose only laterally but Gt_5–syntergum with at least one row of hair-like setae across surface dorsally; syntergum more-or-less uniformly sculptured and coloured so that syntergal flange comparatively inconspicuously differentiated. Ovipositor sheaths pale, yellowish.

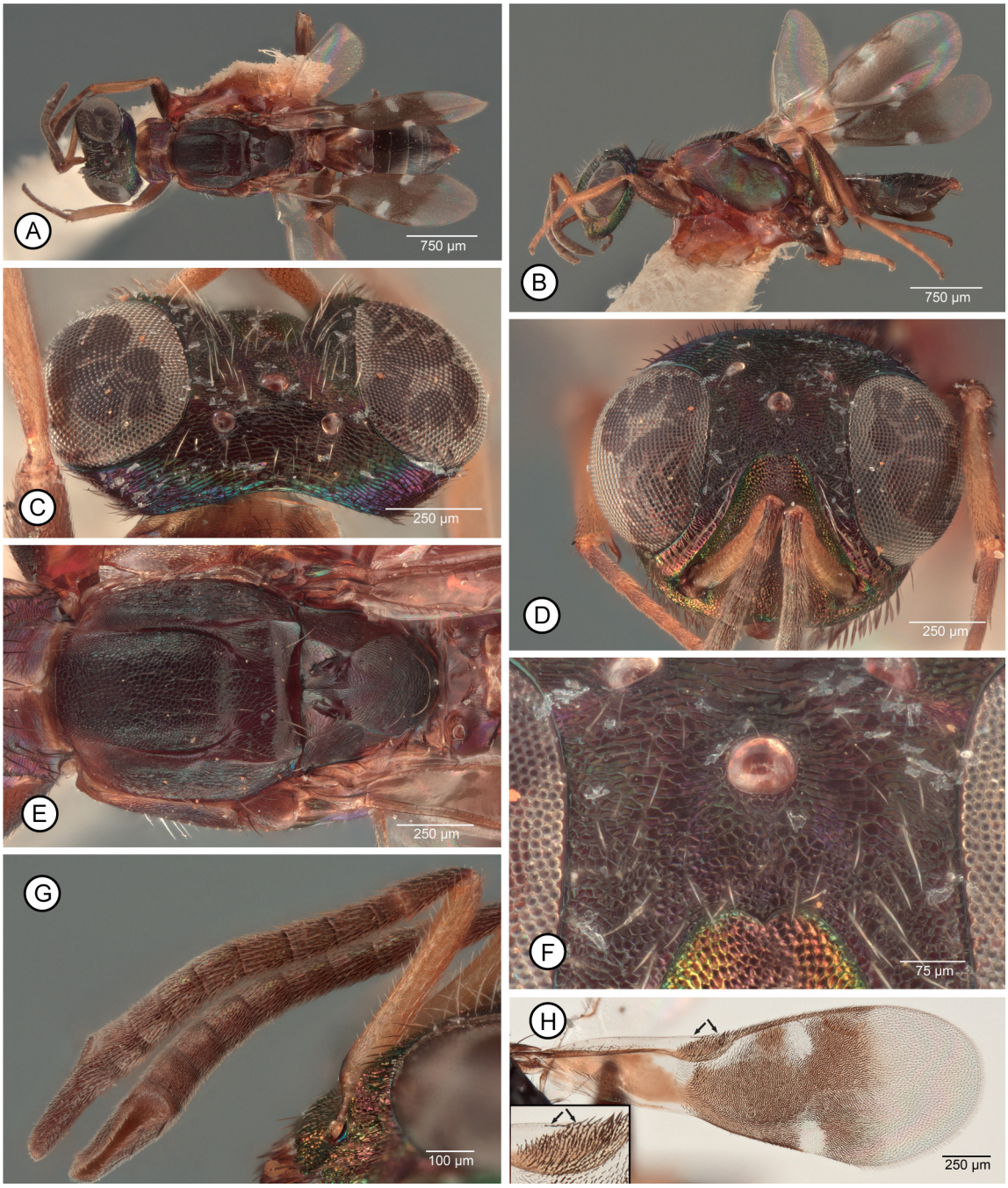

FIGURE 20A–H. *Mesocomys longiscapus* ♀. **A**, dorsal habitus (HT); **B**, lateral habitus (HT); **C**, head, dorsal (HT); **D**, head, frontal (HT); **E**, mesosoma, dorsal (HT); **F**, frontodorsal part of head (HT); **G**, antennae (PT); **H**, fore wing (HT) [arrows point to row of setae along leading margin of costal cell; insert: enlargement of parastigma]. Figure caption abbreviations: HT = holotype, PT = paratype.

MALE. Unknown.

Type material. Holotype ♀ (NHMUK). "T.239 / Uganda | Kampala / IV.1936 | H.C. Taylor / Brit. Mus. | 1956-25 / NHMUK 011515667 / HOLOTYPE ♀ | *Mesocomys* | *longiscapus* Gibson". Holotype mounted by mesosoma on top of point such that head directed toward left, but uncontorted, and entire (Figs 20A, B).

Paratype (1♀ NHMUK). Same data as holotype except NHMUK 01151566, and labelled with paratype label.

Etymology. A combination of the Latin words *longus*, long, and *scapus*, stem, in reference to the comparatively long scape of females, which is one of two principal features to distinguish females from those of *M. anelliformis*.

Distribution. AFROTROPICAL: Uganda.

Biology. Host: unknown.

Remarks. As discussed under *M. anelliformis*, *M. longiscapus* is hypothesized as most likely the sister species of *M. anelliformis* based on an extensively infuscate basal cell that is continuously infuscate into the disc along the mediocubital fold (*cf.* Figs 18H & 20H), and possibly on a secondarily reduced marginal vein. Females of the two species are differentiated most conspicuously by the keyed antennal differences. Other, less conspicuous observed differences between females are not included in the key because more specimens are required to more confidently assess whether these truly represent interspecific differences or one or more may result from incomplete knowledge of intraspecific variation. Other described features that differ among available females of *M. longiscapus* and *M. anelliformis* include the following: 1) costal cell dorsally with short row of dark hair-like setae along leading margin in front of parastigma (Fig. 20H: arrows) *versus* costal cell dorsally without row of setae along leading margin (Fig. 18H), though both with dark lanceolate setae apically in costal cell in front of parastigma (Figs 18H, 20H); 2) frons mostly imbricate to pustulate with surface of sculptural cells flat to slightly convex (Fig. 20F) *versus* sculpture reticulate with concave cells (Fig. 18E); 3) distinctly lanceolate dark setae of fore wing disc more extensive, extending apically beyond anterior and posterior hyaline regions posteriorly, and anteriorly partly beyond stigmal vein toward postmarginal vein *versus* setae hair-like posteriorly beyond posterior hyaline region and lanceolate anteriorly only to stigmal vein; 4) acropleuron quite distinctly, longitudinally striate mesally below level of fore wing base (Fig. 27B) *versus* almost smooth (Fig. 27A); and 5) scrobal depression dorsally quite distinctly M-like arched (Fig. 20F) *versus* evenly arched (Fig. 18E). Sculpture of the prepectus also differs noticeably, though prepectal sculpture is variable in some other species, such as *M. pulchriceps*. Of the above five features, the first is unique to *M. longiscapus* among *pulchriceps*-group species.

The unknown males of *M. longiscapus* are undoubtedly similar to those of *M. anelliformis* in having a shallowly emarginate clypeus, as for their conspecific females. If further similar to females, males of *M. longiscapus* may also have a basal cell that is setose at least along the length of the mediocubital fold and a costal cell with a row of setae closely paralleling the leading margin apically (*cf.* Fig. 19D: ser) rather than obliquely angled into the cell, and may differ from *M. anelliformis* males by antennal structure, as discussed under the latter species. Further collections are also necessary to determine whether males have the scrobal depression dorsally somewhat M-like emarginate as for known females (Fig. 20F).

Mesocomys orientalis Ferrière

Figs 21, 22, 23A–H, 24A–C, 27C & D

Mesocomys orientalis Ferrière, 1935: 150–152, fig. 5 (female). Described from 14♀ and 10♂ syntypes; lectotype ♀, here designated (NHMUK).

Mesocomys orientalis; Ferrière, 1951: 265 (keyed); Khan, 1983: 656–658 (redescription), figs 1–8 (female), figs 9, 10 (male); Mani, 1989: 668–669 (redescription), fig. 156H, I (female); Narendran & Sheela, 1995: 311 (keyed); Ahmed *et al*., 1995: 259–261 (redescription); Yang *et al*., 2015: 167 (keyed), 170 (Chinese description and data), 257 (English data summary), fig. 89 (female); Yao *et al*., 2009: 155 (keyed).

Mesocomys atulyus Narendran in Narendran & Sheela, 1995: 308–310, figs 1–4 (female), figs 5, 6 (male). Described from holotype ♀ and paratype ♂ (both DZUC). **New synonymy**.

Description. FEMALE (habitus: Figs 21A, B, E, F). Length = 2.1–4.1 mm. Head (Figs 22A, B) usually with distinct greenish lustre at least extensively on interantennal protuberance, parascrobal region, lower face and gena, usually also with variably extensive and distinct green to bluish-green lustre on frontovertex under at least some angles of light (Fig. 22E), and often with variably distinct reddish-violaceous lustre on one or more of following: within scrobes, scrobal depression dorsally, interantennal prominence mediolongitudinally, across lower face between toruli, and sometimes in part on parascrobal region and frontovertex (Figs 22A, B). Face with upper parascrobal region and frons mesh-like coriaceous or if somewhat coriaceous-imbricate then at least surface of all sculptural cells flat (Figs 22A, B, D, E), frontovertex alutaceous (Fig. 22B), and lower parascrobal region more transversely reticulate-imbricate roughened. Clypeus with apical margin deeply, ∩-like emarginate medially (Fig. 22C: arrow). Head measurements: HL = 2.3–3.8, HH = 4.0–6.5, HW = 4.5–7.8, TL = 0.7–1.4, EH = 2.3–4.0, EW = 1.7–3.0, MS = 1.4–2.3, IOD = 0.40–0.42, MPOD: OOL: POL: LOL = 1.0: 1.2–1.3: 2.7–3.0: 1.6–2.0, and with dso 2.0–2.6× aod. Scrobal depression dorsally evenly ∩-like arched (Figs 22A, B, D, E), the dorsal margin sometimes transverse (Fig. 22A) but not distinctly emarginate. Labiomaxillary complex with maxillary palps dark brown but labial palps slightly paler. Antenna (Figs 22F–H) with scape sometimes entirely yellow but usually dark at least ventrobasally

and sometimes with up to almost basal half brownish (often more extensively on inner than outer surface); pedicel and flagellum sometimes similarly brown (Fig. 22G), and pedicel sometimes with green lustre dorsally, but often pedicel and/or variable number of basal funiculars at least noticeably paler than apical funiculars and/or clava (excluding micropilose sensory region); scape broadest subbasally and narrowed apically, with ventral margin sinuate, and about 4.0–4.2× as long as greatest width; pedicel equal to or slightly longer than twice apical width and equal in length or slightly longer than combined length of basal three funiculars; flagellum with all funiculars transverse and increasing in width apically such that apical funiculars strongly transverse; clava equal in length or slightly longer than combined length of apical four funiculars.

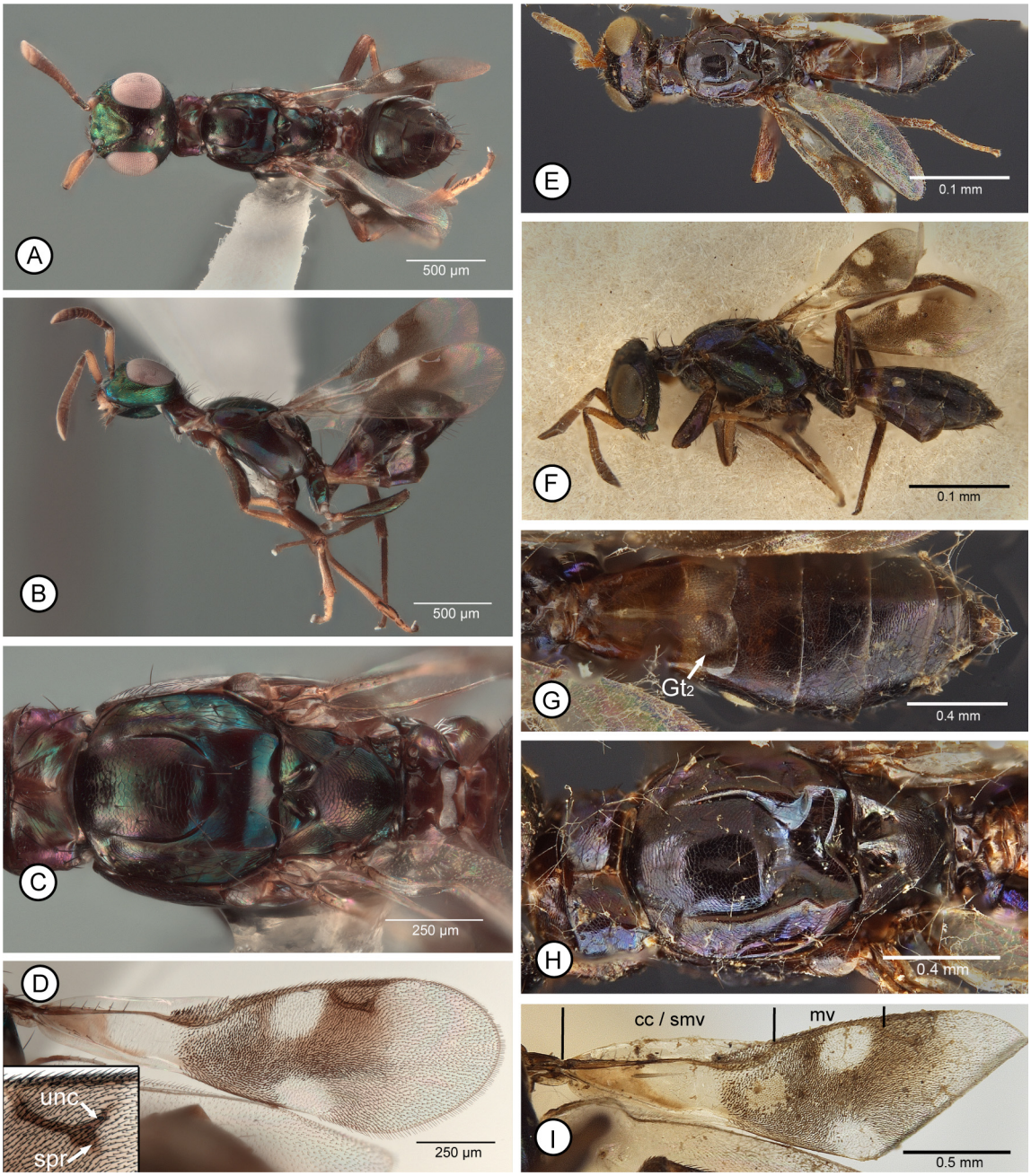

FIGURE 21A–I. *Mesocomys orientalis* ♀. ***A–D***, (#41): **A**, dorsal habitus; **B**, lateral habitus; **C**, mesosoma, dorsal; **D**, fore wing [insert: enlargement of stigmal vein]. ***E–I***, *M. atulyus* holotype: **E**, dorsal habitus; **F**, lateral habitus; **G**, gaster, dorsal; **H**, mesosoma, dorsal; **I**, fore wing. [See 'Methods' and Table 1 for explanation of abbreviations.]

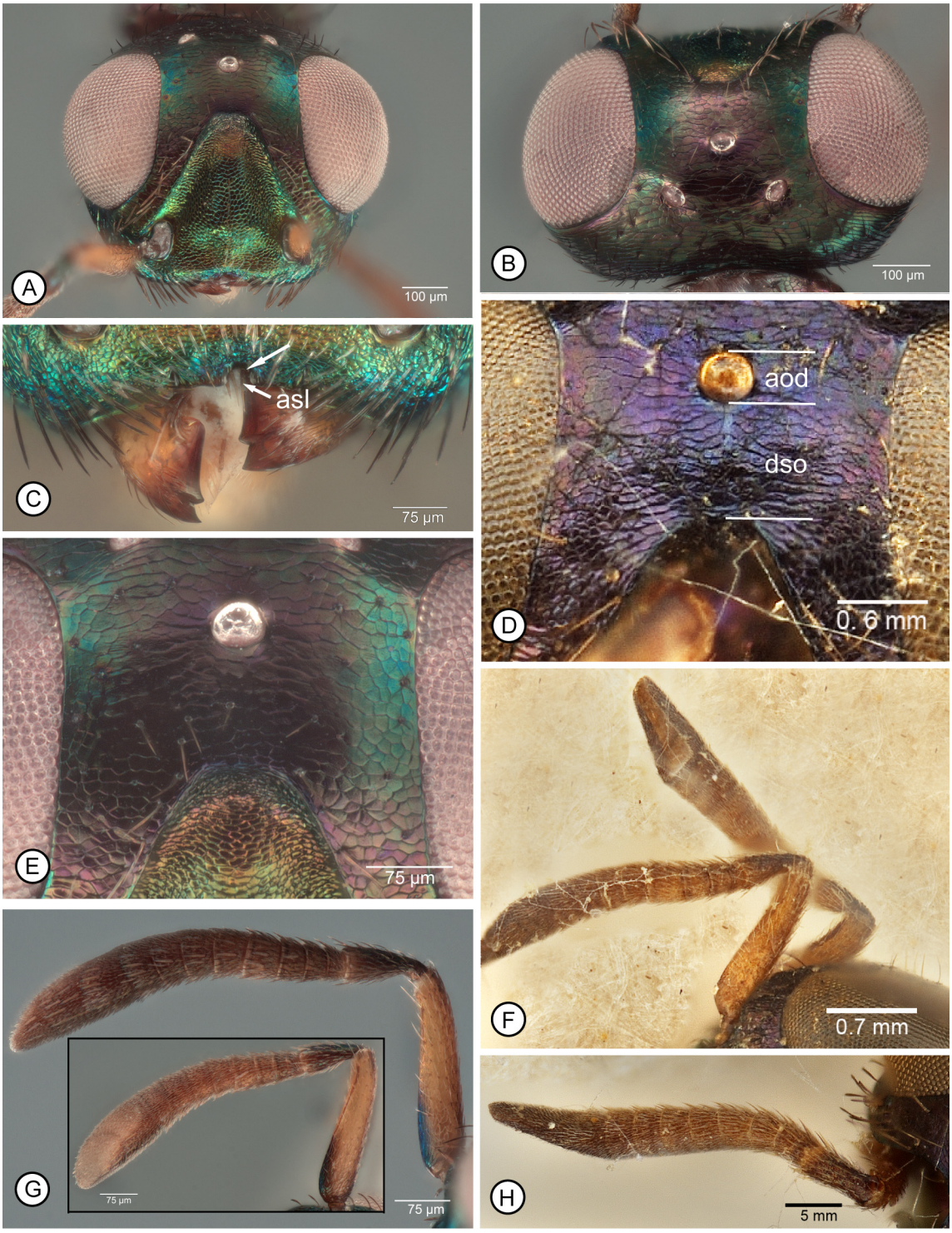

FIGURE 22A–H. *Mesocomys orientalis* ♀. **A**, head, frontal (#41); **B**, head, dorsal (#41); **C**, lower face (#41) [arrow points to margin of incised clypeus]. ***D & E***, frontodorsal part of head: **D**, *M. atulyus* (holotype); **E**, #41. ***F–H***, antennae: **F**, *M. atulyus* (holotype); **G**, outer view [insert: inner view] (#41); **H**, *M. atulyus* (holotype), dorsal view. [See 'Methods' and Table 1 for explanation of abbreviations.]

Mesosoma dorsally mostly dark brown (Fig. 21H) or with slight reddish-violaceous lustre under some angles of light except concave posterior part of mesoscutum usually variably distinctly and extensively green to blue and sometimes, less distinctly, elsewhere (Fig. 21C); in lateral view (Figs 27C, D) mostly brown to dark with coppery to reddish-violaceous or sometimes with green, blue and/or purple lustres under some angles of light. Mesoscutum (Figs 21C, H) with convex anterior part of medial lobe finely mesh-like coriaceous, the posterior depressed part

with similar though less distinct to subeffaced sculpture, and lateral lobe also mesh-like coriaceous; mesoscutum, excluding parapsidal band, variably extensively and conspicuously setose, sometimes with setae mostly aligned in longitudinal row on either side of midline, but depressed posterior part with only 4 long, bristle-like setae. Scutellar-axillar complex mesh-like coriaceous; with 2 or 3 hair-like setae within each axillar depression and scutellum with 2 longer, bristle-like setae laterally. Prepectus (Figs 27C, D) mesh-like coriaceous or mesh-like imbricate to shallowly reticulate anteriorly or anteroventrally. Acropleuron (Figs 27C, D) finely sculptured, mesh-like coriaceous-alutaceous anterodorsally near lateral margin of mesoscutum, similarly but more longitudinally coriaceous dorsally and ventrally and very finely, minutely sculptured to almost smooth mesally below level of wing bases, but mesh-like coriaceous over about posterior half, the sculpture becoming increasingly larger and more isodiametric posteriorly except usually more elongate posterodorsally. Front leg (Figs 21B, F) with femur at least extensively dark, but usually paler dorsoapically and often with anterior surface variably extensively basally to entirely pale; tibia sometimes entirely pale but at least apically and often with dorsal and/or inner surfaces pale; tarsus pale or with apical tarsomere darker. Middle leg (Figs 21B, F) with femur mostly dark but at least pale apically, and usually with anterior surface variably extensively apically and basally to entirely variably distinctly paler; tibia sometimes almost entirely pale, though usually with more distinct, narrow pale band subbasally and tibial spur at least orangish and usually dark brown in distinct contrast to tarsomeres; tarsus with at least basal four tarsomeres pale except for dark pegs. Hind leg (Figs 21B, F) mostly dark, but at least trochantellus and often femur apically and tibia basally paler. Fore wing (Figs 21D, I) with costal cell hyaline or at most only slightly, comparatively inconspicuously brownish-infuscate apically in front of parastigma; basal cell brownish-infuscate over at most about basal half except more extensively along mediocubital fold, though not extending to disc, cubital area hyaline, and vanal area at least very slightly brownish-infuscate basally; disc extensively brownish-infuscate basally except with slender, often comparatively inconspicuous hyaline band along parastigma to base of marginal vein, and with separated anterior and posterior hyaline regions behind marginal vein apically, the anterior region extending to or almost to junction of marginal and stigmal veins, and wing hyaline apically beyond about level of postmarginal vein or more extensively posteriorly toward posterior hyaline region. Fore wing (Figs 21D, I) with costal cell dorsally bare except densely setose with hair-like or only slightly lanceolate dark setae in front of parastigma; basal cell with row of 3–8 hair-like setae along mediocubital fold basally, and with a few short, white, hair-like setae apically adjacent to parastigma and infuscate part of disc; disc with setae white in anterior and posterior hyaline regions, but otherwise dark brown and extensively hair-like except distinctly lanceolate mediolongitudinally from base of infuscate region to and between anterior and posterior hyaline regions, the setae more hair-like posterior of cubital fold basal to posterior hyaline region and apically beyond anterior and posterior hyaline regions; stigmal vein apically curved into uncus or with only short, stub-like, comparatively inconspicuous spur (Fig. 21D, insert: spr) projecting beyond uncus (Fig. 21D, insert: unc); measurements of cc: mv: pmv: stv = 4.8–5.5: 2.0–2.4: 1.3–1.5: 1.0.

Gaster often completely dark brown (Figs 21A, B, E–G) or with variably distinct green to bluish lustre over apical three tergites under some angles of light, but St_1 usually variably distinctly paler and Gt_2 (Fig. 21G: Gt_2) and St_2 at least hyaline with colour of underlying sclerites showing through (Fig. 21G) and sometimes Gt_1 paler to white mediolongitudinally and/or Gt_2 and St_2 variably distinctly paler brown to yellowish so as to form variably broad and distinct subbasal pale band in dorsal and/or lateral (*cf*. Fig. 25C) views near apical margin of Gt_1; Gt_1 dorsally shiny, at most very obscurely mesh-like coriaceous, and bare but with hair-like setae laterally; Gt_2 similar to Gt_1 but at least subsequent tergites finely mesh-like coriaceous-alutaceous or at most Gt_2 and Gt_3 coriaceous-reticulate (surface of sculptural cells flat but formed by slightly raised ridges) and at least apical three tergites with at least one row of setae across tergite; syntergum more-or-less uniformly sculptured and coloured so that syntergal flange comparatively inconspicuously differentiated. Ovipositor sheaths pale, yellowish.

MALE (habitus: Figs 23A, B). Length = 1.7–3.5 mm. Head (Fig. 23C) with face green to bluish-green except usually for some coppery to reddish-violaceous lustre under some angles of light. Face with upper parascrobal region and frons (Fig. 24A) at most only slightly roughened, mesh-like coriaceous in smaller individuals to coriaceous-imbricate in larger individuals, but with surface of sculptural cells flat (Fig. 24A); vertex transversely alutaceous to alutaceous-reticulate with surface of sculptural cells at most shallowly depressed so not distinctly strigose. Clypeus with apical margin deeply, ∩-like emarginate medially (*cf*. Fig. 22C: arrow). Head measurements: HL = 2.1–4.0, HH = 3.0–5.8, HW = 3.6–7.2, EH = 1.5–3.5, EL = 1.9–2.9, MS = 1.0–2.0, IOD 0.40–0.42× HW, MPOD: OOL: POL: LOL = 0.7–1.3: 0.6–1.1: 1.8–3.4: 1.0–2.2, and dso 1.2–1.4× aod. Scrobal depression dorsally evenly ∩-like arched to slightly M-like emarginate (Fig. 24A). Labiomaxillary complex with maxillary and labial palps yellow.

Antenna (Fig. 23E) variably extensively pale, the flagellum, pedicel, and scape dorsoapically sometimes brown, particularly in smaller individuals, but usually scape, pedicel, and flagellum at least basally, yellowish-brown to yellow, though clava usually somewhat darker brownish; scape about 3.1–3.9× as long as wide; pedicel about 2.7–4.0× as long as apical width and at least almost as long as, and sometimes slightly longer than, combined length of basal four funiculars; flagellum clavate; fl_1 similar in size to fl_2, with all funiculars slightly transverse or only fl_4 quadrate, and clava about 1.6–1.9× as long as wide and subequal in length to combined length of apical three funiculars.

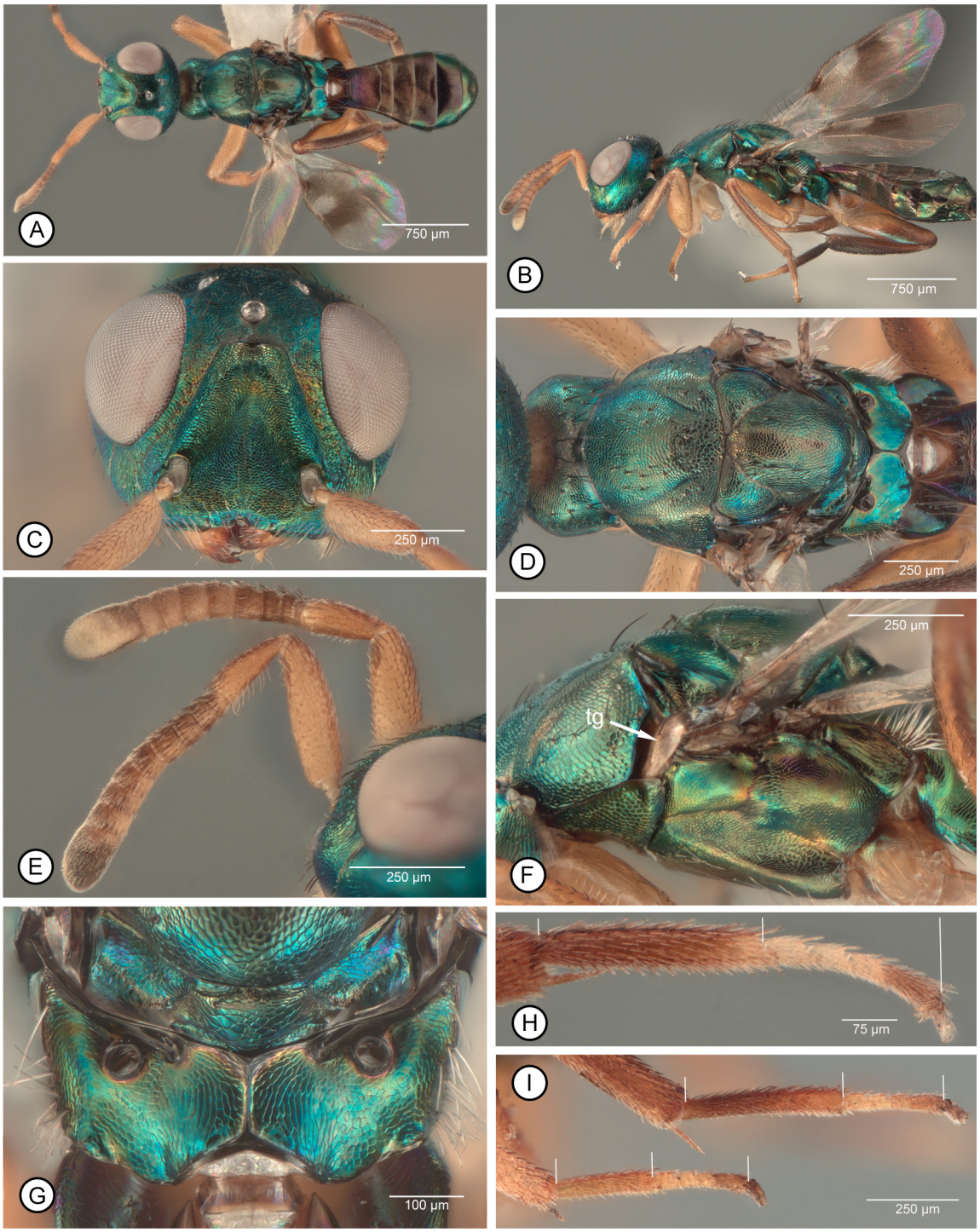

FIGURE 23A–I. *Mesocomys* species ♂. ***A–H***, *M. orientalis*: **A**, dorsal habitus (#70); **B**, lateral habitus (#70); **C**, head, frontal (#69); **D**, dorsal mesosoma (#69); **E**, antennae (#70); **F**, lateral mesosoma (#71) [tg = tegula]; **G**, metanotum and propodeum (#69); **H**, metatarsus (#42). **I**, *M. pulchriceps* (#68), metatarsus (upper) and mesotarsus (lower). [Vertical lines in Figs 23H & I indicate dorsal length of basitarsus and combined length of apical four tarsomeres.]

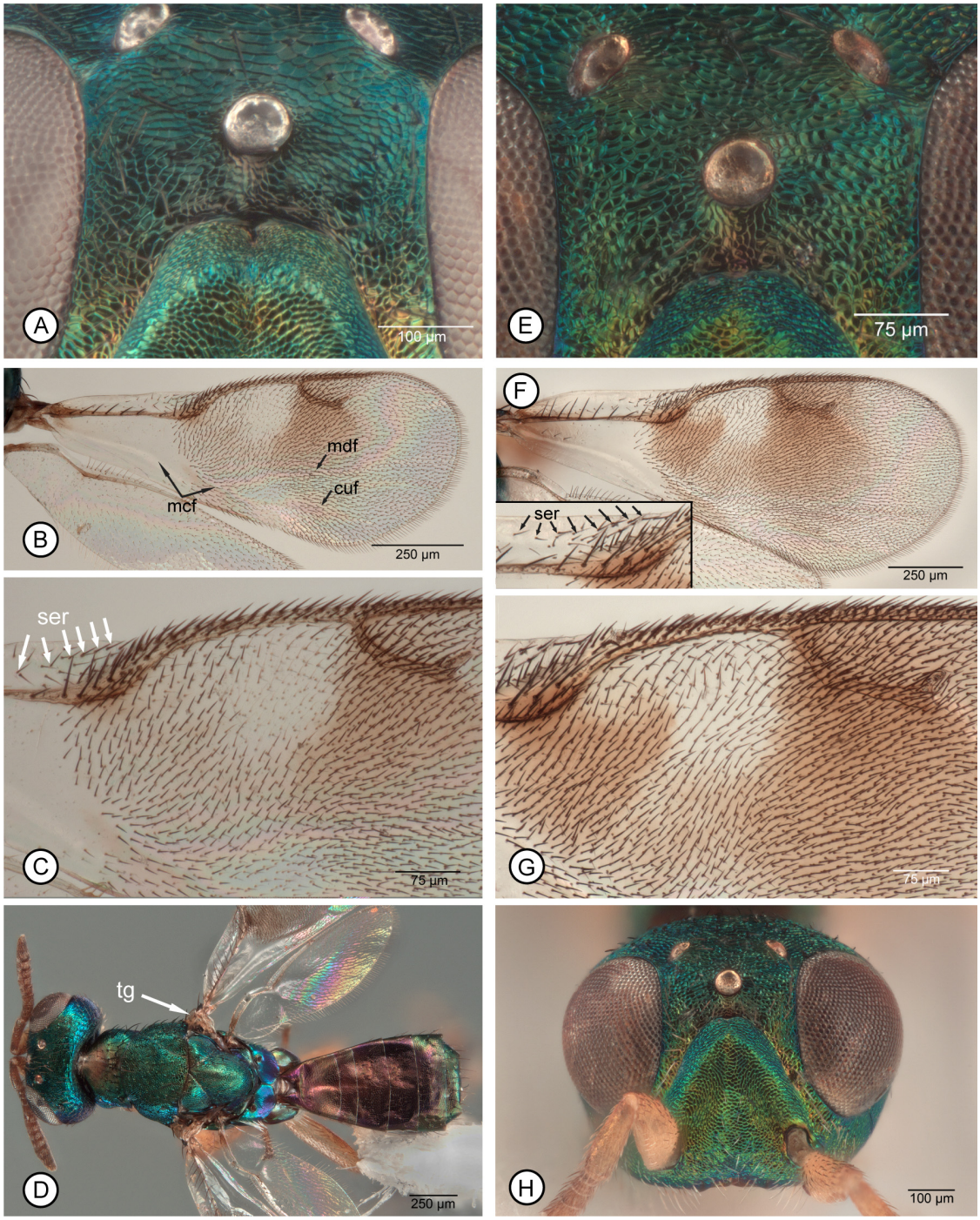

FIGURE 24A–H. *Mesocomys* species ♂. ***A–C***, *M. orientalis*: **A**, frontodorsal part of head (#69); **B**, fore wing (#43); **C**, middle part of fore wing (#43). ***D–H***, *M. pulchriceps*: **D**, dorsal habitus (#44), **E**, frontodorsal part of head (#45); **F**, fore wing (#44) [insert: enlargement of apex of costal cell]; **G**, middle part of fore wing (#44); **H**, head, frontal (#45). [See 'Methods' and Table 1 for explanation of abbreviations.]

Mesosoma dorsally (Fig. 23D) similarly green to bluish-green as head except propodeum often more blue to purple and usually with variably extensive coppery to reddish-violaceous lustre on one or more of pronotum, mesoscutum, and scutellar-axillar complex medially under different angles of light; in lateral view (Fig. 23F) similar in colour to dorsal surface and often with some coppery to reddish-violaceous lustre under different angles of light, but mesopleurosternum without differentiated, paler, Y-like set of lines (Fig. 23F). Tegula sometimes brown to brownish-hyaline, particularly in smaller individuals, to orangish or yellow (Fig. 23F: tg). Mesoscutum (Fig. 23D) with medial lobe mesh-like coriaceous to variably extensively shallowly reticulate, at least posteriorly toward scutellar-

axillar complex; scutellar-axillar complex with axillae similarly or more finely sculptured than mesoscutal medial lobe, but at least scutellum mesh-like coriaceous medially and posteriorly and somewhat more imbricate laterally. Legs usually with procoxa entirely pale (Figs 23B, F), though sometimes only ventrally in smaller individuals, mesocoxa at least ventrally and sometimes almost entirely pale (Fig. 23F), but metacoxa dark with green lustre except sometimes extreme apex (Fig. 23B); front leg beyond coxa sometimes entirely, similarly pale as coxa (Figs 23A, B), though often femur more brownish-yellow and sometimes in smaller individuals variably extensively dark brown with some green lustre, at least over posterior surface; middle leg beyond coxa often entirely pale, including tibial spur, except sometimes basal tarsomere and apical one or two tarsomeres at least slightly darker brown than medial tarsomeres (Fig. 23B), though in smaller individuals femur and tibia variably dark brown and tibial spur, basal tarsomere and one or two apical tarsomeres similarly or somewhat darker brown than femur and tibia; hind leg beyond coxa sometimes dark in smaller individuals except for paler trochanter and trochantellus and at least tarsomeres 2 and 3 to 2–5 white to brownish-white compared to darker basitarsomere, though sometimes femur paler basally, brownish-yellow, and sometimes entirely paler dorsally, and tibia sometimes also paler basally; mesotarsus with basitarsus about 0.7–0.9× and metatarsus with basitarsus (Fig. 23H) about 1.1.–1.4× combined length of respective apical four tarsomeres, with larger individuals having a relatively more elongate basitarsus. Fore wing (Fig. 24B) with basal cell hyaline, but disc variably light to dark brownish-infuscate between about base of parastigma and level of apex of stigmal vein except paler to hyaline behind medial fold (Fig. 24B: mdf) or cubital fold (Fig. 24B: cuf) and apically beyond about level of apex of stigmal vein (often more faintly infuscate behind parastigma than between postmarginal and stigmal veins and behind stigmal vein), and with hyaline region behind about apical half of marginal vein opposite of smaller hyaline region adjacent to posterior margin of wing, with setae within hyaline regions behind marginal vein white but dark elsewhere (Figs 24B, C); costal cell ventrally sometimes with single row of setae along most of length in smaller individuals, but larger individuals often with two rows of setae along most of length, though then setae interrupted from more numerous setae in front of parastigma by bare region basal to parastigma, and costal cell dorsoapically with row of setae extending obliquely into cell rather than closely paralleling leading margin (Fig. 24C: ser); basal cell entirely bare basal to parastigma (Fig. 24B); stigmal vein apically expanded and truncate or with variably distinct uncus, and often with at least short, stub-like spur projecting beyond uncus (Fig. 24C); measurements of cc: mv: pmv: stv = 3.8–4.1: 1.6–2.1: 1.4–1.9: 1.0.

Gaster dark brown except often for variably extensive green lustre apically (Fig. 23A).

Type material examined. *Mesocomys orientalis*. Lectotype ♀ (hereby designated, NHMUK). Specimen not re-examined for study, but examined in 2015 at NHMUK, with following data based on notes taken at that time and on image of designated lectotype and type labels provided by N. Dale-Skey Papilloud (NHMUK) in 2018: "Type [red-bordered circular label] / BURMA. | Rangoon. | F.J. Meggitt. / Pres. by | Imp. Inst. Ent. | Brit. Mus. | 1933-375. / *Mesocomys* | *orientalis* ♀ | Ch. Ferriere det. ['det.' crossed out] Type / B.M. TYPE | HYM. | 5.1,038 / NHMUK 010198547"; also newly labelled with "LECTOTYPE ♀ | *Mesocomys*| *orientalis* | Ferrière". Lectotype glued by left acropleuron on top of card point (right side faced upwards), uncontorted, and entire.

Paralectotypes examined, here designated: 12♀ and 9♂ (NHMUK) all with similar label data as for lectotype but without yellow-bordered "Co-type" label; also newly labelled with "PARALECTOTYPE | *Mesocomys* | *orientalis* | Ferrière". The type material is associated with another three cards with linear eggs masses.

Mesocomys atulyus. Holotype ♀ (DZUC; photomicrographs examined, Figs 21E–I): "Holo | type [red-bordered circular label] / ♀ *Mesocomys atulyus* | sp. nov. | Det. Narendran T.C 1993 / INDIA: Kerala | Cali. Uni. Campus | 18.i.1988 | T.C. Narendran / Host: *Antheraea* sp. | (Lepidoptera: Sturniidae [*sic*]) / 2577".

Other material examined. ORIENTAL. **BANGLADESH**. Rajshahi, 27.VI.1986, M. Husain, ex. egg *Euproctis fraterna* on *Castor*, CIE A19038 (5♀ NHMUK). **CHINA**. ***Fujian***. Shaowu County, Longhu, 450m, 28.IV.2015 (4♀ FAFU). ***Fuzhou***. Fuzhou, 27.VIII.1954, egg of *Dendrolimus* sp. (7♀ IZCAS). ***Guangdong***. VIII.1974, Ren Hui, ex. *Dendrolimus punctatus* (10♀, 1♂ IZCAS). Deqing, 18.V.1973, *Dendrolimus* sp. (1♀ IZCAS). Guoungzhou—V.1978, Lasiocampidae sp. (1♀, 3♂ IZCAS); 3 (1♀ NHMUK), 3-6 (1♀ NHMUK).V.1983, 6.V.1983 (1♀ NHMUK), 2.VI.1983 (1♀ NHMUK), 7.VI.1983 (1♀ NHMUK), Z. Bouček; Shipai, 8.VIII.1954, egg of *Dendrolimus* sp. (2♀ IZCAS). ***Guangxi***. Nanning, Lin Wei (1♀ IZCAS). ***Hainan***. Hainan I., Tien Fong Mts., 21.V.1983, Z. Bouček (1♀ NHMUK). ***Hong Kong***. Tai Lung N.T., ex. egg *Dendrolimus punctatus*, CIE A4274 (1♀ NHMUK). ***Hunan***. Changsha, 26.VI.1978, Xinwang Tong (1♀ IZCAS). Dao-An, V.1975 (1♂ IZCAS). Dao County, V.1979 (2♀ IZCAS). ***Jiangsu***. Nanjing, 1957 (1♀ IZCAS). ***Yunnan***, Gejiu, 1985, Guoxiang Li (1♀ IZCAS). Laijiang Forest, IV.1984, Jianghong Wei, egg of *Dendrolimus* sp. (6♀ IZCAS). **INDIA**. ***Odisha***. Orissa, 9.X.1988, ex. *Trav-*

ella bishnu [*sic*], CIE A20268 (1♀ NHMUK). ***Telangana***. Hyderabad—Rayandra Nagar, VIII.1980, lep. eggs on Jamun [*Syzgium cumini* (L.) (Myrtaceae)], CIE A12750 (7♀, 10♂ NHMUK, 1♂ CNC Photo 2018-43); VIII.1980, R.C. Joshi, eggs on *Syzygium jambolanum* [= *S. cumini*], CIE A12750 (10♀, 2♂ NHMUK). ***Uttarakhand***. Dehra Dun, 7.IX.1936, S.N. Chatterjee, ex. eggs of *Trabala vischnou* [*sic*] (1♀, 3♂ NHMUK). ***Uttar Pradesh***. Aligarh, botanical garden, 27°84′10″N 78°04′31′S, 185m, 3.XI.2003, J. Heraty, DNA voucher D# 2320 (1♀ UCRC). Muzaffarnagar, fm. Sanatan Dharm College, ex. eggs *Trabala vishnu* [*sic*], CIE A18410 (3♀ NHMUK). ***West Bengal***. Godapiasal, 17.II.1985, sp. Pn. associated with *Shorea robusta* [Roth (Dipterocarpaceae)], CIE A17293 (1♀, 2♂ NHMUK). Kalyani Univ., sp. P.g. on *Shorea robusta*, CIE A6647 (1♀ NHMUK). **INDONESIA**. Java, Barat, Bogor, Darmaga Cikarawang forest, 1.III.1989, Noni Wanta, eggs of *Calliteara cerigoides* (3♀, 3♂ NHMUK). **MALAYASIA**. Malaya, Penang Genting, 14.II.1948, H.T. Pagden, ex. egg mass, CIE coll. No. 11298 (18♀, 10♂ NHMUK, 1♂ CNC Photo 2018-42). **TAIWAN**. Pindung, 22.368106°N 120.595308°E, coll. VIII.2018 using *Antherae pernyi* sentinel eggs, lab reared on eggs of *A. pernyi*, 12.IX.2018, J.C Hsu (9♀ CNC). Taipei, 25.017365°N 121.539100°E, collected using *Antherae pernyi* sentinel eggs, lab reared on eggs of *A. pernyi*, J.C. Hsu — collected 2017, reared 17.VIII.2018 (13♀ CNC); collected 20.VII.2018, reared 22.VIII.2018 (8♀ CNC); collected VIII.2018, reared 12.IX.2018 (4♀ CNC); collected II.2019, reared 8.V.2019 (10♀, 14♂ CNC, 3♂ CNC Photo 2018-69, -70, -71). Taipei, 25.017365°N 121.539100°E, collected V.2008 from *Tessaratoma papillosa*, lab reared on *Antherae pernyi* eggs (F2 generation) (4♀ CNC). **THAILAND**. Bangkok, 14.IX.1979, K. Charernsom, ex. egg *Trabala vishnu* [*sic*] (3♀, 1♂ NHMUK). Prachuap, Khiri Khan, Khao Sam Roi Yot NP Abbey, 12º13.091'N 99º56.109'E, 1-8.II.2009, Sorat, MT T4183 (1♀ CNC, CNC Photo 2018-41).

Distribution. ORIENTAL: Bangladesh (Ali & Karim 1991), China [*Fujian, *Fuzhou, *Guangdong, *Guangxi, *Hainan, *Hong Kong, Hunan (Yang *et al*. 2015), *Jiangsu, *Yunnan], India [*Odisha, *Telangana, *Uttarakhand, Uttar Pradesh (Khan 1983), *West Bengal], Indonesia [Java (Ferrière 1935), Sumatra (Messer *et al*. 1992)], *Malaysia, Myanmar (Ferrière 1935), *Taiwan, *Thailand.

Biology. Hosts: HEMIPTERA. **Tessaratomidae**. **Tessaratoma papillosa* (Drury). LEPIDOPTERA. **Erebidae**. *Euproctis fraterna* Moore (Ahmed *et al.* 1995) on *Ricinus communis* L. (Euphorbiaceae) (Hossain *et al.* 1995). **Lasiocampidae**. *Dendrolimus punctatus* (Walker) defoliating *Pinus massoniana* Lamb. (Pinaceae) and *Lebeda nobilis* Walker defoliating *Camellia oleifera* Abel. (Theaceae) (Yang *et al*. 2015); *Metanastria hyrtaca* Cramer (Josh *et al*. 1983); *Trabala vishnou* (Lefèbvre) (Khan 1983). **Lymantriidae**. *Calliteara cerigoides* (Walker) on *Hopea odorata* Roxb. & *Shorea javanica* Koord. & Valeton (Dipterocarpaceae) (Messer *et al*. 1992). **Saturniidae**. **Antherea pernyi* (Guérin-Méneville); *Cricula trifenestrata* (Helfer) on *Mangifera indica* L. (Anacardiaceae) (Ali & Karim 1991).

Remarks. *Mesocomys orientalis* is the only species of the *pulchriceps* group yet known from the Oriental region and thus is readily distinguished from other *Mesocomys* in the region, though some *M. pulchriceps* from the Afrotropical region are very similar in structure and sculpture and could be easily misidentified for *M. orientalis* without their site of collection. Females of *M. orientalis* always have the upper parascrobal region and frons mesh-like coriaceous (Fig. 22E) to coriaceous-imbricate (Fig. 22D), but with the surface of all the sculptural cells flat (Figs 22A, B, D, E), whereas females of *M. pulchriceps* are variable in sculpture, from quite distinctly reticulate (Fig. 26D) to variably less extensively and coarsely sculptured so sometimes to be almost entirely coriaceous to imbricate with only some of the sculpture on the frons defined by very fine, raised ridges and some of the sculptural cells on the upper parascrobal region slightly depressed medially. Oblique lighting filtered through translucent film is necessary to differentiate these subtle differences (see Material and methods).

Males of *M. orientalis* and *M. pulchriceps* usually are more easily distinguished from each other than are females because in addition to the same sculptural differences of the head they differ in fore wing setal colour. Males of *M. orientalis* have white setae within the hyaline regions behind the marginal vein so that the setae are comparatively inconspicuous relative to the other setae (Figs 24B, C), whereas males of *M. pulchriceps* have all the setae dark, including in the hyaline regions behind the marginal vein, so these setae are as conspicuous as elsewhere (Figs 24F, G). Males of *M. pulchriceps* also typically have the mesotibial spur obviously darker than the mesotarsomeres so as to more distinctly contrast in colour, whereas *M. orientalis* males have the mesotibial spur more similar in colour to the tarsomeres, though varying from similarly pale to similarly dark. Features shared in common between *M. orientalis* and *M. pulchriceps* males that differ from those of *M. anelliformis* are discussed above under the latter species.

When Narendran (*in* Narendran & Sheela 1995) described *M. atulyus*, the species was keyed with *M. orientalis* but, among other minor differences, was differentiated by: antenna mostly brown (Fig. 22F) *versus* scape yellow

with a green spot ventrally, anterior ocellus separated from scrobal depression by 2× *versus* about 1× ocellar diameter, pedicel 1.5× *versus* 2.75× as long as apical width, and submarginal vein 3.0× *versus* a trifle over 2.3× the length of the marginal vein. However, females of *M. orientalis* that I examined show wide variation in antennal colour, from almost entirely brown except for the scape (Fig. 22G) to having the antenna mostly yellow and darker only apically. Further, the scrobal depression of *M. orientalis* females is always separated from the anterior ocellus by at least about twice the longitudinal diameter of the ocellus (Figs 22D, E). It is possible that the head of the female identified as *M. orientalis* by Narendran was somewhat collapsed, which is not unusual for smaller, air-dried individuals, in which case the dorsal limit of the scrobal depression can be difficult to determine accurately, and thus he may have erred in his measurement. Similarly, even though the pedicel was stated as only 1.5 times as long as wide in the key, in the description it was stated as 2.2 times as long as wide, which is confirmed by images of the holotype antennae (Figs 22F, H). Finally, as seen from the image of the holotype fore wing, length of the costal cell or submarginal vein (Fig. 21I: cc/smv) is only about twice, not three times, the length of the marginal vein (Fig. 21I: mv). The single male was described as having both the antennae and legs dark brown, which is more unusual for typical *M. orientalis* males (Figs 23A, B). Smaller males often have the flagellum and the legs darker than larger males, but the male of *M. atulyus* was described as 3.2 mm in length, toward the higher end of the range in size for males of the species. However, based on the discrepancies in the original description relative to the images of the holotype of *M. atulyus* (Figs 21E–I), I consider *M. atulyus* as conspecific with *M. orientalis* and newly synonymize the former name under the latter.

Mesocomys pauliani Ferrière

Figs 25, 27E

Mesocomys pauliani Ferrière, 1951: 263–265, fig. 1 (female). Described from 3♀ syntypes; lectotype ♀, here designated (MHNG).

Description. FEMALE (habitus: Figs 25A, C). Length about 2.7–3.9 mm. Head (Fig. 25D) with frontovertex and upper parascrobal region mostly dark but sometimes with variably distinct green and/or reddish-violaceous lustre under some angles of light, and remainder of face mostly with much more distinct reddish-violaceous lustre, though usually with some green on lower face under some angles of light (Figs 25E, F). Face with upper parascrobal region and frons coriaceous-alutaceous to slightly imbricate, but sculptural cells flat, not concave, ocellar triangle and vertex more distinctly transversely alutaceous, and lower parascrobal region transversely reticulate-imbricate roughened. Clypeus with apical margin deeply, ∩-like emarginate medially (Figs 25E, F: arrow). Head measurements: HL = 2.8–3.3 [3.2], HH = 4.6–5.7 [6.0], HW = 5.4–[6.8], TL = 1.0–[1.2], EH = 3.0–[3.6], EW = 2.4–[2.7], MS = 1.5–[2.0], IOD 0.37–0.39 [0.35]× HW, MPOD: OOL: POL: LOL = 1.0: 1.0–1.2: 2.5–3.0: 1.8–2.1 [0.9: 1.1: 2.8: 1.8], and with dso 2.5–2.9 [2.5:1.0]× aod. Scrobal depression dorsally evenly ∩-like arched (Fig. 25D) or only very slightly emarginate medially (less distinctly than Fig. 20F). Labiomaxillary complex with maxillary palps dark brown (Fig. 25C) but labial palps slightly paler. Antenna (Fig. 25I) with scape entirely yellow or brownish basally, with pedicel and funiculars variably extensively pale, entirely yellow to almost entirely brown, but at least somewhat paler ventrally, and clava dark except micropilose sensory area paler (Fig. 25I); scape broadest subbasally and narrowed apically, with ventral margin sinuate, and about [3.6]–3.9× as long as greatest width; pedicel equal to or slightly longer than twice apical width and subequal in length to combined length of basal three funiculars; flagellum with all funiculars transverse and increasing in width apically such that apical funiculars strongly transverse; clava subequal in length to combined length of apical four funiculars.

Mesosoma dorsally (Figs 25A, G) mostly dark brown but convex part of mesoscutal medical lobe usually reddish-violaceous to bluish-purple posteriorly and concave posterior part, or at least inclined inner surfaces of lateral lobes, variably distinctly bluish-purple; in lateral view dark brown but with at least slight green, blue to purple or reddish-violaceous lustres under different angles of light (Figs 25G). Mesoscutum (Fig. 25G) with convex anterior part of medial lobe and outer inclined surface of lateral lobe finely mesh-like coriaceous, and depressed posterior part of medial lobe somewhat shinier and even more finely, less distinctly mesh-like coriaceous to almost smooth medially; mesoscutum, excluding parapsidal band, uniformly though comparatively sparsely setose with brownish hair-like setae except depressed posterior part with only 4 setae, an anterior and a posterior paramedial pair of somewhat longer, more bristle-like setae. Scutellar-axillar complex (Fig. 25G) mesh-like coriaceous; with 2 or 3

hair-like setae within each axillar depression and scutellum with 2 similar hair-like setae on each side laterally along length, the posterior-most setae longest. Prepectus mesh-like coriaceous (Fig. 27E). Acropleuron (Fig. 27E) finely sculptured, mesh-like coriaceous-alutaceous anterodorsally near lateral margin of mesoscutum, similarly but more longitudinally coriaceous dorsally and ventrally and very finely, minutely sculptured to almost smooth mesally below level of wing bases, but mesh-like coriaceous or inconspicuously coriaceous-reticulate over about posterior half, the sculpture becoming increasingly larger and more isodiametric posteriorly except usually more elongate posterodorsally. Front leg (Fig. 25C) with femur dark brown except variably distinctly paler apically; tibia with at least posterior surface mostly dark brown, but anterior and/or dorsal surfaces and apex pale; tarsus with basal four tarsomeres pale and apical tarsomere dark. Middle leg (Fig. 25C) mostly dark brown, including tibial spur, but femur slightly paler apically, tibia variably distinctly paler apically and with narrow pale band subbasally, and at least basal four tarsomeres pale excluding dark pegs. Hind leg (Fig. 25C) mostly dark brown, but trochanter and trochantellus distinctly paler, femur slightly paler apically, and tibia narrowly paler basally; tarsus sometimes entirely pale, but usually variably distinctly bicoloured, variably darker brown basally and apically and at least slightly paler mesally. Fore wing (Figs 25B, H) with costal cell hyaline except brownish-infuscate apically in front of parastigma; basal cell brownish-infuscate over about basal half except more extensively along mediocubital fold to near discal infuscation, but the two infuscate regions separated at least narrowly, cubital area hyaline, and vanal area brownish-infuscate basally but more hyaline posteriorly and apically; disc extensively brownish-infuscate basally (sometimes slightly darker behind marginal vein basal to anterior hyaline region) except with distinct, slender hyaline region along parastigma and base of marginal vein, and with separated anterior and posterior hyaline regions behind marginal vein apically, the anterior region extending to or almost to junction of marginal and stigmal veins, and wing hyaline apically beyond about level of postmarginal vein or somewhat more extensively posteriorly toward posterior hyaline region. Fore wing (Fig. 25H) with costal cell dorsally bare except densely setose with mostly slightly lanceolate dark setae in infuscate region in front of parastigma; basal cell with 6 or 7 dark, hair-like setae along mediocubital fold basally, and with a few short, white, hair-like setae apically adjacent to parastigma and infuscate part of disc; disc with setae white within anterior and posterior hyaline regions behind marginal vein but otherwise dark and mostly hair-like, distinctly lanceolate only mesally from base of infuscate region to, and between, anterior and posterior hyaline regions to at most about level equal with apex of hyaline regions, the setae more hair-like anterobasally in hyaline region along parastigma, posterobasally behind cubital fold to posterior hyaline region, and apically beyond anterior and posterior hyaline regions; stigmal vein apically curved into uncus (Fig. 25H), but without spur projecting beyond uncus; measurements of cc: mv: pmv: stv = 5.1–6.3: 3.0–3.8: 1.7–2.2: 1.0 [5.1: 3.0: 2.0: 1.0].

Gaster usually completely brown, though often somewhat paler brown basally and darker brown apically with at least slight green to bluish lustre over apical three tergites under some angles of light, and with Gt_1 often paler mediolongitudinally and Gt_1 and/or Gt_2 hyaline so that colour of underlying sclerite shows through, but only rarely with distinct subbasal pale band (Fig. 25C) formed by transverse, yellowish-white band on Gt_2 and similarly pale St_2; Gt_1 and Gt_2 dorsally shiny, at most very obscurely mesh-like coriaceous, and bare but with hair-like setae laterally; Gt_3–syntergum similarly or somewhat increasingly more coarsely mesh-like coriaceous-alutaceous or at most Gt_2 and/or Gt_3 obscurely coriaceous-reticulate (surface of sculptural cells flat but formed by slightly raised ridges) and increasingly more setose dorsally such that at least apical two tergites with row of setae across tergite; syntergum more-or-less uniformly sculptured and coloured so that syntergal flange comparatively inconspicuously differentiated. Ovipositor sheaths pale, yellowish.

MALE. Unknown.

Type material examined. Lectotype ♀ (hereby designated, MHNG): "I. S. Madagascar | Parasite des ponte ? | de *Schinus-molle* | Tjimbazaza | Elevage du 7.I.48 (No 73) | Naissance le 9.II.48 (A.R.) / *Mesocomys* | *pauliani* | Ferrière. Cotype / Paratypus / MHNG | ENTO ♀ | 00013399"; also newly labelled with "LECTOTYPE ♀ | *Mesocomys* | *pauliani* Ferrière". Lectotype (Fig. 25B) minutien mounted through mesoscutum, with head and gaster detached and glued to card rectangle along with host egg (Fig. 25B, insert), uncontorted, and entire except following missing: left antenna beyond fl_1, apical three tarsomeres of right front leg, right hind leg beyond coxa, and right hind wing.

Paralectotypes examined, here designated: 2♀ (MHNG), with similar labels as lectotype and newly labelled with "PARALECTOTYPE ♀ | *Mesocomys*| *pauliani* Ferrière". One of the designated paralectotypes has an original label with "*Mesocomys pauliani* Ferrière Type". This female is not designated as the lectotype because of its condition, lacking its wings and gaster as well as the antennae beyond the scapes, right hind leg and right mesotibia and tarsus.

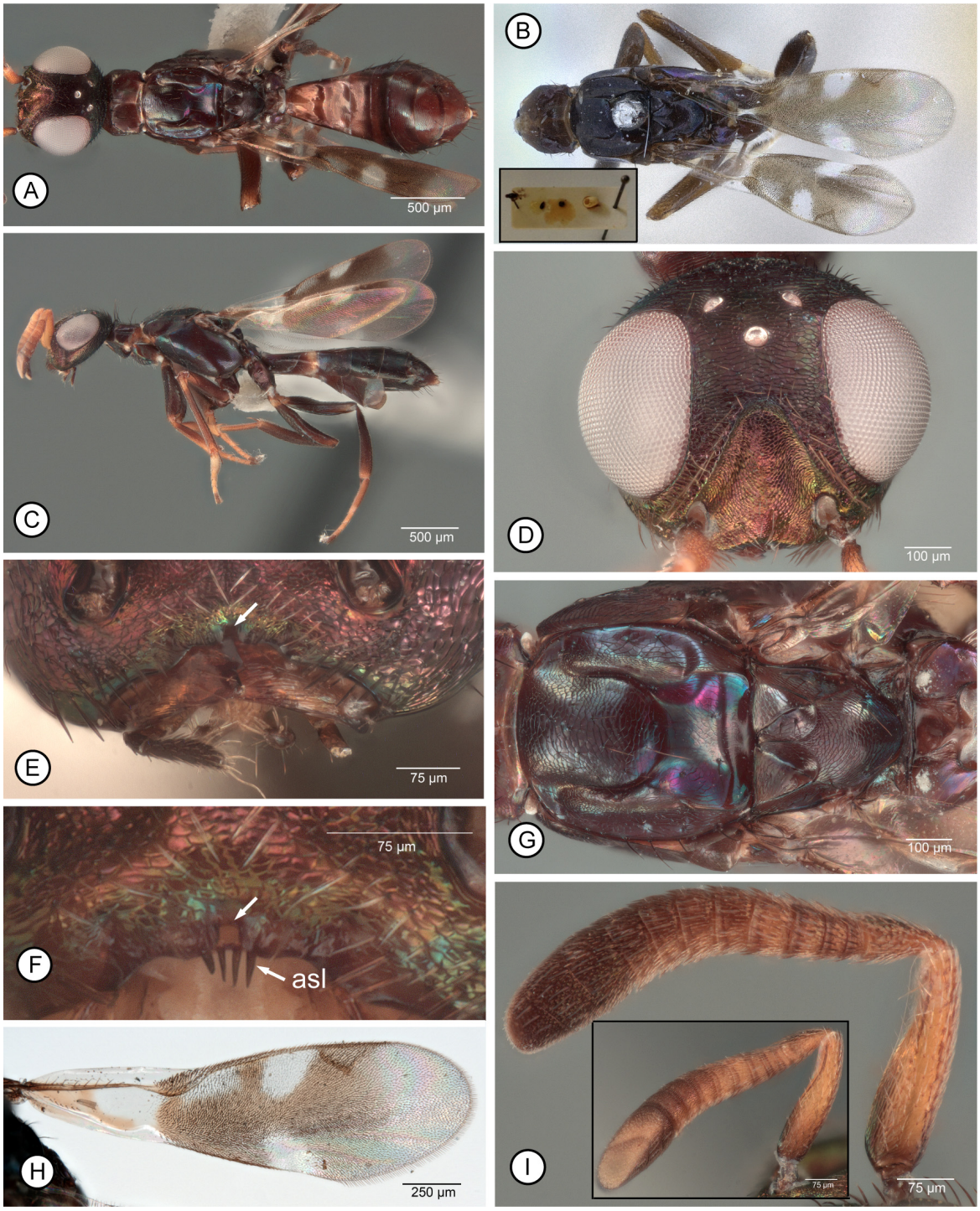

FIGURE 25A–I. *Mesocomys pauliani* ♀. **A**, dorsal habitus (#48); **B**, lectotype. dorsal habitus [insert: card with pinned mesosoma and head, gaster and egg glued to card]; **C**, lateral habitus (#49); **D**, head, frontal (#48); **E**, lower face (#51) [arrow points to margin of incised clypeus]; **F**, clypeus and underlying labrum (#50) [arrow points to margin of incised clypeus; asl = apical setae of labrum]; **G**, mesonotum and propodeum (#48); **H**, fore wing (lectotype); **I**, antenna, outer view [insert: antenna, inner view] (#48).

Although the original description states the type material is in the "Muséum de Paris" (MNHN), the syntypic series was discovered in MHNG.

Other material examined. AFROTROPICAL. **MADAGASCAR**. Province de Antananarivo, botanic garden near entrance to Andasibe National Park, 18°55′58″S 48°24′47″E, 1025m, 1-5.IX.2001, R. Harin′Hala, CAS MT-tropical forest, MA-01-08B-11 (1♀ CASC). Province de Fianarantsoa, Forêt d′Atsirakambiaty, 7.6 km 285° WNW Itremo, 20°35′36″S 46°33′38″E, 1550m, 22-26.I.2003, Fisher, Giswold *et al*., CAS beating low veg. montaine rain-

forest, BLF7152, CASC: CASENT 2070914 (2♀ CASC, 1♀ CNC Photo 2018-49). Province de Mahajanga, Réserve d'Ankorirka, 10.6 km 13°NE de Tsaramandroso, 16°16′2″S 46°2′55″E, 210m, 9-14.IV. 2001, Fisher, Giswold *et al*., CAS MT-tropical dry forest, BLF 3665, CASLOT 005404, CASENT 2013020 (1♀ CASC, CNC Photo 2018-48). Region du Centre-Sud, Vallée de L'Ihosy, 1901, Ch. Alluaud (1♀ NHMUK, NHMUK 011515740). Tulear, Berenty, V.1983, J.S. Noyes & M.C. Day, BMNH(E) 1983-201 (1♀ NHMUK, NHMUK 010834562, CNC Photo 2018-50). Tulear, Berenty, 12 km NW Amboasary, 5-15.V.1983, J.S. Noyes & M.C. Day (1♀ NHMUK, NHMUK 011515669, CNC Photo 2018-51).

Distribution. AFROTROPICAL: Madagascar.

Biology. Host: LEPIDOPTERA. **Saturniidae**. *Antherina suraka* (Boisduval) on *Schinus molle* L. (Anacardiaceae) (Ferrière 1951).

Remarks. *Mesocomys pauliani* is the only species of *Mesocomys* known from Madagascar other than for *M. pulchriceps*. Females are recognized in part by the marginal vein being at least three times as long as the stigmal vein (Fig. 25H), which is the longest within the *pulchriceps* group. As discussed under *M. anelliformis*, females are more similar to *albitarsis*-group females in this feature (*cf*. Fig. 2F), which conflicts with several other features that support *M. pauliani* as part of a monophyletic lineage with *M. orientalis* and *M. pulchriceps*. Unfortunately, because males of *M. pauliani* are unknown, such potentially informative features as setal patterns of the basal and costal cells, colour of the tegula and coxae, and relative lengths of the basitarsi of the middle and hind legs are not known. However, one possible indicator that *M. pauliani* might be the sister of *M. orientalis* + *M. pulchriceps* is the development of an evident stigmal vein spur in at least larger females of the latter two species (Figs 21D, 26H: spr), though this is a variable feature that appears to be correlated, at least in part, with specimen size. Females of *M. pauliani* (Fig. 25D) share with both sexes of *M. orientalis* a finely sculptured, coriaceous (Figs 22E, 24A) to coriaceous-imbricate (Fig. 22D) upper parascrobal region and frons, whereas both sexes of all other *Mesocomys* have a more coarsely roughened, variably reticulate upper parascrobal region and frons, which could support *M. orientalis* and *M. pauliani* as sister species. However, head sculpture is quite variable for *M. pulchriceps* and intergrades with that of *M. orientalis* (see under these species).

Mesocomys pulchriceps Cameron

Figs 2H, 23I, 24D–H, 26, 27F–H

Mesocomys pulchriceps Cameron, 1905: 211. Described from at least 2♀ syntypes; lectotype ♀, here designated (NHMUK).

Anastatus vuilleti Crawford, 1912: 5–6. Described from 8♀ and 5♂ syntypes; lectotype ♀, here designated (USNM). **New synonymy**.

Mesocomys pulchriceps Cameron; Ferrière, 1930a: 35–36 (data); Ferrière, 1951: 265 (keyed); Berg, 1970: 138 (life history, description of immature stages), figs 1–6 (immature stages), fig. 7 (female); Gibson, 1995, figs 142, 200, 267, 299, 338 (female); Narendran & Sheela, 1995: 310 (keyed).

Mesocomys vuilleti (Crawford); Ferrière, 1930a: 36 (new combination, stated as probably a variety of *M. pulchriceps*); Ferrière, 1951: 265 (keyed); Fusu *et al*., 2015: 475 (list of slide mounted Risbec material in MNHN).

Mesocomys Vuilleti [*sic*]; Risbec, 1951a: 191 (two unnamed varieties described), figs 120a, b, 123a (female); Risbec, 1952: 74 (redescription).

Description. FEMALE (habitus: Figs 26A, B). Length = 2.0–4.2 mm. Head sometimes entirely or almost entirely green in smaller individuals, but usually with variably extensive reddish-violaceous or, more rarely, violaceous to purple lustre on one or more of following: parascrobal region, in scrobes and/or across scrobal depression dorsally, interantennal prominence mediolongitudinally to almost entirely, across lower face between toruli, gena, and sometimes on frontovertex in part. Face with upper parascrobal region and frons variably extensively and distinctly roughened, usually mesh-like reticulate (Fig. 26D) to reticulate-imbricate, but at least some sculpture on frons defined by fine, raised ridges and/or upper parascrobal region with some sculptural cells slightly depressed or with tiny medial pit, with frontovertex alutaceous to transversely reticulate-strigose, and lower parascrobal region transversely reticulate-imbricate roughened. Clypeus with apical margin deeply, ∩-like emarginate medially (Fig. 26F: arrow). Head measurements: HL = 2.0–3.8, HH = 4.0–7.0, HW = 4.7–8.6, TL = 0.9–1.5, EH = 2.3–4.6, EW = 1.9–3.3, MS = 1.4–2.6, IOD 0.36–0.43× HW, MPOD: OOL: POL: LOL = 1.0: 0.8–1.1: 2.7–3.3: 1.9–2.2, and with dso 1.8–2.5× aod. Scrobal depression dorsally evenly ∩-like arched (Fig. 26D) to variably distinctly M-like emar-

ginate medially (*cf.* Fig. 20F). Labiomaxillary complex with maxillary palps dark brown but labial palps slightly paler. Antenna (Fig. 26G) rarely entirely brown, but usually scape at least partly and often mostly yellow, and pedicel and flagellum brown or variably paler to entirely yellow except pedicel dorsally and clava darker; scape broadest subbasally and narrowed apically, with ventral margin sinuate, and about 4.1–5.1× as long as greatest width; pedicel about 2.0–2.5× as long as apical width and slightly longer than combined length of basal three funiculars; flagellum with all funiculars transverse and increasing in width apically such that apical funiculars strongly transverse; clava equal in length or slightly longer than combined length of apical four funiculars.

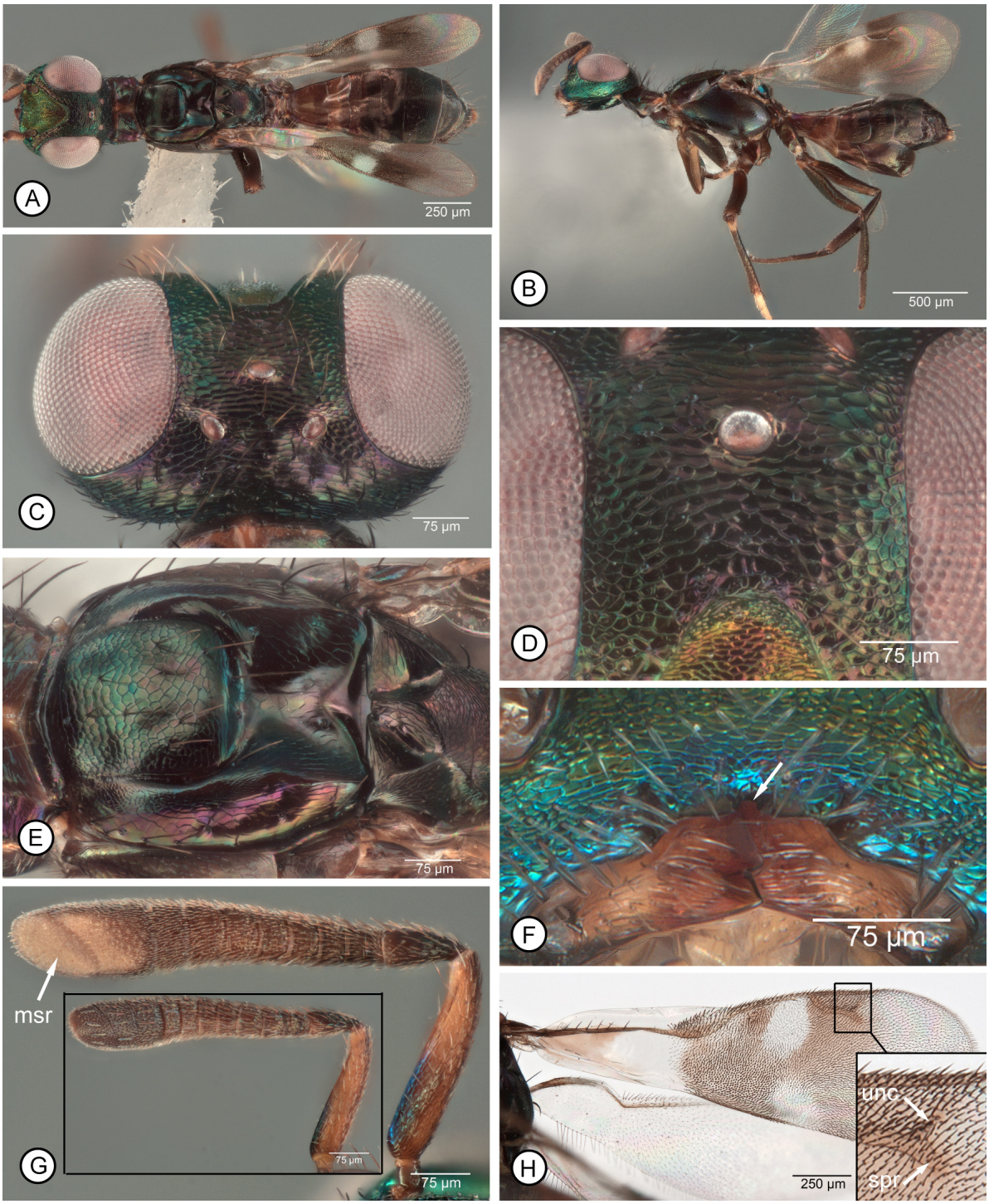

FIGURE 26A–H. *Mesocomys pulchriceps* ♀. ***A–G*** (#47): **A**, dorsal habitus; **B**, lateral habitus; **C**, dorsal head; **D**, frontodorsal part of head; **E**, mesonotum; **F**, lower face [arrow points to margin of incised clypeus]; **G**, antenna, inner view [insert: antenna, outer view]. **H**, fore wing (#46) [insert: enlargement of apex of stigmal vein]. [See 'Methods' and Table 1 for explanation of abbreviations.]

Mesosoma dorsally mostly dark (Fig. 26A) though usually with variably extensive and distinct greenish and/or reddish-violaceous lustre under some angles of light (Fig. 26E), and pronotal neck sometimes paler, yellowish-brown to orangish-yellow; in lateral view usually similarly dark with various metallic lustres (Figs 27F, G) as mesonotum, except larger individuals sometimes with prepectus variably paler (Fig. 27G) similar to pronotal neck. Mesoscutum (Fig. 26E) with convex anterior part of medial lobe mesh-like coriaceous in smaller individuals to very shallowly reticulate with sculptural cells formed by only very fine raised ridges in larger individuals, posterior depressed part with similar or finer mesh-like sculpture, and lateral lobe mesh-like coriaceous; mesoscutum, excluding parapsidal band, variably extensively and conspicuously setose, sometimes with setae mostly aligned in longitudinal row on either side of midline, but depressed posterior part with only 4 long, bristle-like setae. Scutellar-axillar complex mesh-like coriaceous; with 1 or 2 hair-like setae within each axillar depression and scutellum with 2 longer, bristle-like setae laterally. Prepectus mesh-like coriaceous (Fig. 27F) to reticulate (Fig. 27G). Acropleuron (Figs 27F, G) variably coarsely but mostly mesh-like sculptured, with more finely, minutely sculptured region mesally below level of wing bases. Front leg sometimes similarly pale as prepectus, but more commonly mostly dark (Fig. 26B) except tarsus and dorsal and/or anterior surface of tibia variably extensively pale. Middle leg beyond coxa rarely similarly pale as front leg except for brownish-orange to dark tibial spur and dark mesotarsal pegs, but usually mostly dark (Fig. 26B), including tibial spur, except femur variably extensively paler apically, tibia pale basally or subbasally, and at least basal four tarsomeres pale except for dark pegs. Hind leg sometimes similarly pale as front and hind legs, but usually mostly dark (Fig. 26B) with at least trochantellus and often femur apically and tibia basally paler. Fore wing (Fig. 26H) with costal cell hyaline or at most only slightly, comparatively inconspicuously brownish-infuscate apically in front of parastigma; basal cell brownish-infuscate over at most about basal half except sometimes somewhat more extensively along mediocubital fold, but infuscation almost always separated from discal infuscation (see Remarks), and cubital and vanal areas hyaline or at most very slightly brownish-infuscate basally; disc extensively brownish-infuscate basally, often variably distinctly darker behind marginal vein basal to anterior hyaline region, but with slender though often comparatively inconspicuous hyaline band along parastigma to base of marginal vein, and with separated anterior and posterior hyaline regions behind marginal vein, the anterior region extending to or almost to junction of marginal and stigmal veins, and wing hyaline apically beyond about level of postmarginal vein or more extensively posteriorly toward posterior hyaline region. Fore wing (Fig. 26H) with costal cell dorsally bare except densely setose with hair-like or only slightly lanceolate dark setae in front of parastigma; basal cell sometimes completely bare, but more commonly with row of 2–8 hair-like setae along mediocubital fold basally, and with a few short, white, hair-like setae apically adjacent to parastigma and infuscate part of disc; disc with setae white in anterior and posterior hyaline regions, but otherwise dark brown and lanceolate at least mediolongitudinally from base of infuscate region to base or apex of anterior and posterior hyaline regions, the setae more hair-like posterior of cubital fold basal to posterior hyaline region, often within hyaline region along parastigma, and apically beyond anterior and posterior hyaline regions; stigmal vein with variably long, often conspicuous spur (Fig. 26H, insert: spr) projecting beyond uncus (Fig. 26H, insert: unc); measurements of cc: mv: pmv: stv = 4.8–5.6: 1.5–2.3: 1.2–1.5: 1.0.

Gaster usually completely dark brown (Figs 26A, B) except often with variably distinct green to bluish lustre over apical 3 or 4 tergites under some angles of light, with Gt_1 and/or Gt_2 and St_1 hyaline such that colour of underlying sclerites shows through or at most with Gt_1 and Gt_2 paler, lighter brown to orangish-brown dorsally without a distinct white band subbasally, though rarely with a very slender white band in lateral view (*cf*. Fig. 25C). Gaster with tergites mesh-like coriaceous basally to very shallowly mesh-like reticulate apically, with Gt_1 and Gt_2 base dorsally and usually shinier than more apical tergites, but at least apical three tergites with at least one row of setae across tergite; syntergum more-or-less uniformly sculptured and uniformly coloured or only extreme apex pale so that syntergal flange comparatively inconspicuously differentiated. Ovipositor sheaths pale, yellowish.

MALE (habitus: 24D). Length = 1.7–3.5 mm. Head (Fig. 24H) with face usually mostly green to bluish green except usually for some coppery to reddish-violaceous lustre under some angles of light, and sometimes frontovertex more distinctly bluish (Fig. 24D). Face with upper parascrobal region and frons distinctly roughened, mesh-like reticulate (Fig. 24E); vertex more transversely alutaceous-reticulate to reticulate. Clypeus with apical margin deeply, ∩-like emarginate medially (*cf*. Fig. 22C: arrow). Head measurements: HL = 2.3–4.0, HH = 3.2–5.9, HW = 3.9–7.3, EH = 2.0–3.5, EL = 1.7–2.9, MS = 1.0–2.0, IOD 0.39–0.41× HW, MPOD: OOL: POL: LOL = 1.0: 0.7–1.0: 2.6–2.8: 1.5–2.0, and with dso 0.7–1.2× aod. Scrobal depression dorsally evenly ∩-like arched (Figs 24E, H). Labiomaxillary complex with maxillary and labial palps yellow. Antenna (*cf*. Fig. 23E) variably extensively pale,

the flagellum, pedicel, and scape apically sometimes brown, particularly in smaller individuals, but usually scape, pedicel, and flagellum at least basally, yellowish-brown to yellow, though clava usually somewhat darker brownish; scape about 3.2–3.6× as long as wide; pedicel about 2.5–3.4× as long as apical width and almost as long as, and sometimes slightly longer than, combined length of basal four funiculars; flagellum clavate; fl_1 similar in size to fl_2, with all funiculars slightly transverse or only fl_4 quadrate, and clava about 1.9–2.2× as long as wide and subequal in length to combined length of apical three funiculars.

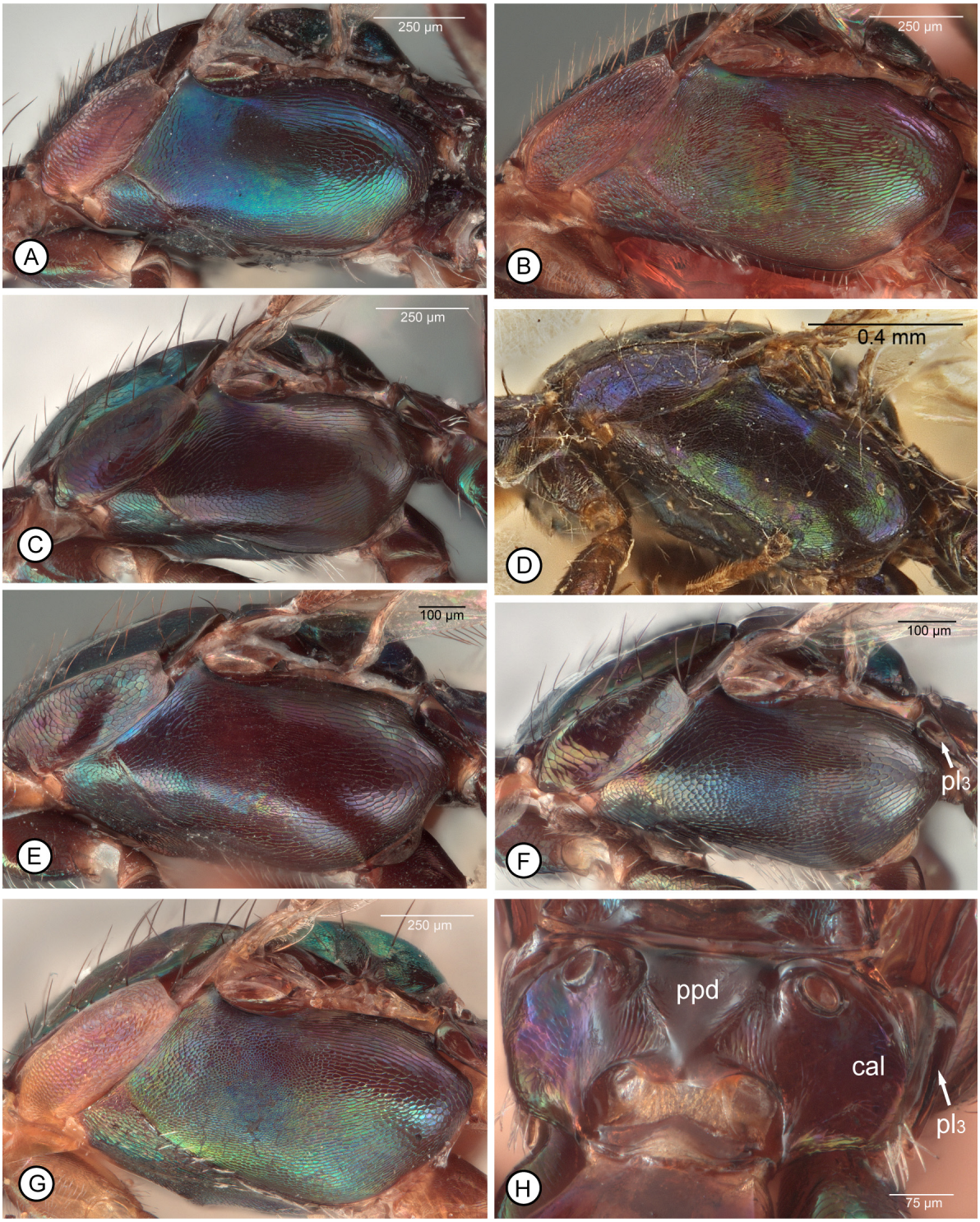

FIGURE 27A–H. *Mesocomys* species ♀. ***A–G***, lateral mesosoma: **A**, *M. anelliformis* (holotype); **B**, *M. longiscapus* (holotype); **C**, *M. orientalis* (#41); **D**, *M. orientalis* (*M. atulyus* holotype); **E**, *M. pauliani* (#49); **F**, *M. pulchriceps* (#47); **G**, *M. pulchriceps* (#63). **H**, *M. pulchriceps*, propodeum (#64). [See 'Methods' and Table 1 for explanation of abbreviations.]

Mesosoma dorsally (Fig. 24D) similarly green to bluish-green as head except propodeum often more blue to purple, and often with variably extensive coppery to reddish-violaceous lustre on one or more of pronotum, mesoscutum, and scutellar-axillar complex medially under different angles of light; in lateral view similar in colour to dorsal surface and often with some coppery to reddish-violaceous lustre under different angles of light, but mesopleurosternum without differentiated, paler, Y-like set of lines (*cf*. Fig. 23F). Tegula dark brown, particularly in smaller individuals, to orangish or yellow (Fig. 24D: tg). Mesoscutum (Fig. 24D) with medial lobe mesh-like coriaceous to variably extensively, shallowly reticulate, at least posteriorly toward scutellar-axillar complex; scutellar-axillar complex with axillae similarly or more finely sculptured than mesoscutal medial lobe, but at least scutellum mesh-like coriaceous medially and posteriorly and somewhat more imbricate laterally. Legs highly variable in colour, from mostly pale except for brownish-infuscate to dark mesotibial spur, metacoxa, metatibia and metabasitarsus, to almost entirely dark, including all coxae and mesotibial spur, except for variably pale to white basal tarsomeres of front leg and with at least second and third and sometimes first to third tarsomeres of middle leg (first tarsomere at least slightly darker, more yellowish-orange, than whitish second and third tarsomeres) and second and third tarsomeres of hind leg pale so as to contrast variably distinctly with other tarsomeres (Fig. 23I); mesotarsus with basitarsus about 0.6–1.1× and metatarsus with basitarsus about 0.9–1.7× combined length of respective apical four tarsomeres (Fig. 23I), with larger individuals having a relatively more elongate basitarsus. Fore wing (Fig. 24F) with basal cell hyaline (apparent basal infuscation in Fig. 24F an artefact because of underlying leg), but disc variably light to dark brownish-infuscate between about base of parastigma and level of apex of stigmal vein except paler to hyaline behind medial or cubital fold and apically beyond about level of apex of stigmal vein (often more faintly infuscate behind parastigma than between postmarginal and stigmal veins and behind stigmal vein), and unless infuscation comparatively faint then with hyaline region behind about apical half of marginal vein, and smaller hyaline region adjacent to posterior margin of wing, but with all setae dark, including in hyaline regions behind marginal vein (Figs 24F, G); costal cell ventrally with single row of setae, though setal row usually interrupted from more numerous setae in front of parastigma by bare region basal to parastigma, and dorsally with 1 or 2 rows of setae apically that extend obliquely into cell rather than paralleling leading margin (Fig. 24F: ser); basal cell often entirely bare basal to base of parastigma but sometimes with up to 4 setae along mediocubital fold basally; stigmal vein apically expanded and truncate or with variably distinct uncus, and often with at least short, stub-like spur projecting beyond uncus (Fig. 24G); measurements of cc: mv: pmv: stv = 3.1–3.8: 1.2–1.6: 1.5–1.7: 1.0.

Gaster dark brown except often for variably extensive green lustre apically (Fig. 24D).

Type material examined. *Mesocomys pulchriceps*. Lectotype ♀ (here designated, NHMUK). Specimen not re-examined for this study, but examined in 2015 at NHMUK, with following data based on notes taken at that time and on image of designated lectotype and type labels provided by N. Dale-Skey Papilloud (NHMUK) in 2018: "Type [red-bordered circular label] / Cameron Coll. | 1905-192. / *Mesocomys* | *pulchriceps* | Cam. Type | Cape Colony / B.M. TYPE | HYM. | 5.1,037 / NHMUK 010198546"; also newly labelled with "LECTOTYPE ♀ | *Mesocomys* | *pulchriceps* Cameron". Lectotype glued by venter of mesosoma across apex of card triangle, uncontorted, and entire except following missing: almost entire right clava; left protarsus beyond third tarsomere.

Paralectotype ♀ (here designated, NHMUK). "Brak [the "r" obscure] Kloof | Mrs. | White | Nov. / [*sic*] 03 [front of label, hand written; printed on back of label is: ALBANY | MUSEUM | GRAHAMS | TOWN] / 33 / P. Cameron Coll. | 1914-110 / *Mesocomys* | *pulchriceps* | Cam. / NHMUK011509255"; also newly labelled with "PARALECTOTYPE ♀ | *Mesocomys* | *pulchriceps* Cameron". Paralectotype glued by venter of mesosoma onto rectangular card with front legs folded under the mesosoma, uncontorted but fore wings glued together and folded upwards over the propodeum to the right of the specimen, with the gaster detached and glued basally to the top of the metafemora in a dorsally projected position such that the folded wings are partly covered and the venation basal to the stigmal vein is not visible, and with the right hind wing detached and glued to the outer surface of the right metafemur; missing are: head and antennae, left mesotarsis, and left metatarsis beyond basitarsus.

Based on information from N. Dale-Skey Papilloud (personal communication), the here designated paralectotype was located in the unincorporated accessions of NHMUK as of only March, 2018. The associated numbers "1905-192" and "1914-110" of the lectotype and paralectotype, respectively, refer to NHMUK accession numbers, with the year the specimen was obtained and the accession register number—"1905-192" is cited as "114 Hymenoptera (chiefly types) from various localities, purchased from P. Cameron", and "1914-110" as "10,000 Hymenoptera (P. Cameron collection) including 1500 type specimens from various localities, purchased from Mr J Summer Pollitt, solicitor and agent for Mrs Louis Lechner, sister of the late Mr Peter Cameron". The meaning or relevance of the number "33" label for the paralectotype is unknown.

Cameron (1905) did not state how many specimens he had before him when describing *M. pulchriceps*, which is not unusual for Cameron's species descriptions (Notton *et al*. 2009). Only a single body length measurement, 3 mm, is given in the species description and nothing in the genus or species descriptions would indicate more than one female. However, distribution was given as "Cape Colony. Grahamstown; Brak Kloof" (Cameron 1905, p. 211). Based on the method of punctuation used for distribution of other newly described species in the same publication, the semicolon indicates he had at least two females, one from Grahamstown and one from Brak Kloof. In the introduction to the paper, Cameron also stated that species described in the paper included, among others, "species in the Collection of the Albany Museum, Grahamstown, collected by Mrs. G. White, Mrs. Pringle, and Misses Daly and Sole in the neighbourhood of Grahamstown" (Cameron 1905, p. 195). Based on its label data, including the species name label in the same handwriting as for the here designated lectotype, the Brak Kloof specimen must be part of the original type series. The lectotype differs in being mounted on a triangular point rather than a rectangular card and lacks any collection data other than "Cape Colony". The different method of mounting and information provided indicates it may have been collected by one of the individuals listed in the introduction other than Mrs. White, the collector of the paralectotype. However, because it has the species name label in the same handwriting as the paralectotype it most likely is the specimen cited from Grahamstown. The head from the Brak Kloof female may have been lost subsequent to the original description, but some structures described for the genus are present but cannot be seen because of its condition and method of mounting, such as dilation of the profemur and fore wing features. It is likely that Cameron mostly used the Cape Colony female for his description of *M. pulchriceps* and for this reason labelled it as "Type". According to N. Dale-Skey Papilloud (personal communication), the Hymenoptera primary types were segregated during World War II and the primary type number labels (such as 5.1,037) added at that time. Because the Cape Colony female has the species name and "Type" written in Cameron's handwriting, was purchased from Cameron as part of a collection of "chiefly types", and is the more complete specimen that shows relevant specific features, I hereby designate it as lectotype of *M. pulchriceps* Cameron.

Anastatus vuilleti. Lectotype ♀ (hereby designated, USNM): "Koulikoro | French | Soudan / Ex eggs | *Cerina* [*sic*] | n. sp. / J. Vuillet | coll. / Type | No. 14343 | U.S.N.M. / *Anastatus* | *vuilleti* | Cwfd Type"; also newly labelled with "LECTOTYPE ♀ | *Anastatus* | *vuilleti* Crawford". Lectotype glued by left side on top of triangular point such that right side faced upwards and head pointed to right, uncontorted, and entire.

Paralectotypes examined, here designated: 7♀ and 5♂ (USNM) with similar collection label data as for lectotype, but all with "Paratype No. 14343 U.S.N.M." label except one male with USNM "Type No. 14343" label as for lectotype; all newly labelled with "PARALECTOTYPE | *Anastatus* | *vuilleti* Crawford".

Other material examined. AFROTROPICAL. **ANGOLA**. Chianga, V.1972, M. Helena, pu. *Papilio demodocus*, no. 1268 (3♀, 1♂ NHMUK). **BOTSWANA**. Lesenepole, 22°31S 27°32′E, 5.II.2001, A.J. Gardiner, ex. eggs *Imbrasia belina* (7♀, 2♂ SANC). Maunatlala, 22.36S 27.38E, II.2001, 14.II.2001, A.J. Gardiner, ex. eggs *Imbrasia belina* (20♀, 15♂ SANC). **BURKINO FASSO**. 11.VI.1991, M. Ouedraogo, ex. eggs *Cirina butyrospermi* (4♀, 1♂ NHMUK). **CAMEROON**. Musone, Mboanoong, 11.XII.1981, S.G. Compton (1♂ SAMC). **CÔTE D'IVOIRE**. Bingerville, 25.IV.1943, H. Alibert, ex. eggs of [?] (6♀ NHMUK). **ERITREA**. Asmara—25.V.1946, Dr. G. Jannone, ex. eggs *Holocera smilax* (8♀ NHMUK); 2350m, 10.VII.1948 (6♂ NHMUK), 4.VIII.1948 (15♀, 6♂ NHMUK), G. de Lotto, ex. eggs *Pachypasa* sp.; 30.IX.1946, G. de Lotto, ex. eggs *Holocerina angulata* (Aur.) (5♀, 3♂ NHMUK). **ESWATINI** [Swaziland]. IX.1961, ex. eggs *Nudaurelia c. cytherea* (2♀, 1♂ CNC; 2♀, 1♂ + unmounted ♀♀ & ♂♂ SANC). Usutu Forest, VII.1959, ex. egg *Nudaurelia cytherea* (1♀ USNM). **GHANA**. Aburi, Gold Coast, I.1916, W.H. Patterson, ex. Lepidoptera ova (4♀ NHMUK, 1♀ CNC Photo 2018-64). Jirapa, UWR, Tafo, 28.VI.1988, E.O. Manu, ex. eggs lep. sp., CIE A20305 (2♀ NHMUK). New Tafo-Akim Cocoa Research Institute, VIII.2000, E.A. Dwomoh, associated with *Butyrospermum parkii* (Sapotaceae) (2♀, 1♂ + unmounted ♂♂ SANC). **KENYA**. em. V.1955, ex. *Cirina forda*, per W.A. Smith (7♀ NHMUK). Eastern Prov., base of Ukasi Hill, 0.82103°S 38.54443°E, 613m, 21.XI-5.XII.2011, R. Copeland, *Acacia*/*Commiphora* savanna (1♀ NMK). Mwingi, Mathyakani, 12.XI.1995, D. Kimbu, ex. eggs wild silkmoth (4♀ SANC). **MADAGASCAR**. Rég. Sud de I'Ile, Bekily, II.36 (1♀ NHMUK; 17♀, 1♂ MNHN), II.37 (3♀ MNHN), ex. oeufs *Bunaea aslans*. **MALAWI**. Zomba, 1913, E. Ballard, ex. Lepidoptera egg (1♀ NHMUK). **MALI**. Koulikoro, Haut Senegal-Niger, J. Vuillet, ex. *Cirina butyrospermi* (2♀, 12♂ USNM). **NAMIBIA**. Etemba, 20 km SW, 21.31S 15.32E, 11.III.1987, R. Oberprieler, ex. eggs *Usta wallengrenii* (8♀ CNC; 5♀ + unmounted ♀♀ SANC). Okahandja, 3-9.II.1928, R.E. Turner (2♀ NHMUK). **NIGER**. Rég. de Zinder, Sultanat du Damagherim, Dungass, Mission Tilho, IX.1910, Dr. R. Gaillard (2♀, 5♂ MNHN). **NIGERIA**. Ile-Ife, Oyo State, 13 (1♂ NHMUK), 21 (1♀ NHMUK).II.1988, B.A. Matammi, ex. eggs *Trabala.* N. Nigeria,

IV.1928, H. Liddiard (11♀, 4♂ NHMUK). Nsukka, M.C. Eluwa, ex. mantid ootheca (4♀ NHMUK). **SENEGAL**. Bambey—J. Risbec, ex. eggs *Cirina butyrospermi* (7♀ NHMUK); ex. eggs on Cade (46♀, 28♂ NHMUK). **SOUTH AFRICA**. ex. eggs, 1979 (3♀, 1♂ NHMUK). XII.1958, G.C. Clark, ex. eggs *Cirina forda* (12♀, 2♂ NHMUK). Alldays, 50 km NE, X.1993, C. Styles, ex. eggs *Imbrasia belina* on *Colophospermum mopane* (Fabaceae) (4♀ SANC). Bander, XII.1955, B.v.d.B., ex. *N. belina* on *C. mopane* (2♀, 2♂ SANC). Bloemfontien—XII.1917, J.C. Faure, ex. eggs *Gonimbrasia tyrrhea* (9♀, 1♂ NHMUK); O.F.S., XII.1917 (2♀, 2♂ NHMUK). Bloubergstrand C.P., VIII.1979, M.J. Hassell, ex. ?*Nudaurelia* eggs on *Euclea* sp. (Ebenaceae) (4♀ SANC). Bouberg Strand, 33 18 CD, IV.1977, V.B. Whitehead, ex. *N. cytherea* eggs (9♀ SAMC). Bredasdorp – Elim T-Junction, coll. 25.VII.2016, em. 5XI.2016, M. Brink, ex. Lasiocampidae eggs on *Leucadendron* (2♀, 1♂ SANC). Cape Colony, ex. eggs Lepidoptera (2♀ NHMUK). Cape of Good Hope Nature Reserve, Olifantsbos, 34°16′S 18°23′E, strandveld, coll. 23.II.1998, em. 2.XII.1998, S. van Noort, ex. saturniid egg (33♀, 4♂ SAMC, 1♀ CNC Photo 2018-46, 1♂ CNC Photo 2018-44). Cape Town, XI.1976, H.L. O'Hefferman, ex. eggs *Nudaurelia cytherea* (6♀, 5♂ NHMUK); nr Cape Town, E.E. Hamm (1♂ NHMUK). Clan Syndicate, II.1915, C.B. Hardenberg (4♂ NHMUK). Dikombe, Merweville Koup C.P. (2♀ SAMC). Dendron, 15.XII.1966, M.v.d. Berg (3♀, 4♂ SANC). D'Nyala Nat. Res., Ellisras Dist., 23.45S 27.49E, 17-20.XII.1987, M.W. Menseli (1♀ SANC). Dohne, XII.1921, H.K. Munro, ex. eggs *Gonimbrasia tyrrhea* (4♀, 32♂ NHMUK). Duinepos, 33º11.670'S 18º08.325'E, 5.X.2011, S. van Noort, ex. Saturniidae eggs on *Euclea racemosa* (9♀, 1♂ SANC). Durban, Marley [associated with unidentified Lep. eggs] (2♀ SAMC). Elgin C.P., VI.1951, J.H. Grobler, ex. eggs *Nudaurelia cytherea capenis* (1♀ NHMUK; 1♀, 1♂ SANC). Eston, 18 (1♀ NHMUK), 20 (3♀, 1♂ NHMUK).IX.1915, C.B. Hardenberg. Grabouw C.P., Vyeboom, 5.I.1973, H. Geertsema (1♂ SANC). Gransbaai C.P., Uilenkraalmond, 2.X.1956, D.v.V. Webb, ex. eggs *Nudaurelia cytherea capensis* (2♀ NHMUK; 6♀ SANC). George, 23.I.1931, C.J. Joubert, ex. eggs *Nudaurelia cytherea* (1♀, 1♂ NHMUK). Grahamstown, 14.IX.1990, S. van Noort, ex. eggs *Bunaea alcinoe*, cabbage tree emperor moth (1♀, 1♂ SAMC). Groenfontein, Malmesburg, 14.V.1973, H. Geertsema (1♂ SANC). Hans Merensky Res, XI.1981, R. Oberprieler, ex. eggs *Gynanisa maia* on *Colophospermum mopane* (Fabaceae) (5♀ SANC). Howick, 1904.46, J.P. Cregoe, ex. *Saturnia appollonia* (7♀, 3♂ NHMUK). Humansdorp, X.1958, J.S. Taylor, ex. eggs *Nudaurelia cytherea capensis* (3♀ NHMUK). Koppies Nat. Res., 22-23.II.1993, M. Stiller, swept off *Acacia karoo* (3♀ SANC). Kraaifontein, 29.XII.1972, H. Geertsema (1♀ SANC). Ladismith C.P., XI.1977, S. Neser—(14♀, 8♂ CNC; 14♀, 9♂ + unmounted ♀♀ & ♂♂ SANC), Barrydale Rd. (3♀, 2♂ + unmounted ♀♀ & ♂♂ SANC). Lamloch, 34º19.80'S 19º04.91'E, 20-30.XI.2000, S. van Noort, ex. eggs on *Rhus lucida* stem (15♀, 3♂ SANC). La Motte C.P., Meerlust D, H. Geertsema, ex. egg *N. cytherea* (1♀, 6♂ SANC). Louis Trichardt, III.1935, T.J. Naude (6♀ SANC). Louis Trichardt district, III.1935, T.J. Naude, ex. eggs *Gonometa rufobrunnea* (4♀, 1♂ NHMUK), ex. eggs *Gonimbrasia belina* (6♀ NHMUK). Mossel Bay, XII.1921, R.E. Turner (2♀ NHMUK). New Hanover, (1♀NHMUK), X.1915 (4♀ NHMUK), 17.IX.1915, (3♀, 1♂ NHMUK), C.B. Hardenberg. Nigel, GAU, 26.25S 28.28E, IX.1963, G.H. Hepburn, ex. eggs *Philotherma rosa* (Druce) on *Eucalyptus macarthurii* (Myrtiaceae) (5♀, 2♂ CNC; 5♀, 2♂ + unmounted ♀♀ & ♂♂ SANC). Nwanedi Nature Pres., 22.33.9S 30.24.9E, c.500m, 5.IV.1997, S. Neser & M. Stiller, beating *Acacia nilotica* (1♀ SANC). Nylsvley Res., I.1978, S. Nunn, ex. eggs *Cirina forda* on *Burkea africana* (Fabaceae) (6♀, 1♂ SANC). Pietermaritzburg, J.A. Hunt, eggs found on wattle (1♀, 2♂ NHMUK). Port Elizabeth, G.C. Clark, XII.58 ex. eggs *Cirina forda* (12♀, 8♂ NHMUK). Pretoria—IX.1965, D. Webb, *Nudaurelia cytherea capenis* (1♀ USNM); X.1965, M. Holmes, *Cirina forda* (1♀ USNM); X.1965, M. Holmes, ex. *C. forda* on *B. africana* (2♀, 2♂ SANC); X.1992, R. Oberprieler, ex. eggs *Cirina forda* on *Burkea africana* (Fabaceae) (4♀, 1♂ SANC); II.1983, R. Oberprieler, ex. eggs *Bunaea alcinoe* (10♀, 2♂ CNC, 1♂ CNC Photo 2018-68; 11♀, 5♂ + unmounted ♀♀ SANC, 1♀ CNC Photo 2018-63). Swellendam, 9-14.XII.1931, R.E. Turner (1♀ NHMUK). N. Transvaal, XI.1965, M.v.d. Berg, *Gonimbrasia belina* (1♀ USNM), *Heniocha appollonia* (1♀ USNM). Umlalazi Nature Res., 1.5 km E Mtuzini, X.1978, R.M. Miller (1♀ CNC). Van Reenen, Drakensberg, 55-5600 ft., X.1926, R.E. Turner (2♀ NHMUK). Wolseley C.P., H. Geertsema, ex. eggs *Nudaurelia cytherea*—III.1972 (5♀ SANC), Kluitjieskraal, 5.I.1971 (3♀, 4♂ SANC). **TANZANIA**. Tanga, West Usambara, Mgwashi env., 04.763099°S 38.474956°E, 1460m, 31.I-1.II.2015, P. Janšta & J. Straka, sweep herbal & shrub veg. along rd., cultural savanna (1♀ CNC, CNC Photo 2018-47). **UGANDA**. Kampala—10.V.1953, D.G. Sevastopulo, ex. eggs Lasiocampid sp. from mango (6♀, 2♂ NHMUK); 4.XII.1930, H. Hargreaves, eggs on leaf *Eucalyptus* [Myrtaceae] (2♀ NHMUK). Kawanda, IX.1939, H.C. Taylor (2♀ NHMUK). Kibale N.P., Kanyawara Biol. Station, 00°33′54.4″N 30°21′29.8″E, 1509m, 30.V-6.VI.2010 (1♀ AICF, DNA voucher LFMM00111_0101), 27.VI-4.VII.2010 (1♀ AICF), S. Katusabe. **ZIMBABWE**. Harare, XI.1986, A. Watsham, ex. unidentified Lep. egg mass (17♀ CNC). Makumbi Miss., V.1974, A. Watsham (1♀ NHMUK). Manyoli Estates, Inyanga, em. II.1992, ex.

ova *Imbrasia carnegei* (Saturniidae) (6♀, 4♂ CNC; 6♀, 4♂ + unmounted ♀♀ SANC). Mazoe, A. Watsham (2♀ NHMUK). Salisbury—9.XII.1911, R.W. Jack (1♀ NHMUK); A. Watsham, eggs on *Jubernalia* [Fabaceae] (34♀, 3♂ NHMUK). Warren Hulls, 16.X.1974, A.T. Weaving (6♀, 1♂ NHMUK, ♂ CNC Photo 2018-45).

Distribution. AFROTROPICAL: *Angola, Botswana (Ditlhogo 1996), *Burkino Fasso, *Cameroon, Côte d'Ivoire (Risbec 1951), *Eritrea, *Eswatini, *Ghana, *Kenya, Madagascar (Risbec 1952), *Malawi, Mali (Crawford 1912), *Namibia, *Niger, *Nigeria, Senegal (Risbec 1951), South Africa (Cameron 1905), Sudan (Thompson 1955), *Tanzania, *Uganda, *Zimbabwe.

Biology. Hosts: LEPIDOPTERA. **Bombycidae** (Ferrière 1930a). **Eupterotidae**. *Janomima mariana* (White) [as *J. westwoodi* Aurivillius] (Berg 1970). **Hesperiidae**. *Pelopidas mathias* (Fabricius) [as *Parnara*] (Risbec 1951). **Lasiocampidae**. *Chrysopsyche imparilis* Aurivillius & *C. ladburyi* B. Baker [= *C. imparilis*] (Risbec 1951a); *Eutricha capensis* L. [as *Pachypasa*], *Gonometa postica* Walker & *G. rufobrunnea* (Aurivillius) and *Lechriolepis ochraceola* Strand (Berg 1970); **Philotherma rosa* (Druce); **Trabala* sp.; *Trichopisthia monteiroi* Druce (Berg 1970). **Nymphalidae**. *Charaxes jasius* (L.) [as *C. epijasius* Reich] (Risbec 1951a). **Papilionidae**. **Papilio demodocus* Esper. **Saturniidae**. *Argema mimosae* (Boisduval) and *Bunaea alcinoe* (Stoll) (Berg 1970), [?] *B. aslans* (Risbec 1952), *B. aslauga* Kirby (Risbec 1951a); *Cirina butyrospermi* (Vuillet) (Crawford 1912), *C. forda* (Westwood) (Berg 1970); *Epiphora bauhiniae* (Guérin-Méneville) (Risbec 1951a), *E. mythimnia* (Westwood), *Gonimbrasia belina* (Westwood) [as *Nudaurelia*] and *G. cytherea* (Fabricius) [as *Nudaurelia c. cytherea* by Berg (1970) and as *N. cytherea capensis* (Stoll) by Ferrière (1930a)], *G. tyrrhea* (Cramer) (Ferrière 1930a); *Gynanisa maja* (Klug) and *Heniocha dyops* (Maassen) (Berg 1970), **H. apollonia* (Cramer); **Holocerina angulata* (Aurivillius), **H. smilax* (Westwood); **Imbrasia carnegiei* [?]; *Pselaphelia aurata* (Westwood) [as *Nudaurelia*] and *Pseudobunaea epithyrena* (Maassen & Weymer) [as *Lobobunaea*] (Berg 1970), *P. irius* (Fab.) (Berg 1974b); *Urota sinope* (Westwood) and *Usta terpsichore* (Maassen & Weymer) [as *Heniocha*] (Berg 1970); **Usta wallengrenii* (Felder & Felder). *MANTODEA. Mantidae. Unidentified species.

Berg (1970, 1971a, 1971b, 1972, 1974a, 1974b) and Webb (1961) investigated aspects of the biology of *M. pulchriceps*.

Remarks. This is the most commonly collected and widely distributed species of *Mesocomys* in Africa. Perhaps because of this, females exhibit the most variability among examined *pulchriceps*-group species, including variation in the extent of infuscation within the basal cell. Almost all observed females have the basal cell entirely hyaline or brownish-infuscate only within about its basal half except sometimes more extensively along the mediocubital fold (Fig. 26H), that is, similar to *M. orientalis* (Fig. 21D) and *M. pauliani* (Fig. 25H). However, a single female from Ile-Ife, Nigeria, reared from a *Trabala* sp. egg, has the basal infuscate region extending comparatively broadly along the mediocubital fold into the disc similar to females of *M. anelliformis* (Fig. 18H) and *M. longiscapus* (Fig. 20H). Unlike in these latter two species, the marginal vein of the Ile-Ife female is quite short, only about twice as long as the stigmal vein, and the clypeus is deeply emarginate (*cf.* Fig. 26F) as for other *M. pulchriceps* females. Sculpture of the upper parascrobal region and frons is also variable among examined specimens. Females typically have the upper parascrobal region and frons quite distinctly roughened, mesh-like reticulate (Fig. 26D) to reticulate-imbricate, but the region sometimes is less strongly sculptured so that at one extreme the sculpture of the frons is formed only in part by very fine ridges and the sculptural cells of the upper parascrobal region are mostly flat (coriaceous) though with at least a few of the cells shallowly depressed or with a tiny pit centrally. As noted under *M. orientalis*, oblique lighting filtered through translucent film is necessary to correctly differentiate this extreme of sculpture from the entirely coriaceous (Fig. 22E) to coriaceous-imbricate (Fig. 22D) sculpture of *M. orientalis*, in which the surface of all the sculptural cells are flat. The extremes in sculpture for *M. pulchriceps* are only partially correlated with size of the individual because although smaller females typically have a more finely sculptured head, even some of the smallest have the frons and upper parascrobal region quite obviously reticulate. Colour of the body is also variable, including that of the antenna, but also of the pronotal neck, prepectus and legs. In most individuals, including smaller ones, the pronotum and prepectus (Fig. 27F) as well as most of the legs are similarly dark (Fig. 26B); however, a few larger females have the pronotal neck, prepectus (Fig. 27G), and the legs obviously paler, more-or-less similarly brownish-orange to orange. Such females also have quite a strongly reticulate prepectus rather than the finely coriaceous prepectus typical of dark females, though the sculpture intergrades among all examined females. The stigmal vein also often has a distinct spur (Fig. 26H, insert: spr) extending beyond the uncus (Fig. 26H, insert: unc) and if this was included as part of the length of the stigmal vein it would result in an even shorter marginal vein relative to the stigmal vein than given in the description. None of the examined females have

a distinct white band subbasally on the gaster, at least dorsally, though sometimes the first two gastral tergites are paler, lighter brown to orangish-brown and, as for females of most species, under some angles of light the first one or two tergites can be seen to be hyaline (*cf*. Fig. 21G: Gt_2). This is not obvious for many specimens because the dark colour of the underlying tergites shows through and the hyaline condition of Gt_1 and Gt_2 is often only distinct if the tergites are raised slightly above the other tergites.

Males of *M. pulchriceps* are most similar to those of *M. orientalis*, being differentiated by the features given in the key and as discussed under the latter species, though the males of *M. pauliani*, which is allopatric with *M. pulchriceps* in Madagascar, are unknown.

Acknowledgements

The individuals associated with the collections listed under 'Material and methods' are thanked for the loan or gifts of specimens which made this revision possible, most particularly Yong-Ming Chen and Lian-Sheng Zang (JLAU) for the reared material that stimulated this work. These two individuals and Ling-Fei Peng (FAFU) also provided English translations of parts of Yao *et al*. (2009) and other relevant Chinese literature; Huanxi Cao (IZ-CAS) provided English translations of the label data for all IZCAS-cited specimens, and Ling-Fei Peng identified the FAFU-cited specimens. Natalie Dale-Skey Papilloud (NHMUK) is thanked for providing cited information and for photographs of the labels of NHMUK *Mesocomys* type material, and other individuals listed under 'Material and methods' are also thanked for providing photographs of some type material. Simon van Noort (SAMC) is thanked for information concerning voucher material from van Noort *et al.* (2007) and L-F. Peng for providing additional information relevant to voucher material of Lin *et al*. (2017). Lucian Fusu (AICF), S. van Noort and N. Dale-Skey Papilloud are also thanked for comprehensive reviews of an earlier version of this manuscript; any remaining errors are entirely my own.

References

Ahmed, K.N., Husain, M.M. & Pramanik, S.H.A. (1995) Morphology of the egg parasite, *Mesocomys orientalis* Ferrière (Hymenoptera: Eupelmidae). *Journal of the Asiatic Society of Bangladesh*, 21, 259–261.

Ali, M.I. & Karim, M.A. (1991) Notes on the biology, behaviour and biocontrol agents of mango defoliator *Cricula trifenestrata* (Lepidoptera: Saturniidae). *Bangladesh Journal of Entomology*, 1, 83–87.

Anonymous **(**1965) Studies on the control of pine moth, *Dendrolimus spectabilis* Butler. *Entomological Research Bulletin, Seoul*, 1, 1–109.

Ashmead, W.H. (1904) Descriptions of new Hymenoptera from Japan. II. *Journal of the New York Entomological Society*, 12 (3), 146–165.

Berg, M.A. van den (1970) The biology and development of *Mesocomys pulchriceps* Cam. (Hym., Eupelmidae), a parasite of the eggs of Saturniidae in South Africa. *Phytophylactica*, 2, 137–144.

Berg, M.A. van den (1971a) Studies on the egg parasites of the mopani emperor moth *Nudaurelia belina* (Westw.) (Lep., Saturniidae). *Phytophylactica*, 3, 33–36.

Berg, M.A. van den (1971b) Studies on the induction and termination of diapause in *Mesocomys pulchriceps* Cam. (Hym. Eupelmidae) an egg parasite of Saturniidae (Lep.). P*hytophylactica*, 3, 85–88.

Berg, M.A. van den (1972) Studies on the longevity of, and number of eggs parasitised by *Mesocomys pulchriceps* Cam. (Hymenoptera: Eupelmidae), an egg parasite of Saturniidae (Lepidoptera). *Phytophylactica*, 4 (4), 113–117.

Berg, M.A. van den (1974a) Natural enemies and diseases of the forest insect *Nudaurelia cytherea clarki* Geertsema (Lepidoptera: Saturniidae). *Phytophylactica*, 6 (1), 39–44.

Berg, M.A. van den (1974b) Natural enemies and diseases of the forest insects *Pseudobunaea irius* (F.) and *Holocerina smilax* (Westw.) (Lepidoptera: Saturniidae). *Phytophylactica*, 6 (1), 69–72.

Boldt, P.E. & White, R.E. (1992) Life history and larval description of *Exema elliptica* Karren (Coleoptera: Chrysomelidae) on *Baccharis halimifolia* L. (Asteraceae) in Texas. *Proceedings of the Entomological Society of Washington*, 94 (1), 83–90.

Bouček, Z. (1979) Description of a new eupelmid parasite (Hymenoptera: Chalcidoidea) of cockroaches in India. *Bulletin of Entomological Research*, 69, 93–96.
https://doi.org/10.1017/S0007485300017922

Bouček, Z. (1988) *Australasian Chalcidoidea (Hymenoptera). A biosystematic revision of genera of fourteen families, with a reclassification of species*. CAB International, Wallingford, 832 pp.

Brèthes, J. (1922) Himenópteros y Dípteros de varias procedencias. *Anales de la Sociedad Científica Argentina*, 93, 119–146.

Burks, B.D. (1967) The North American species of *Anastatus* Motschulsky (Hymenoptera: Eupelmidae). *Transactions of the*

Entomological Society of America, 93, 423–431.
Cameron, P. (1905) On some new genera and species of Hymenoptera from Cape Colony and Transvaal. *Transactions of the South African Philosophical Society*, 15, 195–257.
https://doi.org/10.1080/21560382.1904.9626440
Chen, Y.M., Gibson, G.A.P., Peng, L.F., Iqbal, A. & Zang, L.S. (2019) *Anastatus* Motschulsky (Hymenoptera, Eupelmidae): egg parasitoids of *Caligula japonica* Moore (Lepidoptera, Saturniidae) in China. *ZooKeys*, 881, 109–134.
https://doi.org/10.3897/zookeys.881.34646
Chen, Y.-M., Qu, X.-R., Li, T.-H., Iqbal, A., Wang, X., Ren, Z.-Y., Desneux, N. & Zang, L.-S. (2020) Performances of six eupelmid egg parasitoids from China on Japanese giant silkworm *Caligula japonica* with different host age regimes. *Journal of Pest Science*. [in press]
https://doi.org/10.1007/s10340-020-01271-1
Chu, J.T. (1937) Notes on the hymenopterous parasites of the pine caterpillar *Dendrolimus punctatus* Walker in China. *Entomology and Phytopathology*, 5 (4–6), 56–103.
Clausen, C.P. (1927) The bionomics of *Anastatus albitarsis* Ashm., parasitic in the eggs of *Dictyoploca japonica* Moore (Hymen.). *Annals of the Entomological Society of America*, 20 (4), 461–472, pl. XXIII.
https://doi.org/10.1093/aesa/20.4.461
Crawford, J.C. (1912) Descriptions of new Hymenoptera. No 4. *Proceedings of the United States National Museum*, 42, 1–10.
https://doi.org/10.5479/si.00963801.42-1880.1
Ditlhogo, M.K. (1996) *The natural history of Imbrasía belina (Westwood) (Lepidoptera: Saturniidae), and some factors affecting its abundance in north-eastern Botswana*. Ph.D. Thesis, University of Manitoba, Winnipeg, Manitoba. [unknown pagination]
Fang, H.L. & Hu, H.J. (1993) Parasitic rate and control effect of *Anastatus albitarsis* on *Dendrolimus punctatus*. *Forest Research*, 6 (6), 703–706.
Ferrière, C. (1930a) On some egg parasites from Africa. *Bulletin of Entomological Research*, 21 (1), 33–44.
https://doi.org/10.1017/S0007485300021532
Ferrière, C. (1930b) Notes on Asiatic Chalcidoidea. *Bulletin of Entomological Research*, 21 (3), 353–360.
https://doi.org/10.1017/S000748530002188X
Ferrière, C. (1935) Notes on some bred exotic Eupelmidae (Hym. Chalc.). *Stylops*, IV, 145–153.
https://doi.org/10.1111/j.1365-3113.1935.tb00580.x
Ferrière, C. (1951) Parasites des oeufs d'un saturnide a Madagascar. *Mémoires de l'Institut Scientifique de Madagascar (A)*, 5 (2), 263–268.
Fourcroy, A.F. de. (1875) *Entomologia Parisiensis, sive catalogus Insectorum, quae in agro parisiensi reperiuntus—secundum methodam Geoffraeriam in sectiones, genera et species distributii; cui addita sunt nomina trivialia et fere recentae novae species*, 2, 233–544.
Fry, J.M. (1989) *Natural enemy databank, 1987. A catalogue of natural enemies of arthropods derived from records in the CIBC Natural Enemy Databank.* CAB International, Wallingford, Oxford, 115 pp.
Fukaya, S. (1936) On the hymenopterous parasitoids of gypsy moth. *Japanese Journal of Applied Zoology*, 8, 332–335.
Fusu, L. & Polaszek, A. (2017) Description, DNA barcoding and phylogenetic placement of a remarkable new species of *Eopelma* (Hymenoptera: Eupelmidae) from Borneo. *Zootaxa*, 4263 (3), 557–566.
https://doi.org/10.11646/zootaxa.4263.3.7
Fusu, L., Ebrahimi, E., Siebold, C. & Villemant, C. (2015) Revision of the Eupelmidae Walker, 1833 described by Jean Risbec. Part 1: the slide mounted specimens housed at the Muséum national d'Histoire naturelle in Paris. *Zoosystema*, 37 (3), 457–480.
https://doi.org/10.5252/z2015n3a3
Ge, Q.J., Xia, Y., Jiang, X.G. & Xu, T.L. (1996) The study of parasitism of four egg enemies on *Lymantria dissoluta* Swinhoe. *Journal of Nanjing Forestry University*, 20 (4), 45–48.
Gibson, G.A.P. (1986) Mesothoracic skeletomusculature and mechanics of flight and jumping in Eupelminae (Hymenoptera, Chalcidoidea: Eupelmidae). *The Canadian Entomologist*, 118 (7), 691–728.
https://doi.org/10.4039/Ent118691-7
Gibson, G.A.P. (1995) Parasitic wasps of the subfamily Eupelminae: classification and revision of world genera (Hymenoptera: Chalcidoidea: Eupelmidae). *Memoirs on Entomology, International*, 5, i–v + 1–421.
Gibson, G.A.P. (2004) A new species of *Oozetetes* DeSantis (Hymenoptera: Chalcidoidea: Eupelmidae) attacking oothecae of *Nyctibora acaciana* Roth (Orthoptera: Blattellidae). *Journal of Hymenoptera Research*, 13, 13–23.
Gibson, G.A.P. (2016) Revision of the Neotropical genus *Macreupelmus* Ashmead (Hymenoptera: Chalcidoidea: Eupelmidae). *Zootaxa*, 4161 (1), 81–115.
https://doi.org/10.11646/zootaxa.4161.1.3
Gibson, G.A.P. (2017a) Revision of *Eopelma* Gibson (Hymenoptera: Chalcidoidea: Eupelmidae: Neanastatinae). *Proceedings of the Entomological Society of Washington*, 119 (Special Issue), 741–777.
https://doi.org/10.4289/0013-8797.119.SpecialIssue.741
Gibson, G.A.P. (2017b) Synonymy of *Reikosiella* Yoshimoto under *Merostenus* Walker (Hymenoptera: Chalcidoidea: Eupelmidae), with a checklist of world species and a revision of those species with brachypterous females. *Zootaxa*, 4255 (1),

1–65.
https://doi.org/10.11646/zootaxa.4255.1.1
Gibson, G.A.P. (2020) Redescription of *Anastatus mantoidae* Motschulsky, the type species of *Anastatus* Motschulsky 1859, and *Anastatus echidna* (Motschulsky), the type species of *Cacotropia* Motschulsky 1863, with respect to taxonomy of *Anastatus* (Hymenoptera: Eupelmidae: Eupelminae). *Zootaxa*, 4748 (3), 485–513.
https://doi.org/10.11646/zootaxa.4748.3.5
Gibson, G.A.P. & Fusu, L. (2016) Revision of the Palaearctic species of *Eupelmus* (*Eupelmus*) Dalman (Hymenoptera: Chalcidoidea: Eupelmidae). *Zootaxa*, 4081 (1), 1–331.
https://doi.org/10.11646/zootaxa.4081.1.1
Girault, A.A. (1927) *Thysanoptera nova Australiensis. II.* Private publication, Brisbane, 2 pp.
He, J.H. & Chen, X.X. (1990) Studies on ten species of *Aleiodes* Wesmael parasitic on the forest insect pests in China: (Hymenoptera: Braconidae). *Acta Zootaxonomica Sinica*, 15 (2), 201–208.
Herting, B. (1976) *A catalogue of parasites and predators of terrestrial arthropods. Section A. Host or Prey/Enemy. Lepidoptera, Part 2 (Macrolepidoptera). Vol. 7*. Commonwealth Agricultural Bureaux, Commonwealth Institute of Biological Control, Farnham Royal, 221 pp.
Hirose, Y. (1964) The activity of the egg parasite of the pine-moth, *Dendrolimus spectabilis* Butler in the Japanese black pine forest on the sea coast. *Science Bulletin of the Faculty of Agriculture, Kyushu University*, 21 (1), 13–24.
Hirose, Y. (1969) Comparative ecology of some Hymenopterous egg parasites of the pine moth, *Dendrolimus spectabilis* Butler (Lepidoptera: Lasiocampidae), with special reference to the factors affecting their efficiency as natural enemies. *Science Bulletin of the Faculty of Agriculture, Kyushu University*, 24 (2), 115–148.
Hossain, M.M., Ali, S.H. & Rahim, A. (1995) Some lepidopteran and homopteran pests and parasites of castor (*Ricinus communis* L.). *Bangladesh Journal of Scientific and Industrial Research*, 30, 265–267.
Howard, L.O. (1892) The hymenopterous parasites of spiders. *Proceedings of the Entomological Society of Washington*, 2, 290–302.
Ishii, T. (1938) Chalcidoid- and proctotrypoid-wasps reared from *Dendrolimus spectabilis* Butler and *D. albolineatus* Matsumura and their insect parasites, with descriptions of three new species. *Kontyû*, 12 (3), 97–105.
Josh, R.C. & Uttamasamy Kameswara Rao, P. (1983) New record of the egg parasite *Mesocomys orientalis* Ferriere (Eupelmidae: Hymenoptera) on *Metanastria hyrtaca* Cam. *Madras Agricultural Journal*, 70 (12), 833.
Kalina, V. (1981) The Palaearctic species of the genus *Anastatus* Motschulsky, 1860 (Hymenoptera, Chalcidoidea, Eupelmidae) with descriptions of new species. *Silvaecultura Tropica et Subtropica*, *Prague*, 8, 3–25.
Kalina, V. (1984) New genera and species of Palaearctic Eupelmidae (Hymenoptera, Chalcidoidea). *Silvaecultura Tropica et Subtropica, Prague*, 10, 1–29.
Khan, M.A. (1983) First record of *Mesocomys* Cam. (Hym.: Chalcidoidea, Eupelmidae) in India. *Journal of the Bombay Natural History Society*, 80 (3), 656–658.
Kioko, E.N. (1998) *Biodiversity of wild silkmoths (Lepidoptera) and their potential for silk production in East Africa*. Ph.D. thesis, Kenyatta University, Nairobi, 151 pp.
Koidzumi, K. & Shibata, K. (1940) Studies on *Eriogyna pyretorum* Westw, and its fishing thread. XI. Epiparisites. *Journal of the Society of Tropical Agriculture*, 12 (4), 259–265.
Kononov, A., Ustyantsev, K., Wang, B., Mastro, V.C, Fet, V., Blinov, A. & Baranchikov, Y. (2016) Genetic diversity among eight *Dendrolimus species* in Eurasia (Lepidoptera: Lasiocampidae) inferred from mitochondrial COI and COII, and nuclear ITS2 markers. *BMC Genetics*, 17 (Supplement 3), 173–191.
https://doi.org/10.1186/s12863-016-0463-5
Lin, H., Fu., L., Lin, J., Hua, Y., Han, X., Zheng, J., He, H., Zhang, F. & Liang, G. (2017) Main species of parasitoid natural enemy insects within *Dendrolimus houi* (Lajonquiere) in the forest of *Cryptomeria fortunei* (Hooibrenk). *Chinese Journal of Biological Control*, 33 (6), 842–848.
Mani, M.S. (1989) *The fauna of India and the adjacent countries: Chalcidoidea (Hymenoptera). Part 1: Introduction. Agaontidae, Torymidae, Leucospididae, Chalcididae, Eurytomidae, Perilampidae, Eucharidae, Cleonymidae, Miscogasteridae, Pteromalidae, Eupelmidae and Encyrtidae*. Zoological Survey of India, Calcutta, xlv + 1067 pp.
Mathur, R.N. (1956) A new species of *Anastatus* Motschulsky (Chalcidoidea: Eupelmidae) from Kashmir. *Proceedings of the Royal Entomological Society of London*, 25, 93–97.
https://doi.org/10.1111/j.1365-3113.1956.tb01100.x
Messer, A.D., Wanta, N.N. & Sunjaya, X. (1992) Biological and ecological studies of *Calliteara cerigoides* (Lepidoptera, Lymantriidae), a polyphagous defoliator of southeast Asian Dipterocarpaceae. *Japanese Journal of Entomology*, 60, 191–202.
Muesebeck, C.F.W. & Dohanian, S.M. (1927) A study in hyperparasitism, with particular reference to the parasites of *Apanteles melanoscelus* (Ratzeburg). *Bulletin of the United States Department of Agriculture*, No. 1487, 1–35.
https://doi.org/10.5962/bhl.title.108942
Narendran, T.C. & Sheela, S. (1995) A new species and key to species of *Mesocomys* Cameron (Hymenoptera: Eupelmidae). *Journal of Ecobiology*, 7 (4), 307–311.
Ni, L.X., Tong, X.W. & Lao, X.M. (1994) Influence of multiparasitism of egg parasitoids of pine lasiocampids on efficacy of biological control. *Acta Entomologica Sinica*, 37 (2), 145–152.

Notton, D.G., Buffington, M.L. & van Noort, S. (2009) The status of the type material of *Pycnostigmus rostratus* Cameron (Hymenoptera, Figitidae, Pycnostigminae). *Journal of Natural History*, 43, 181–184. https://doi.org/10.1080/00222930802250142

Noyes, J.S. (2019) Universal Chalcidoidea Database. Online. Available from: https://www.nhm.ac.uk/chalcidoids (accessed 1 August 2019).

Özdikmen, H. (2011) New names for some preoccupied specific epithets in Chalcidoidea II: families Eupelmidae, Eurytomidae, Mymaridae, Perilampidae, Pteromalidae, Torymidae (Hymenoptera: Parasitica). *Munis Entomology & Zoology*, 6 (2), 832–855.

Peng, J.W., Ma, W.Y., Wang, X.L. & Zuo, Y.X. (1984) Influence of enhancement of host egg supply on population increase of egg parasites in pine forests. *Acta Entomologica Sinica*, 27 (1), 39–47.

Perkins, R.C.L. (1906) Leaf-hoppers and their natural enemies (VIII). *Bulletin of the Hawaiian Sugar Planters' Association Experiment Station*, Entomology Series, 1, 239–267.

Prinsloo, G.L. (1980) An illustrated guide to the families of African Chalcidoidea (Insecta: Hymenoptera). *Department of Agriculture and Fisheries Science Bulletin, Republic of South Africa*, 395, 1–66.

Qin, J., Zhang, Y., Zhou, X., Kong, X., Wei, S., Ward, R.D. & Zhang, A.-B. (2015) Mitochondrial phylogenomics and genetic relationships of closely related pine moth (Lasiocampidae: *Dendrolimus*) species in China, using whole mitochondrial genomes. *BMC Genomics*, 16, 1–12. https://doi.org/10.1186/s12864-015-1566-5

Risbec, J. (1951a) I. Les Chalcidoïdes d'A.O.F. *Mémoires de l'Institute Français d'Afrique Noire*, 13, 1–410.

Risbec, J. (1951b) Chalcidoïdes d'A.O.F. *Bulletin de l'Institut Français d'Afrique Noire*, 13, 1110–1130.

Risbec, J. (1952) Contribution à l'étude des Chalcidoïdes de Madagascar. *Mémoires de l'Institute Scientifique de Madagascar (Série E)*, 2, 449 pp.

Risbec, J. (1955) Hyménoptères parasites du Cameroun. *Bulletin de l'Institut Français d'Afrique Noire (A)*, 17(1), 191–266.

Schaefer, P.W., Kanimatsu, K. & Lee, H.P. (1988) Egg parasitism in *Lymantria dispar* (Lepidoptera, Lymantriidae) in Japan and South Korea. *Kontyû*, 56, 430–444.

Schedl, K.E. (1936) Der Schwamms spinner (*Porthetria dispar* L.) in Euroasien, Afrika und Neuengland. *Monographien zur Angewandten Entomologie*, 12, 69–170.

Sheng, J.K. (1998) A new species of genus *Mesocomys* (Hymenoptera: Eupelmidae) from China. *Entomological Sinica*, 5 (1), 26–28. https://doi.org/10.1111/j.1744-7917.1998.tb00291.x

Sheng, J.K. & Wang, G.H. (1996) A new species of *Mesocomys* from China (Hymenoptera: Chalcidoidea: Eupelmidae). *Acta Agriculturae Universitatis Jiangxiensis*, 18 (4), 416–418.

Schmiedeknecht, O. (1909) Hymenoptera fam. Chalcididae. *In*: *Genera Insectorum*. *Vol. 97*. P. Wytsman, Brussels, pp. 1–550.

Subba Rao, B.R. (1957) Some new species of Indian Hymenoptera. *Proceedings Indian Academy of Sciences (B)*, 46, 376–390.

Talamas, E.J., Buffington, M.L. & Hoelmer, K. (2017) Revision of Palearctic *Trissolcus* Ashmead (Hymenoptera, Scelionidae). *Journal of Hymenoptera Research*, 225, 3–186. https://doi.org/10.3897/jhr.56.10158

Thompson, W.R. **(**1955) Section 2. Host parasite catalogue, Part 3. Hosts of the Hymenoptera (Calliceratid to Evaniid). *In*: A catalogue of the parasites and predators of insect pests. Commonwealth Agricultural Bureaux, The Commonwealth Institute of Biological Control, Ottawa, pp. 191–332.

Tong, X.W. (1987) New host records of Chalcidoidea. *Natural Enemies of Insects*, 9, 54.

Tong, X.W. & Ni, L.X. (1989) Bionomics of *Pseudanastatus albitarsis* Ashmead and its utilization in controlling *Dendrolimus punctatus* Walker. *Acta Entomologica Sinica*, 32 (4), 451–458.

Tong, X.W. & Ni, L.X. **(**1990) Studies on relationship between density of host eggs, parasitic rate and number released of *Trichogramma dendrolimi* and *Pseudanastatus albitarsis*. *Forest Pests and Diseases*, 1, 5–7.

Urich, F.W., Scott H. & Waterston, J. (1922) Note on the dipterous bat-parasite *Cyclopodia greeffi* Karsch, and on a new species of hymenopterous (chalcid) parasite bred from it. *Proceeding of the Zoological Society of London*, 32, 471–477. https://doi.org/10.1111/j.1096-3642.1922.tb02153.x

van Noort, S., Stone, G.N., Whitehead, V.B. & Nieves-Aldrey, J.-L. (2007) Biology of *Rhoophilus loewi* (Hymenoptera: Cynipoidea: Cynipidae), with implications for the evolution of inquilinism in gall wasps. *Biological Journal of the Linnean Society*, 90, 153–172. https://doi.org/10.1111/j.1095-8312.2007.00719.x

Vasic, K. & Minic, D. (1979) Fauna of hyperparasites in cocoons of solitary *Apanteles* species and *Meteorus versicolor* Nees., of primary parasites of the gypsy moth (*Porthetria dispar* L.) and the satin moth (*Leucoma salicis* L.) in Yugoslavia. *Archiv Bioloskih Nauka, Belgrade*, 28, 175–188.

Veldtman, R., McGeoch, M.A. & Scholz, C.H. (2004) Parasitoids of Southern African wild silk moths (Lepidoptera). *African Entomology*, 12 (1), 117–122.

Viggiani, G. & Tremblay, E. (1978) Nuovi reperti sulla specializzazione morfotipica di *Anastatus bifasciatus* (Geoffroy) (Eupelmidae) agli ospiti. *Atti XI Congresso Nazionale Italiano di Entomologia*, 1978, pp. 321–322.

Walker, F. (1872) Part 5. Encyrtidae (continuation), Myinidae, Eupelmidae, Cleonymidae, Spalangidae and Pirenidae. *Notes on*

Chalcidiae, London, 1872, pp. 71–88, 16 figs.
Wang, W.X. (1990) Sex allocation by parasitic Hymenoptera. *Chinese Journal of Biological Control*, 6, 173–178.
Waterston, J. (1915) Chalcidoidea bred from *Glossina morsitans* in North Rhodesia. *Bulletin of Entomological Research*, 6, 69–82.
https://doi.org/10.1017/S0007485300043431
Webb, D.v.V. (1961) Preliminary investigations on the biology, ecology and control of Emperor moths, *Nudaurelia cytherea capensis* Stoll., and *Gonimbrasia tyrrhea* Cr., attacking trees and shrubs in the western and south-western Cape Province. *Technical Communications, Department of Agricultural Technical Services, South Africa*, No 12, 44–51.
Weseloh, R.M., Wallner, W.E. & Hoy, M.A. (1979) Possible deleterious effects of releasing *Anastatus kashmirensis*, a facultative hyperparasite of the Gypsy moth. *Environmental Entomology*, 8, 174–177.
https://doi.org/10.1093/ee/8.1.174
Wheeler, A.G. Jr. & Miller, G.L. (1990) *Leptoglossus fulvicornis* (Heteroptera: Coreidae) a specialist on magnolia fruits: seasonal history, habits and descriptions of immature stages. *Annals of the Entomological Society of America*, 83 (4), 753–765.
https://doi.org/10.1093/aesa/83.4.753
Xu, Y.X., Sun, X.G., Han, R.D. & He, Z. (2006) Parasitoids of *Dendrolimus punctatus* in China. *Chinese Journal of Applied Entomology*, 43, 767–773.
Yang, Z.Q., Yao, Y.X. & Cao, L.M. (2015) *Chalcidoidea parasitizing forest defoliators (Hymenoptera)*. Science Press, Beijing, 283 pp., 21 pls.
Yao, Y.X., Yang, Z.Q. & Zhao, W.X. (2009) Descriptions of four new species in the genus *Mesocomys* (Hymenoptera, Eupelmidae) parasitizing eggs of defoliators from China. *Acta Zootaxonomica Sinica*, 34 (1), 155–160.
Yasumatsu, K. & Watanabe, C. (1964) *A tentative catalogue of insect natural enemies of injurious insects in Japan. Part 1. Parasite-predator host catalogue.* Entomology Laboratory, Faculty of Agriculture, Kyushu University, Fukuoka, 166 pp.